MARTIN MARIETTA DENVER DIVISION

APPLICATION OF REMOTE-SENSING TECHNIQUES TO THE GEOLOGY OF THE BONANZA VOLCANIC CENTER

By

Ronald W. Marrs

Remote Sensing Report 73-1

NASA Grant NGL 06-001-015
National Aeronautics and Space Administration
Office of University Affairs
Washington, D.C. 20546

March 1973

REMOTE SENSING PROJECTS

DEPARTMENT OF GEOLOGY

COLORADO SCHOOL OF MINES • GOLDEN, COLORADO

APPLICATION OF REMOTE-SENSING TECHNIQUES TO THE GEOLOGY OF THE BONANZA VOLCANIC CENTER

By

Ronald W. Marrs

Remote Sensing Report 73-1

Bonanza Remote Sensing Project
Department of Geology
Colorado School of Mines
Golden, Colorado

NASA Grant NGL 06-001-015

Approved for Publication: 

Keenan Lee
Principal Investigator

March 1973

Page Intentionally Left Blank

ABSTRACT

A program for evaluating remote sensing as an aid to geologic mapping has been under way at the Colorado School of Mines for the past four years. Data tested in this evaluation include color and color infrared photography, multiband photography, low sun-angle photography, thermal infrared scanner imagery, and side-looking airborne radar.

The relative utility of color and color infrared photography was tested as it was used to refine geologic maps in previously mapped areas, as field photos while mapping in the field, and in making photogeologic maps prior to field mapping. The latter technique served as a test of the maximum utility of the photography. In this application the photography was used successfully to locate 75% of all faults in a portion of the geologically complex Bonanza volcanic center and to map and correctly identify 93% of all Quaternary deposits and 62% of all areas of Tertiary volcanic outcrop in the area.

Attempts were made to enhance geologically significant contrasts and to detect and delineate lithologically and structurally important features using multiband photography. The multiband techniques were generally unsuccessful in the heavily forested volcanic terrain of the Bonanza area. Color-additive viewing of the multiband

photography also failed to produce any obvious contrast improvement.

Daytime thermal infrared imagery was useful for locating faults despite strong interference from topography. Pre-dawn thermal imagery was also affected by topography in areas of high relief, but revealed moisture and vegetation patterns in areas of low relief. Some of these patterns proved to be geologically significant.

Low sun-angle photography was more useful than available side-looking radar for geologic mapping in the Bonanza volcanic center where the main object of low-angle illumination was enhancement of topographically expressed structures. The low sun-angle photography has its major advantage in superior resolution, but lacks the flexibility of side-looking radar with regard to "look-direction". For both sensors, the best illumination direction is one which is very nearly perpendicular to the structural trends and "looks down" the dominant topographic slope.

Geologic mapping done in conjunction with the remote-sensing evaluations of the previously unmapped area to the south and west of the central Bonanza mining district confirms the existence of the Bonanza caldera and demonstrates that structures related to the formation of the caldera dominate the geology of the area.

The Oligocene volcanic sequence of the Bonanza volcanic center is typical of volcanism in and around the San Juan volcanic field. It begins with intermediate andesitic flows and breccias, followed by more silicic pre- and intracaldera lavas and ash flows, and terminates with small, latitic and rhyolitic flows. Caldera collapse is associated with the eruption of the middle ash-flow sequence which serves as a geologic marker for the structural interpretation and as an indicator of the geologic evolution of the magma which produced the Bonanza volcanic pile.

Interpretation of the structural pattern of the Bonanza area as the result of large-scale subsidence is supported by all the observed structural and stratigraphic relationships, and is further confirmed by gravity data (Karig, 1965).

The radial and concentric pattern of faulting which resulted from collapse of the Bonanza caldera has controlled post-volcanic ore deposition in the area. Mineralogical similarities among deposits demonstrate that mineralizing fluids moved out along radial fractures. The largest areas of alteration and mineralization are located at the intersections of the major radial and concentric faults.

Evidence of post-caldera movements on the Western Boundary Fault of the Bonanza caldera and the coincidence of the

Western Boundary Fault of the caldera with the west boundary fault of the Arkansas Valley graben indicates that the caldera fault system has been undergoing additional displacement as a part of the presently active Rio Grande rift system. This late movement helps to explain why the west boundary of the Bonanza caldera shows more structural displacement than the east boundary.

CONTENTS

ILLUSTRATIONS

Page

ACKNOWLEDGMENTS

The work presented in this report was performed as research in connection with the Bonanza Remote-Sensing Project at the Colorado School of Mines. I am indebted to the administration and faculty of the Colorado School of Mines and to the National Aeronautics and Space Administration (NASA Grant NGL 06-001-015) for providing the financial assistance which made this work possible.

I gratefully acknowledge the advice and assistance of Drs. R. C. Epis, J. J. Finney, Keenan Lee, and R. G. Reeves, who have given freely of their time and effort during the course of this investigation. Acknowledgments are also due the residents and land owners in the Bonanza area who allowed me access to their property and provided me with considerable information regarding the development and history of the district. I wish to acknowledge especially the cooperation and assistance of Mr. and Mrs. Kempner of the ED Ranch, who in addition to their abundant hospitality, furnished me many interesting and colorful details about the history of the area.

I also am thankful for the steadfast support of my wife, Glenna, who helped in innumerable ways throughout the course of this work.

INTRODUCTION

The Bonanza mining district lies along the southeast edge of the Colorado Mineral Belt near the junction of the Sawatch Range, the Sangre de Cristo Mountains, and the San Juan volcanic field (fig. 1). The southwest Bonanza area includes much of the region loosely defined as the "Bonanza volcanic center" and encompasses the area south and west of the central Bonanza mining district which was previously mapped by H. B. Patton (1915) and W. S. Burbank (1932). The area lies 25 miles south-southwest of Salida, the county seat of Chaffee County and is immediately north of Saguache, the county seat of Saguache County. Bonanza is nestled in the Kerber Creek valley near the northeast boundary of the area. Access to the area is by several county roads and numerous jeep trails that extend north and west away from U. S. Highway 285 between Salida and Saguache. The Villa Grove-Bonanza road (Saguache County 16) is the major access route (fig. 2).

Most of the southwest Bonanza area lies within Rio Grande National Forest, but the areas along Kerber Creek and Saguache Creek belong to private ranches (fig. 2). Most of the area is mountainous and much is heavily forested (fig. 3). Elevations range from 8,000 ft in the Findley Gulch area to more than 13,200 ft in the mountains west of Bonanza.

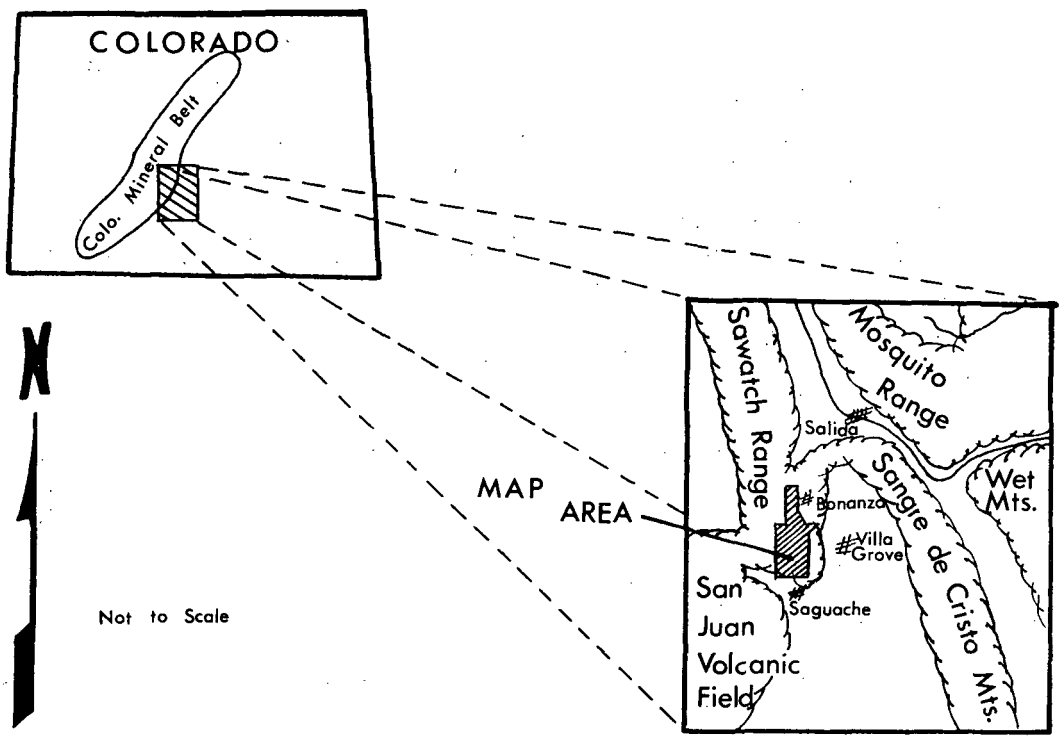

Figure 1. Index map of south-central Colorado and the southwest Bonanza area (cross-hatched area).

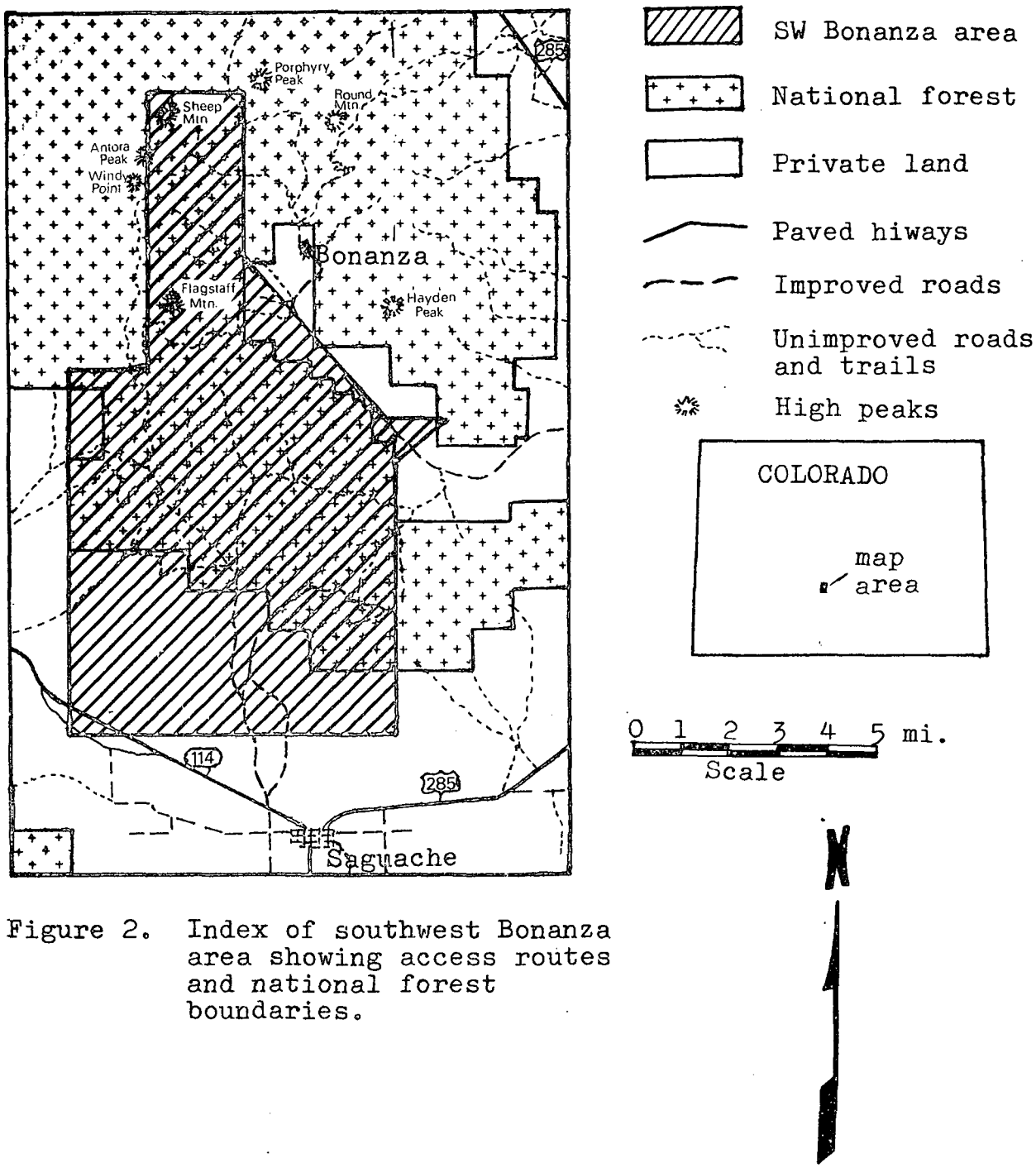

Figure 2. Index of southwest Bonanza area showing access routes and national forest boundaries.

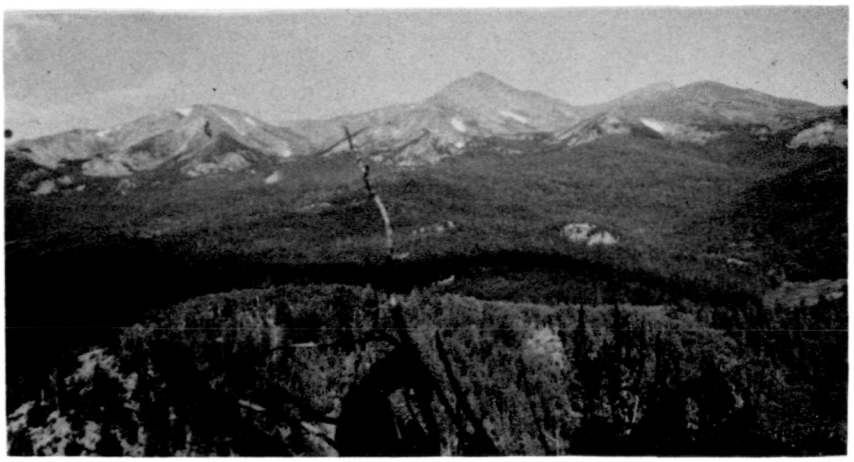

Figure 3. View westward across the northern Bonanza area. Windy Point, Antora Peak, and Sheep Mountain are seen along the skyline from left to right. The topographic depression in the central part of the photograph is the northern Kerber Creek drainage.

This report is the result of a dual purpose study which was conducted from July 1969 thru March 1972. The aims of the study were: 1) to evaluate remote-sensing techniques as tools for geologic mapping, and 2) to derive a geologic map and a structural and stratigraphic interpretation of the geology of the previously unmapped southwest Bonanza area.

Reports on various aspects of the remote-sensing evaluations have been included in the regular reports of the Bonanza Remote-Sensing Project under NASA Grant NGL 06-001-015 (Lee and others, March 1970, p. 27-28; Lee and others, Jan. 1971, p. 38-45; Reeves and others, June 1971, p. 13-16; Reeves and others, Oct. 1971, p. 4-7; Knepper and others, March 1972, p. 14-16). Two papers, one dealing with the geology of the Bonanza area and the other with the remote-sensing evaluations, were presented at the regional meeting of the Rocky Mountain Section of the Geological Society of America in Laramie, Wyoming, on May 11-12, 1972 (Marrs, 1972a; 1972b). Papers dealing with geology and remote-sensing applications in the Bonanza area and the surrounding region have been published in the New Mexico Geological Society Guidebook (Knepper and Marrs, 1971) and the Proceedings of the Eighth International Symposium on Remote Sensing of Environment (Knepper and Marrs, 1972).

Throughout this report, selected examples of the various remote-sensing data used and their interpretations illustrate the utility of the data and the problems encountered in their use. The techniques that were studied and evaluated include:

1. Photogeologic interpretation of color and color infrared photography (both high- and low-altitude)
2. Photogeologic interpretation of multiband photography
   a. Standard techniques of photogeologic interpretation
   b. Color-additive techniques
   c. Video image processing
   d. Digital enhancement techniques
3. Photogeologic interpretation of low sun-angle photography
4. Video image processing and geologic interpretation of thermal infrared scanner data (including mid-day and pre-dawn imagery in 3-5 μm and 8-14 μm bands)
5. Geologic interpretation of side-looking airborne radar imagery

The information that resulted from these remote-sensing interpretations was checked and supplemented by field mapping, spectral measurements, and laboratory petrographic studies.

The field mapping, which required most of three summer field seasons (a total of 36 weeks), provided the basic ground control necessary for proper evaluation of the remote-sensing techniques and insured that the final

geologic map would be as accurate and complete as possible. The remote-sensing interpretations were carefully checked against the field data and were supplemented by detailed field investigation in areas where the remote-sensing interpretations were inadequate or misleading.

Field and laboratory spectral reflectivity determinations provided a quantitative base from which to assess the likelihood of discrimination between various lithologic units by remote sensing. These spectral determinations were made only on a few samples which were chosen to represent major lithologies. Therefore, the spectral measurements provided only enough information to draw very general conclusions about descriminable units.

Laboratory petrographic studies are a significant portion of the investigation because they provide 1) the detailed mineralogical data for correlation of various units and groups in the volcanic sequence; 2) mineralogical, structural, and textural data which indicate various relationships between units and groups and allow for more complete interpretation of the magmatic, stratigraphic, and structural evolution of the area; 3) textural and mineralogical information for interpretation of spectral measurements.

The entire mass of data was then compiled into a geologic map of the southwest Bonanza area. This work was combined with data from the reports of others who have

worked in adjacent areas to produce a structural and stratigraphic interpretation of the region. The regional relationships outlined in this report may provide insight into the geologic history and tectonic development of south-central Colorado.

HISTORICAL SKETCH

The first settlers came to the Kerber valley in the 1860's. Most of these settlers were homesteaders who came to establish farms and ranches, but even during these first years a few ventured into the surrounding mountains to prospect. John G. Huntington, a U.S. mineral surveyor, surveyed most of the pre-emptions taken up by the settlers and mapped parts of the Bonanza area as early as 1873.

The earliest recorded geological survey of the area was completed in 1874 by F. M. Endlich as part of the U.S. Territorial Survey under the direction of F. V. Hayden. Endlich described the upper Kerber valley as having the appearance of "a huge crater containing a number of small eruptive cones" (1874, p. 343). More detailed geologic maps of the Bonanza mining district were compiled by H. B. Patton (1915) and students of the Colorado School of Mines, and W. S. Burbank of the U.S. Geological Survey (1932). More recently, graduate students from the Colorado School of Mines have mapped areas to the southeast (R. J. Bridwell, 1968), southwest (D. L. Bruns, 1971), east (J. D. Mayhew, 1969), and north (H. A. Perry, 1971) of the central mining district. D. H. Knepper is presently completing a regional geologic map including these and other areas to the north and east.

The first mining claim in the Bonanza area was staked by E. Durfey in the late 1870's, but was never recorded because the vein soon gave out (Kempner, 1971, p. 6). Many prospectors passed through the area in the 1870's on their way west to the gold fields, but the few silver and lead prospects that were found in the district did not stir much interest. The gold rush finally hit the district in 1880 with the location of many promising claims (fig. 4); including the Rawley, the Bonanza, the Manitou, and the Josephine. Several towns sprang up along the Kerber valley; among them were Bonanza (fig. 5), Kerber City, Sedgwick, Exchequer, Parkville, and Claytonia. In addition, many of the larger mines supported substantial camps. The population of the district is estimated to have been as high as 40,000 at one time (Kempner, 1971, p. 8).

The rush of the 1880's died almost as suddenly as it had begun, and the town of Bonanza gradually absorbed the few people that remained, while the other towns and camps disappeared. Today, even Bonanza is dying. There are no businesses in the town and no post office or school. Only a few summer cabins mark the site of the once-bustling mining community.

Over the years, only a very few mines of the Bonanza district have survived for any length of time. Even these have suffered from various management and production problems and, in general, have not been very profitable.

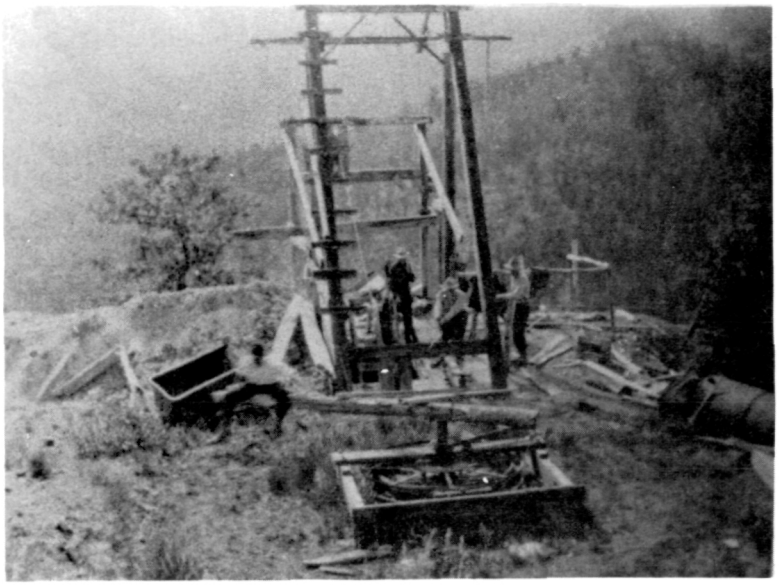

Figure 4. The Black Bess mine (after Hudson and Bigley, 1915). This scene is typical of the activity around Bonanza between 1880 and 1920.

Figure 5. Bonanza in 1880 (after Ransom and Damon, 1915). The "floating" population of the Bonanza area was estimated at 40,000 about this time.

Minor booms brought new life to the area as new discoveries were made, as new capital became available, or as changing prices allowed mines to be brought into production. But each time the activity subsided. As a result, the overall production figures for the district are unimpressive. Burbank (Vanderwilt, 1947, p. 445) estimated the total production of the district prior to 1946 to be about $9,000,000; but some feel that this estimate is too conservative (Kempner, 1972, personal communication).

Recent efforts to locate new ore bodies in the Bonanza area have employed modern techniques, including geophysical surveys, color air-photo analysis, and diamond drilling. These, too, have failed to produce any significant finds, but they emphasize the fact that many people believe untapped reserves lie within the Bonanza district.

CLIMATE AND VEGETATION

Both climate and vegetation influence the applicability of remote-sensing techniques. Therefore, a brief description of the climate and vegetation of the Bonanza area is warranted.

The prime control on the climate of the Bonanza area is its location in the semi-arid region of western North America, but the local climate is directly controlled by terrain. The mountains of Colorado act as a barrier to the dominant west-to-east flow of air and create an anomalous climatic condition. The mean annual precipitation in mountainous areas, such as Bonanza, is approximately 50 inches per year compared to the 15 inches per year normally received in a semi-arid region. The temperatures in the area vary from -35° to 90°F as an average annual minimum and maximum, with a mean annual temperature near 35°F.

Most of the precipitation in the summer results from thundershowers that commonly dump more than an inch of precipitation in a few minutes (generally in a restricted area). These torrential rains are responsible for the greatest portion of the visible erosion in the area. General rains are more prevalent during the spring and fall when mid-day temperatures are moderate. Snow is

common from mid-September to May, and protected portions of the higher peaks are generally snow-covered for seven or eight months each year. There are no permanent snow fields in the area.

Vegetation is controlled by the climate and soil-type. Since both climate and soils are strongly influenced by topography, elevation is a natural parameter on which to base a subdivision of vegetation life-zones. According to Preston's classification (1968) the four life-zones present in the southwest Bonanza area are: 1) Upper Austral or Transition (below 9,000'), 2) Canadian (9,000-11,000'), 3) Hudsonian (11,000-11,800'), and 4) Alpine (above timber line). The elevation ranges are arbitrary and can vary under local conditions.

The dominantly conifer forests of the Bonanza area include a great variety of tree species. Douglas fir (Pseudotsuga taxifolia) and ponderosa pine (Pinus ponderosa) are the dominant species, but juniper (Juniperus monosperma), pinon pine (Pinus edulis), lodgepole pine (Pinus contorta latifolia), Colorado blue spruce (Picea pungens), subalpine fir (Abies lasiocarpa), Engelmann spruce (Picea engelmanii), bristlecone pine (Pinus aristata), and quaking aspen (Populus tremuloides) are also found within their respective life-zones. Figure 6 shows the normal elevation ranges of most of the species in the Bonanza area. The lower elevations,

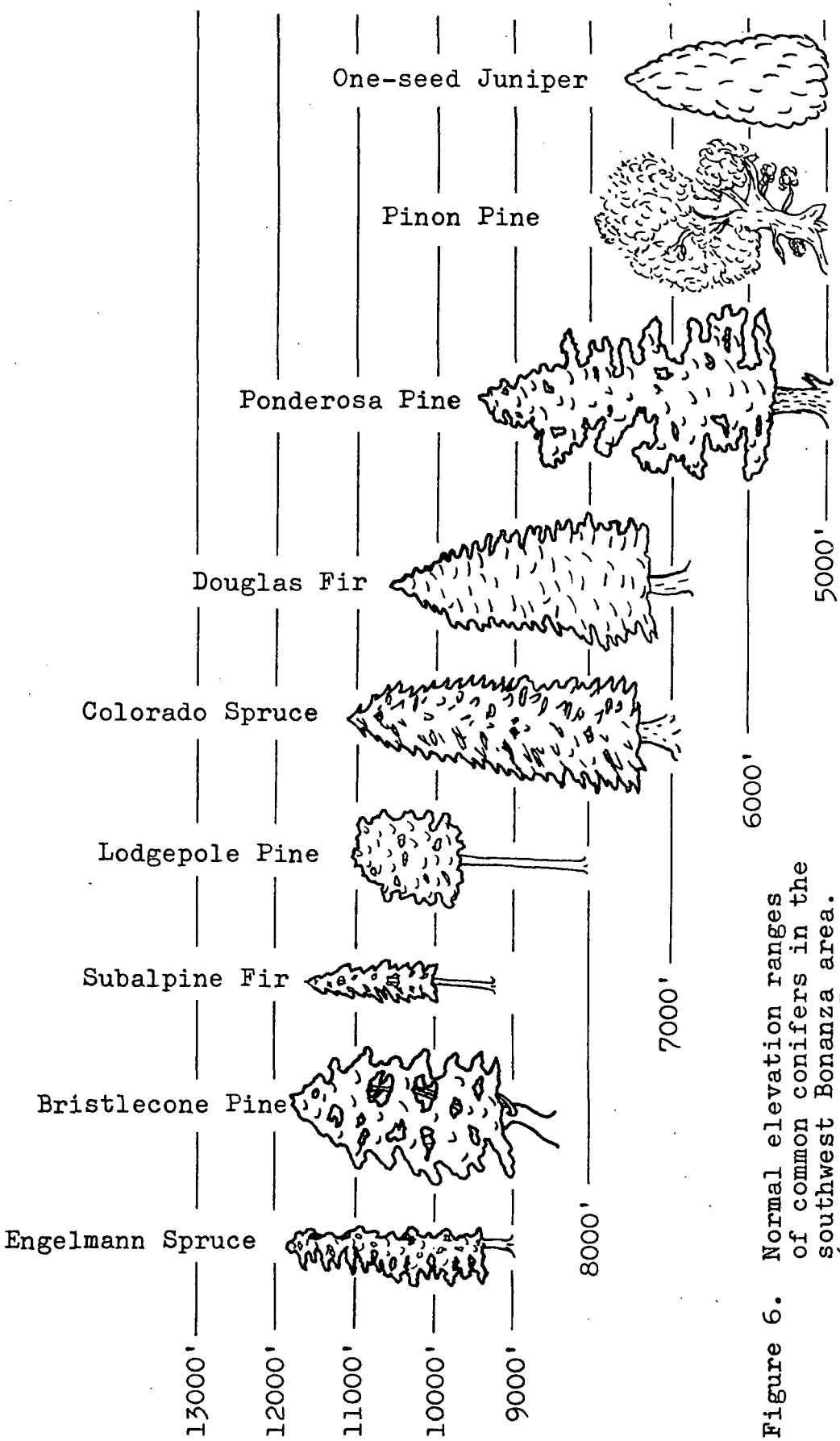

Figure 6. Normal elevation ranges of common conifers in the southwest Bonanza area. (modified after LeRoy, personal communication; and Preston, 1968)

particularly areas of low relief, are characterized by shrubs such as rabbitbrush (Chrysothamnus spp.), greasewood (Sarcobatus vermiculatus), and sagebrush (Artemisia spinescens) along with a great variety of grasses and wildflowers. Greasewood is particularly interesting because it is concentrated in areas of poor drainage where the soil is alkaline. Sometimes such areas are associated with faults which have inhibited the flow of ground water.

Above timberline most of the gentler slopes are covered by a mat of grasses, sedges, and alpine wildflowers. The steeper outcrops have very little soil, but support some moss and lichen.

LITHOLOGIC SEQUENCE

The Bonanza volcanic center lies at the northeastern edge of the San Juan volcanic field (T 44 thru 49 N and R 5 thru 9 E), and most investigators prefer to think of the Bonanza volcanic pile as part of the San Juan field, or as part of a huge volcanic field that once included both the San Juan and Thirty-nine Mile volcanic fields (Steven and Epis, 1968). Tertiary volcanic sequences embrace the bulk of lithologies exposed in the southwest Bonanza area; but Precambrian igneous and metamorphic rocks, Paleozoic sedimentary rocks, and Quaternary deposits are also present. Figure 7 is a generalized columnar section which shows the usual relationship observed between the various units mapped.

The volcanic rocks of the Bonanza area were erupted onto a low-relief erosion surface cut mainly in Precambrian igneous and metamorphic rocks. A maximum relief of 2,000 ft is estimated for this surface on the basis of variations in thickness of the lowermost volcanic units. Scattered remnants of folded and faulted Paleozoic sedimentary rocks were present on the surface where their position along synclinal axes or under thrust plates had protected them from erosion. This surface was completely inundated by the Tertiary volcanic flows. Some of these pre-volcanic lithologies have since been exhumed by erosion and crop out along the edge of the volcanic pile and in erosional windows cut through the

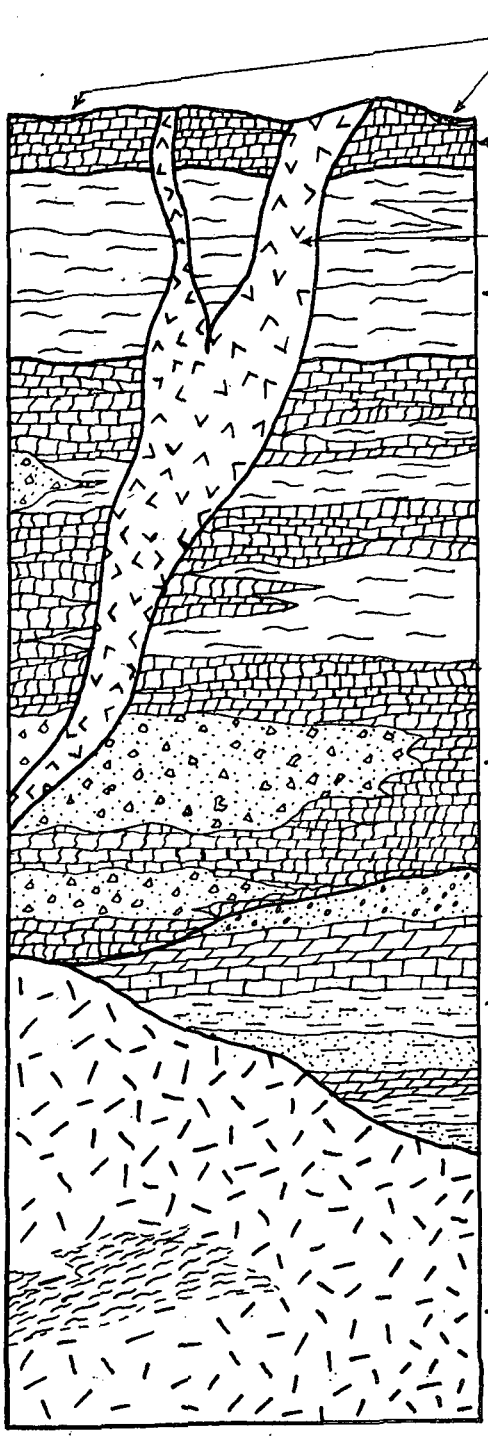

Quaternary gravel and alluvium: Consists primarily of clay, sand, and gravel derived from volcanic materials.

Tertiary intrusive bodies ranging in composition from gabbro to rhyolite throughout the Bonanza volcanic center. Those of the southwest Bonanza area are leucocratic, biotite aphanites.

Tertiary upper volcanic sequence (300-1000 ft thick where exposed): Includes hornblende biotite andesite, latite, and latite ash-flow tuff.

Tertiary Bonanza Formation (450-1000 ft thick): A sequence of biotite latite ash-flow tuffs consisting of at least eight ash flows.

Tertiary Rawley Formation (generally 1500-2000 ft thick): A complex sequence composed of many dissimilar volcanic lithologies including basalt, andesite, and latite flows, lapilli tuffs, water-laid tuffs, and breccias.

Paleozoic sedimentary rocks (≈1700 ft thick): Includes sandstone, dolomite, limestone, shale, and siltstone ranging in age from Cambrian to Permian.

Precambrian igneous and metamorphic rocks: Consisting of quartz monzonite, quartz diorite, amphibolite gneiss and schist.

Figure 7. Generalized columnar section showing the usual relationships among the major lithologic units of the southwest Bonanza area.

volcanic rocks. Most of the outcrops of Precambrian and Paleozoic rocks occur in the southern part of the southwest Bonanza area (plate 1). Quaternary deposits are concentrated along the major drainages and in the San Luis Valley, which lies south and east of the Bonanza area.

The geologic, petrographic, and spectral characteristics of the various lithologies are included in the following descriptions. The locations where the samples were taken are identified on Plate 1 (in pocket). Martin-Marietta Corporation provided infrared spectral reflectance measurements on selected rock samples using a Gier-Dunkle parabolic reflectometer. These reflectance data are available as part of the "First Year Summary Report" of the Bonanza Project (Gliozzi and others, 1970).

Precambrian Igneous and Metamorphic Rocks

Precambrian rocks crop out at seven locations in the southwest Bonanza area (plate 1). The largest outcrop lies along the eastern edge of the area near Graveyard Gulch. Other exposures of Precambrian igneous and metamorphic rocks occur along the southern edge of the volcanic pile in Findley Gulch and Saguache Valley. In these areas, the Quaternary deposits lap onto the edges of the low Precambrian outcrops. One large patch of Precambrian rocks in Sections 19 and 20, T 45 N, R 8 E is exposed through an erosional window in the volcanic rocks, and a smaller

outcrop can be seen through an erosional window in Sections 29 and 30, T 46 N, R 7 E. Yet another small outcrop of Precambrian rocks occurs in fault contact with the lower volcanic units in Section 30, T 46 N, R 7 E; and several small outcrops of quartz monzonite occur along various segments of the Columbia Creek Fault (Sec 30, T 46 N, R 8 E).

In all these outcrops, the field relationships indicate that the Tertiary volcanic flows were erupted directly onto an erosion surface cut on the Precambrian igneous and metamorphic rocks. No remnants of Paleozoic or Mesozoic sedimentary rocks were found in normal stratigraphic contact with the Precambrian rocks in these areas. Therefore, the Precambrian age of these units was inferred from their lithologic similarity to Precambrian rocks in nearby areas.

Precambrian rocks of the southwest Bonanza area include quartz monzonite, gneiss, quartz diorite and schist. The quartz monzonite is a pinkish, coarsely crystalline, porphyritic-phaneritic rock. The pink color is due to abundant, large, pink microcline crystals. Generally, only a small amount of muscovite and/or biotite is present. Previous workers in the Bonanza area have called this rock a granite, but thin section studies (appendix A, p. A-5) establish a plagioclase/microcline ratio characteristic of quartz monzonite (Williams, Turner and Gilbert, 1954).

The Precambrian gneiss is typically a finely crystalline biotite-hornblende gneiss. Plagioclase-rich bands alternate with the bands rich in finely crystalline mafic minerals. The hornblende crystals are well-aligned, giving the rock a nematoblastic texture. Width of banding varies from fine (1 mm) to medium (1 cm) and the rock is well-foliated parallel to banding. There is considerable variation in the percentage of minerals. In places, the gneiss grades into schist as the mafic constituents become more predominant.

Outcrops of Precambrian rocks in the northern part of the southwest Bonanza area are quartz monzonite, while outcrops further south are composed of gneiss and schist intruded by small quartz diorite bodies. In areas where the quartz diorite occurs with gneiss and schist, there are zones where they occur together as migmatite (PRC 10). The migmatite has some veins of quartz and oligoclase parallel to the foliation of the gneiss and schist and others cross-cutting the foliation and parallel to joints. This relationship demonstrates that the Precambrian quartz diorite intruded the gneiss and schist. In some areas a migmatite was formed as the leucocratic intrusive penetrated the gneiss and schist.

Infrared spectral measurements were made on samples of three of the Precambrian lithologies; the quartz diorite, the hornblende gneiss, and the migmatite (figs. 8 thru 11).

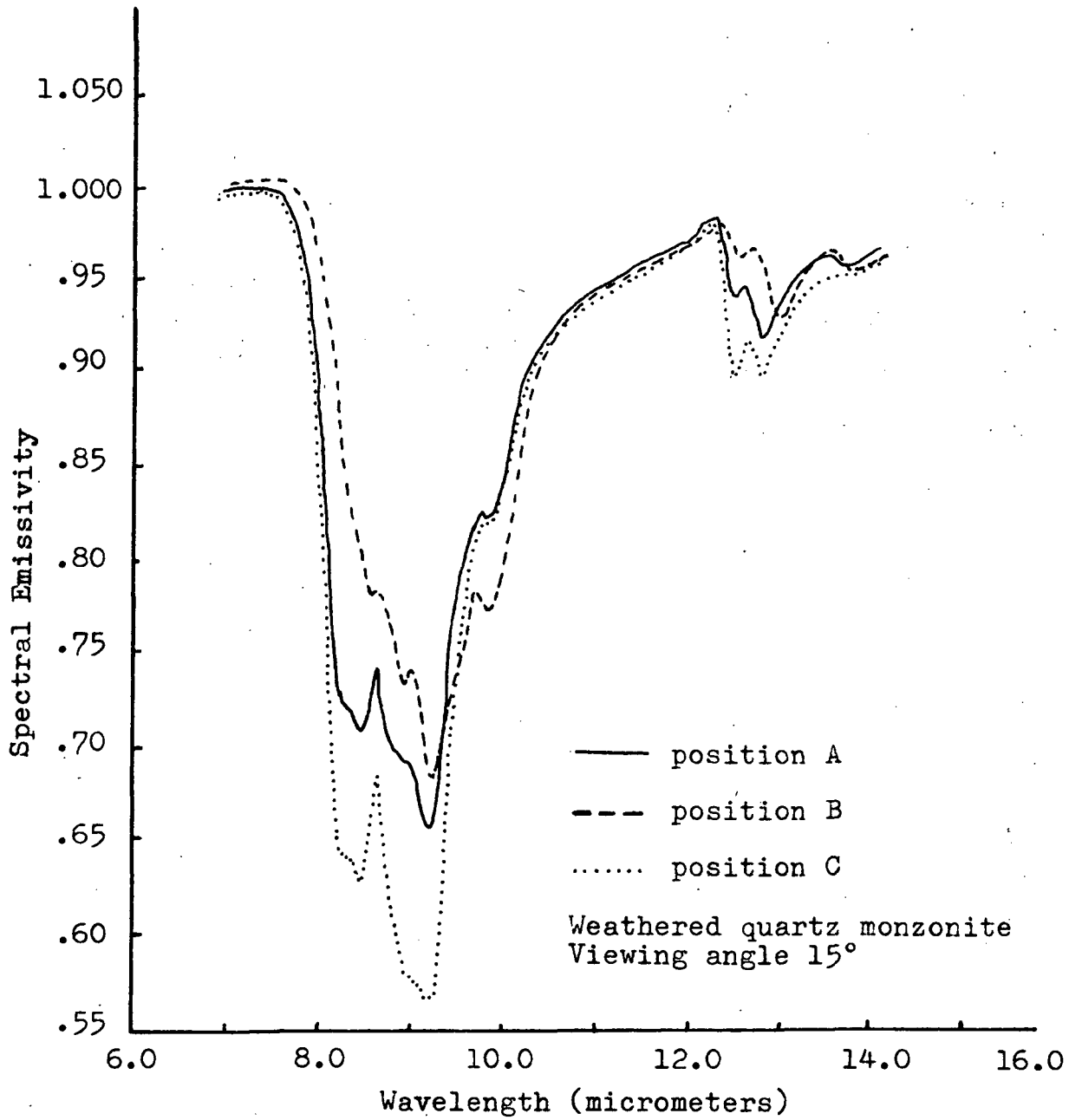

Figure 8. Variations in spectral emissivity with changing target point on a weathered sample (PRC-8). Fluctuations in spectral emissivity with target point are similar for other samples on both fresh and weathered surfaces. (After Gliozzi and others, 1970)

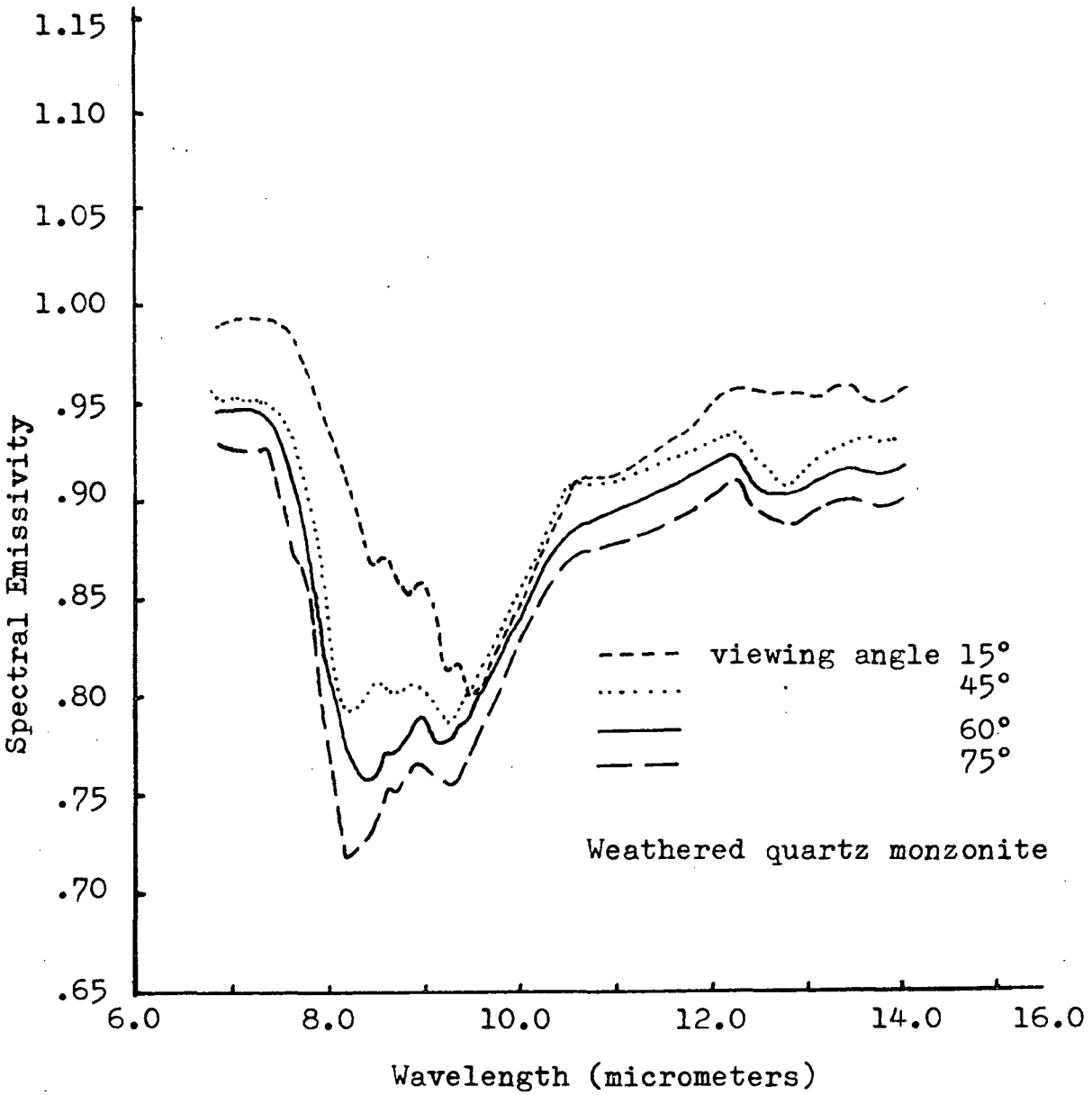

Figure 9. Variations in spectral emissivity with viewing angle on a weathered surface (PRC-8). Spectral emissivity changes with viewing angle are equally pronounced for other samples on weathered and freshly cut surfaces. (After Gliozzi and others, 1970)

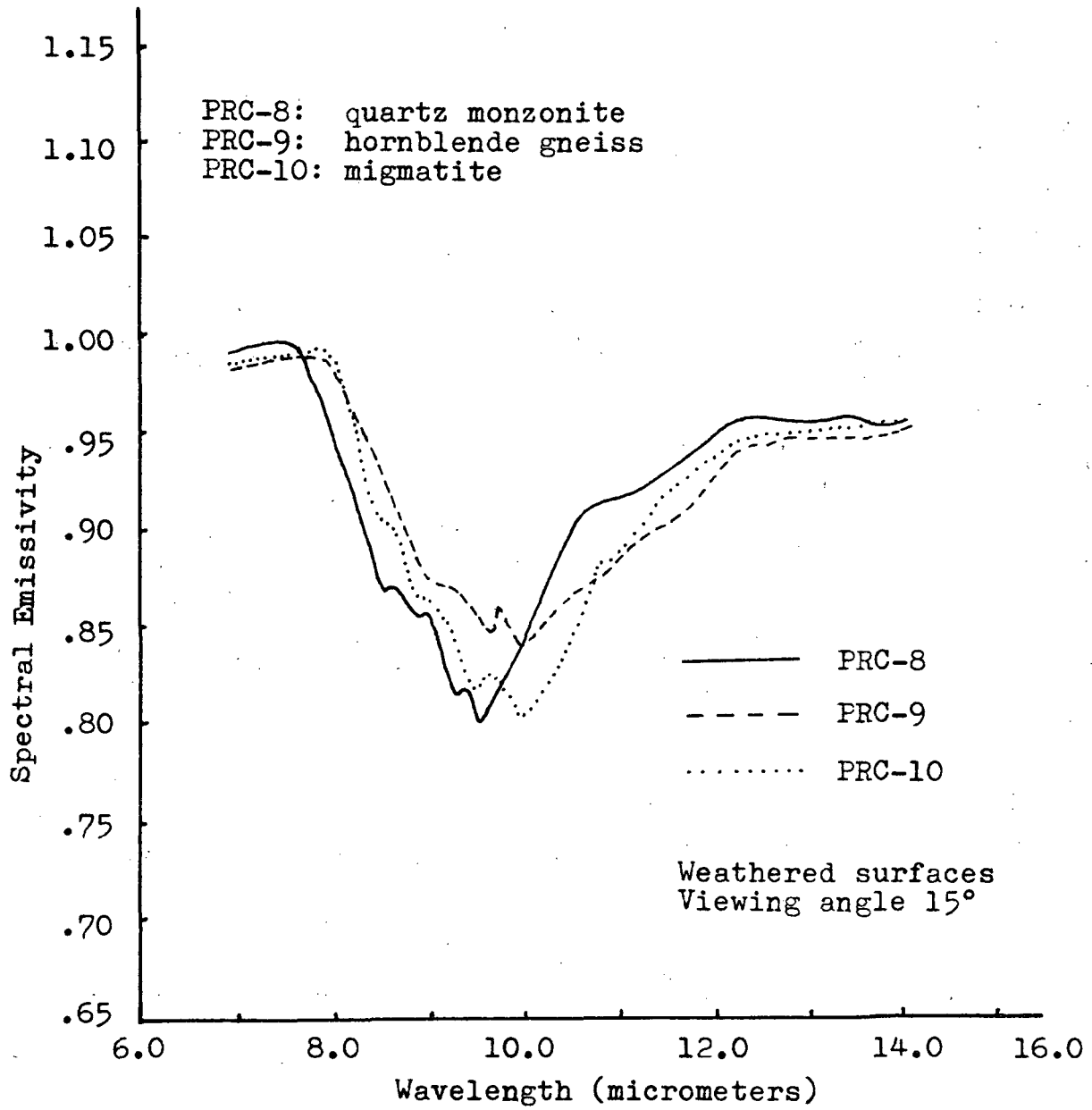

Figure 10. Comparison of spectral emissivity curves measured on weathered surfaces of three samples. Differences between these spectral emissivity curves are no greater than those between curves measured for single samples at various target points and viewing angles. (After Gliozzi and others, 1970)

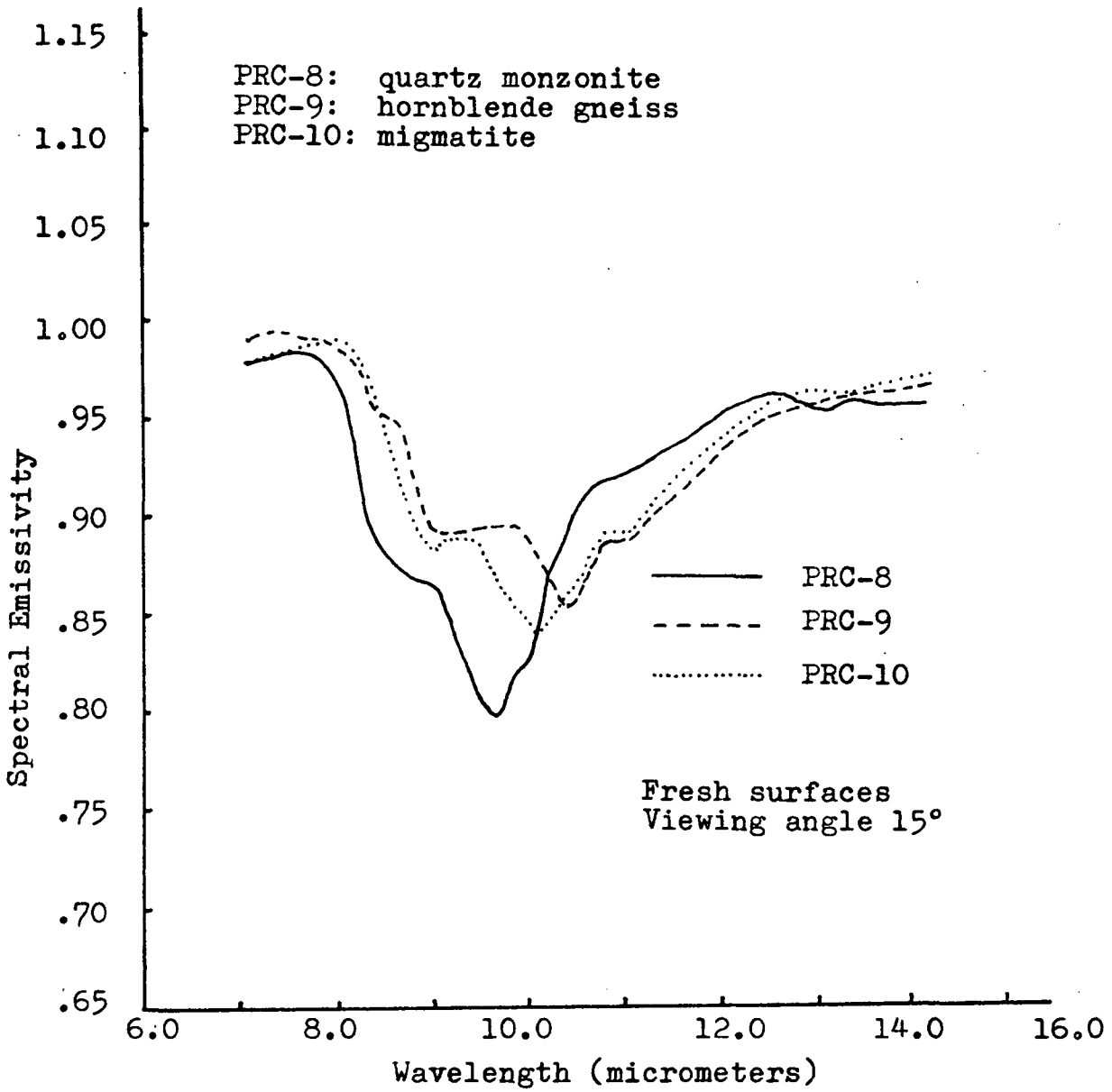

Figure 11. Comparison of spectral emissivity curves measured on freshly cut surfaces of three samples. Differences between these spectral emissivity curves are no greater than differences between curves measured for single samples at various target points and viewing angles. (After Gliozzi and others, 1970)

These measurements show a wide variation in spectral emissivity with viewing angle, texture, and location on the sample, for the three samples. The inhomogeneity of the samples, both in texture and composition, is probably the major cause of the observed variations. As a result, no reliable spectral signature could be established for any of the three rock types tested.

Paleozoic Sedimentary Rocks

Only two exposures of Paleozoic sedimentary rocks were found in the southwest Bonanza area (plate 1). Both are in the southeastern part of the area. The larger exposure lies in Sections 28, 32, and 33, T 46 N, R 8 E, and is partially covered by a patch of Quaternary gravels. The smaller outcrop is only a few hundred feet wide and lies along the east edge of Section 33, T 46 N, R 8 E. Both outcrops are remnants preserved in a syncline. The folded Paleozoic sedimentary units were covered by the Tertiary volcanic flows, and are now re-exposed in erosional windows through the volcanics.

Only shales and sandstones of Pennsylvanian age are exposed in the smaller outcrop, but the larger outcrop reveals a sequence of Cambrian, Ordovician, Devonian, Mississippian and Pennsylvanian units.

Since the Paleozoic sedimentary units occupy such a small portion of the southwest Bonanza area and were somewhat incidental to this study, only a brief description of these units will be given here. More complete discussions of the structure and stratigraphy of the Paleozoic units of the Kerber area are given by Burbank (1932) and Bridwell (1968).

The Sawatch Formation of Cambrian age, is the basal unit of the Paleozoic sequence in the southwest Bonanza area. It is hard, fine- to medium-grained quartz sandstone about 15 ft thick that stands out as a resistant ridge. It has been postulated that the sediments of the Sawatch Formation were deposited in a shallow seaway between two highlands (the Colorado Sag), which connected larger marine bodies to the east and west (Haun and Kent, 1965, p. 1783). The Sawatch Formation lies unconformably on Precambrian crystalline rocks, but has a gradational contact with the overlying Manitou Formation of early Ordovician age. The Manitou Formation consists of approximately 200 ft of thin-bedded, brown dolomite containing nodules of dark colored chert. This dolomite is also resistant to erosion. Other Ordovician units in the area are the Harding Formation and the Fremont Formation. The Harding Formation is a 75-ft-thick sequence of grey, fine- to coarse-grained, siliceously-cemented sandstones. It

disconformably overlies the Manitou Formation. The Fremont is a 260-ft-thick sequence of grey, massive dolomites interbedded with sandy dolomites. These lie conformably upon the Harding. The Fremont dolomite characteristically forms rough pit-and-cusp weathering surfaces.

All of the Ordovician units were deposited in the Colorado Sag, but sea-level apparently fluctuated considerably, and withdrew from the area for a time after deposition of the Manitou Formation.

No Silurian units are present in the area. If Silurian rocks were ever deposited, they were completely eroded away before the deposition of the Chaffee Formation of Devonian age.

The Chaffee Formation consists of the Parting Member (≈40 ft thick) and the Dyer Member (≈100 ft thick). The reddish colored Parting Member is made up of quartzites, shales, silts, and sandstones which lie unconformably on the Fremont Formation. Fossils indicate that it was deposited in late Devonian time. The Parting grades upward into the tan dolomite, limestone, and shale of the Dyer Member. Both appear to have been deposited in a shallow sea that transgressed eastward across the Colorado Sag (Haun and Kent, 1965, p. 1785).

As the sea continued to deepen during the Mississippian period, the Leadville Formation was deposited. This fine-grained, blue-grey limestone is about 250 ft thick in the

southwest Bonanza area. The Leadville Formation is conformable with the underlying Dyer Member and unconformable with the overlying Kerber Formation. The irregular upper surface of the Leadville Formation is the result of a long period of erosion that occurred after the area was uplifted in late Mississippian time.

The Kerber Formation, which is named for exposures along Kerber Creek, is a sequence of coarse sandstones and carbonaceous shales of Pennsylvanian age. Its contact with the overlying Minturn Formation is not exposed in the southwest Bonanza area, so the contact relationship and thicknesses were not determined. In nearby areas, the Kerber is conformable with the red-beds of the Minturn Formation (Bridwell, 1968, p. 24). Fossil evidence indicates the red sandstone-shale sequence of the Minturn was deposited during the latter part of the Pennsylvanian period.

Incomplete exposure and possible repeated sections due to faulting make it impossible to determine accurately the thickness of the Pennsylvanian-Permian section in the Kerber area, but it appears to be at least 1,000 ft thick. The Kerber Formation is at least 200 ft thick, and more than 800 ft of Minturn red-beds are exposed in the area.

The Kerber and Minturn Formations were deposited in a narrow, northwest-trending trough lying between two elongate highlands (Knepper and Marrs, 1971, p. 259).

The observed sequence of sedimentary rocks resulted from combined fluvial and marine deposition in this narrow trough.

In order to simplify the map presentation of the Paleozoic units in the southwest Bonanza area, they have been grouped together into two map units. These units were designated the "lower Paleozoic" sequence and "upper Paleozoic" sequence and include Cambrian through Mississippian units and Pennsylvanian units respectively.

Detailed thermal infrared spectral reflectance measurements and petrographic studies were made on only one of the Paleozoic lithologies, the dolomite of the Manitou Formation (this paper, p. 129-130, and p. 225). The infrared spectral measurements indicate that there is a good chance for discrimination of the Manitou dolomite in the infrared region because the rock is sufficiently homogeneous to yield a fairly reliable spectral signature. Field measurements on other Paleozoic lithologies indicated that reliable spectra could not be readily established, so the Manitou was chosen as the test lithology because it was apparent that it offered the best possibility for discrimination from aircraft altitudes.

Mesozoic Lithologies

No Mesozoic formations occur in the southwest Bonanza area. The only unit in the area that might be considered Mesozoic in age is a tectonic breccia (M_{tb}) that is exposed in several outcrops near the junction of Little Kerber Creek with Kerber Creek (Sec 27, T 46 N, R 8 E). Only one of these outcrops is within the map area. It occurs on the easternmost point of the ridge separating the two drainages. Figure 12 is a photograph of this outcrop showing the distinctive weathering pattern of the breccia.

The tectonic breccia is composed largely of blocks and smaller particles of the Precambrian quartz monzonite previously described. However, it also contains a few blocks of Paleozoic sedimentary rocks. Many of the rock fragments are rounded and the interstices between them filled with finer rock particles. The entire rock mass has been so tightly compressed that the larger rock fragments are bound within the finer material, and even the fine material is difficult to scrape away.

The outcrops of the tectonic breccia are in an area where considerable thrusting took place within the Precambrian-Paleozoic sequence, and the breccia is believed to have formed along the sole of one of these thrusts. The grinding action has caused the rocks to become broken,

Figure 12. Tectonic breccia at the junction of Little Kerber and Kerber creeks. Note the rounding of the large blocks, the extreme variation in the size of rock fragments, and the steepness of the slope which reflects, in part, the reconsolidation of the mass.

rounded, and mixed together. The jumble of rock material was then reconsolidated under the tremendous pressure of the overthrust plate. The origin of the breccia is thought to be unrelated to the volcanic activity because its exposures are limited to areas of known thrusting, and because there are no apparent interrelationships between the volcanic rocks and the breccia. The contact between the breccia and the overlying volcanic unit is an erosional one and the breccia shows very little effect of heating from the volcanic units in contact with it.

Two theories have been advanced to explain the origin of the tectonic breccia. Burbank (1932, p. 41) interpreted the breccia outcrops as klippen representing the sole of a thrust plate which moved northward along a shallow-dipping thrust plane. Dissimilarities between the dip-angles of the thrust planes and overall characteristics of the breccia outcrops and the Kerber Thrust front led Burbank to conclude that the breccia klippen are remnants of a thrust older than the Kerber Thrust. Bridwell (1968) interpreted the breccia outcrops as remnants of a land-slide caught beneath the advancing front of the Kerber Thrust. These interpretations, the supporting evidence for each, and my own observations are discussed in greater detail in the "structural geology" section of this report.

A maximum age for tectonic breccia is late Pennsylvanian because boulders of the Minturn Formation are the youngest rocks found in the breccia. The overlying Oligocene volcanic rocks give a minimum age limit for the breccia by their stratigraphic relationship and the fact that there are no volcanic rock fragments in the breccia. However, a better estimate for the age of the breccia might be late Cretaceous or early Tertiary if one accepts the evidence presented by workers in adjacent areas who feel the thrusting is associated with a second stage of the Laramide Orogeny (Bridwell, 1968; Burbank and Goddard, 1937; Karig, 1963).

Tertiary Volcanic Rocks

The Oligocene volcanic rocks of the Bonanza area constitute an eruptive sequence typical of south-central Colorado (Turner and Verhoogan, 1960). The sequence is divisible into three major groups: a basal group of lavas and breccias of intermediate composition, a middle group of silicic ash-flow tuffs, and an upper group of intertongueing silicic and intermediate flows. This sequence parallels those in the San Juan volcanic field to the southwest (Steven and Epis, 1968) and the Thirtynine-mile field to the northeast (Epis and Chapin, 1968).

According to Turner and Verhoogen (1960, p. 275) this pattern of volcanism is characteristic of an orogenic area immediately following uplift of a folded geosynclinal mass. The Rocky Mountains can hardly be considered a "typical" geosynclinal area, but the widespread volcanism in Oligocene time did follow a major period of uplift. In a more recent discussion of andesitic volcanism, McBirney (1969, p. 506) suggests that such sequences are characteristic of areas of continental tectonic uplift, especially epeirogenic uplift. He feels that the magma producing this association must have resulted from partial melting of crustal materials.

It appears that there are two processes which could have contributed to increasing silica content of the erupted magmas with time. The magma might become more silicic by progressively assimilating silicic material from the chamber walls, or the mafic constituents of the melt might crystallize and settle toward the bottom of the magma chamber. Eruptions from the upper part of the chamber would become progressively more silicic as the process continued. The formation of a zoned magma would also explain the eruption of a late bi-modal sequence associated with collapse of the chamber roof. New conduits opening as a result of fracturing and collapse would tap the magma chamber at different levels allowing magma from two or more compositional zones to be erupted simultaneously.

Rawley Formation (T_r): The lower third of the volcanic sequence in the southwest Bonanza area consists of a complex group of basalt, andesite, and latite flows, lapilli tuffs, water-laid tuffs, and breccias which were erupted from several centers in and around the Bonanza area. The basal portion of this lower group is largely composed of basalt and andesite flows and laharic breccias.

The flow rocks are typically grey to black hornblende biotite basalts and andesites with fine and medium phenocrysts in an aphanitic groundmass (fig. 13). Mineralogically, these lower flows are relatively simple, but show a tendency toward more complexity upward through the sequence. For example, the lowermost flows contain a single variety of plagioclase (appendix A, p. A-12), while later flows exhibit two or more generations of plagioclase phenocrysts (appendix A, p. A-13). Presumably, these trends reflect the changes in temperature and pressure in the magma chamber. As volcanic activity continued, the temperature-pressure changes coupled with the changing mineralogical composition of the melt caused late-formed crystals to be of different composition and character than those first formed.

The laharic breccias are most abundant in the southern part of the area and are usually white to tan in color with numerous dark lapilli and blocks in a light-colored, ashy matrix. The blocks and lapilli are mostly fragments

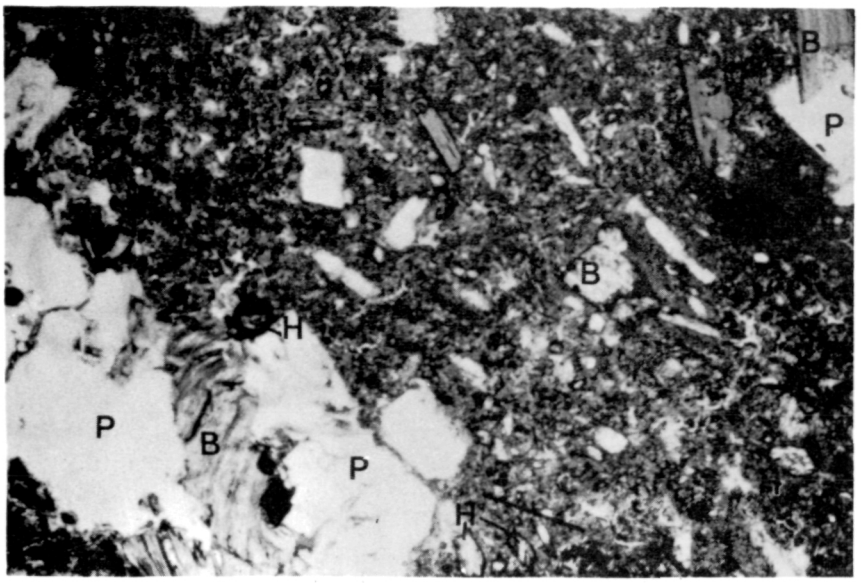

Scale 1 mm

Figure 13. Photomicrograph of hornblende biotite andesite of the lower Rawley Formation (PRC-16, p. A-11, plane polarized light, X30). Note the deformed biotite crystal. (P=plagioclase, B=biotite, H=hornblende)

Figure 14. Laharic breccia of the Rawley Formation exposed along Little Kerber Creek. Bedrock outcrops in the foreground and on the horizon show knobby character like that of granite. Normal slopes between prominant outcrops develop a sandy, well-drained soil which supports grass and cacti. The large andesitic blocks in the right foreground are 2-3 ft in diam.

of andesite and latite, although a few fragments of Precambrian igneous and metamorphic rocks occur in some of the lahars. The matrix of the lahars is mostly volcanic ash and pumice. The texture and composition of these units attest to their origin as mud flows. The lateral extent of individual lahars is quite limited and thicknesses vary erratically. Most outcrops show thicknesses on the order of 10 or 20 ft, but a few outcrops occur where the total thickness of the lahars exceeds 100 ft. Imbrication of the included rock fragments is extremely rare and no definite flow pattern can be established. Apparently, the lahars were cool when emplaced, because there is no evidence of baking or welding, and they are poorly consolidated. Outcrops are easily eroded and, often, poorly exposed. However, in larger areas of outcrop, the weathered laharic breccias form a rounded, knobby topography similar to granitic igneous rocks (fig. 14) and are impossible to distinguish from adjacent exposures of quartz monzonite on aerial photographs.

The upper part of the lower volcanic group is largely made up of grey and red-brown andesite and latite flows, andesitic autobreccias, and lapilli tuffs. The flow units are grey hornblende andesites and red-brown, hornblende biotite latites which commonly exhibit two or three distinct sizes of plagioclase phenocrysts and other mineralogical complexities. Some show well-developed

columnar jointing or platy foliation (figs. 15 and 16). The autobreccias are similar in composition to the flow rocks. They probably have a very similar origin, but have been forcefully remobilized after partially solidifying.

Water-laid tuffs are locally present throughout the sequence. They are white to tan in color and are composed of ash, pumice, and crystal fragments. These, along with the ash in the laharic breccias are evidence of some explosive volcanism which was contemporaneous with the dominant flow-eruptions. Sorting and graded bedding are common in the water-laid tuffs.

The lower group of flows attains a total thickness of more than 2,500 ft in parts of the Bonanza area. Areas where the total thickness of the lower flows can be measured or estimated are rare, but the average thickness is on the order of 1,500 to 2,000 ft. The minimum thickness of the Rawley Formation is believed to occur near the mouth of Tennessee Gulch where the Paleozoic sedimentary rocks are separated from the middle ash-flow sequence by a few tens of feet of Rawley flows. The thicknesses of the lower flow sequence is largely controlled by the topographic relief of the paleo surface which was inundated by the Rawley flows. The extremely rapid lateral variations in thickness which occur in the Rawley Formation are

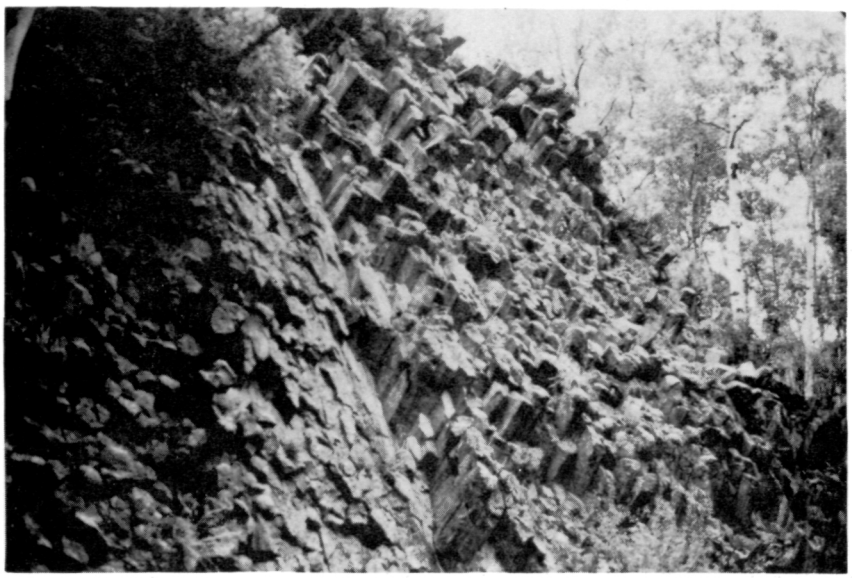

Figure 15. Well-developed columnar jointing in andesite of the Rawley Formation near Sawlog Gulch trail. Columns are approximately 6-8 in. in diam.

Figure 16. Platy foliation in andesite of the Rawley Formation near Lucky Boy Gulch.

exemplified by the fact that the Bear Creek Mining Co. (Cook, 1960) drilled nearly 2,000 ft into lavas of the Rawley Formation at a location just 1 mile north of Tennessee Gulch where the minimum Rawley thickness was observed.

Dips in the Rawley Formation and the overlying units suggest that they formed a large shield volcano centered in the Bonanza area. The wide distribution of overlying flows and lack of Precambrian lithic fragments in the upper flows of the middle group indicate that the pre-existing topography was nearly covered by the Rawley flows and the lower flows of the middle ash-flow group.

Many of the flows of the Rawley Formation are local in extent. The flows were erupted from numerous separate vents (which are now concealed) and flowed into the area from different directions. This resulted in a very complex sequence that exhibits rapid lithologic changes, both horizontally and vertically. Accordingly, it is often impossible to correlate basal units from one place to another in the structurally complex Bonanza area. Cook (1960) reported that it was impossible to reliably correlate the units of the basal sequence between drill holes less than 1 mile apart.

The Rawley Formation, as defined in this report, is equivalent in age and lithology to the Rawley andesite and Hayden Peak latite mapped by Burbank (1932), Mayhew

(1969), Perry (1971), and Bruns and others (1971) in adjacent areas. Bruns and others (1971) have established the correlation of the Rawley andesite with rocks mapped as lower Conejos Formation in the San Juan field. The ages for the Rawley andesite (33.4 m.y. and 34.2 m.y.) reported by Lipman and others (1970) support this correlation.

Both the Rawley and Conejos have been formally accepted as formations by the Geologic Names Committee of the U.S. Geologic Survey, but the term, Conejos, has been applied to many rock units in the 30-35 m.y. age range. Thus, the more restricted name, Rawley, which was defined by Burbank (1932) for the lower sequence of volcanics in the Bonanza area, and has since been formally accepted as a formation name, will be used in this report.

The definition of the Rawley Formation in this report differs from that of Burbank (1932) and Mayhew (1969) only because I have included within the Rawley Formation latite flows that may be equivalent to the "Hayden Peak latite" which was mapped as a separate unit by Burbank and Mayhew.

Bonanza Formation (T_b): The middle group of volcanic rocks in the southwest Bonanza area consists almost entirely of latite ash-flow tuffs. These ash flows were erupted onto the eroded surface of the intermediate volcanic rocks of the Rawley Formation. The lower ash flows filled the valleys

and flooded the topography. Then, the upper ash flows spread out from the source area in broad sheets. But even these broad sheets are not continuous. At some locations in the southwest part of the area, the Rawley Formation is directly overlain by flows of the upper volcanic sequence. These localities probably represent high topography at the time the Bonanza flows were erupted. These high areas may never have been covered by the Bonanza ash flows or the Bonanza flows may have been eroded away prior to eruption of the upper flow sequence. Nearby outcrops of ash-flow units typical of the lower Bonanza sequence suggest that the latter is probably the case. In the central part of the district, the ash-flow sequence attains a thickness of more than 1,000 ft and the units are welded together so that individual flows are texturally indistinguishable. The flows normally thin to less than 500 ft in the southern part of the map area and are separated by cooling breaks into distinct cooling units (fig. 17). Overall, the middle ash-flow sequence is remarkably uniform in composition and character. Its wide distribution, relatively rapid emplacement, and distinct character make it invaluable as a geologic marker and structural datum. In addition, minor textural and compositional variations within the ash flows reflect the cooling and eruptive history of the sequence.

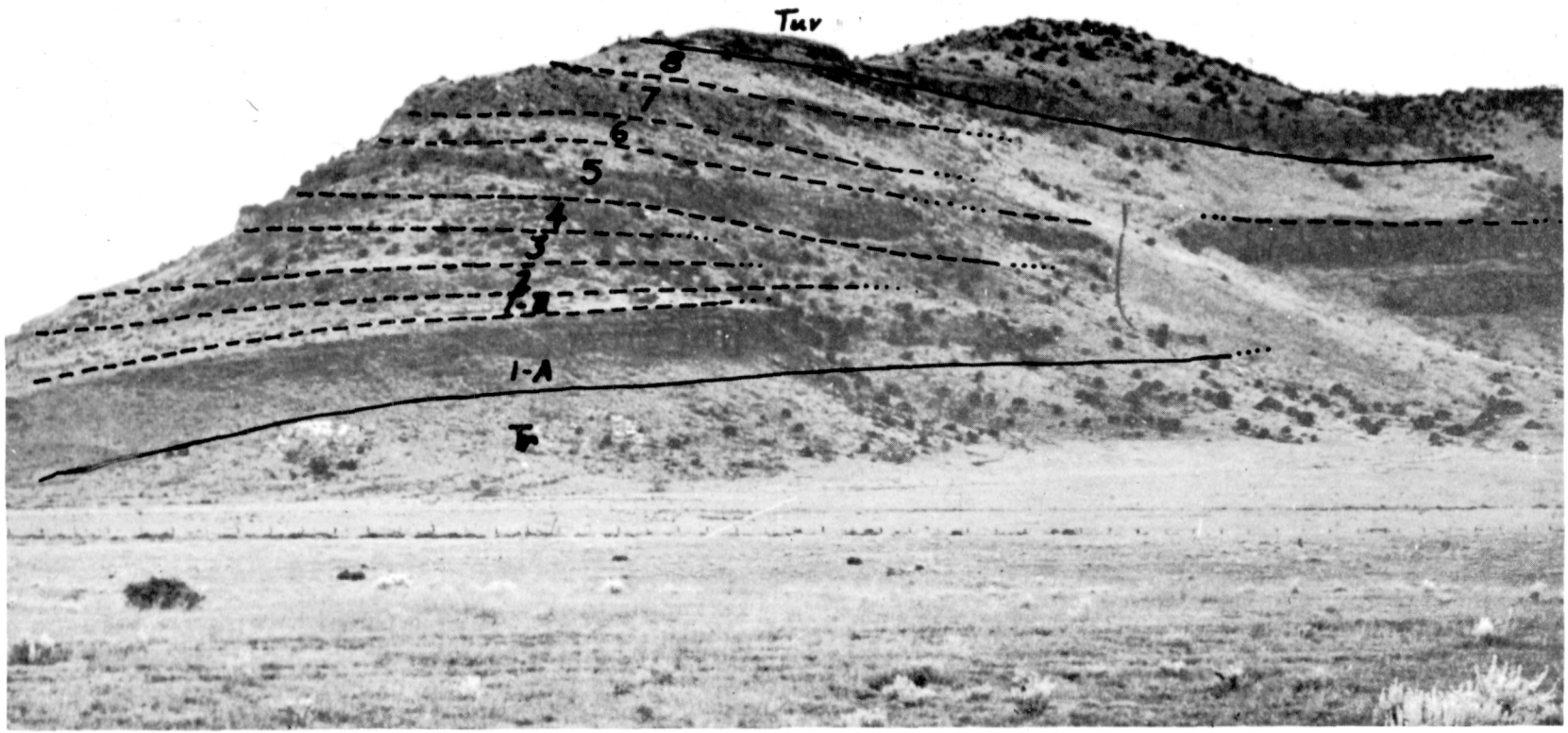

Figure 17. Photograph of Bonanza Formation exposed on Findley Ridge. Note: Solid lines represent the upper and lower contacts of the Bonanza Formation; dashed lines are boundaries of mineralogical subdivisions. The Bonanza Formation is underlain by a volcanic conglomerate of the Rawley Formation (T_r) and capped by a latite flow of the upper volcanic sequence (T_{uv}). Note the five distinct topographic breaks (above units 1-A, 2, 4, 5, and 7) that reflect the more significant cooling breaks in the sequence.

Mineralogically the Bonanza Formation is made up of biotite latite ash flows that exhibit distinct platy foliation parallel to compaction layering (fig. 18). Purplish-grey andesitic lithic fragments with diameters ranging from 1 mm to 250 mm are common throughout the ash-flow sequence, but are most abundant in the lower flows. Other characteristics of the ash flows are the large (0.5 mm to 2 mm in diam), hexagonal biotite flakes that are usually a rusty, red-brown color and the wavey lenses of compacted pumice which appear as wisps of white in the red-brown latite (figs. 19 and 20). These compacted pumice fragments weather easily and enhance the eutaxitic structure apparent in most outcrops.

The Bonanza ash-flow tuffs were first mapped and described by Patton (1915) as latitic lava flows with a prominent flow-texture and inclusions of andesite. He includes photographs of hand specimens and thin sections in his report which show the compacted pumice lapilli and other features characteristic of the Bonanza ash-flow sequence (1915, p. 34). Burbank (1932) also mapped the ash flows as the Bonanza latite, but Mayhew (1969) recognized the unit as an ash-flow sequence and suggested that the name be changed to the Bonanza tuff. This usage has since been adopted by others (Bruns, 1971; Bruns and others, 1971; Knepper and Marrs, 1971). The U.S. Geological Survey has

Figure 18. Outcrop of Bonanza Formation showing typical foliation parallel to compaction planes. Outcrop is located on the north side of Highway 114 approximately 7 miles west of Saguache (NE¼, Sec 24, T 45 N, R 6 E).

Figure 19. Altered Bonanza latite at the Cocomonga mine (after Burbank, 1932, plate 7). Note the striking flow structure emphasized by the elongation of the white, compacted pumice fragments.

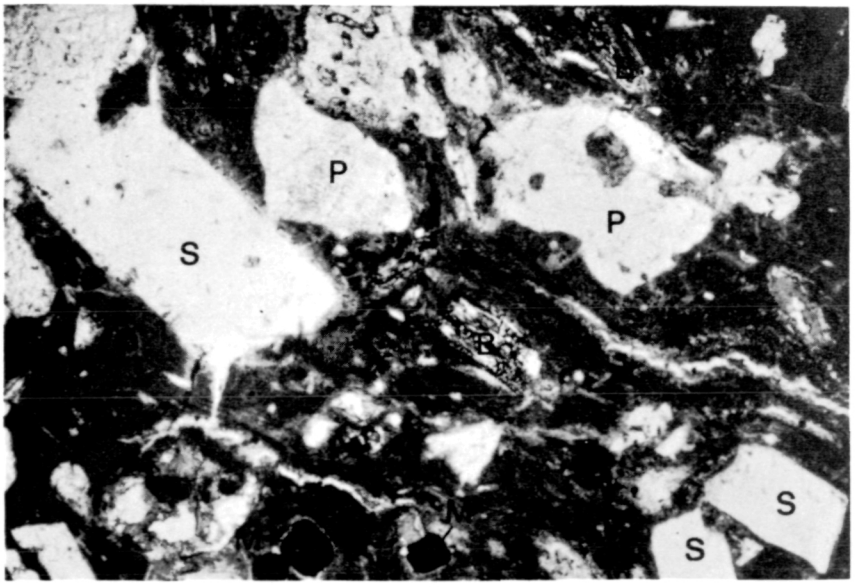

1 mm
Scale

Figure 20. Photomicrograph of biotite latite ash-flow tuff of the Bonanza Formation. (PRC-15, p. A-21, plane polarized light, X30, P=plagioclase, S=sanidine, B=biotite, M=magnetite). Welding and compaction of vitroclastic matrix are evident.

since accepted "Bonanza" as a formal formation name (McGlauphlin, 1972, personal communication). In this report the middle ash-flow sequence will be called the Bonanza Formation.

An excellent exposure of the Bonanza Formation (Sec 28, T 45 N, R 7 E) occurs at the south end of the ridge west of Findley Gulch (hereafter called Findley Ridge). This exposure can be seen from State Highway 114 between Saguache and Gunnison, and can be easily reached from the Findley Gulch road (fig. 21). The Findley Ridge exposure presents the most complete and accessible section of the Bonanza Formation seen in the Bonanza area. Therefore, I propose that the exposed section be designated a "principal reference section" for the Bonanza Formation.

Figure 17 is a photograph of the Bonanza Formation on Findley Ridge. From the photograph it is apparent that the Bonanza can be separated into at least five units on the basis of topographically-expressed cooling breaks. However, detailed inspection of the rock outcrops and petrographic analysis (appendix A, p. A-22 - A-37) reveal that the section should be divided into at least eight units on the basis of mineralogy. Figure 22 shows the relationship between the topography and these mineralogical subdivisions at the point where the section was

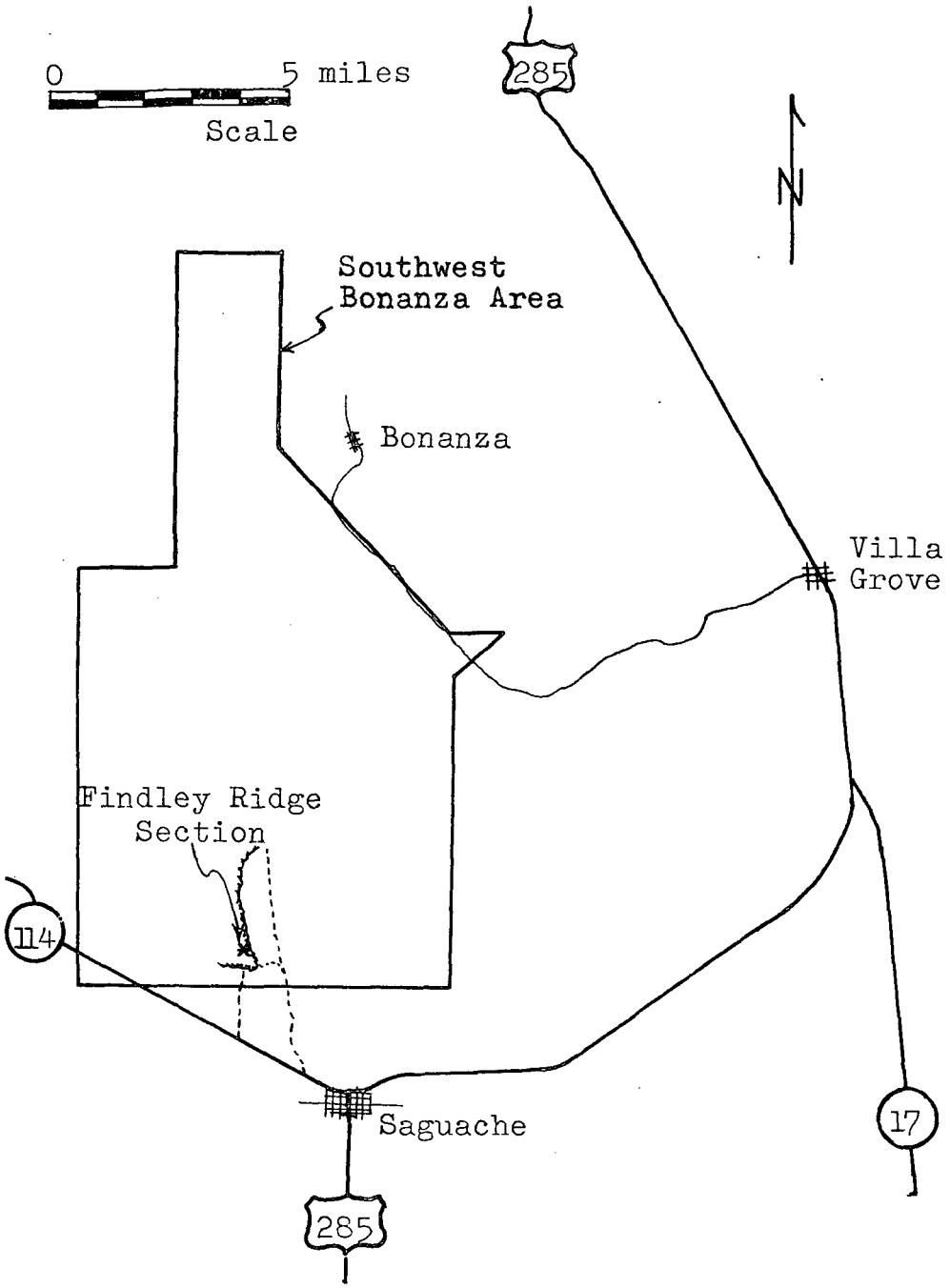

Figure 21. Index map showing the location of the proposed principal reference section for the Bonanza Formation.

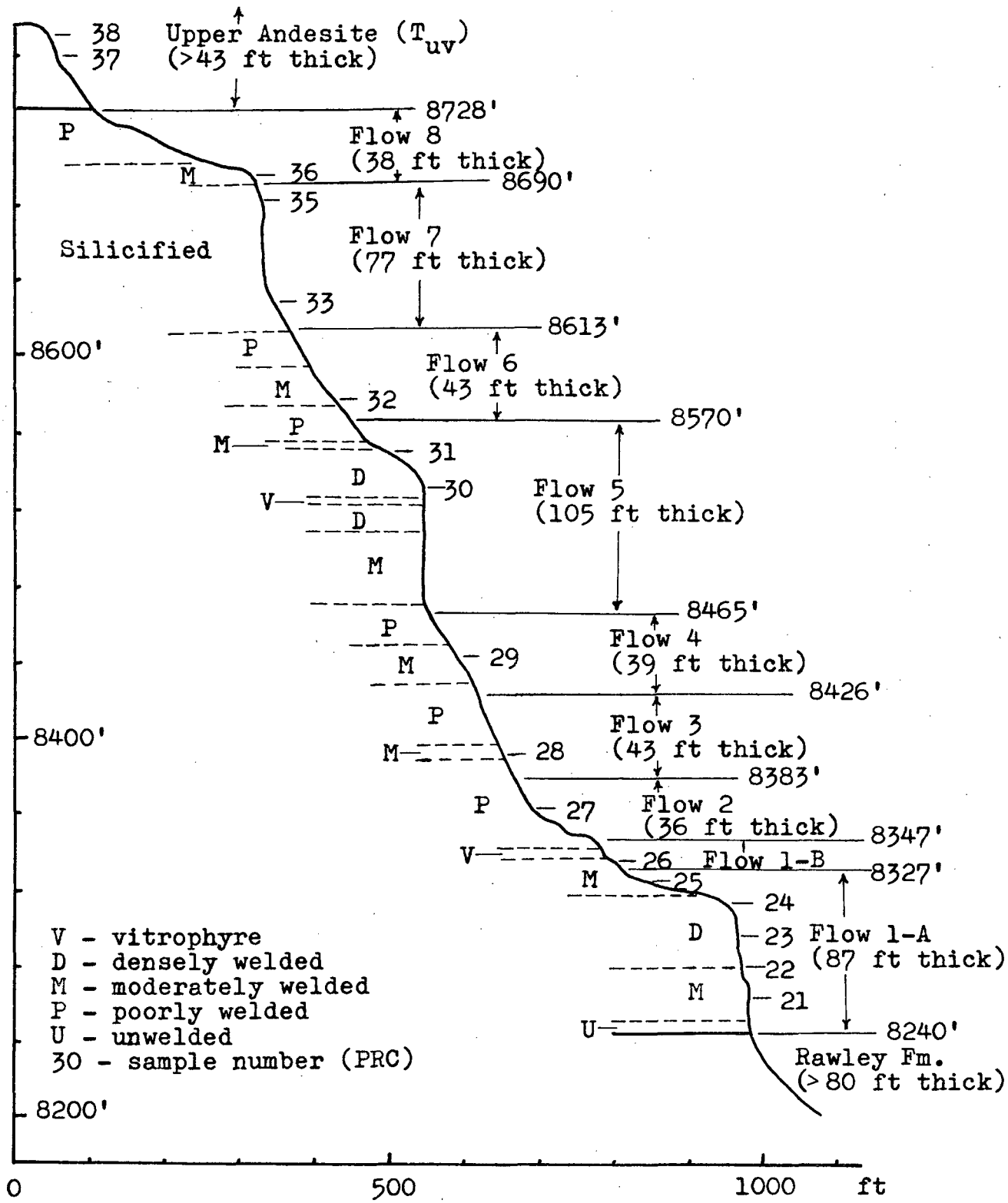

Figure 22. Measured section of Bonanza Formation on Findley Ridge. Elevations (amsl) are referenced to bench mark (8770 ft). Vertical exaggeration is 2½.

measured. The major topographic breaks correspond roughly to the unit boundaries because the ash-flow units are vertically zoned with respect to welding intensity and exhibit corresponding changes in their resistance to erosion. The usual pattern of welding zonation for a particular flow is a central, densely welded zone between upper and lower, moderately welded zones that grade into poorly welded zones toward the top and bottom of the flow. Variations of this pattern are dependent on the thickness and temperature of the individual flows and the time lapses between flow eruptions. Some flows were not hot enough nor thick enough to produce a highly welded or moderately welded zone. Others have had the upper unwelded zone removed by erosion prior to emplacement of the succeeding flow. Some flows were erupted in such a rapid sequence that they welded together as a compound cooling unit, while others had sufficient time to develop the normal zonation of a simple cooling unit.

Considerable textural and mineralogical detail is evident in the outcrops of Bonanza Formation exposed along Findley Ridge. Megascopic examination of these outcrops revealed several general trends, but thin section analysis of a suite of fifteen samples from the Findley Ridge section provided considerably more detail regarding vertical variations in texture and mineralogy.

Some of the textural trends appear to be related to minor differences in the eruptive mechanisms which produced the individual ash flows while other textural trends reflect the cooling histories of the different flows. The mineralogical variations observed in the Bonanza ash flows are largely the result of changing composition of the source magma as it evolved in response to pressure and temperature change and to the removal of material by eruption.

Similarities among the various flows of the Bonanza sequence and the continuity of certain mineralogical trends suggest a definite relationship among the various flows, while second-order variations in the textures and mineralogies of the ash-flow sequence serve as indicators of particular interrelationships. For example, compound cooling units, variations in type and quantity of lithic fragments, and rhythmic patterns in flow mineralogies aid in estimating time lapses between consecutive eruptions and in determining sources and eruptive mechanisms for individual flows.

Many of the observed lithologic variations, particularly those dependent on cooling history, are local in extent and have little significance with regard to regional patterns. Others reflect conditions that influence an entire flow or flow sequence.

A volcanic conglomerate of the Rawley Formation (>80 ft thick) crops out along the base of Findley Ridge. This conglomerate is mostly composed of white volcanic ash and coarse sand; but pebbles, cobbles, and even boulders of volcanic material are also common. The composition of this unit is similar to many of the laharic breccias of the Rawley Formation, but much of the coarser material is partially rounded and coarse stratification and graded bedding are present, indicating transport by water. The conglomerate is poorly consolidated and erodes easily. Consequently, it is poorly exposed on the relatively gentle slope along the base of Findley Ridge. The sparsely exposed stratification gives low dips (4-9°) to the southwest, and the contact between the conglomerate and the overlying ash-flow tuff is slightly unconformable. Only 80 ft of the Rawley conglomerate was exposed at the measured section, but northward along the ridge, the Rawley-Bonanza contact rises until it is approximately 200 ft up the ridge slope.

The basal unit of the Bonanza Formation (1-A, fig. 22) is 87 ft thick and composed of moderately- to densely welded latite ash-flow tuff which appears red-brown in its prominant outcrop. The thin, poorly welded

and poorly exposed zone at the base of unit 1-A is light-colored and punky. Numerous andesitic lithic fragments give the lower unwelded zone an appearance similar to the underlying volcanic conglomerate. Closer inspection reveals the flattened pumice fragments and a pyroclastic texture which distinguish it as an ash-flow tuff.

The more densely welded middle and upper portion of unit 1-A stands out as a prominent cliff and exhibits large-scale columnar jointing (fig. 17). Platy foliation parallel to compaction layering is common. Flattened pumice fragments weather easily from the exposed surfaces and give the rock a vesicular appearance. Biotite, which is abundant as golden-brown, hexagonal plates, is the chief mafic mineral. Angular, andesitic lithic fragments (up to 1 ft in diam) are abundant throughout the flow, but decrease in abundance upward. In the densely welded part of the flow, the grey lithic fragments have a slight purplish hue.

Thin section analysis (appendix A, p. A-22 - A-26) show abundant fine to medium, subhedral biotite, sanidine, and plagioclase crystals in a matrix of pumice and brown glass. Considerable compaction is evidenced by the flattened pumice fragments and glass shards in the matrix. Many of the crystals are broken or bent. Most lithic

fragments exhibit no evidence of exposure to weathering. The lithic fragments represent many different flows and some intrusive rocks. All these features are characteristic of ash flows. The material was erupted with such violence that many of the crystal fragments were broken and fragments of the chamber and vent walls were torn off and incorporated into the flow. As the extremely fluid material rushed away from the vent, the lithic fragments sank and were concentrated near the base of the flow in spite of the extreme turbulence. The superheated melt cooled rapidly as particles and fluid globules forming ash, glass shards, and matrix glass. The mass was still hot when it came to rest and the central portion welded together as it cooled and compacted.

The mineralogy of flow 1-A suggests the source magma was relatively mafic. Augite is present in minor amounts. The sanidine/plagioclase ratio is low and calcic andesine is common. Zoned plagioclase crystals are most calcic at the core, indicating that the source magma was becoming more silicic with time.

There is a slight decrease in welding intensity near the top of flow 1-A which results in a break in slope and a covered zone above the cliff-forming central portion of the flow. Flow 1-A may have a thin, poorly welded upper zone; but it and the contact with the overlying flow (1-B) is covered.

Flow 1-B (20 ft thick) crops out as a narrow vitrophyre and highly welded zone which together form a small cliff. Petrologically and mineralogically flow 1-B is practically identical to flow 1-A; therefore, it was not designated as a mineralogically independent unit. 1-B was distinguished from flow 1-A on the basis of the marked increase in welding intensity and a noticeable increase in the abundance of lithic fragments. Some of the lithic fragments in flow 1-B are latite ash-flow tuff (similar to flow 1-A) rather than andesite. These lithic fragments demonstrate that 1-B was a separate eruption which tore through or flowed across a lithified ash-flow sequence. The compositional similarities between flows 1-A and 1-B are strong evidence that they were erupted from the same source.

The extreme welding observed in ash flow 1-B seems unusual when one considers the meager thickness of the flow in the measured section (≈20 ft). However, the flow thickens considerably to the south, and appears to pinch out completely just north of the measured section. Thus, flow 1-B may not be as thin as it first appears. Rather, the major direction from which flow 1-B entered the area may have been slightly different than that of flow 1-A, with the result that the Findley Ridge section is very near the north edge of flow 1-B.

Ash flow 2 (36 ft thick) is a poorly- to moderately welded, light-grey, biotite latite ash-flow tuff which occupies the lower part of a covered slope. Further south along Findley Ridge it becomes more densely welded and stands out as a small cliff in some places. To the north, the outcrop is buried under talus. The flow apparently pinches out or merges with adjacent flows in the buried area, because it is indistinguishable in the massive outcrops north of the talus-covered slope.

The composition of flow 2 is considerably different from that of flow 1. The andesitic lithic fragments are noticeably smaller and fewer. The crystals constitute a smaller portion of the whole rock, but this may reflect only the lesser degree of compaction. The sanidine/plagioclase ratio is slightly higher than that of flow 1 (6/7 vs 1/3), and augite is absent. The plagioclase composition, the hexagonal biotite flakes, and the purple-grey andesitic lithic fragments are remarkably similar to those of flow 1.

The similarities between flow 1 and flow 2 demonstrate that they have a similar origin and are probably products of the same source material. The difference in abundance of lithics suggests a slightly different mode of eruption (i.e. less violent or through an already open vent). The mineralogical differences indicate that the

magma had changed composition since the earlier eruptions, or that flow 2 issued from a vent that tapped the magma chamber at a slightly higher level than the vent for flow 1.

Flow 3 (43 ft thick) is a poorly- to moderately welded biotite latite ash flow which forms no prominent outcrops near the Findley Ridge section. Complete sampling of the unit was impossible because it is almost entirely covered. Flow 3, like flow 2, pinches out or merges with other flows under the talus slope to the north.

The samples and their analyses (appendix A, p. A-29) demonstrate that flow 3 is compositionally distinct from both flows 1 and 2. Lithic fragments are small and very sparse; augite is absent; and the sanidine/plagioclase ratio is low ($\approx 1/3$). The plagioclase composition (An_{29-47}), the character and abundance of biotite flakes, and the presence of lithics show that flow 3 is closely related to flows 1 and 2. The overall composition of flow 3 is intermediate between that of flows 1 and 2; so it is probable that most of the compositional variations observed are related to changes in level of eruption from a zoned magma rather than to compositional evolution of the magma itself.

Ash flow 4 (39 ft thick) is a moderately welded, grey to red-brown latite ash flow which supports a discontinuous cliff about midway up Findley Ridge. The flow is best exposed at the very tip of the ridge and appears to merge with flow 5 north of the measured section. A broad, poorly welded zone at the top of the flow forms a covered slope on which the upper contact of the flow is concealed.

Lithic fragments are practically absent from flow 4, but there are a few small andesitic lapilli (< ½ in. in diam) scattered through the flow.

The mineralogy of flow 4 is similar to that of flow 2, with no augite and a sanidine/plagioclase ratio of ≈2/3. Again, the composition and character of the crystals indicate that flow 4 originated from the same source as the lower flows. The composition of the erupted magma is very nearly identical to that of flow 2 and suggests that both the source and eruption mechanism may have been the same for flows 2 and 4.

Flow 5 (105 ft thick) is well exposed as a prominent cliff halfway up Findley Ridge. It has a thin, basal unwelded zone which is poorly exposed at the base of the cliff. Flow 5 exhibits all gradations of welding, including a black vitrophyre near the middle of the flow. The basal part of the flow is distinguished by an abundance of large, flattened pumice fragments and fragments of black vitrophyre.

Removal of the pumice fragments by weathering produces a vesicular aspect with elongate cavities paralleling the platy compaction foliation. The color of the rock varies from light-buff to red or black depending upon the degree of welding. Small purple-grey lithic lapilli are present throughout the flow but are most abundant in the lower part. Both the upper and lower contacts of flow 5 are obscured on poorly exposed slopes which reflect the decrease in welding intensity toward these contacts.

The mineralogy of flow 5 is slightly different from the mineralogy of all the previous flows. In addition to the abundant hexagonal plates of biotite, there are substantial amounts of augite and a few hornblende crystals. The sanidine/plagioclase ratio is ≈1/1.

The texture and appearance of flow 5 is much like flow 1, and augite is present as it is in flow 1. With these strong similarities, it seems likely that the source and eruption mechanism was the same for flows 1 and 5. The increased sanidine/plagioclase ratio (1/3 vs 1/1) might be due to compositional evolution in the source magma.

Ash flow 6 (43 ft thick) is a light-grey poorly welded ash-flow tuff which crops out very sparsely on the slope above the cliff formed by flow 5. Flow 6 contains abundant, small, andesitic lithic fragments, and many of the flattened pumice fragments are replaced by chalcedony.

The mineralogy of flow 6 is comparable to that of flows 2 and 4. No augite or hornblende is present, and the sanidine/plagioclase ratio is ≈3/4. The only notable difference between flow 6 and flows 2 and 4 is the plagioclase composition (An_{23-44}, An_{27-48}, An_{30-48} respectively).

On the basis of these observations, it is postulated that flows 2, 4, and 6 shared a common source, and that the minor variation in plagioclase composition is related to gradual compositional changes in the source magma.

Flow 7 of the Bonanza Formation (77 ft thick) is distinctive both in appearance and composition. It is a massive, light-grey to pinkish-grey flow which is poorly- to moderately welded, but resistant because of extreme silicification. Flow 7 crops out as a 50-ft-high cliff near the top of Findley Ridge. Large-scale, columnar jointing has developed perpendicular to the flow surfaces, but foliation is very poorly developed.

The petrography and mineralogy of flow 7 is strikingly different from other flows of the Bonanza sequence. There are numerous small lithic fragments, but they include light-grey ash-flow tuff and brick-red latites in addition to the normal grey andesite lithics. Biotite is the only mafic present, but the flakes are not so numerous as in other units. Large, glassy sanidine crystals contrast sharply with the light-grey matrix. Thin-section analysis reveal that the matrix is largely composed of microcrystalline

quartz rather than pumice and glass as in other flows of the Bonanza Formation. Elongate vesicles (or replaced pumice fragments) are completely filled with secondary quartz.

The intense and remarkably homogeneous silicification of the entire unit is probably the most peculiar characteristic of flow 7, but the mineralogical differences may be more significant. The high sanidine/plagioclase ratio (≈3/1), the deficiency in mafics, and the odd varieties of lithic fragments suggest a different source magma for flow 7.

Ash flow 8 (38 ft thick) is a poorly welded, light-grey, crystal-rich ash flow which is poorly exposed in the flat area above the cliff formed by flow 7.

Numerous grey, andesitic lithic fragments are present along with abundant hexagonal flakes of biotite. The composition of flow 8 is similar to that of flows 1, 3, and 5. Augite is present in minor amounts and the sanidine/plagioclase ratio is ≈2/5. The observed relationships between flows 7 and 8 also support the hypothesis that the major mineralogical changes reflect differences in the source magma or eruption mechanism; while minor mineralogical changes are related to changes in the magma composition.

A dark-grey, platy-foliated, hornblende biotite andesite of the upper volcanic sequence caps Findley Ridge. This andesite lies conformably on flow 8 of the Bonanza Formation.

It crops out as a distinctive slabby cliff, which can be traced the entire length of Findley Ridge.

Thin-section studies (appendix A, p. A-43 and A-44) show that the andesite is composed of strongly aligned phenocrysts of plagioclase, biotite, and magnetite in a pilotaxitic microcrystalline groundmass. It is readily distinguished from flows of the Bonanza Formation because it lacks the distinctive lithic fragments and compaction structures.

The entire sequence of Bonanza ash-flow tuffs exposed in Findley Ridge is 488 ft thick at the line of measured section. However, the measured thicknesses are not valid through even a small horizontal distance because flows can be seen thickening and wedging out within a few-hundred feet of the measured section. Nevertheless, the Findley Ridge section has served as a valuable reference section for mapping in the southwest Bonanza area. The unique characteristics of the described flows have proven recognizable in many parts of the area.

In addition to the compositional and textural variations that are characteristic of all ash-flows, several trends and patterns can be seen in the Bonanza Formation which are useful as marker patterns. These trends and patterns are also significant with respect to the geologic history of the area.

1. Lithic fragments are abundant in the lower portion of each flow and are most abundant in the lower flows of the sequence. This suggests that each flow erupted explosively, causing rock fragments to be torn from the walls of the vent. These lithic fragments settled toward the bottom of each flow as it flowed outward from the vent. Later flows may have erupted from vents opened by the early ash-flow eruptions. As a result, they contain fewer lithic fragments.

2. Flows 1, 3, 5, and 8 are compositionally similar and flows 2, 4, and 6 are similar. Together they make up a pattern of alternating flows which probably tapped a zoned magma at different levels.

3. Flow 7 is unique in texture and composition and probably originated from a distinct magma zone or source.

4. The sanidine/plagioclase ratio increases upward through each flow set (1, 3, 5, 8 and 2, 4, 6), and plagioclase becomes less calcic upward through the sequence. These variations probably reflect a gradual evolution of the source magma which, by continued differentiation, was becoming more and more silicic as the mafic constituents crystallized and settled toward the bottom of the magma chamber.

In mapping the Bonanza Formation throughout the southwest Bonanza area, several other significant features were noted:

1. The presence of a few angular lithic fragments of Precambrian rocks along with the abundant andesitic lithic fragments suggests that the Bonanza ash flows vented explosively through Precambrian crystalline rocks and lavas of the Rawley Formation.

2. The welding together of various ash flows shows that they were erupted in a rapid sequence.

3. Thinning of the ash flows and decrease in welding intensity away from the central Bonanza area indicate that the source of the ash flows was within the central Bonanza area. Local "pinching-out" of individual flows described in the Findley Ridge section may simply reflect the fact that the portion of the flow cropping out on Findley Ridge entered the area from a slightly different direction.

Seven of the eight units of the Bonanza Formation may be considered "typical" and bear enough similarity to one another that they are interpreted as products of a single magma. The other flow, flow 7, is considerably different. It contains an unusual variety of lithic fragments, is relatively crystal poor, contains almost no mafic minerals and has a very high percentage of sanidine in comparison to other flows of the Bonanza Formation. In addition, it is poorly compacted, highly silicified, and sandwiched between flows that have typical textures and compositions. The compositional differences between flow 7 and the other

flows and its relationship to them suggest that it was erupted from a separate source, but is related in time and mode of occurrence to the Bonanza ash-flow tuff sequence.

Burbank (1932) mapped a unit similar to flow 7 in the central Bonanza district. He recognized that it was distinct from the normal biotite- and lithic-rich latites found lower in the Bonanza sequence. He mapped the lithic- and crystal-poor, rhyolitic ash flow as the uppermost flow in the Bonanza sequence, and called it the upper Bonanza latite. Burbank does not mention a flow similar to his lower Bonanza latite overlying or included in his upper Bonanza group, but he does suggest the possibility that the upper and lower Bonanza units had different sources (1932, p. 22).

The Bonanza Formation is found throughout the southwest Bonanza area and in previously mapped areas to the north (Perry, 1971) and southwest (Bruns, 1971). Its wide distribution and the substantial thicknesses emphasize the fact that the Bonanza Formation could be present over a much broader area than it is presently known. The Bonanza ash flows intertongue with volcanic rocks of the San Juan volcanic field to the southwest (Bruns and others, 1971) and, although no such outcrops are reported, they could also extend far to the northwest and northeast of the Bonanza center. Such outcrops, if present, would certainly

aid in establishing the relationship between the Bonanza volcanic center and the Thirtynine Mile volcanic field.

Because the flows of the Bonanza Formation were deposited rapidly over a broad area, they are invaluable as a marker sequence. Also, the eruption of the Bonanza ash-flow sequence appears to be intimately associated with the collapse of the Bonanza caldera. Consequently, much of the structural history of the Bonanza area can be deciphered through interpretation of displacements and attitudes marked by the Bonanza flows. These relationships are discussed more fully in the "Structural Geology" section of this report.

The precise age of the Bonanza Formation is not yet known, but its stratigraphic position above the Rawley Formation (33.4 m.y. and 34.2 m.y.) and below the Sapinero Mesa tuff (Bruns and others, 1971) dated at older than 28 m.y. (Lipman and others, 1970) allows its age to be estimated at approximately 30 m.y. (i.e. early Oligocene). Samples of the Bonanza Formation have been collected and submitted for age dating, but the analyses have not yet been completed.

Upper Volcanic Sequence (T_{uv}): The upper sequence of volcanic rocks in the Bonanza area varies from 300 to 1,000 ft thick and includes various andesite and latite flows similar to those of the underlying Rawley Formation. They are identifiable largely because the Bonanza Formation separates them from the Rawley Formation. In areas where the Bonanza Formation is absent, it is extremely difficult to establish the contact between the Rawley Formation and the flows of the upper sequence.

Individual flows of the upper sequence are generally very local in extent and, they, like the Rawley flows, intertongue with flows from various centers. Along the north edge of the Bonanza center (Sec 10, 11, 14 and 15; T 47 N, R 7 E) they are found intertongueing with silicic volcanic units that appear to have been extruded from major fracture zones. The composite sequence is distinctly bi-modal, and, according to McBirney (1969, p. 506), typical of a mature volcano where a minor amount of rhyolitic magma has evolved from the more basic magma.

The upper volcanic sequence of the southwest Bonanza area includes the Squirrel Gulch latite and the Brewer Creek latite mapped by Burbank (1932), and the andesite of Ford Creek mapped by Bruns (1971) in the Lake Mountain Northeast quadrangle. Although all the units mapped by Burbank are formally recognized formations, the Brewer

Creek and Squirrel Gulch were not recognized as mappable units in the southwest Bonanza area. In this report, they have been grouped with other flows as part of the upper volcanic sequence. The upper volcanic sequence is also equivalent to the younger andesite and younger ash-flow tuff mapped by Mayhew (1969) and contemporaneous with the Porphyry Peak rhyolite (Burbank, 1932) and the Hayden Peak quartz latite (Mayhew, 1969).

The flow units of the upper sequence have previously been mapped as latites. Chemically, they may be latites, but petrographically, they are andesites (appendix A, p. A-39 thru A-47). Many of these andesites are mineralogically more complex than those of the Rawley Formation. For example, sample PRC-2 exhibits zoned plagioclase crystals which have calcic cores surrounded by more sodic rims, hornblende crystals with augite cores (fig. 23), and two generations of hornblende crystals; one exhibiting reaction rims of magnetite. These complexities reflect the longer period of evolution of these later andesite flows.

Most of the andesites of the upper sequence are surprisingly similar in their mineralogic compositions considering their probable origin from different centers and their widely different textures and appearances. For example, the rather massive dark grey to black andesite mapped by Burbank as Squirrel Gulch latite (samples PRC-2 and PRC-14) weathers to a tan color except for the

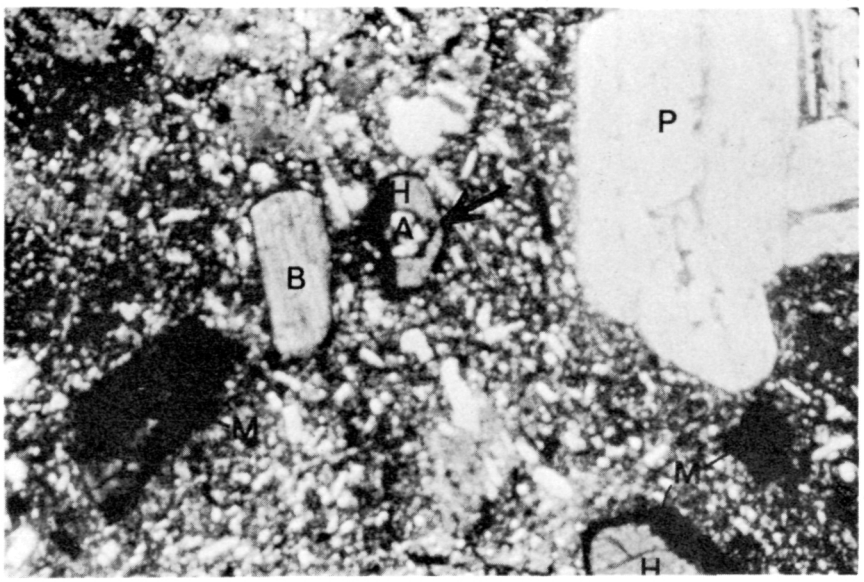

Figure 23. Photomicrograph of biotite hornblende andesite of the upper volcanic sequence. (PRC-2, p. A-39, plane polarized light, X30, P=plagioclase, B=biotite, A=augite, H=hornblende, M=magnetite) Note hornblende crystal with augite core. Groundmass consists mostly of plagioclase microlites.

conspicuous black hornblende crystals. The overlying andesite flow (Burbank's Brewer Creek latite, PRC-17) weathers to a red-brown color and exhibits rusty-colored biotite flakes as the most apparent mafic. These flows are petrographically similar and may have been erupted from a single vent (probably somewhere in the central Bonanza district), but they are quite distinct in the field. Another flow which is found directly overlying the Bonanza Formation in the southwest part of the map area (as does the Squirrel Gulch in the central Bonanza area) is very similar in composition to flows of the upper volcanic sequence of the central Bonanza area (samples PRC-37 and PRC-38), but it has a coarser groundmass and exhibits platy foliation reflecting a pilotaxitic structure. This unit probably originated from a separate source which may have been located to the west or southwest of the central Bonanza area, but it is compositionally similar to flows found in the central Bonanza area.

Late Silicic Flows and Intrusives (T_i): Another group of volcanic rocks having particular significance are the silicic flows and intrusives of the central Bonanza areas. This group includes all the intrusive bodies mapped in the southwest Bonanza area and the Porphyry Peak rhyolite which was mapped by Burbank (1932) and extends into the northern part

of the southwest Bonanza area. These lithologies are grouped together as a single unit because they are believed to be genetically related.

The Porphyry Peak rhyolite was mapped and described by both Patton (1915) and Burbank (1932). It is a series of light-colored latite and rhyolite flows named for exposures on Porphyry Peak in the northeastern corner of the map area (Sec 2, T 47 N, R 7 E). The lower flows of the Porphyry Peak sequence are crystal-poor latites with sparse phenocrysts of plagioclase and sanidine. Higher in the sequence, the flows become more rhyolitic and contain quartz and sanidine phenocrysts. The upper flows commonly exhibit a platy foliation which parallels flow structure. Flows of the Porphyry Peak sequence are characterized by glassy quartz and feldspar phenocrysts set in a light-grey to buff groundmass which weathers to near-white. The single sample of Porphyry Peak rhyolite petrographically analyzed for this study (PRC-40) represents a flow in which the dominant phenocrysts are sanidine with minor amounts of plagioclase and biotite. However, the groundmass contains sufficient quartz concentrated in zones parallel to the flow structure to require the sample to be classified as rhyolite. Biotite is the only important mafic mineral in the Porphyry Peak flows and generally occurs as fresh, yellowish flakes.

The above-mentioned compositional variations in the Porphyry Peak sequence denote a trend toward more silicic flows, upward through the sequence. This trend may reflect continued differentiation of the rhyolite magma during eruption, or the selective eruption from a differentiated magma with the more silicic (upper) differentiates being erupted last. The latter possibility requires the vent system to tap the magma chamber some distance below its top, allowing the more mafic differentiates to be erupted from beneath the silicic concentrates at the top of the chamber. Because this mechanism is relatively complex, I favor "continuing differentiation" as most probable.

Burbank found flows of the Porphyry Peak rhyolite lying directly on Squirrel Gulch latite and overlain by Brewer Creek latite (Burbank, 1932, p. 26). This relationship demonstrates that the Porphyry Peak rhyolite was erupted contemporaneously with the upper sequence of intermediate lavas. However, the Porphyry Peak sequence is mineralogically very different from the latites and andesites of the upper volcanic sequence. These mineralogical differences, coupled with the contemporaneous relationship demonstrate that the two sequences were erupted from separate vents. The Porphyry Peak flows appear to have been erupted along major faults which developed in conjunction with the earlier volcanism.

Several Tertiary intrusive bodies have been mapped in the central Bonanza district (Patton, 1915; Burbank, 1932, and Mayhew, 1969). They range in composition from gabbro to rhyolite and are found in contact with all formations mapped in the area, except the Porphyry Peak rhyolite. They were emplaced during or after the eruption of the upper volcanic sequence and their distribution demonstrates that they intruded along fractures and faults of the structurally complex central Bonanza area.

The Eagle Gulch "latite" is the largest intrusive body in the Bonanza area. Burbank (1932, p. 32) described the Eagle Gulch latite as having a crystalline groundmass with the smaller particles of the groundmass hardly distinguishable. Apparently, he classified the Eagle Gulch as a latite despite its phaneritic groundmass. According to the system used in this report (Williams, Turner, and Gilbert, 1954) it is a porphyritic quartz monzonite. The Eagle Gulch intrusive is a light-grey, porphyritic-phaneritic, quartz monzonite body that crops out over a 2-sq-mi area along Eagle Gulch. The entire outcrop area lies within the area mapped by Burbank, but I studied thin sections of the Eagle Gulch latite (appendix A, p. A-49) because I expected to find similar intrusive bodies in the southwest Bonanza area, or to discover flows which would correlate with the Eagle Gulch intrusive as a source vent. No such intrusive bodies or flows were found in the southwest Bonanza area.

The only intrusives mapped in the southwest Bonanza area are two vein-like, leucocratic, biotite aphanites in the vicinity of upper U.S. Gulch (Sec 13, T 46 N, R 7 E and Sec 7, 18, and 19, T 46 N, R 8 E). These intrusives are narrow, dike-like bodies that have been intruded along fault zones. Near their contacts with the andesitic country rock, they contain numerous angular fragments of altered andesite. The andesitic country rock has been strongly silicified and altered for several hundred feet out from the intrusive contact, but no economic mineralization has yet been found associated with these intrusives.

The two intrusives in the U.S. Gulch area have a texture quite different from intrusive bodies in the central Bonanza area. The alternating size-zonations of microlites (appendix A, p. A-50) probably represent flow structure, but no other fabric or structure could be detected in this finely crystalline rock. The overall composition of the intrusive material is uncertain, but the light color and identifiable microlites suggest that it is intermediate or silicic.

The silicic and intermediate intrusive bodies mapped in the southwest Bonanza area are similar to the Porphyry Peak rhyolite in that they were also emplaced along major fractures during a late phase of volcanic activity. These similarities suggest that the Porphyry Peak and other late

silicic intrusives are related in origin, despite the obvious textural differences. Certainly, both are representative of late silicic intrusive activity which probably accompanied the dying stages of volcanism in the Bonanza center. Because of this probable relationship, I have grouped the intrusives of the U.S. Gulch area with the Porphyry Peak rhyolite as a single map unit.

Quaternary Deposits

Most of the southwest Bonanza area is presently undergoing active erosion, and Quaternary deposits are limited in extent. The bulk of the Quaternary deposits is gravels, talus, and alluvium concentrated along stream valleys.

Geologically, the most significant of the deposits are the older terrace gravels which occur as small remnants along Kerber Creek and near the junction of Kerber and Little Kerber Creeks. These are preserved as broad terraces in a few areas of low relief. The older terrace gravels are identifiable both by their topographic position with respect to modern streams and by the condition of the rock material in the gravels. The gravels in the Bonanza area are largely composed of materials derived from the Bonanza volcanic pile, but contain some fragments of older rock units, some of which may have been caught up in the volcanic rocks as lithic fragments. Pebbles, cobbles, and boulders

of the older terrace gravels often show extreme effects of weathering. Some are so strongly weathered that they can be disaggregated by hand. A reasonably mature soil has developed on these gravel terraces, and can be seen exposed along gullies which disect the older terrace gravels. The light colored "A" horizon is generally 3-5 ft thick and the underlying red-brown "B" horizon is at least 5 ft thick, with the base usually unexposed.

The terrace gravels are particularly important because they can be used as indicators of erosional cycles, and can be correlated with terraces outside the Bonanza area to establish ages for related geologic features. In the upper San Luis and Arkansas Valleys, some of the older terraces are displaced by recent faulting (Knepper and Marrs, 1971). A similar situation is suspected in the Bonanza area (Sec 5, T 45 N, R 8 E), which is adjacent and structurally related to the San Luis-Arkansas Valley system.

The only Quaternary deposits mapped in the mountains of the southwest Bonanza area were a few landslides. The largest of these was a slide (or slump) on the east side of Poison Gulch (Sec 7, T 45 N, R 7 E). The area is identifiable as a landslide by the irregular, hummocky topography, and the erratic dips measured on rocks in the area. The slide mass has retained much of its original stratigraphic zonation. A broad, irregular, band of

Bonanza Formation can be traced through the central part of the slide mass and is flanked on either side by andesitic flow rocks. The present topography and the stratigraphic sequence on the steep ridge southwest of the slide area indicate that it was the source of the landslide.

The effects of glaciation are evident in the high peaks surrounding the upper Kerber Creek drainage. Most of the tributary streams that flow into Kerber Creek from the west head in the glacial cirques of the mountains west of Bonanza. However, no mappable glacial deposits were found in the Bonanza area. The morrainal material deposited by the glaciers of the Bonanza area has been removed by post-glacial erosion.

STRUCTURAL GEOLOGY

The earliest insight into geologic structure of the Bonanza volcanic center was provided by F. M. Endlich, who worked with F. V. Hayden in making the territorial surveys of the 1870's. Endlich described his impressions of the Bonanza area as seen from the top of Antora Peak (1874, p. 343):

> "A mass of high andesitic mountains occurs about five to six miles south of Mount Ouray, upon one of which station 24 is located at an elevation of 13,400 ft., and throughout that portion of the volcanic country a number of peaks nearly as high occur, forming an almost regular horseshoe, studded with numerous smaller hills inside. When seen in the field, the impression produced by it was that of one huge crater edge, containing within its limits a number of smaller eruptive cones."

No detailed geologic observations are recorded for the Bonanza area until H. B. Patton (1915) and a group of Colorado School of Mines students mapped part of the central Bonanza mining district in the summer of 1912. Many of the geologic units defined in this early work are still recognized in the area. Patton constructed a map of the various units in the central district and based his brief assessment of the structure on foliation dips which he observed. He did not observe the complex faulting later mapped by Burbank (1932) in the same area. Patton noticed a dominant west-dip in the flows of the northern part of the district and the opposing dips in the southern part of

his map area led him to suggest a synclinal fold in the volcanic rocks of that area (1915, p. 61):

> "In the southern portion of the district, the Bonanza latite appears to have been folded into a synclinal arch. The axis of the fold is approximately north and south. West of this arch the flowage planes dip to the west, and east of it to the east."

Patton's description is one of an anticline rather than a syncline, but the described fold is a realistic interpretation of the features he observed.

In 1926 and 1927, W. S. Burbank, of the U.S. Geological Survey, mapped the central Bonanza mining district. His map area encompasses the area mapped by Patton (fig. 24), but also includes an area to the southeast in which he did reconnaissance mapping. Burbank spent more than 9 months mapping the Bonanza district, and his work is very detailed. Much of Burbank's geologic interpretation has been repeatedly verified by work in adjacent areas. The volcanic sequence defined by Burbank is very similar to the one described by Patton, but his structural interpretation is quite different. Burbank mapped a complex system of post-volcanic faults and foliation attitudes which he interpreted as the result of post-volcanic collapse (1932, p. VIII):

> "Presumably, the extrusion of lavas resulted in such a loss of volume and supporting force of the intrusive body that the crust failed and subsided locally under its own weight. The older lavas were broken into many small fault flocks which were thrown downward in successive steps toward a central area of collapse."

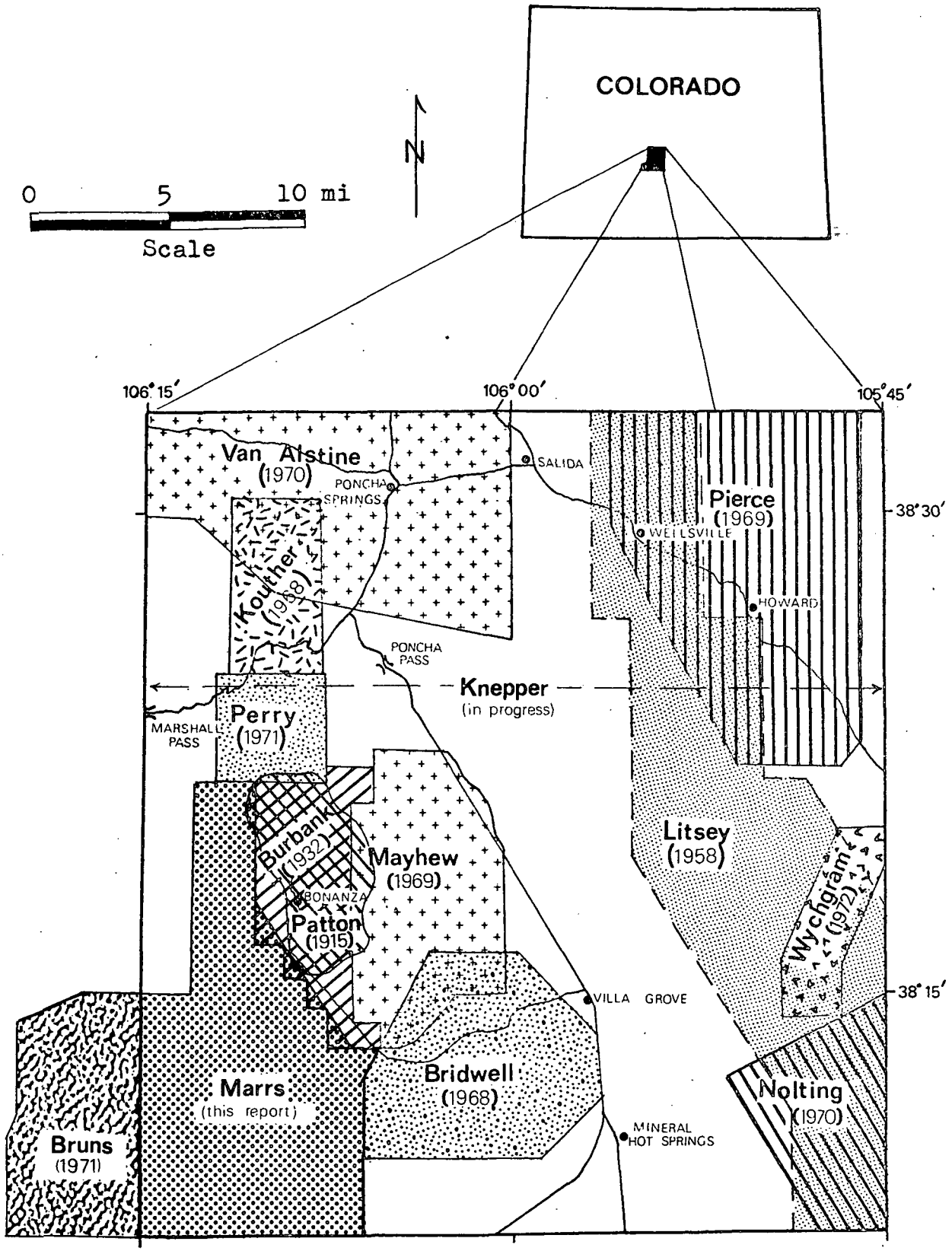

Figure 24. Index map of the Bonanza area, showing areas mapped by various investigators.

Graduate students from the Colorado School of Mines have since mapped areas adjacent to the central mining district (fig. 24). The structural interpretation made in each of these areas concurs, to a large degree, with Burbank's idea of post-volcanic collapse.

Pre-Volcanic Structure

Considerable insight into the pre-volcanic structure and geologic history is provided by Burbank's reconnaissance work to the southeast of the Bonanza district and later investigations which have dealt with the Precambrian and Paleozoic sequences exposed in that area.

The only structure observed in the Precambrian rocks of the southwest Bonanza area is the northwest-trending foliation in the hornblende gneiss of the southern part of the area. This trend has also been recognized in Precambrian rocks north of the Bonanza district (Perry, 1971, p. 38), where it was attributed to the uplift of the Sawatch Arch because the observed foliation trends parallel the axis of the Sawatch Uplift.

The Paleozoic sedimentary units and Precambrian crystalline rocks east of the Bonanza volcanic field are folded into a series of northwest-trending anticlines and synclines which extend northwestward under the edge of the Oligocene flows of the Bonanza volcanic pile (Bridwell,

1968, plate 1). Northwest-trending, high-angle thrust faults have formed along the southwest flanks of some of these folds as complimentary structures. These folds and thrusts are thought to have formed as a first stage of late Cretaceous Laramide deformation in response to a northeast-southwest compressive stress, and have also been correlated with uplift of the Sawatch Arch (Bridwell, 1968, p. 77).

The Paleozoic sedimentary outcrops within the southwest Bonanza area represent the southwest flank of one of the northwest-trending synclines. They are exposed through erosional windows in the volcanic rocks. The dips in these paleozoic sedimentary units range from 30° northeast in the lower part of the section, near Little Kerber Creek, to 60° northeast in the upper units that are exposed north of Columbia Gulch. The units exhibiting steeper dips lie nearer to the synclinal axis.

A second stage of Laramide deformation has thrust Precambrian and Paleozoic units northward over the folded and faulted Paleozoic sedimentary rocks. Bridwell (1968, p. 63) and others have attributed this thrusting to the uplift of a highland (the Sierra Blanca massif) in the area of the present San Luis Valley.

Two remnants of these thrust plates are exposed in the southwest Bonanza area (plate 1). At one location the Manitou Formation is thrust over the Minturn Formation

(Sec 28, T 46 N, R 8 E; plate 3, cross section F-F'). Here, the thrust front trends northward with the overthrust material on the east, but the trend of this small outcrop of the thrust front is probably not indicative of the direction of thrusting.

Outcrops of the Mesozoic tectonic breccia (Sec 27, T 46 N, R 8 E) have been interpreted as material caught along the sole of a thrust fault. This material was brecciated and reconsolidated by the tectonic forces associated with second-stage Laramide thrusting. Thus, the breccia represents an outcrop of the sole of a thrust fault; probably the same thrust fault that is exposed in Section 28, T 46 N, R 8 E.

The front of the north-northwest-trending Kerber thrust fault is exposed along the east edge of the southwest Bonanza area, less than one mile south of the previously described outcrops of thrust-plate remnants. The proximity of these outcrops to the major thrust sheet suggests that they may be outlying remnants (klippen) of the Kerber thrust plate. Burbank (1932, plate 3) mapped the Kerber thrust and the tectonic-breccia klippen in his reconnaissance study of the area, but he did not map the small thrust outcrop in Section 27, T 46 N, R 8 E. Burbank (1932, p. 40) believes that the tectonic-breccia outcrop is of sufficiently different character and

attitude from the main Kerber thrust that it represents a separate, older, thrust sheet. His strongest evidence that the breccia klippen are not part of the Kerber thrust are marked changes in dip and repeated section of the Minturn Formation that indicate a hidden fault lying along Little Kerber Creek. Bridwell (1968, p. 62), on the other hand, postulated that similar petrographic properties of all the overthrust Precambrian rocks require that the outliers and the Kerber thrust are related. He acknowledges that the megascopic texture and composition of the breccia is unlike anything seen along the main Kerber thrust and that the attitude of the fault planes are significantly different. To explain these discrepancies, Bridwell suggests that the tectonic breccia might have been formed when a landslide "released from the advancing toe of the thrust" was overridden by the thrust plate. He feels that the difference in fault plane attitudes can be explained by a decrease in the dip angle of the thrust plane near the surface.

Bridwell's interpretation of the thrust plate remnants seems reasonable in view of the almost certain correlation of the tectonic breccia with the thrust outcrop north of Columbia Gulch and the closer similarity of style between that thrust remnant and the main Kerber thrust. The flattening (or even minor undulation) of the thrust plane

required by this interpretation is also reasonable in the light of current ideas on stress release associated with thrust faulting in the Rocky Mountains (Prucha and others, 1965).

My investigation of the area failed to produce any evidence which would allow a definite conclusion as to which hypothesis is correct. Rounding of the breccia blocks could have resulted from paleo-weathering, tectonic grinding, or recent weathering. The breccia outliers may or may not be a part of the Kerber thrust plate. However, there is considerable evidence for faulting of the volcanic units along Little Kerber Creek. This post-Oligocene faulting may have been controlled by an older zone of weakness which would correspond to the Little Kerber thrust fault inferred by Burbank (1932, p. 39).

No evidence was found to indicate that the Little Kerber thrust, postulated by Burbank, is older than the Kerber thrust. It seems equally likely that Little Kerber thrust is contemporaneous with the Kerber thrust and simply represents a sliver of that thrust.

Volcanic and Post-Volcanic Structure

Volcanic and post-volcanic structural adjustments in the southwest Bonanza area have resulted in a well-developed pattern of radial and concentric faults centered near the

town of Bonanza. The radial faults are vertical or high-angle faults which generally show relatively little total displacement. Slip directions vary considerably, with some of the radial faults being normal and others, reverse. Some radial faults show normal displacements along some sections and reverse displacements at other points. Strike-slip displacements are generally not significant.

The concentric faults of the southwest Bonanza area are also high-angle normal or reverse faults with dominant dip directions inward, toward the center of the fault pattern. Most of the concentric faults show significant (>100 ft) displacements and some have very large displacements (>1,000 ft). Concentric faults near the central part of the Bonanza district usually show large, normal displacements. Consequently, the central Bonanza area has been down-dropped substantially with respect to the outlying portions of the southwest Bonanza area, forming the central Bonanza caldera.

Of particular interest within the pattern of concentric faulting is the "Western Bouldary Fault" which runs along the east flank of the high mountains west of Bonanza. This fault shows a particularly large normal displacement (at least 2,000 ft) and defines the western rim of the Bonanza caldera. At the north end of the area, the Western Boundary Fault joins a major normal fault which is responsible for

much of the down-to-the-east displacement along the western side of the upper Arkansas Valley. To the south, the Western Boundary Fault of the Bonanza caldera splays out into several faults as it swings eastward to form the southern perimeter of the central collapse zone. Therefore, the southern boundary of the Bonanza caldera is defined by a series of down-to-the-north step faults. The displacements on each of these step faults is not nearly so great (1,000 ft maximum) as that seen along the Western Boundary Fault and the total displacement tends to decrease eastward along the concentric faults of the southern caldera boundary. One particularly interesting feature occurs at the southern end of the Lucky Boy Fault as it curves southward across Little Kerber Creek. This fault begins to die out eastward, but curves around and splays out into a series of minor radial faults, forming an epicycloidal pattern.

Concentric faults farther from the central area of collapse are nearly vertical. They show smaller displacements than those near the center, and sometimes have displacements opposite those seen nearer the center; that is, the side toward the central area is structurally higher. The steepening of dips on the concentric faults as one proceeds outward from the center is interpreted as a function of the level of exposure and the geometry of the

faults. Burbank (1932, p. 46-54) presents evidence that the dips of the concentric faults decrease with depth. This conclusion is based on steeply outward-dipping foliations in volcanic units affected by the faults. Dips in the central Bonanza area are commonly so steep that they are difficult to explain as normally-occurring slopes or the flanks of the volcanic pile. When projected, they yield an incredibly high profile for the pre-collapse volcanic pile. Burbank interpreted these oversteepened dips as the result of rotation of the fault blocks as they slid downward along curved fault planes (fig. 25).

Anomalously steep dips are also observed in the southwest Bonanza area and there is a noticeable decrease in foliation dip-angles with increasing distance from the central collapse area. This decrease in foliation dips could result from smaller displacements on the normal, concentric faults in the outlying areas, while the increase in the apparent dip-angle of the faults, outward from the central collapse zone, would be the result of both the smaller displacement, and the fact that a higher level of the fault is exposed at the surface (fig. 26).

The concave upward form of the concentric faults indicates that they formed under horizontal tension like those described by Anderson (1936) in the formation of cone sheets, but with a dominantly upward-directed component of force (fig. 27). This sort of stress system

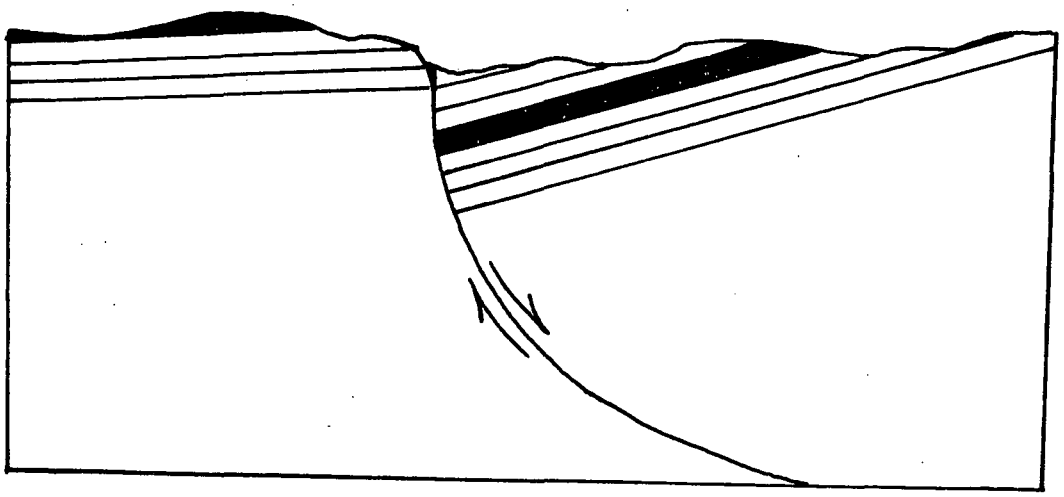

Figure 25. Configurations of a normal fault resulting in steeper dips on the downdropped block (after Burbank, fig. 7, p. 49).

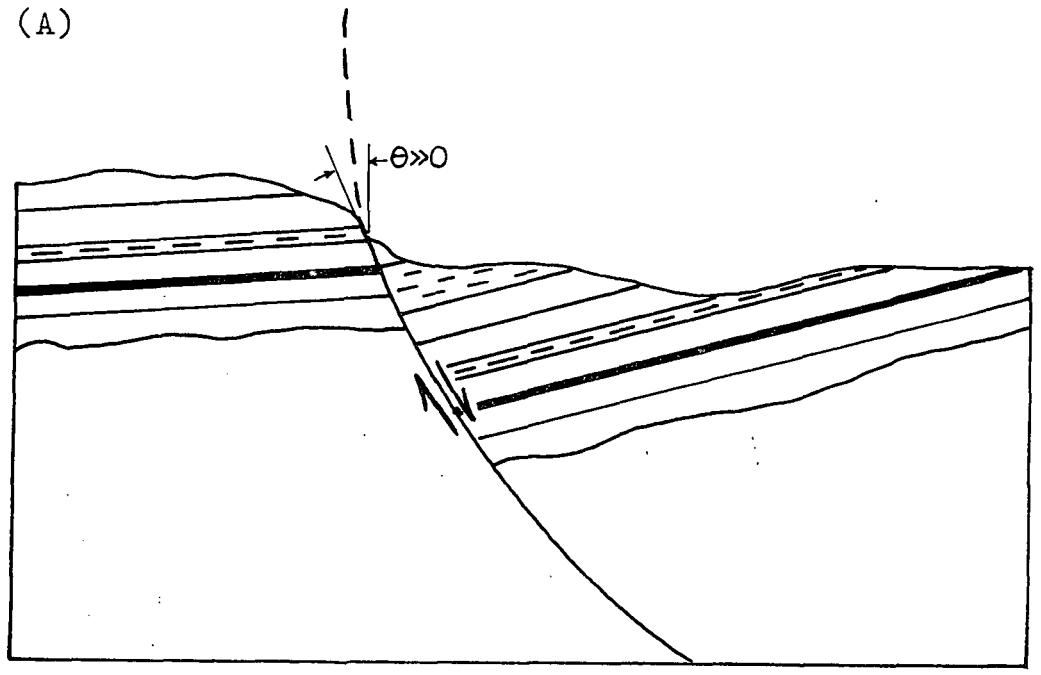

θ = the angular deviation of the fault plane from vertical where the fault plane intersects the surface.

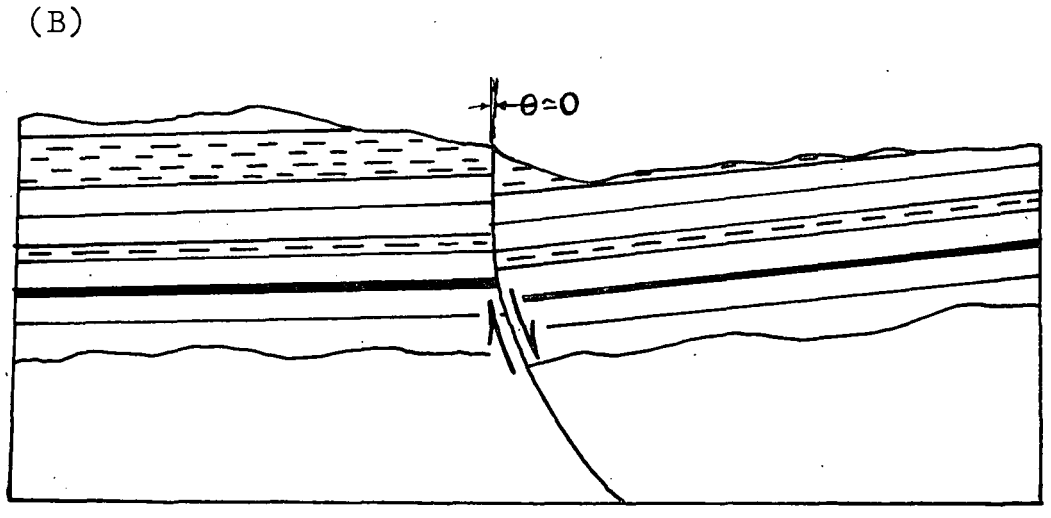

Figure 26. Comparison of normal faults in: (A) the central collapse zone, and (B) an outlying area. The greater movement portrayed in figure A produces steeper dips on the down-thrown block while the lower level of erosion exposes the lower, shallow-dipping portion of the fault not exposed in figure 26-B.

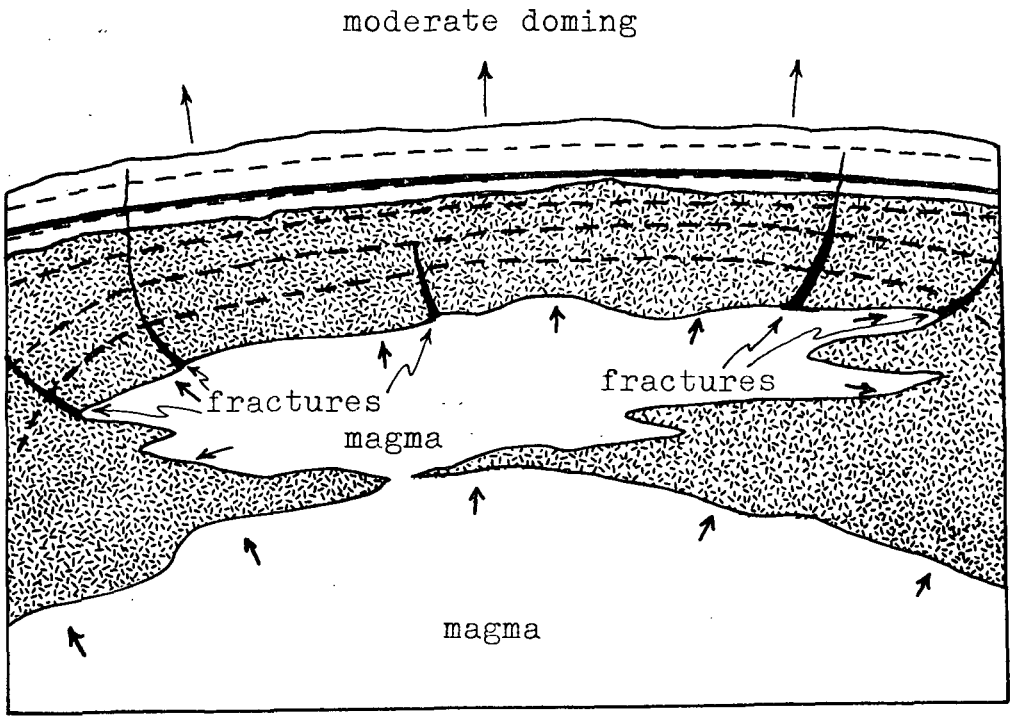

Figure 27. Diagram showing the general configuration of the hypothesized magma chamber and the major stresses during a period of increasing magma pressure. Small arrows in the magma chamber indicate stress. The shapes of the isobaric surfaces are determined largely by the shape and distribution of pressure on the roof of the magma chamber. Assuming equal pressure distribution in the magma chamber and homogeneity (with regard to mechanical strength) of the overlying rocks, the isobars will have the form shown by the dashed lines. An increase in pressure in the magma chamber induces tensile fracturing normal to the isobars. With a flat-topped magma chamber, the result is a series of cone-shaped, concave-inward, high-angle, reverse faults. The shape of the lower portion of the magma chamber is relatively unimportant.

results from increasing pressures in a magma chamber beneath the surface, but requires that the upper surface of the magma chamber be relatively flat rather than parabolic, as in the case given by Anderson. The upward and outward pressure from below should have resulted in reverse movements on the faults and an overall upward displacement of the central area. Presently, however, the central area has been displaced downward, and the movement along most of the fault is normal. This anomalous situation is easily explained if one assumes that the faults formed as a result of upward- and outward-directed forces and that the original displacements were reverse movements. These movements would compliment the "early" doming in the Bonanza center as suggested by Burbank (1932, p. 49). Then, after rapid eruption of a large volume of magma from the underlying chamber, the pressure would be relieved, and the central Bonanza area could have collapsed along these same faults. This pattern of development would explain not only the observed normal displacement on the faults, but also the reverse movements and smaller normal movements on the concentric faults further from the center where the effects of collapse were not so great.

In summary, the overall fault pattern in the southwest Bonanza center is dominated by a series of radial

and concentric faults which intersect at nearly right angles. The concentric faults and fault zones are planes of major displacement which first formed in response to pressure from the underlying magma chamber and then served as planes along which the central caldera area collapsed. The radial faults served as planes of minor structural adjustment between fault blocks, but are, in general, a product of the same stress systems.

The major part of the caldera collapse is believed to be associated with the eruption of the Bonanza ash-flow sequence. Thickness variations, welding intensities, textures, and overall distribution indicate that the source of the Bonanza Formation was somewhere within the central collapse zone of the Bonanza caldera. The distribution of Bonanza flows outside the caldera demonstrates that the major collapse occurred sometime after the Bonanza sequence was erupted. No evidence for "ponding" of the Bonanza Formation was found in the southwest Bonanza area other than the relatively great thicknesses of the Bonanza Formation present in the central caldera area. Also, the occurrence of upper flows of the Bonanza sequence outside the caldera suggests that all the Bonanza flows were erupted before the major subsidence occurred. However, the Bonanza flows appear to represent the last major eruption sequence

in the Bonanza center. The estimated volume of the upper-volcanic sequence (≈10 cu mi) is too small to account for such a large subsidence feature even if the magma chamber beneath the Bonanza center were the source.

A conservative estimate of the volume of the flows of the Bonanza Formation (computed from estimates of outcrop area and thickness) gives approximately 26 cu mi for the volume of erupted material. A similarly conservative estimate for the volume of the Bonanza caldera is approximately 25 cu mi*. Although these estimates are crude, they do indicate that the volume of the erupted ash-flow material and that of the caldera are of the same order of magnitude.

Structural adjustment continued for some time after eruptions ceased in the Bonanza center. Throughout the Bonanza area faults cut even the youngest volcanic units. Mineralization, which affects the entire volcanic sequence, shows trends that are not only controlled by the fault pattern, but are, in many cases, offset by the faults.

Although the major collapse of the Bonanza caldera is believed to have been associated with the eruption of the Bonanza Formation, the eruption of some of the flows of the upper-volcanic sequences may have contributed to the subsidence. Some of the late flows were erupted from small, local centers where magma was squeezed up along

*Assuming an average down-drop of 2,600 ft over a circular area 8 mi in diam.

fractures as the caldera area subsided. Late silicic flows and intrusives tend to be concentrated along the major zone of downward displacement of the central caldera area and their emplacement appears to have been controlled by these faults. The silicic units intertongue with the upper intermediate sequence.

These observations demonstrate that the major caldera faults were present when the late silicic and intermediate rocks were emplaced. Yet these same units are cut by the faults as a result of continued structural adjustment.

Both the intermediate and silicic flows of the late volcanic sequence are displaced by the caldera fault system and none of these flows show evidence of ponding within the caldera. No flows have been found outside the central caldera area which can be petrographically correlated with the late flows inside the caldera, so the total amount of structural adjustment since their emplacement could not be determined.

Some evidence for recent displacement is found along the Western Boundary Fault and at the southern end of the Lucky Boy Fault. The Western Boundary Fault is marked by a prominant cliff (fig. 28) and a series of cold water springs at its outcrop above Mosquito Lake (Sec 10, T 48 N, R 7 E). This cliff was interpreted as a fault-line scarp, and its youthful appearance with respect to topographically

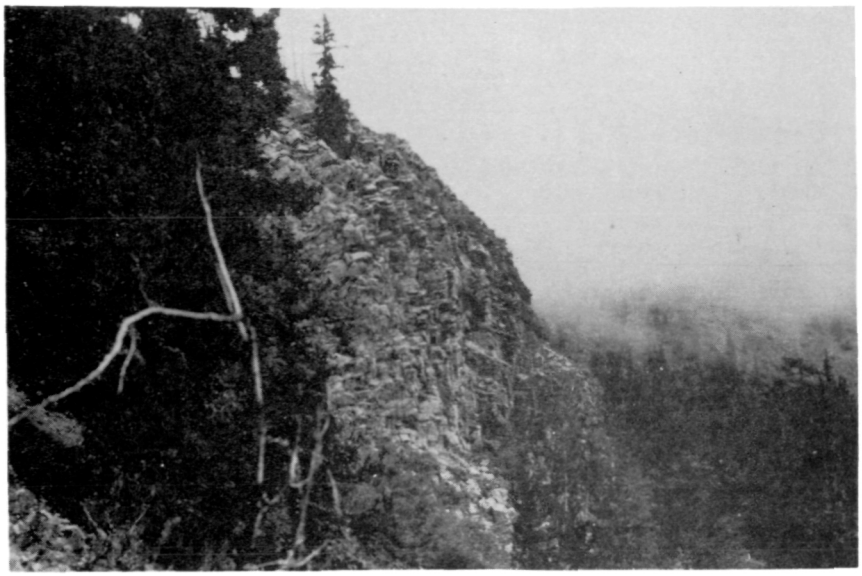

Figure 28. Cliff above Mosquito Lake which may reflect relatively recent fault movement. Hornblende andesites of the Rawley Formation crop out in this youthful scarp. Springs emerge along the base of the cliff.

Figure 29. Brewery Creek as it crosses the zone affected by the Western Boundary Fault. Trees and boulders form natural dams causing the stream to abandon the main channel and flow an erratic coarse down the valley.

expressed structures in other parts of the Bonanza area may reflect relatively recent movement along the fault.

Farther south along this same fault zone, creeks are found crossing the fault which have a very odd bed character. Brewery Creek presents the most striking example of this peculiar form (fig. 29). The stream bed is strewn with large boulders which are sometimes piled high against the trunks of trees. At normal water level the stream flows an erratic coarse in one or more small channels. The small, active channels are often not in the bottom of the main stream channel, instead, they weave along in high-water channels at various levels. At many points the sides of the valley have been or are being actively eroded with new cuts exposing 10- to 15-ft-thick soil profiles and causing the channel to be choked with fallen trees and debris.

Normally, a character like that of Brewery Creek would be attributed to flooding. However, streams in other parts of the central district and even the lower portions of these same streams show no evidence of recent flooding. Long-time residents in the area recall no flood that might have disrupted normal flow patterns in these streams and can remember no time when the stream beds were much different than they are today (Kempner, 1972, personal communication).

An alternate explanation for the anomalous character of these few streams on the west side of the central caldera might be an increase in stream energy and steepened profile caused by recent movement on the Western Boundary Fault which each of the oddly-behaving streams crosses. Admittedly, this explanation is somewhat out of the ordinary, but it does fit the observed conditions.

Still farther south along the Western Boundary Fault (NE¼, Sec 11, T 47 N, R 7 E) the fault trace is marked by a zone of bouldery fault gouge. The topography of this zone is very hummocky and contrasts sharply with the steep slope to the southwest and the relatively low slope to the northeast. A normal drainage pattern has not developed on the hummocky area. Numerous small sink-like lows are present in the fault zone and runoff simply filters into the boulder pile in these low spots.

Again, there is no definite evidence for recent faulting, but the odd topography and complete lack of drainage system across the fault zone could be explained as the result of recent movements along the Western Boundary Fault of the Bonanza caldera.

The Lucky Boy Fault, which is a southern branch of the Western Boundary Fault, cuts across a quaternary gravel terrace as it curves around in an epicycloidal pattern and splays out in a series of radial faults (Sec 5, T 46 N, R 8 E).

At this point the Lucky Boy Fault is expressed as a fault zone with two major components. Minor drainages cut into the older terrace gravels and follow each of the elements of the fault in a set of parallel curves (fig. 30). It is apparent that the fault pattern dominates the drainage across this once-level terrace, suggesting that the Lucky Boy Fault has been reactivated since the deposition of the terrace gravels. In addition, stereoscopic viewing of the area on the color aerial photographs shows that the terrace gravels are displaced slightly across each of the small drainages. These displacements cannot be seen in the field. Local relief and the topographic discontinuity of each drainage completely masks the more subtle, fault-controlled, topographic change across the drainage. A more synoptic view of the area, which shows the overall relationship of each part of the gravel terrace to the other, is necessary in order to see the fault displacements.

None of the evidences discussed above makes an indisputable case for recent structural adjustment in the southwest Bonanza area; but all of the evidence taken together supports the contention that recent structural adjustments have taken place. This is not surprising considering the continuity of the Western Boundary Fault of the Bonanza caldera with the western boundary fault of the Arkansas Valley. Recognizing that the Arkansas Valley is a northern extension of the presently active Rio Grande Rift zone,

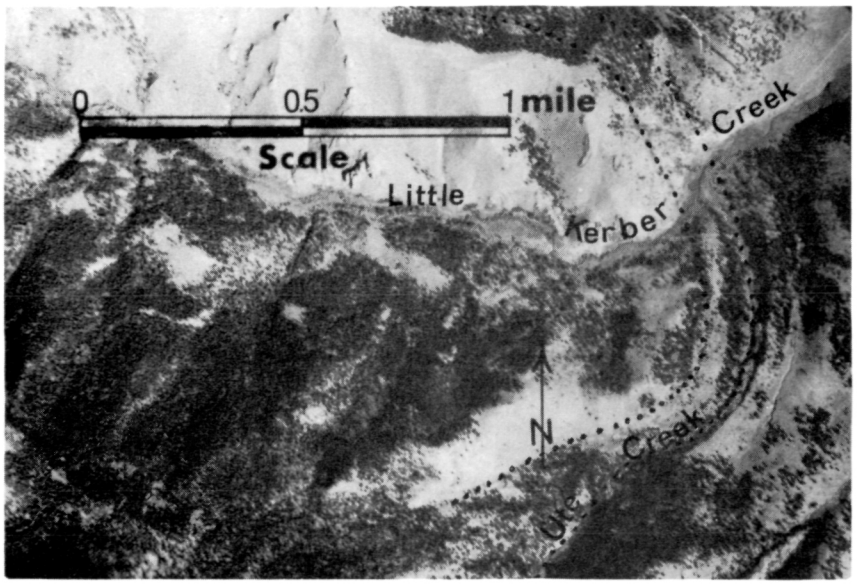

Figure 30. Fault-controlled drainages cutting a gravel terrace at the junction of Ute Creek with Little Kerber Creek. Dotted lines mark the fault terraces. (from a 1:15,000 color aerial photograph taken on NASA Mission 105, October 2, 1969)

one might expect some of the faults of the caldera system to show evidence of recent movement.

These late structural adjustments could account for a large portion of the observed structural displacements on the western side of the caldera. The down-to-the-east movements associated with the Rio Grande Rift system would compliment the original displacement on the Western Boundary Fault of the caldera and would serve to increase the total relative displacement. At the same time, late structural adjustments affecting faults along the eastern rim of the caldera would compensate for the original down-to-the-west displacement. The final result would be a subdued structure along the eastern side of the caldera and an enhanced structure on the western side of the caldera, exactly as observed in the Bonanza area.

Figures 31, 32, and 33 are block diagrams depicting major periods in the structural development of the Bonanza area. Figure 31 represents the beginning of volcanism in early Oligocene time. Intermediate lavas, ash, and pyroclastic material were erupted onto an erosion surface cut on Precambrian crystalline rocks and Paleozoic sedimentary rocks. The San Luis Valley and the Sangre de Cristo Range may not have been present at that time, allowing the Oligocene volcanic flows to spread in all directions, controlled only by the low topography of the Precambrian-

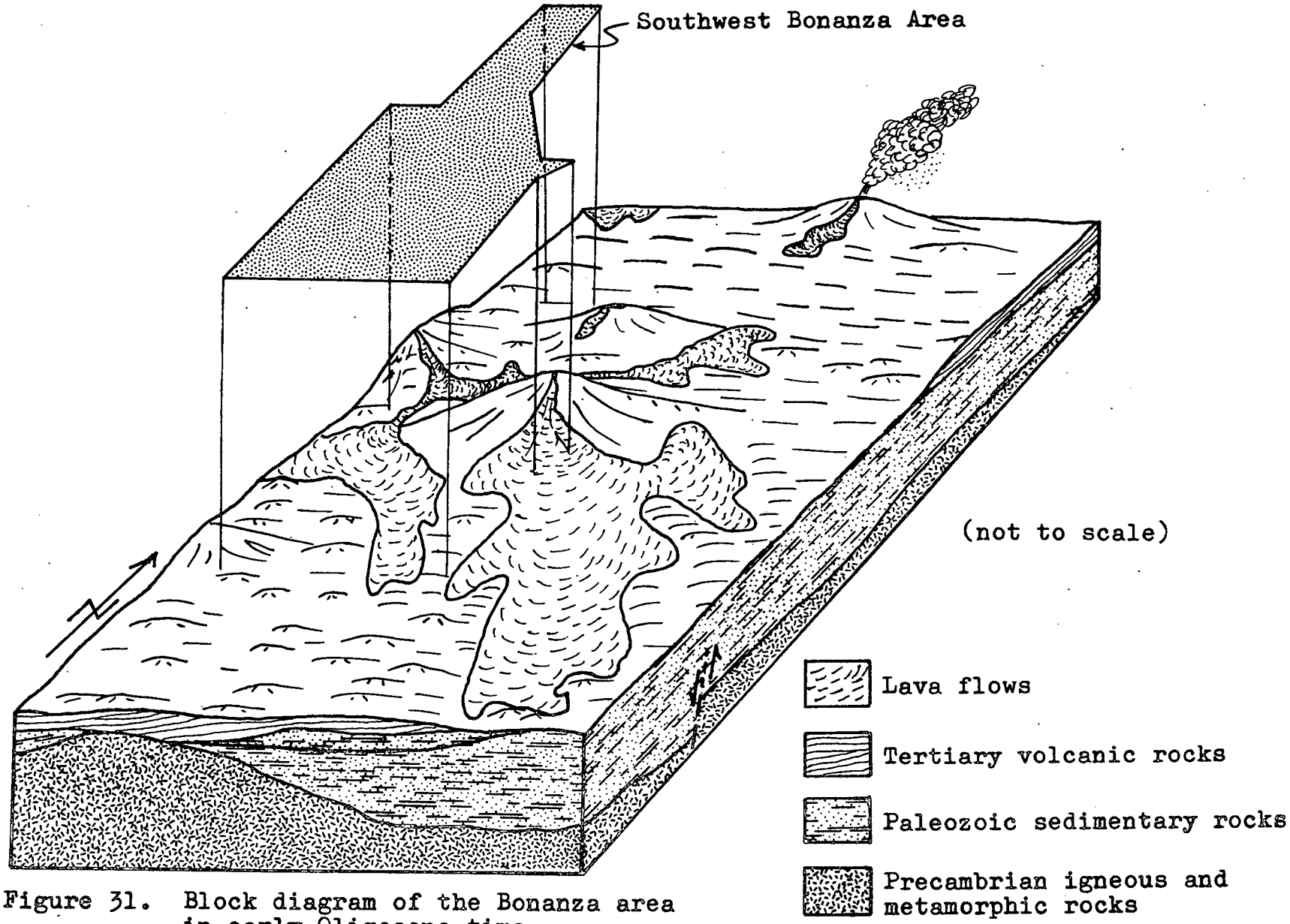

Figure 31. Block diagram of the Bonanza area in early Oligocene time.

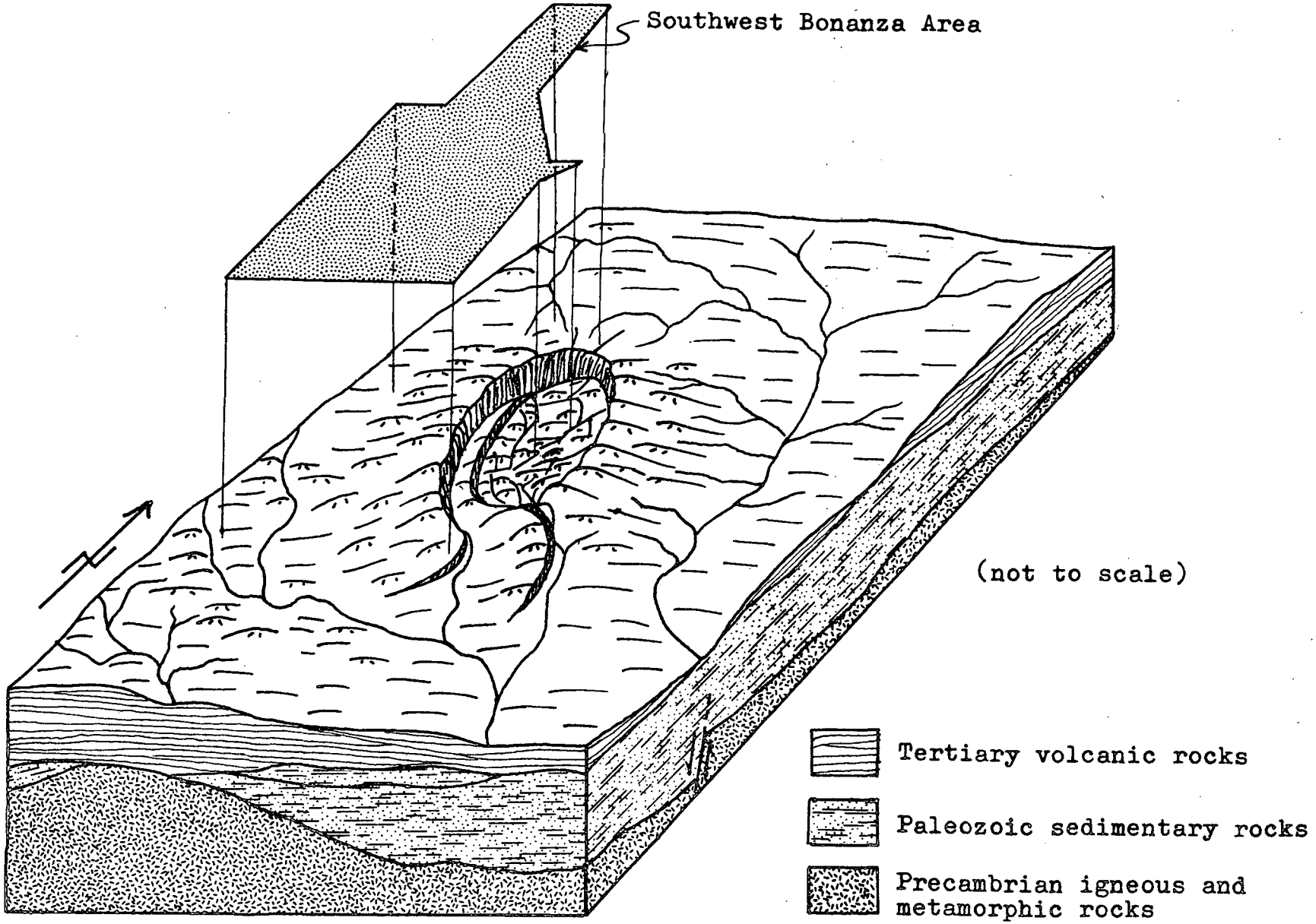

Figure 32. Block diagram of the Bonanza area in late Oligocene time, shortly after eruption of the Bonanza ash-flow tuffs.

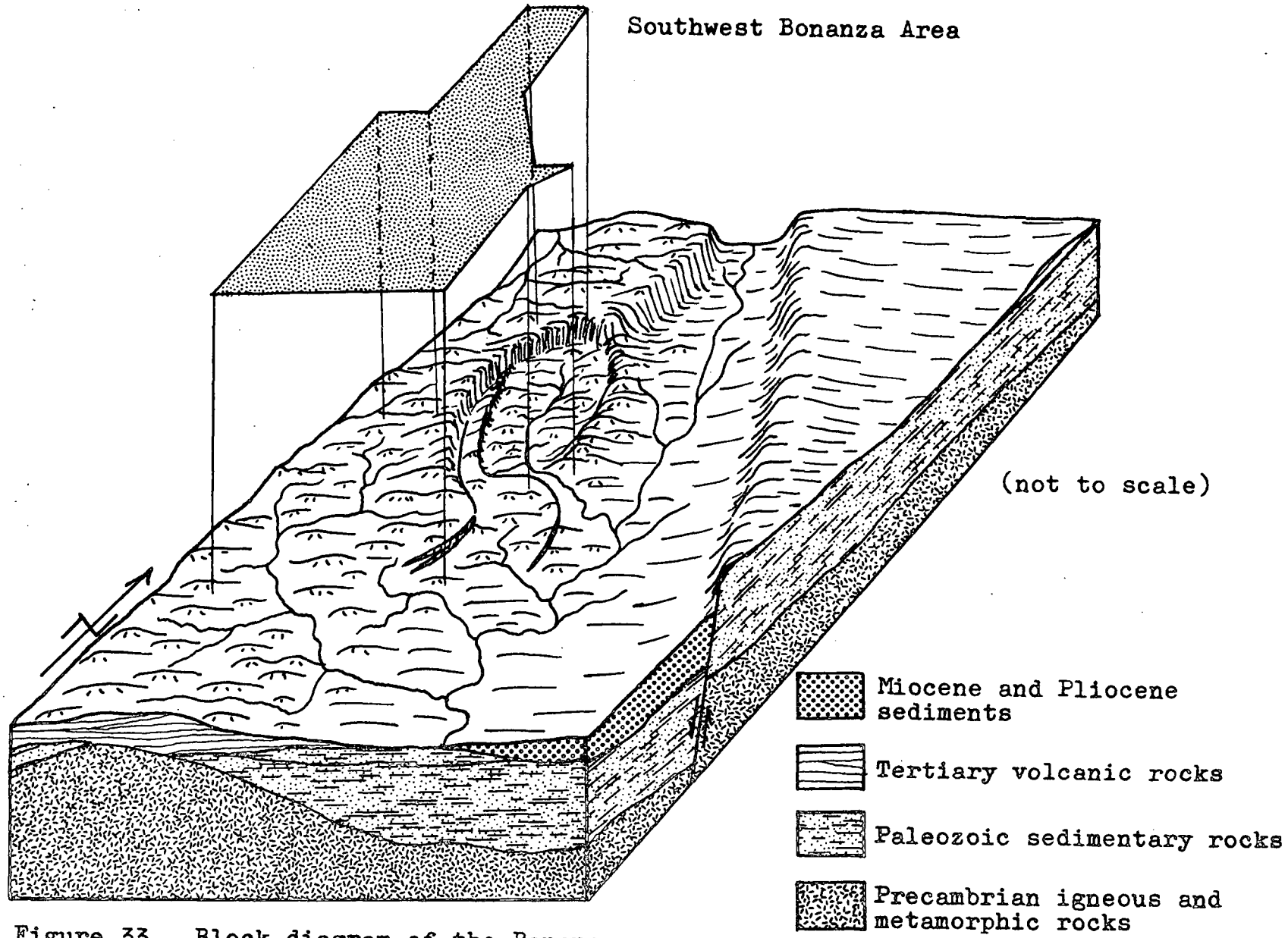

Figure 33. Block diagram of the Bonanza area in early Pliocene time.

Paleozoic plateau. Eruption continued from centers in and around the Bonanza area until a large composite cone had accumulated.

By late Oligocene time (fig. 32) the volcanic activity had evolved through an eruptive sequence which included explosive eruption of the Bonanza ash-flow sequence and ended with eruption of the late bi-modal sequence. Eruption of this vast amount of material reduced the supporting pressure in the magma chamber and allowed the roof of the chamber to collapse, forming the Bonanza caldera. Volcanic activity ceased soon after the collapse and a drainage pattern began to develop. The structure and topography controlled the development of these drainages, causing them to form an annular pattern around the caldera.

In Miocene and Pliocene time (fig. 33), a north-northwest-trending graben began to develop east of the caldera (in the region that is presently the northern San Luis Valley) as a result of regional taphrogenic forces. The Sangre de Cristo range developed along the eastern edge of the graben while the paleo-Arkansas river (then flowing southward into what is now the Rio Grande drainage) deposited vast quantities of clastic debris in the deepening graben (Van Alstine and Lewis, 1960; Van Alstine, 1968). The Bonanza caldera, lying along the western edge of the graben served as a zone of structural weakness which was

reactivated as part of the graben fault system. The resulting down-to-the-east displacement along the caldera faults increased the total displacement along the western side of the caldera, and reduced displacements on the reactivated faults along the eastern edge of the caldera.

The Bonanza caldera is at the point where the Rio Grande rift makes the transition from its expression as a narrow graben (the Arkansas Valley) to the broader, down-to-the-east, hinge structure of the San Luis Valley. The Bonanza caldera may have strongly influenced the development of the northern Rio Grande rift system by serving as a hinge point for this change in structural pattern.

GEOPHYSICAL SURVEYS IN THE BONANZA AREA

A regional gravity survey of the Bonanza area (Karig, 1965) defined a northwest-southeast elongate gravity low corresponding roughly to the central collapse region of the Bonanza caldera (fig. 34).

The steep topography of the Bonanza region limits the accuracy of the Bouguer anomaly map because adequate terrain corrections are difficult or impossible to compute. Therefore, the low-amplitude anomalies superimposed upon the larger anomalies may be spurious, and no attempt should be made to interpret them. However, the regional anomalies are undoubtedly real (assuming 2.67 g/cm^3 is a reasonable approximation for the slab-density).

Interpretation of the Bonanza gravity low is relatively straightforward. The approximation of the observed gravity anomaly with the computed anomaly for an elliptical cylinder (Karig, 1965) is certainly sufficiently accurate within the limits of the survey and the assumptions inherent in the computed model. However, it is significant to note that the observed gravity anomaly extends northwestward well beyond the Western Boundary Fault which marks the limit of the central part of the caldera. This extension of the anomaly might be interpreted as evidence that the central collapse zone extends beyond the Western

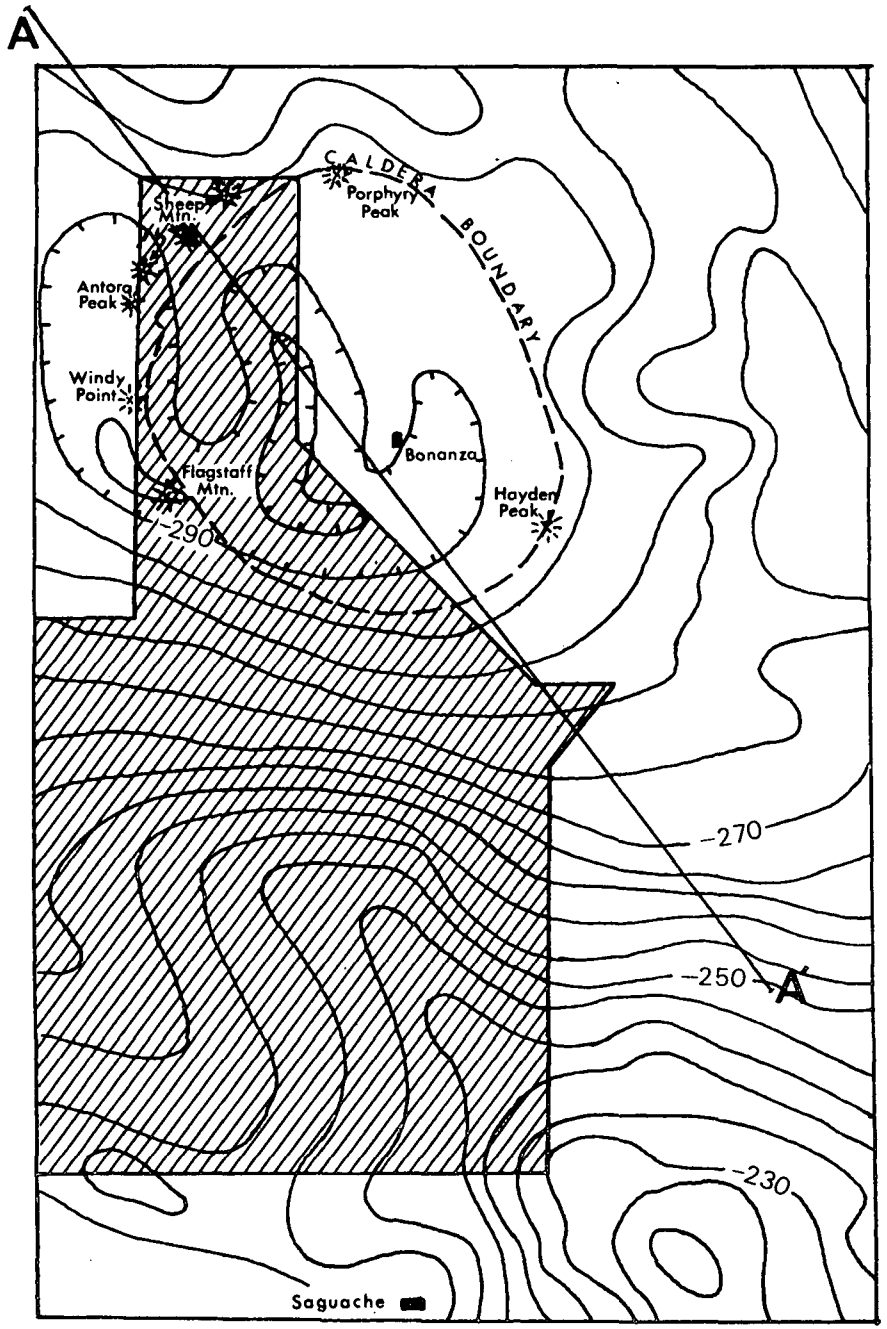

Figure 34. Bouguer gravity map of the Bonanza area (after Karig, 1965).

N

Southwest Bonanza area

-250 Gravity contours (hachures indicate closed lows, contour interval-4 mgal)

Generalized caldera boundary (generalized from plate 1)

Hayden Peak High mountains

A-A' is the line of vertical section for computed model (fig. 36)

0 2 4 6 8 10 mi

Scale

Boundary Fault, but the presence of the Bonanza Formation capping Antora Peak and other mountains along the western caldera rim is ample evidence that the Western Boundary Fault represents the actual limit of the central collapse zone.

A second possible interpretation of the northwest extension of the Bonanza gravity low would be that another low lies immediately northwest of the Bonanza center (beyond the limit of the map). This second low would combine with the observed gravity low to extend the anomaly into the area between the two. Karig's work gives no indication of the regional gravity trends, but work of Gaca (1965) and the regional Bouguer gravity map compiled by the U.S. Air Force (fig. 35) shows a gravity trough trending west-northwest from the Bonanza center into a larger gravity low centered over Blue Mesa Reservoir. However, the regional gravity map shows a divide between the two anomalies indicating that they do not merge. The Bonanza low, as contoured on the regional map corresponds very well to the central collapse zone of the Bonanza caldera. This leaves some doubt as to the validity of the northwest extension of the Bonanza gravity low, but, assuming that it is real, it is unlikely that the regional low trend is solely responsible.

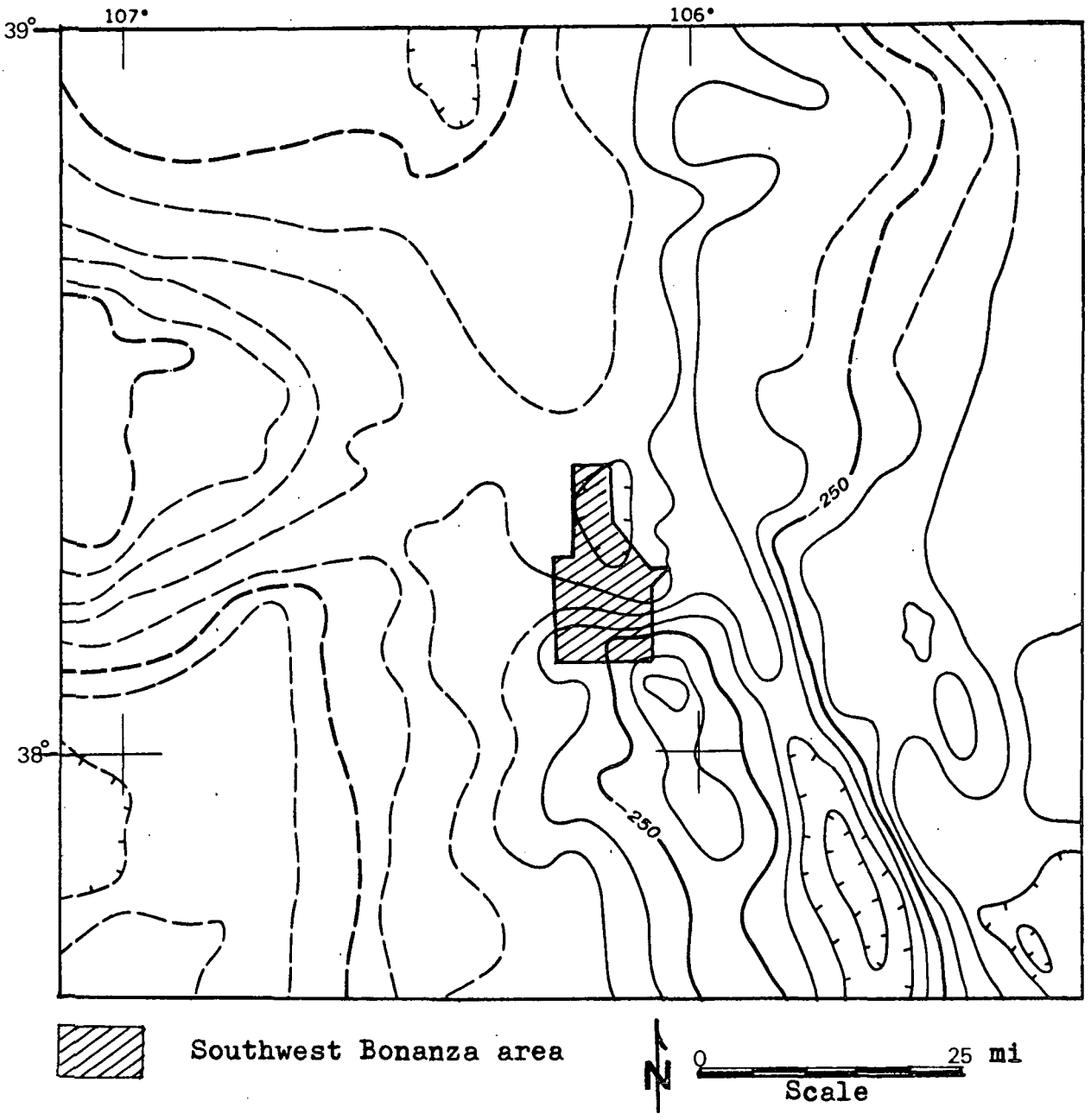

Figure 35. Regional Bouguer gravity map of the Bonanza area showing the relationship of the Bonanza gravity low to regional trends (after U.S. Air Force, 1968, map I-533-B).

A third possible interpretation of the shape of the Bonanza gravity low requires that the cylindrical, low-density mass, proposed by Karig as a model for volcanic rocks within the collapse zone, be tilted westward to allow for a greater volume of low-density material near the Western Boundary Fault.

A tilted elliptical cylinder model was computed for profile A-A' (fig. 34) to be compared to the vertical elliptical cylinder hypothesized by Karig (fig. 36-A). The computed profile for the tilted cylinder fits the observed gravity profile better than does the computed profile for the vertical cylinder. Furthermore, the tilted cylinder model does not require that the low-density mass extend beyond point "X" (fig. 36-A & C), the outcrop point of the Western Boundary Fault. Because the tilted cylinder model fits both the observed gravity profile and the relative structural relationships observed in the Bonanza area, I favor it as the most reasonable interpretation of the Bonanza gravity low.

The considerable discrepancy between the depth of the anomalous body in the computed models (figs. 36-A and 36-C) and the mapped structural relief along the western boundary of the Bonanza caldera (≈2,000 ft) may be due in part to error in the estimates of density contrast and to over-simplification of the models.

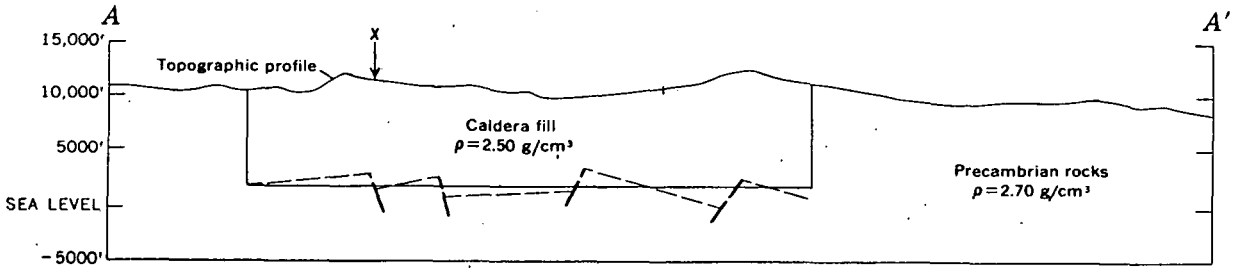

Figure 36-A. A section through a vertical cylindrical mass that will produce a gravity anomaly similar to that observed along profile A-A' (fig. 34) in the Bonanza area (after Karig, 1965).

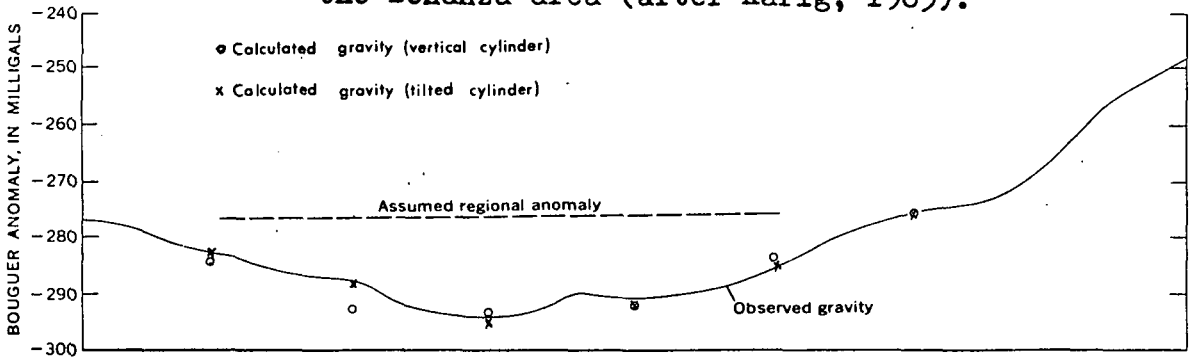

Figure 36-B. Comparison of observed gravity and computed gravity profiles for vertical and tilted cylindrical models.

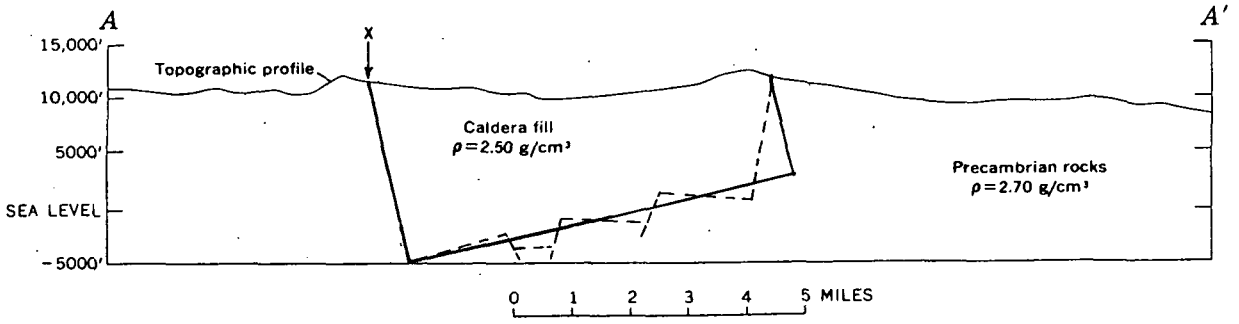

Figure 36-C. A section through a tilted cylindrical mass that will produce the observed gravity anomaly along profile A-A' and is confined to the mapped boundaries of the central caldera.

Note: Body A (hypothesized by Karig, 1965) extends beyond point X (representing position of Western Boundary Fault). Body B allows better correlation between the observed and calculated gravity profiles and does not extend beyond point X. Model B was computed using the Lachenbruch (1957) solid-angle graticule as employed by Karig (1965).

The only magnetic data available for the Bonanza area are the aeromagnetic maps compiled by Zietz and Kirby (1968 and 1972). The 1972 Colorado aeromagnetic map provides the greatest detail, but even it gives only a rough indication of the magnetic field in the Bonanza area. Because a magnetic field is directional, zones of anomalous susceptibility normally produce a matched high and low adjacent to one another and positioned north and south of the anomalous body. Interpretation of the regional magnetic intensity map for the Bonanza area (fig. 37 A, B, C (inset)) suggest that it is a composite anomaly produced by the combination of magnetic fields representing each of several bodies. Three lobes of the anomalous trend lie within the southwest Bonanza area. The southeastern lobe suggests an anomalous body lying near the southeast corner of the southwest Bonanza area. The central lobe suggests a body of high susceptibility in the southern part of the central collapse area, while the northwestern lobe corresponds to an anomalous body in the vicinity of Sheep Mountain. The relatively high relief exhibited in the magnetic contours denotes that the anomalous bodies are at- or near-surface, but the exact nature of anomalous bodies can not be determined. They could represent volcanic plugs or necks, zones of relatively high iron content, or fluctuations along a major basement discontinuity. But, detailed interpretation of such anomalies requires knowledge of the relative susceptibilities of the rocks involved. No

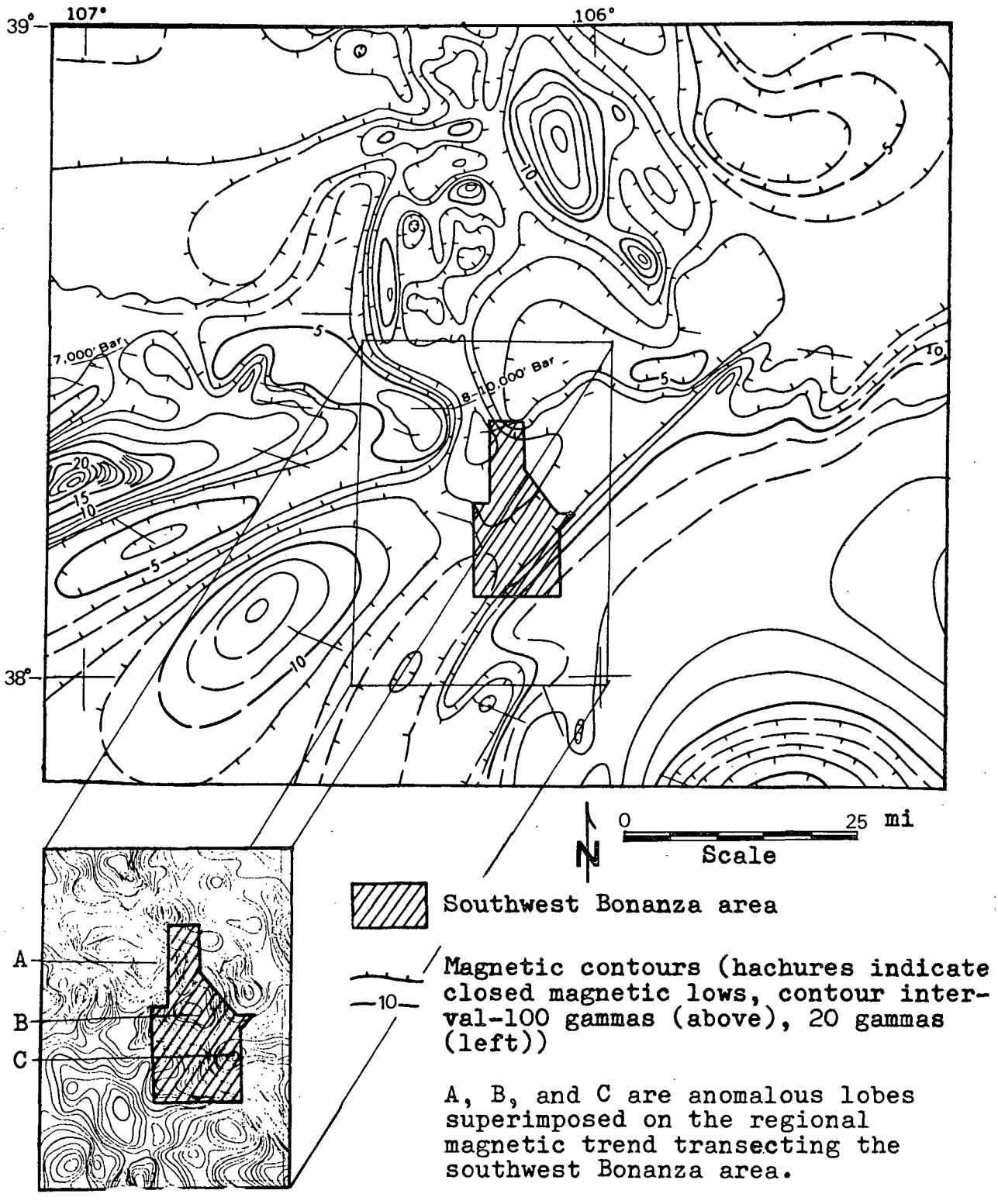

Figure 37. Regional magnetic map of the Bonanza area (generalized map after Zietz and Kirby, 1968, map I-533-A; detailed aeromagnetic map (inset) after Zietz and Kirby, 1972, map GP-880).

such figures are available for the rocks of the Bonanza area and no reasonable generalizations can be made about their relative susceptibilities. Consequently, the only conclusions about the Bonanza area that can be drawn from the magnetic intensity map are: 1) that a major northwest-southeast trend passes through the area, 2) this regional trend is sufficiently strong and continuous to be interpreted as a regional change related to basement structures, and 3) minor lobes along the major northeast-southwest trend reflect near-surface anomalies in the southeast, central, and northwest portions of the southwest Bonanza area, but the significance of these local anomalies could not be determined.

ALTERATION AND MINERALIZATION

Hydrothermal alteration and mineralization are common in the southwest Bonanza area, but are not as intense as in the central mining district mapped by Burbank (1932). Burbank studied the mineralization of the central Bonanza district in detail. He found that the mineralization was fault-controlled and was emplaced during two stages of hydrothermal activity. The first stage of mineralization occurred shortly after the development of many of the faults and fissures and consists mainly of barren silicification. The second stage of mineralization was more favorable for sulfide deposition throughout the district, but the resulting mineral deposits show recognizable differences between the northern and southern parts of the district:

> "According to their mineral contents the principal veins of the district may be divided into two main classes--(1) quartz veins of relatively high sulfide content, carrying lead, zinc, copper, and silver, usually with negligible amounts of gold, and (2) quartz-rhodochrosite-fluorite veins of low sulfide content, only one of which enriched in silver has been productive" (Burbank, 1932, p. 60).

The high-sulfide veins are located, almost exclusively, in the northern part of the district, while the quartz-rhodochrosite-fluorite veins are concentrated in the southern part of the district. Burbank also observed changes in the

mineralization with depth. He found that lead-silver and lead-zinc ores of the northern district increased in copper content with depth (1932, p. VIII).

Mineralization in the southwest Bonanza area exhibits many of the same characteristics described by Burbank in the central mining district. Two stages of hydrothermal activity can be recognized. The first stage produced mostly silicic alteration and was largely confined to the area within and immediately surrounding the Bonanza caldera. The second stage of hydrothermal activity affected rocks throughout the southwest Bonanza area. The major products of this second surge of alteration are the sericitization and propylitization which occurs throughout the area. Some zonation is apparent in this second stage alteration. The most intense sericitization occurs near fractures and faults which must have carried the hydrothermal solutions. Outward from these fractures, the intensity of sericitization decreases and grades into a broad zone of propylitization. The propylitization is widespread and its subtle intensity variations are practically impossible to map, but it, too, decreases in intensity outward from zones of intense alteration.

Mineralization throughout the southwest Bonanza area is associated with the second stage of hydrothermal activity. Each of the areas where significant mineral

development took place (Spook City, Klondike, Columbia, Antora) is characterized by a broad zone of intense sericitization and, in fact, there was some development in each of the major areas of sericitic and propylitic alteration. No definite zonation of the mineral distribution could be established for the area. Very little information was available for the various mines and prospects in the area and none is presently accessible. Surficial distribution of the altered and mineralized zones appears to be entirely controlled by the fracture pattern. A drilling program conducted by the Bear Creek Mining Company (Cook, 1960) is the only work in the southwest Bonanza area that gives any insight into the distribution of alteration with depth. In his analysis of the alteration changes in the three test holes drilled by Bear Creek Company (plate 1, in pocket), Cook states that there is evidence of a solfataric-hydrothermal boundary in hole 1 at 200 ft and that the intensity of hydrothermal activity persists or increases with depth. Cook also noted a horizontal intensity zonation similar to that observed in the southwest Bonanza area.

Both stages of hydrothermal activity affect the oldest and youngest volcanic units in the area, so the mineralization definitely post-dates the last eruptions. The highly silicic vein rocks deposited in the earlier period of

mineralization are commonly brecciated and some have been remineralized during the later stages of hydrothermal activity. Brecciation of the early, silicic, hydrothermal products denotes post-mineralization movement on the caldera faults.

The distribution of altered and mineralized zones in the southwest Bonanza area demonstrates that the caldera fault system provided channels by which the mineralizing fluids moved out from the Bonanza center. Zones of intense sericitization occur along most of the major faults radiating away from the Bonanza center and similarities in the mineralization seen along some of the radial trends demonstrate the continuity of the plumbing system. For instance, the Columbia and Klondike mines, which were the only producers in the district reporting significant amounts of free gold in quartz, are several miles apart, but lie along the same radial trend.

The concentric fracture system surrounding the Bonanza caldera has also exerted some influence on the mineralization. The larger areas of alteration and mineralization (such as the Klondike Mine and Spook City areas) are located at the intersections of major radial and concentric trends. Apparently, the mineralizing fluids moved out along the radial fractures and spread laterally into the fractured country rock where they encountered open

channels. The more intense mineralization at these intersections may also be due, in part, to changes in the temperature and pressure environment of the mineralizing fluids. It seems logical that such changes would occur when a mineralizing fluid, confined within a single channel, encounters open cross-channels. The intensely fractured zones along the major concentric faults provided many such zones and channels.

The alteration and mineralization in the southwest Bonanza area shows no preference for rock type. Most of the mineral deposits of the district and a large proportion of the exposed alteration in the area are within the Rawley Formation, but this appears to be a function of the location and relative abundance of the Rawley rocks with respect to the other lithologies. The Bonanza Formation and units of the upper bi-modal sequence are also altered and mineralized in structurally favorable areas, but the Rawley Formation is lowest in the sequence and most widespread, so it was ordinarily in the most favorable position to receive mineralization.

Many of the faults in the Bonanza area have been active since the last stages of hydrothermal activity. Consequently, the veins are commonly offset by the faults. This fact, again, demonstrates that structural adjustment

continued for some time along the same faults that served as channels for the mineralizing fluids. Because these late movements truncate the trends in mineralization, it is essential to understand the structural system in the area and stress systems that controlled post-mineralization structural activity. In order to successfully explore or develop ore deposits in the area, the structural patterns and controls must be recognized and used as a guide for constructing a model of ore distribution. Several of the remote-sensing techniques used in the southwest Bonanza area (particularly color photography and thermal infrared imagery) can be used as tools to help define this structural pattern.

REMOTE SENSING TECHNIQUES

The data presented in this report were gathered from interpretations of remote-sensing data and from field and laboratory investigations. The remote-sensing data were used in different ways in various regions of the southwest Bonanza area in an attempt to arrive at useful evaluations and comparisons, and yet, keep redundancy of interpretation to a practical minimum. Therefore, the amount of geologic information taken from the photography and imagery varies from area to area, but all features on the geologic map (plate 1, in pocket) that were interpreted from the remote-sensing data are also supported by field evidence. Features that were noted on photography or imagery, but could not be verified by field evidence have been omitted from the geologic map. The map compiled from photogeologic interpretations (plate 2, in pocket) includes even those features that could not be verified.

This section of the report discusses the procedures employed in evaluating the various types of remote-sensing data and the results of these evaluations. Some of the evaluations are limited by lack of data from certain sensors or by the inferior quality of some of the data. All of the evaluations are limited by the inherent subjectivity in the evaluation procedures and restriction

to the special characteristics of the southwest Bonanza test site. The sensors used and evaluated include color and color infrared photography, multiband photography, low sun-angle photography, thermal infrared imagery, infrared spectrometry, side-looking airborne radar, and radar scatterometry.

Spectral Reflectance Measurements

Spectral reflectance measurements were made for selected rock units in the Bonanza area. These measurements included both visible range and photographic-infrared range measurements with a field spectroradiometer and laboratory measurements of thermal infrared reflectances. The thermal infrared reflectance analyses were conducted by Martin Marietta Corporation personnel using a Gier Dunkle parabolic reflectometer. This instrument measures energy reflected from a target in the 7-14 μm range. The operation and capabilities of this instrument are discussed in more detail in Martin Marietta Corporation report (Gliozzi and others, 1970). The plotted spectral emissivities (figs. 8, 9, 10, and 11, p. 22-25) were computed from the measured spectral reflectances using Kirchoff's law ($\epsilon_\lambda = 1-\rho_\lambda$).

spectral emissivity = 1 - spectral reflectance

Reflectances were measured for both freshly cut and weathered surfaces of the rock samples (figs. 10 and 11,

p. 24-25). In addition, the variation in reflectance with position on the sample (fig. 8, p. 22) and viewing angle (fig. 9, p. 23) were evaluated. The following conclusions were drawn from these and other evaluations:

1. Weathering influences spectral signatures in an unpredictable manner. Some spectra appear to be affected only in amplitude, but others show marked changes in character.

2. Viewing-angle affects the amplitude of spectra from rocks which are relatively homogeneous. However, rock samples that are relatively inhomogeneous, either in composition or texture, yield spectra that vary in character with changes in viewing angle.

3. Spectral variations with changing position on the sample were largely dependent on the sample homogeneity. Spectra for the more homogeneous rock types were very similar for different points on the sample surface. Inhomogeneous rocks showed considerably greater variations.

4. The slit-width (i.e. the wavelength resolution) of the instrument is not a critical factor in obtaining representative spectra. The overall character of the spectra for the test samples was not significantly degraded by increasing the slit-width from 50 nm to 250 nm.

These conclusions suggest that considerable difficulty should be expected in trying to apply laboratory-derived spectral recognition criteria to lithologic units in the field, because field applications allow little or no opportunity for control of the critical "rock condition and orientation" parameters. Spectral signatures derived in the field are further complicated by noise introduced by soil, vegetation, moisture, and atmospheric effects. Others who have researched techniques of lithologic identification by spectral signatures (Lyon and Patterson, 1966) have encountered this problem and have had relatively little success in field applications. However, it was anticipated that some of the lithologies of the Bonanza area would exhibit sufficiently strong spectral contrasts to allow some chance for field discrimination with an airborne infrared spectrometer.

Laboratory spectral emissivity curves were derived for samples of the three Precambrian lithologies (figs. 10 and 11) of the Bonanza area and representative samples from each of the three major groups within the volcanic sequence (fig. 38). For both the Precambrian rock samples and the volcanic rock samples, weathering differences, changes in viewing geometry, and inhomogeneities within the samples thwarted efforts to obtain representative emissivity curves. Figure 39 compares emissivity curves

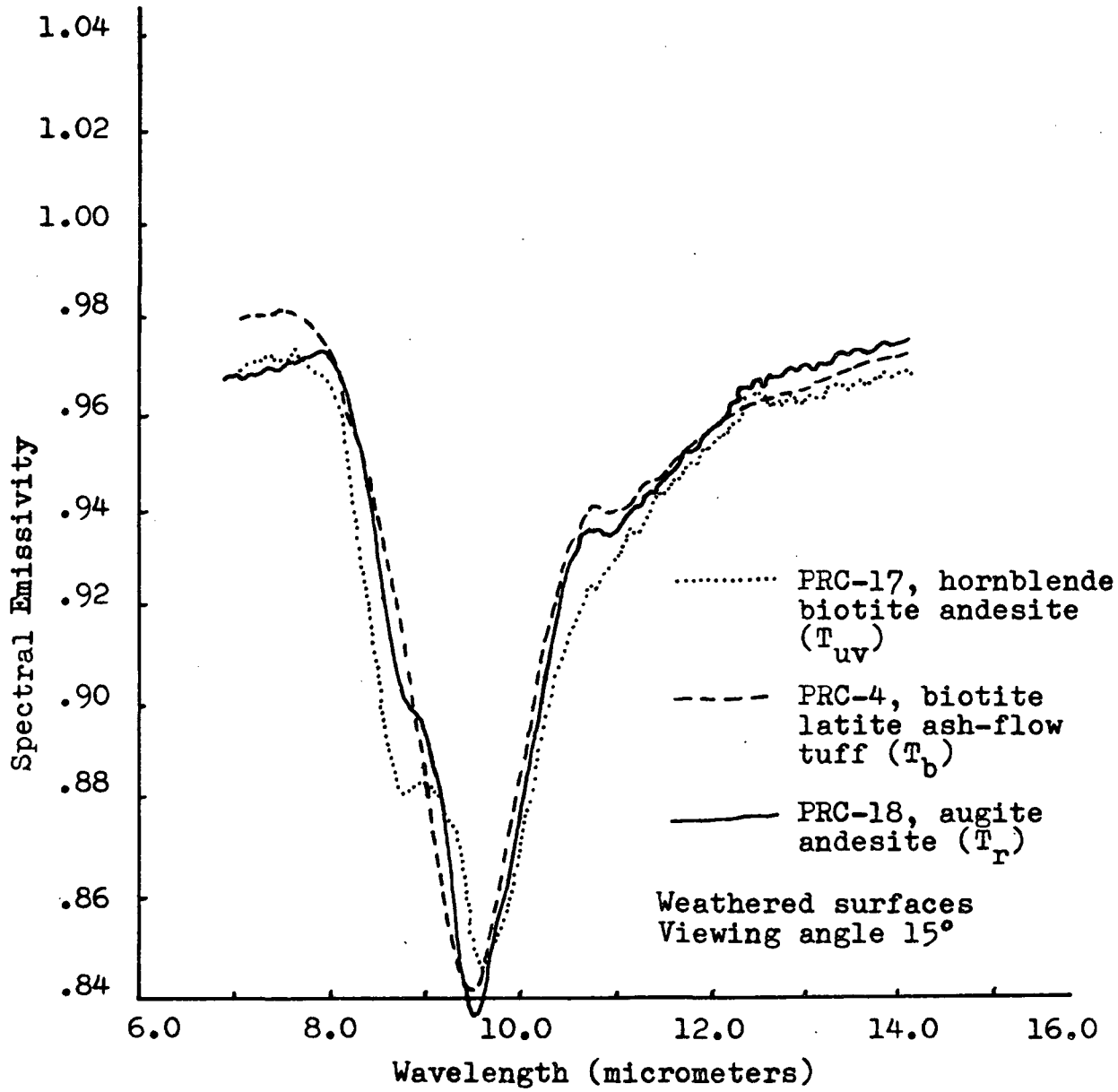

Figure 38. Infrared spectral emissivity curves for major volcanic units of the southwest Bonanza area. Curves for other samples of the same lithologies vary considerably from these which were selected as examples demonstrating that no reliable differences could be established for the three units. (After Gliozzi and others, 1970)

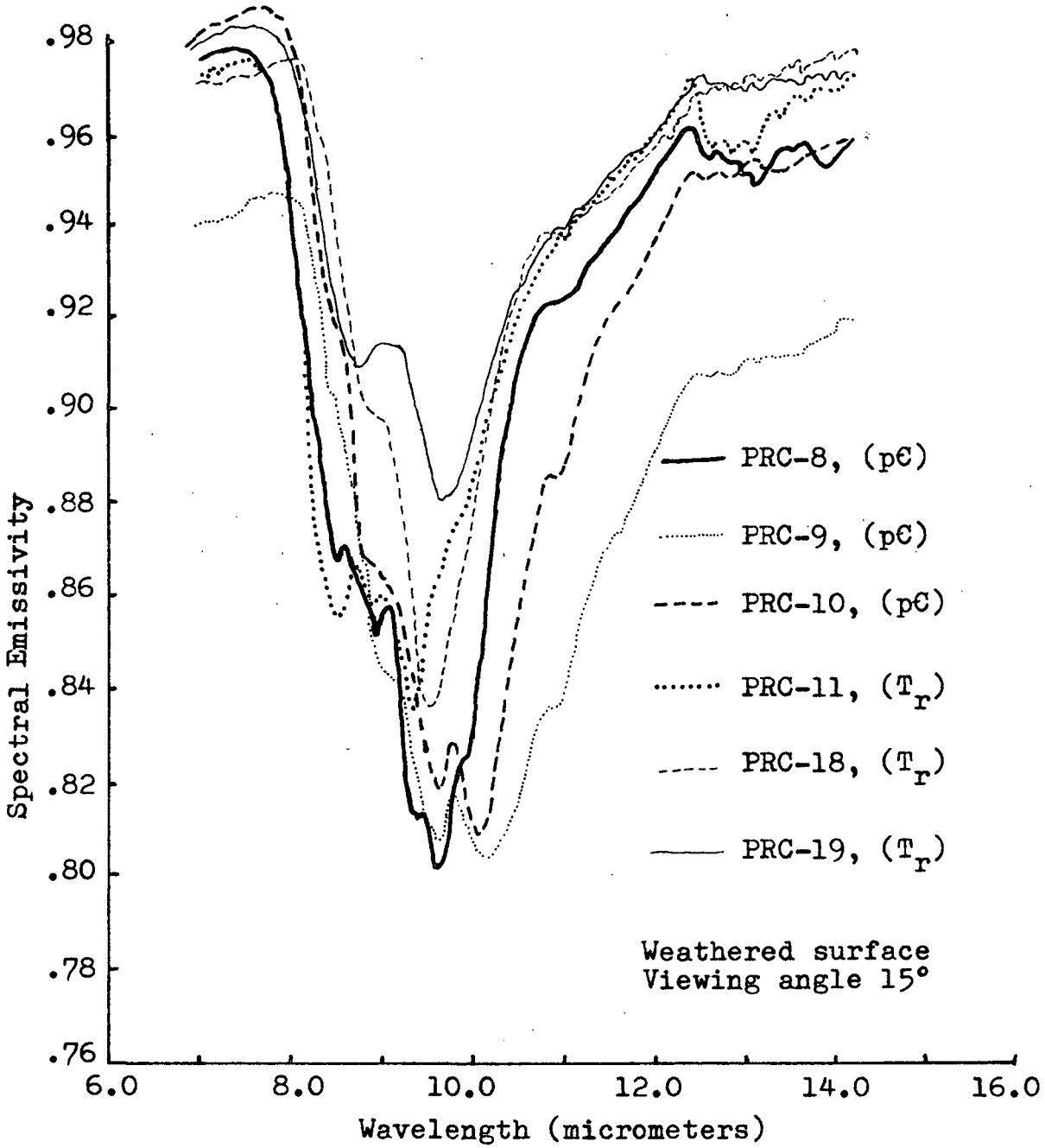

Figure 39. Comparison of emissivity curves for three Precambrian lithologies (PRC-8, quartz monzonite; PRC-9, hornblende gneiss; and PRC-10, migmatite) to emissivity curves for three lithologies of the Rawley Formation (PRC-11, hornblende basalt; PRC-18, augite basalt; and PRC-19, biotite augite basalt). No emissivity characteristics that can be used as a basis for distinction between the Precambrian rocks and the Rawley Formation are apparent. (After Gliozzi and others, 1970)

for the three Precambrian rock samples to three curves obtained for three different samples from the Rawley Formation. No characteristic emissivity differences can be seen that will allow distinction to be made between the Precambrian rocks and the Rawley Formation.

The only lithology tested which consistently gave a unique infrared spectral emissivity curve was dolomite from the Manitou Formation (fig. 40). The dolomite test sample was sufficiently homogeneous that a characteristic emissivity curve could be derived even when test parameters (surface conditions, viewing angle, target point, and instrument resolution) were varied. This result suggests that the Manitou Formation is distinguishable from the tested Precambrian and volcanic rocks in the thermal infrared range. However, outcrop of the Manitou Formation is very limited in the southwest Bonanza area and the ability to distinguish it from other lithologies is of little consequence.

The thermal infrared spectral reflectance measurements left little hope for success in identifying or discriminating important rock units in the Bonanza area with the airborne infrared spectrometer. Nevertheless, plans were made to gather a limited amount of spectrometric data over an area carefully selected on the basis of the anticipated spectral contrast between exposed rock types. Two separate attempts were made to gather spectrometric data in areas where the Manitou Formation was

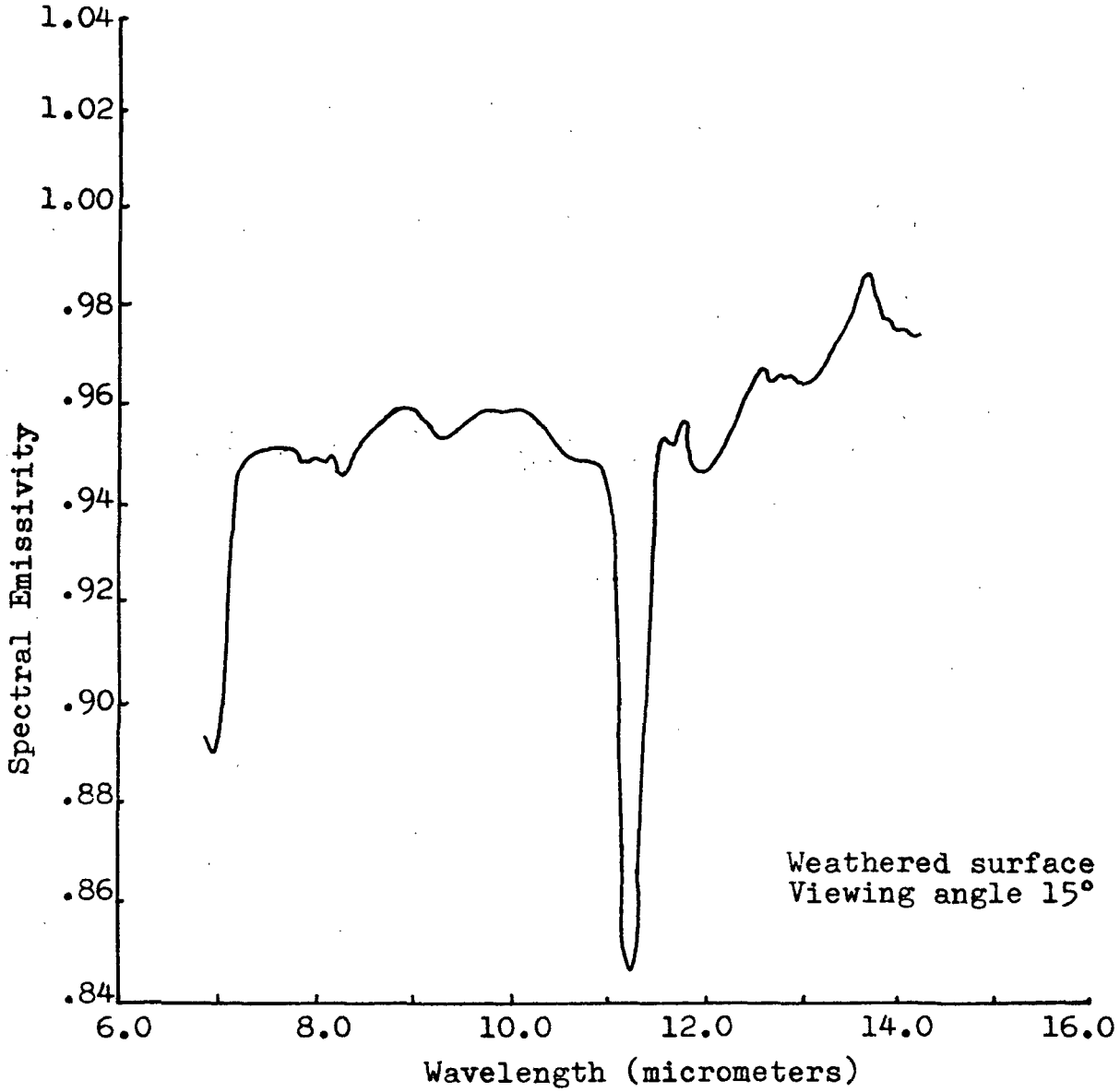

Figure 40. Typical spectral emissivity curve for Manitou dolomite (PRC-7). Measurements on this sample gave similar curves regardless of changes in surface condition, viewing angle, target point, and instrument resolution. The emissivity curve for the Manitou is considerably different from curves derived from all other samples. (After Gliozzi and others, 1970)

exposed in contact with other Paleozoic units and lavas of the Rawley Formation. In the first attempt the data could not be properly correlated to the ground track due to a malfunction of the boresight camera. The second set of spectrometer data, flown on a later mission, has not yet been received. Consequently the spectrometer evaluation is still incomplete.

Spectral reflectance measurements in the visible and near infrared range (400-1100 nm) were made for a few of the Tertiary volcanic units to evaluate the possibilities for distinguishing the Rawley Formation from the underlying Precambrian and Paleozoic lithologies and from the overlying Bonanza Formation using selective band-pass sensors.

The spectral measurements were made on rock outcrops in the field. The energy reflected from selected rock surfaces was recorded using an ISCO (Instrument Specialties Company) spectroradiometer which is capable of measuring incident radiation in a very narrow band ($\approx$25 nm) at selected intervals. These measurements were then ratioed to a similar measurement of incoming solar radiation to determine the reflectance.

$$\text{target reflectance} = \frac{\text{radiation reflected from target}}{\text{solar radiation incident on target}}$$

Measurements of incoming solar radiation were made in one of two ways. At some stations the incoming solar radiation was measured directly by bracketing each suite of target readings with comparable sets of readings taken with the spectroradiometer pointed at the sun. Readings from the two "solar sets" were then averaged to yield a value with which to compare each target reading.

An attempt to eliminate the uncertainty produced in the time differential between target and solar readings was made by taking simultaneous solar readings with a separate instrument. A Kahlsico universal radiation meter was used to take these simultaneous solar readings. The Kahlsico radiation meter does not measure electromagnetic energy in a narrow band, as does the ISCO spectroradiometer. Instead, it measures the total incident radiation in the 300-to 3,000-nm region. In order to make the total radiation measurements of the Kahlsico comparable to the spectral radiation measurements of the ISCO, it was necessary to assume the response of both instruments to be linear with respect to radiation intensity and to assume measured fluctuations of incoming solar radiation result from proportional attenuations of all bands in the spectral region.

With these assumptions, several suites of solar data were collected simultaneously with the Kahlsico radiation meter and the ISCO spectroradiometer. These measurements

were then used to construct a conversion chart (fig. 41) by which the total solar measurements taken with the Kahlsico could be converted to spectral radiation measurements. The relative positions of the conversion lines reflect the effects of the spectral distribution of the incoming solar radiation and the varying response of the ISCO in the different spectral bands. The linearity of the conversion lines as they were plotted on the conversion chart demonstrates that the two assumptions made are generally valid. However, in spectral regions where atmospheric absorption is strongest, the reflected energy level may be too low to be accurately measured. Consequently, these atmospheric absorption bands have been designated as regions of "uncertainty" on each of the reflectance curves.

The spectral curves for various units of the Rawley Formation (fig. 42) show as much, or more, variation between different units of the Rawley as between the Rawley and other formations (figs. 43 and 44). However, most of the Paleozoic sedimentary units exhibit a series of spectral reflectance peaks in the 700- to 1,100-nm range which are not present in any of the spectra of the Rawley Formation. This difference should allow discrimination between many of the paleozoic sedimentary rocks and the Rawley Formation in areas of good outcrop. Spectral

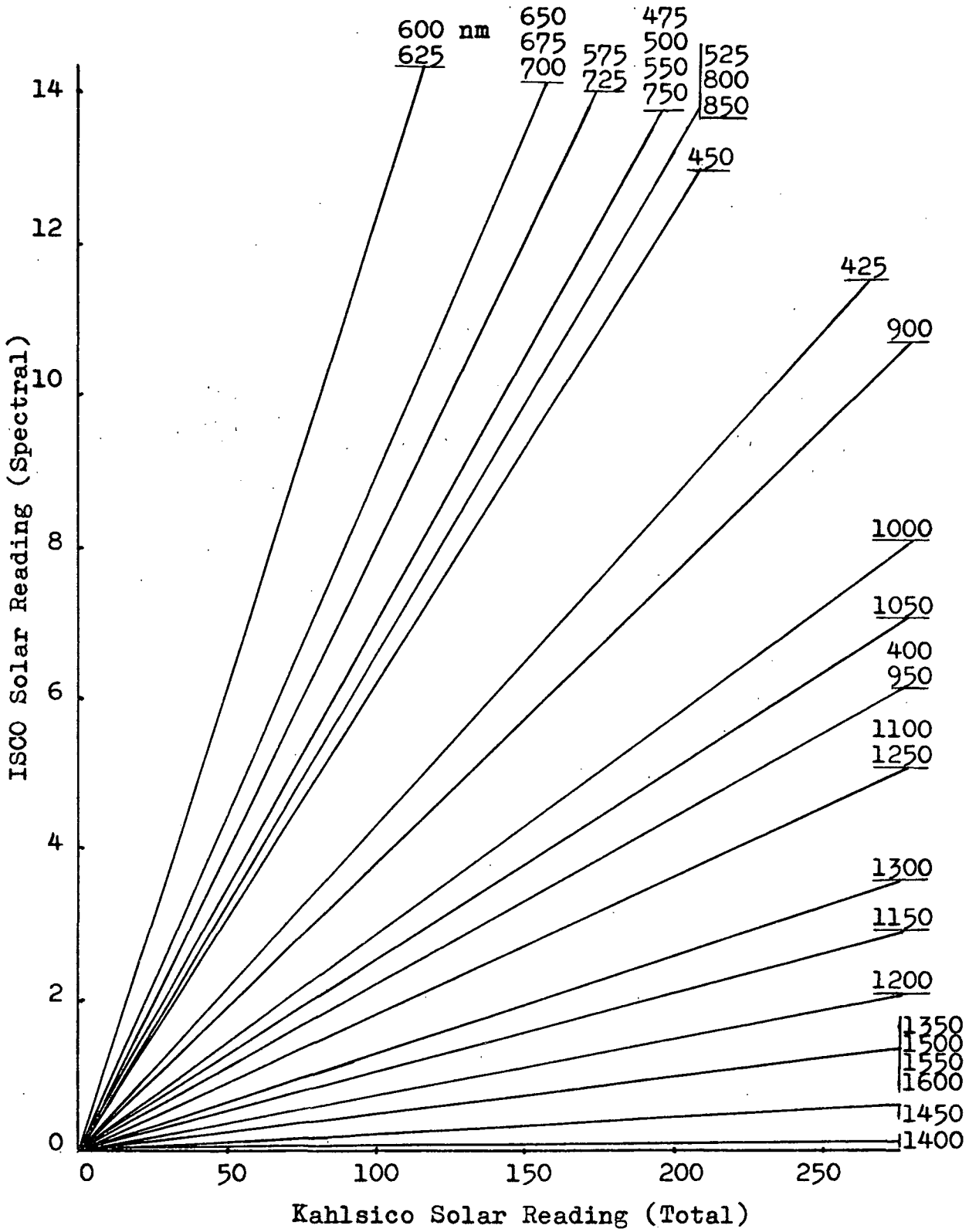

Figure 41. Nomogram for conversion of total solar intensity readings to spectral intensity readings.

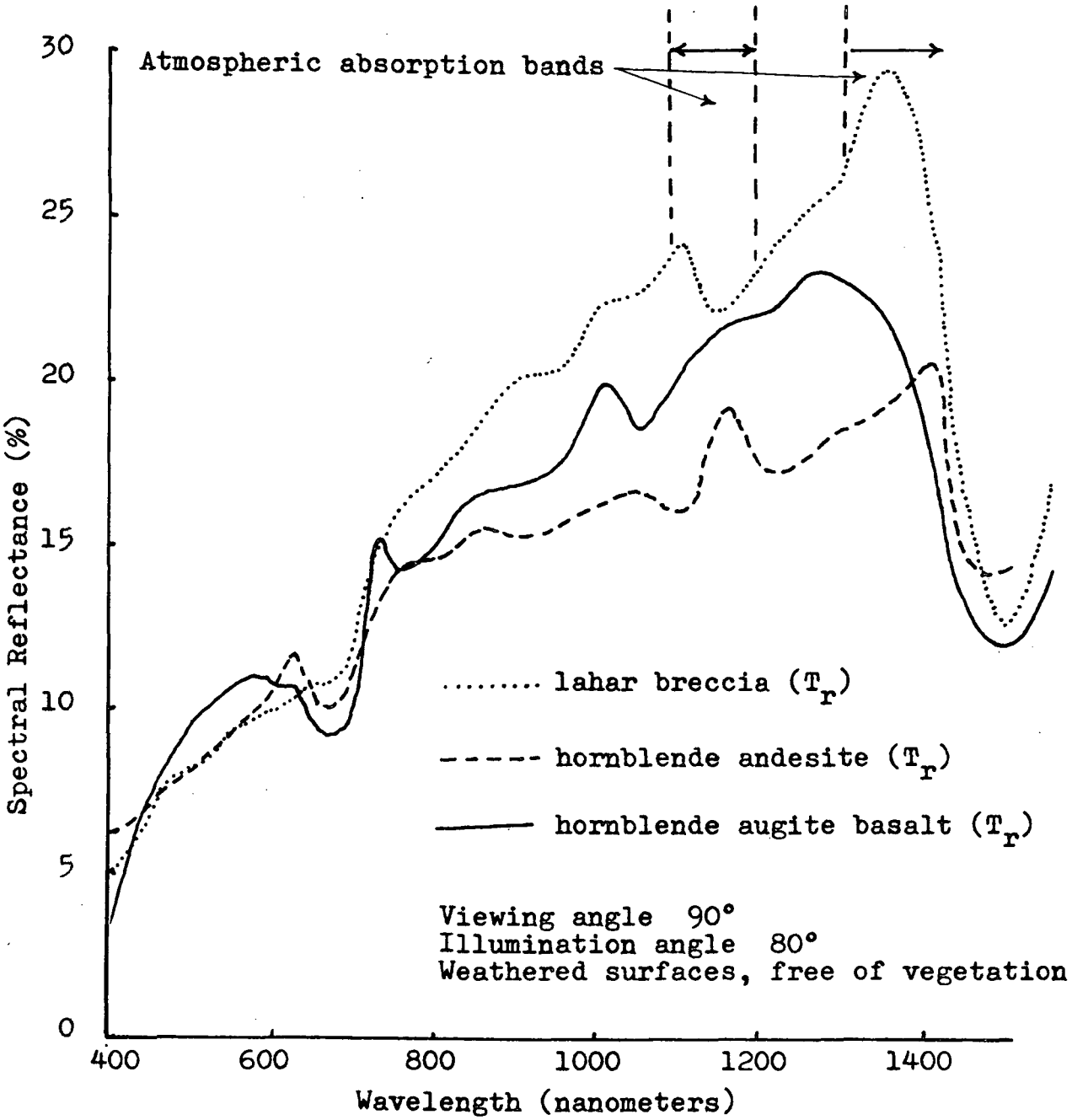

Figure 42. Comparison of visible- and near infrared-range spectral reflectance measurements for three lithologies of the Rawley Formation.

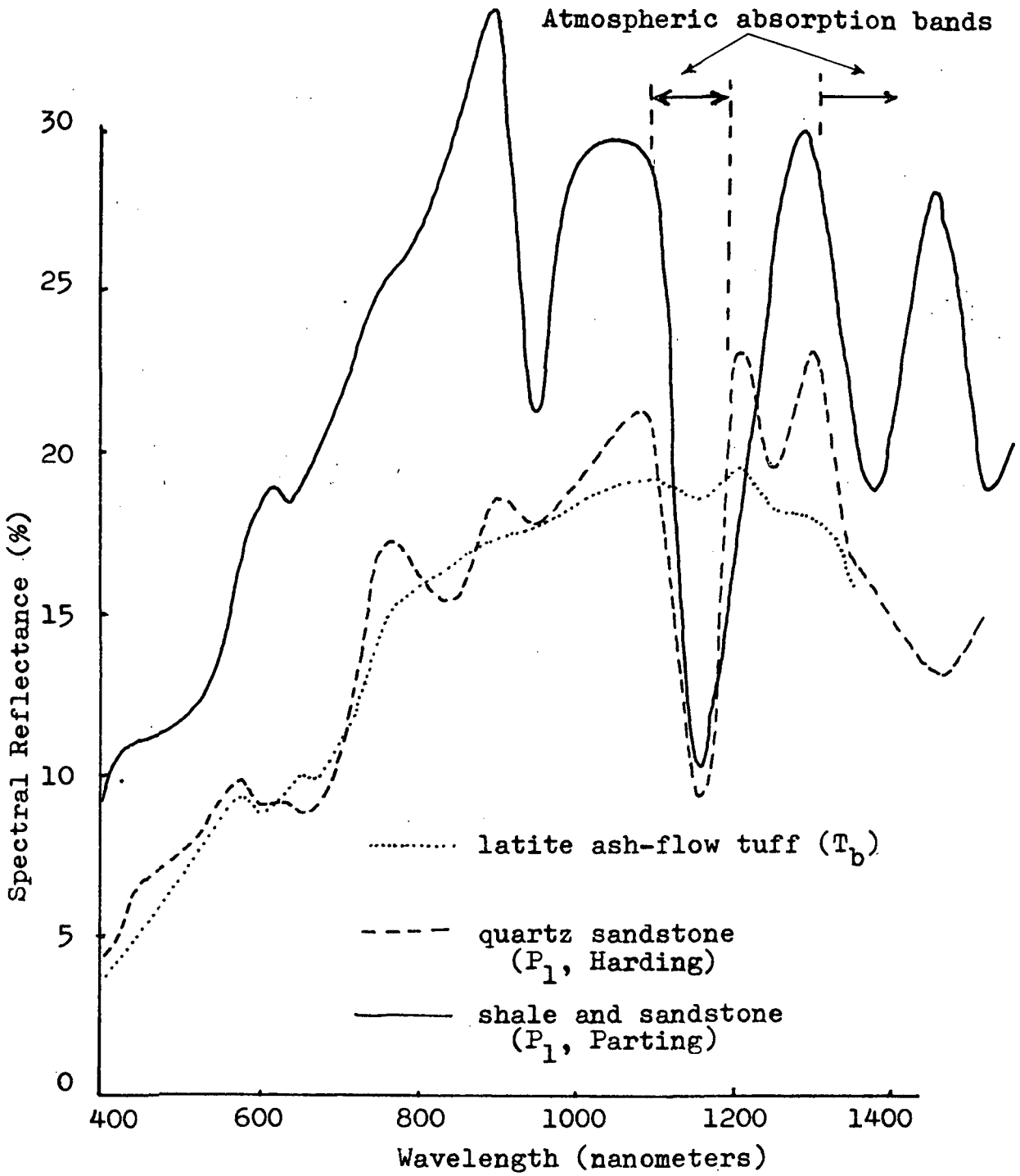

Figure 43. Visible and near infrared spectral reflectance curves for the Bonanza Formation and for two sandstones of the lower Paleozoic sequence. The difference between the curves for the sandstones are much greater than the differences between the curve for the quartz sandstone and the curve for the Bonanza ash-flow tuff.

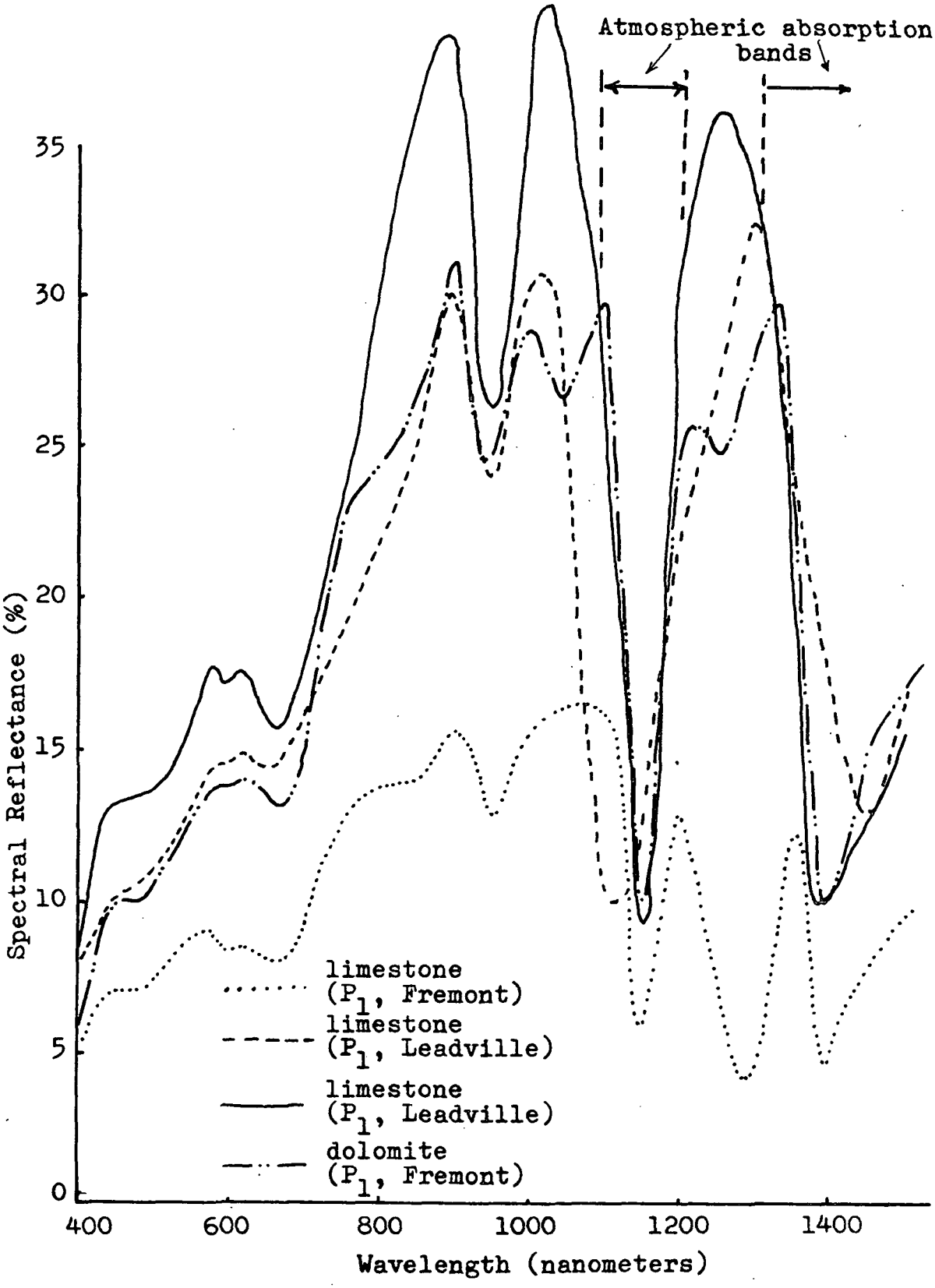

Figure 44. Curves for four carbonate lithologies of the lower Paleozoic sequence. Although total reflectance values vary considerably, all exhibit some common characteristics, such as the reflectance peak in the 820- to 920-nm range.

contrast between the Rawley Formation and the overlying Bonanza Formation is not nearly as apparent. The only characteristics of the Rawley spectral curves which might allow for discrimination are a slight spectral reflectance low in the 600- to 700-nm range, and a reflectance peak in the 1,000- to 1,100-nm range. These same features are also seen on the spectrum for the Bonanza Formation, but are not as strong. The 1,000- to 1,100-nm range lies outside the limit of the near-infrared photographic range, and so, does not lend itself to photographic techniques, but may be imaged by means of a scanner. The 600- to 700-nm range is the red portion of the visible spectrum. The subtle difference between the spectral curves for the Rawley and Bonanza formations in this region suggests band limited photography and additive viewing or ratioing as a means of distinguishing between the two formations. Results of actual multiband analysis (detailed in a later section of this report) indicate that the red band is the best band for Rawley-Bonanza outcrop discrimination. Wherever the Rawley-Bonanza contact is well exposed, it is readily apparent on the red-band photography. However, the Rawley-Bonanza contact is seldom exposed in outcrop, and discrimination of the two formations becomes difficult or impossible in areas of soil or vegetation cover.

Color and Color Infrared Photography

High-Altitude Color and Color Infrared Photography: High-altitude color and color infrared photography of much of the greater Bonanza test site was obtained on flights 8 and 9 of NASA Mission 101 in August, 1969. These data were obtained from NASA's RB-57 aircraft carrying two Wild-Heerbrugg RC-8 aerial cameras and one Zeiss RMK 30-23 aerial camera at an altitude of 60,000 ft above mean sea level (amsl). The RC-8 cameras were equipped with 6-in.-focal-length lenses and synchronized to give identical coverage with color and color infrared photography at a scale of 1:100,000 on a 9- by 9-in. format (fig. 45). The Zeiss camera was equipped with a 12-in.-focal-length lens and was also synchronized with the RC-8 cameras so that it produced non-stereo color infrared photography at a scale of 1:50,000 on a 9- by 9-in. format.

The Mission 101 photography is generally of high quality, with some loss due to cloud cover in the high mountains. Clouds covered about 10% of the southwest Bonanza area at the time of overflight.

Photogeologic interpretation of the Mission 101 color and color infrared photography (fig. 46) demonstrated that the small-scale photography was most useful for delineating regional structural features and some of the more pronounced lithologic variations. Chief among

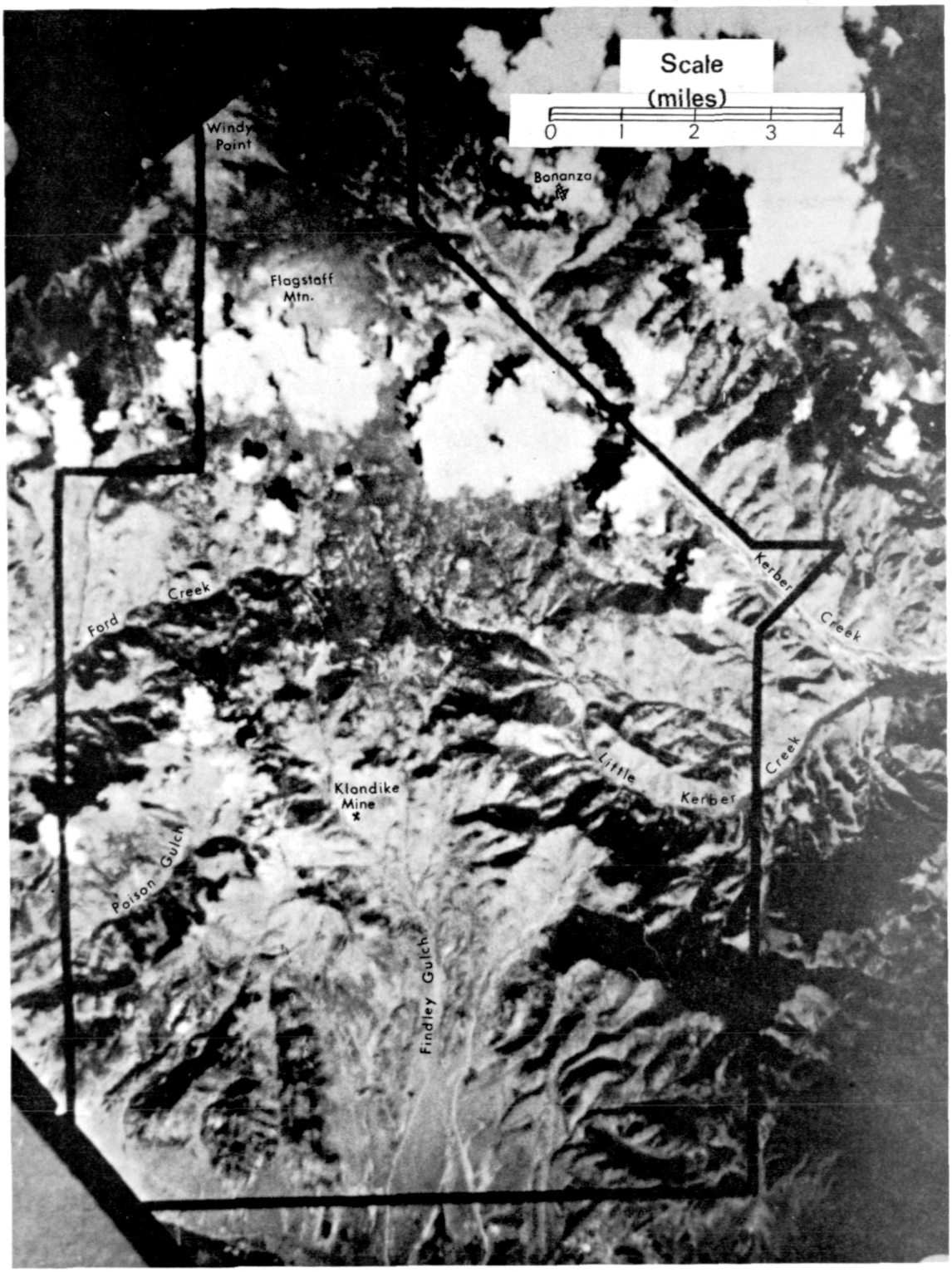

Figure 45. Small-scale (1:100,000) photograph of the southwest Bonanza area. Almost the entire area is covered on a single photograph. This synoptic view is well-suited for regional geologic interpretation. Photo taken from Mission 101 color infrared photograph 5057.

Figure 46.

MISSION 101 - Color & Color Infrared Photography Interpretation

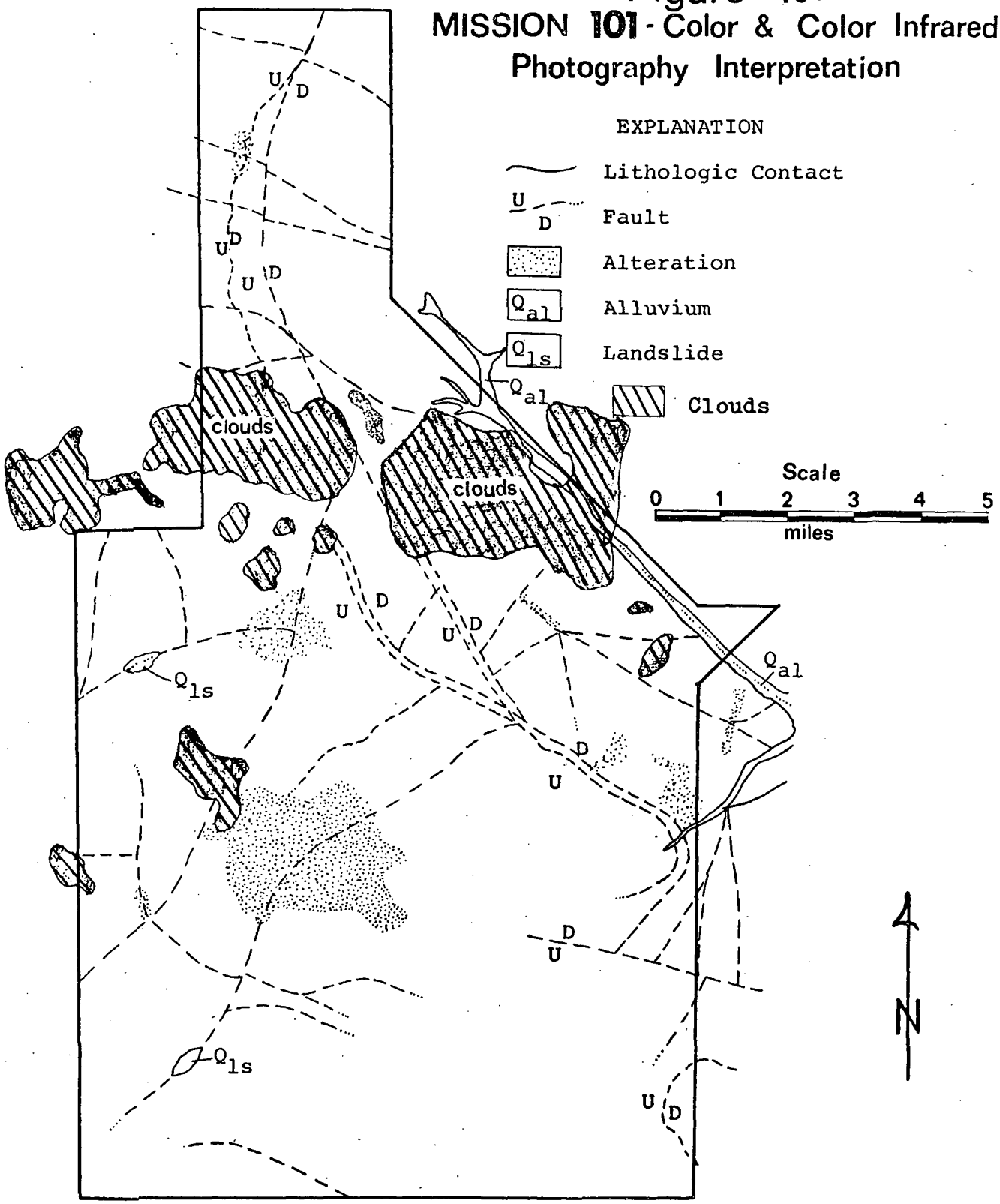

the structurally pertinent features are the topographic alignments and tonal contrasts corresponding to major faults. The Mission 101 photointerpretation was completed prior to field mapping in the northern and western portions of the area. Subsequent field mapping confirmed almost every feature interpreted as a fault from the 101 photography. Most of the faults seen on the high-altitude photography are regional in extent, and have relatively large displacements. Comparison of the photointerpretation with the final geologic map revealed that all faults in the area with displacements greater than 200 ft could be mapped; or at least identified, on the high-altitude photography.

Several of the larger zones of alteration and mineralization are apparent on the high-altitude color and color infrared photography (fig. 46, stippled pattern). These zones are most readily identified and delineated on the color photography where they appear as light buff or yellowish-white areas contrasting with the darker reds, greys, and browns of the unaltered volcanic terrain. Zones of alteration can be seen even in areas of moderately dense forest cover, and in fact, noticeable changes in the density, type, and/or condition of the vegetation can sometimes be related to the distribution of altered rock. In the large, altered area around the Klondike mine, for

example, the trees are fewer than in comparable surrounding areas and field investigations revealed that the ratio of juniper trees to conifers is higher. These changes may be related to soil chemistry, moisture retention, or other factors, but these controlling factors appear to be influenced by the distribution of altered rock.

The larger zones of alteration are more easily delineated on the high-altitude color and color infrared photography than on the low-altitude photography. In such cases, the regional overview provides a definite advantage for consistently locating the indistinct and/or gradational boundaries of the alteration. The general outline of such subtly defined areas is much more difficult to establish on a sequence of large-scale color photos where minor tonal variations between frames and frame boundaries interrupt the overall continuity of the photography.

The high-altitude Zeiss color infrared photography, at a scale of 1:50,000, is of limited utility for defining regional geologic features. The Zeiss photography is very high quality, but is severely limited by the lack of stereoscopic coverage. Also, the intermediate-scale photography (1:50,000) does not provide sufficient coverage per frame for optimun use in regional interpretations nor does it provide the necessary large-scale information to be optimum for detailed geologic investigations. An

accurate appraisal of the utility of the intermediate-scale photography relative to large- (1:15,000) and small-scale (1:100,000) photography was impossible due to the lack of stereoscopic coverage, but the intermediate-scale photography was not considered optimum for any portion of this investigation. It appears that there is no "happy median" which would provide both the regional information and the necessary detail for geologic mapping in the southwest Bonanza area.

Since most lithologic units in the Bonanza area could not be distinguished by direct visual interpretation of the Mission 101 photography, an attempt was made to enhance the contrast between some of these lithologic units by video-image processing. This test was performed by Martin Marietta personnel in their interpretation laboratory. The techniques, equipment, and results of this test are discussed in Martin Marietta Corporation's First Year Summary Report under contract 9-W-06040 (Gliozzi and others, 1970, p. 20-30).

In brief, video-image processing is a technique wherein a scene is viewed by a television camera feeding an electronic gating mechanism which splits the incoming data into several voltage levels (representing grey levels of the scene). The various voltage levels are then assigned different colors and displayed as a color image

on a color picture tube. With proper selection of colors, any particular contrast present in the scene should be enhanced.

Mission 101 color photograph 4723 was used as a test scene for the video-image processor. This photograph covers an area on the southwest side of Antora Peak where the contrasting lithologies are andesites and latites of the Rawley Formation and the Bonanza Formation. The results of the test were disappointing. The Martin Marietta Corporation report states:

> "In this application, the video-image processor was found to be not particularly useful. Apparently the tonal differences of the input image, which are due to shadows, vegetation, and similar superficial causes, are enhanced by the system to the extent that the truly meaningful tones of the rocks themselves are submerged in the profusion of color. Only the most gross spatial outlines can be distinguished." (Gliozzi and others, 1970, p. 28)

It appears that the video-image processor, in its present state of development, is best applied in simpler situations where the meaningful contrasts are relatively constant throughout the scene and are not so completely dominated by "superficial" contrasts.

Low-Altitude Color and Color Infrared Photography: Large-scale (1:15,000) photography of the southwest Bonanza area was obtained by Flight 5 of NASA Mission 105. Mission 105 was requested as a multisensor mission to be flown the week

of 22 September 1969, but equipment problems on the aircraft delayed the flight so that it was finally flown on 2 October 1969. After the mid-day flight on October 2, which obtained low-altitude color and color infrared photography and daytime thermal infrared imagery (3- to 5-μm and 8- to 14-μm bands) in the Bonanza area, the remainder of the flight had to be concelled due to bad weather. Figure 47 is an index map showing the low-altitude photographic coverage of the southwest Bonanza area obtained on Mission 105. The area was completely covered by the Mission 105 photography with the exception of a 1.7-sq-mi area in the extreme southwest corner.

Large-scale (1:9,000) color and color infrared photography was also obtained on NASA Mission 153. Mission 153 was originally scheduled to be flown early in October, 1970; but the Bonanza portion of the Mission was postponed, first because of NASA scheduling and equipment problems, and finally, because of inclement weather. Three lines of color, color infrared, and multiband photography were finally flown on October 27, with some areas snow-covered and the weather worsening. The Mission 153 photography covering the area between Hayden Peak and Saguache was to be supplemented with pre-dawn thermal infrared imagery; but with the snow and bad weather, the infrared portion of the mission was cancelled. The color, color infrared,

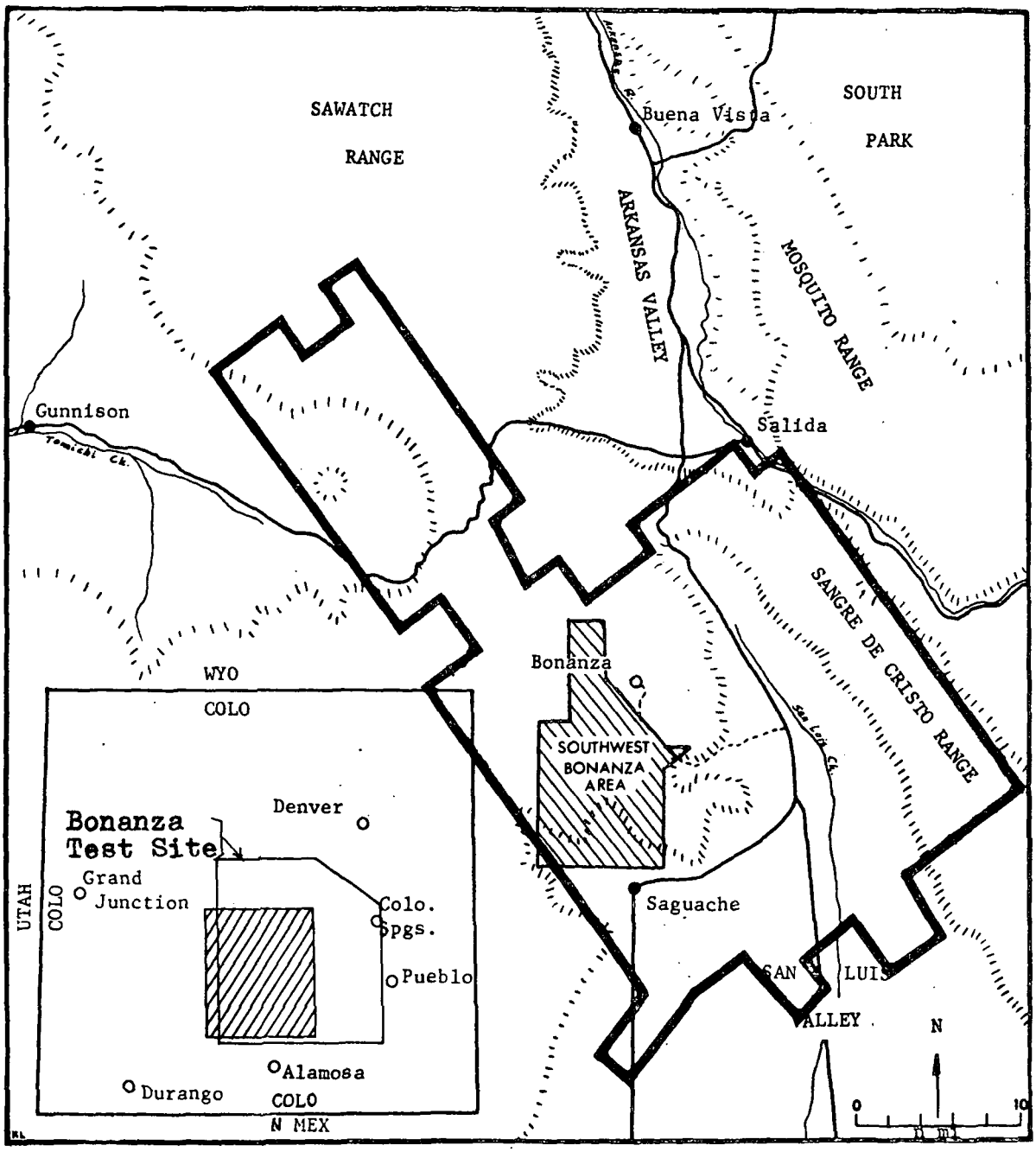

Figure 47. Index map of Mission 105 low-altitude photographic coverage (bold outline) in the southwest Bonanza area (after Lee and others, 1971).

and multiband photography were flown with the hope that they would still provide information for vegetation discrimination in the snow-covered areas and that the melting snow patterns might yield some thermal information.

The resulting photography was practically useless. Almost the entire area between Hayden Peak and Saguache was covered by snow and clouds or cloud shadows. Even contrasts in vegetation, which was not covered by snow, were obscured by the clouds and cloud shadows. It also became apparent that the snow patterns were controlled by wind and topography rather than by melting. As a result, there was very little useful information derived from the Mission 153 low-altitude photography.

The Mission 105 color and color infrared photography were taken with the Wild-Heerbrugg RC-8 cameras on NASA's P3A Electra aircraft. All of the photography lines were flown at an altitude of 17,500 ft amsl, but the terrain elevations vary between 8,500 ft and 13,000 ft, so the scale of the photography ranges from 1:18,000 to 1:9,000. Most of the Mission 105 photography has a scale of about 1:15,000.

The Mission 105 color photography was taken using SO-397 color film and an antivignetting filter. The resulting photography is of excellent quality and entirely cloud free in the southwest Bonanza area. The only

significant problems with this photography are the solar hotspots (overexposed areas that occur directly opposite the aircraft from the sun) and crab. Crab problems result from crosswinds which force the aircraft to head at an angle to the flight line and cause the borders of each frame of photography to lie at an angle to the flight-line direction. At the altitude and sun-angle conditions of Mission 105, the solar hotspots affect the entire northern half of each frame. Thus, the southern half of every frame of Mission 105 photography is slightly underexposed, and the northern half of each frame is slightly overexposed. The crab does not affect the quality of the image in the least, but in some cases it is so severe that stereoscopic viewing of the photography is difficult and transposing data from the photography to maps becomes more difficult.

The Mission 105 color infrared photography was taken with SO-117 film and a suite of filters, including a Wratten 15 (minus-blue) filter, a color-compensating CC20M filter, and a Corning 4600 for additional sensitometric correction. This suite of filters was entirely unsuccessful in achieving the correct color balance and proper exposure. Consequently, the quality of the Mission 105 color infrared photography is quite poor. Large portions of each frame of the Mission 105 color infrared photography

are underexposed due to a combination of problems. The initial exposure-time was too short. This problem was compounded where the photography was underexposed because of the lighting differential produced by the solar hot-spots. Vignetting (darkening outward from the center of each photo frame as a function of the lens transmission characteristics) is also severe. This additional contribution to the underexposure results in almost a total loss of information in the corners of the photos; particularly in the southern corners. These difficulties with the Mission 105 color infrared photography are further compounded because the particular filter combination used tends to bias the photography away from the infrared; resulting in a blue-green photograph which lacks much of the desired information in the infrared band. The quality differences between the Mission 105 color and color infrared photography is so great that an accurate appraisal of the relative utility of the two types of photography is impossible. Only the color photography was used in making most of the photogeologic interpretation in the Bonanza area.

In order to fully evaluate the Mission 105 low-altitude photography as a tool for geologic mapping in the Bonanza area, a three phase program was designed to use the photography in three different roles. The southwest Bonanza

area was divided into three subareas (fig. 48). Plate 2 (in pocket) is a composite photointerpretation map of the southwest Bonanza area which includes all three subareas. Area 1, the southeastern subarea, was mapped in the field, without reference to the Mission 105 photography. After the mapping was completed, the photogeologic interpretation was made and used to refine the original mapping and extend it slightly into areas peripheral to the mapped area.

This use of the photography did result in some refinement of the field map because a few structural and normal lithologic contacts evident as tonal and/or textural contrasts could be traced very accurately on the photography. The photography was particularly effective in delineating the meandering and feather-edge boundaries of Quaternary units (fig. 49). It was not surprising that no trace of many of the contacts mapped in the field could be seen on the photography, because many of the contacts separate lithologically similar units. However, it was very disconcerting to find some contacts between vastly different lithologies could not be seen on the photography. One example of this was the contact between Precambrian quartz monzonite and an andesitic breccia of the Rawley Formation south of Ute Pass (fig. 50); it was quite distinct in the field, but could not be seen at all on either the color or color infrared photography.

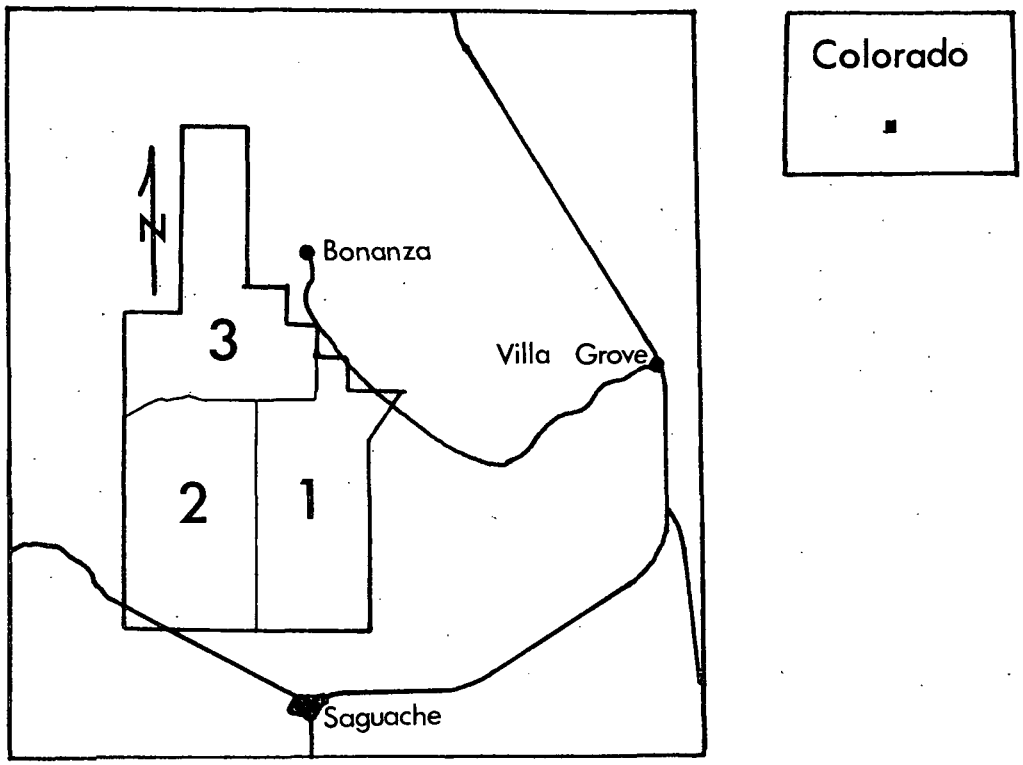

Figure 48. Index map of the Bonanza area showing the subareas in which the Mission 105 photography was used in various roles.

EXPLANATION

Q_p Quaternary pediment

Q_{af} Quaternary alluvial fan

Q_{ls} Quaternary landslide

lithologic contact

possible contact

$\frac{D}{U}$ fault

covered fault

alteration

Figure 49. Black and white print of Mission 105 color photograph of the area west of Findley Gulch with photogeologic interpretations.

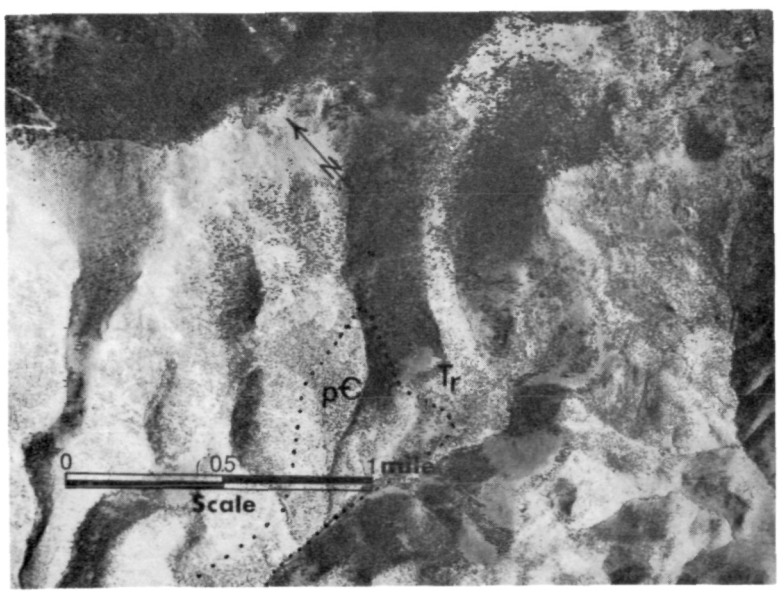

EXPLANATION

T_r Rawley Formation

pC Precambrian quartz monzonite

lithologic contact

Figure 50. Black and white print of Mission 105 color photograph showing the contact between Precambrian quartz monzonite and Rawley andesite south of Ute Pass. This contact could not be seen on the color photography.

Many of the faults that had been mapped in the field appear as lineaments of one sort or another on the photography. These lineaments are usually expressed topographically or as tonal, textural, or color contrasts. Lineaments that were not mapped in the field were also seen on the photography. Field investigation of ten such lineaments revealed various origins for the lineaments. One of the lineaments was a cow trail. Two of the lineaments proved to be minor faults, totally within a single volcanic unit, so that the lithologic contrast across the fault was minor. Two other lineaments represented normal lithologic contacts between flows that had been included within a single map unit. They were valid lithologic contacts which had been considered insignificant for mapping purposes. Two lineaments corresponded to vegetation or topographic anomalies that "cut across" the geology with no apparent geologic significance. The origins of three of the ten lineaments could not be determined. Their geologic significance could not be established because of heavy soil and/or vegetation cover.

Several small, unmapped, light-colored areas were also located on the photography. Field investigation revealed that most of these represented zones of alteration. However, one such area, which appeared identical to the alteration zones, proved to be an outcrop of white ash within a unit of the Rawley Formation.

Photointerpretation in subarea 1 also demonstrates that some Quaternary features and sedimentary outcrops can be reliably located and identified from the photography. The Quaternary units can be identified by their location, form, and geomorphology.

The two areas of sedimentary outcrop which occur in subarea 1 show distinct linear patterns which reflect the bedding. Field observation suggests that the linear patterns are a combination of microtopography, color contrast, and/or moisture and vegetation anomalies.

Field checking of the areas into which the geologic mapping was "extended" by photointerpretation showed that the interpretation in these peripheral areas was quite accurate for a distance of 1 or 2 miles outward from the area of known geology (compare plates 1 and 2).

Area 2, the southwestern subarea (fig. 48), was mapped using the Mission 105 color prints as field photos. That is, the field investigations and photointerpretation were conducted simultaneously. This technique resulted in far more effective use of the photography than the technique used in subarea 1. Lithologic contacts and other geologically significant features were located and traced on the photography and then identified or confirmed in the field. Conversely, if a problem arose while mapping in the field, the photography could be consulted, and possibly reinterpreted; or at least the critical areas of investigation

could be identified, so that the problem could be resolved in minimum time. Comparison of the photointerpretation (plate 2) with the geologic map (plate 1) brings out several features which were interpreted as faults on the photo-interpretation, but are not mapped as faults on the geologic map. They include features that have been erroneously interpreted as faults (cultural features, coincidental lineaments, and misinterpreted geologic features), and features that could not be confirmed as faults. Many of the features that could not be confirmed as faults may, indeed, be faults. In fact, some of these lineaments are so strong and fit so well into the confirmed pattern of faulting that they could hardly represent anything else. However, they were not retained on the geologic map because there is no tangible field evidence to substantiate them. Most significant among these "possible" faults are a series of lineaments cutting northwesterly across the southern part of subarea 1 toward Alkali Spring and the large mineralized area surrounding the Klondike mine. This trend is disrupted in the area of the Klondike mine by several northeast-trending linears, some of which were found to be faults. A pair of northwest-trending linears northwest of the Klondike mine may represent a continuation of the disrupted trend. The significance of these linears could not be definitely established, but it is quite

possible that the entire northwest-trending sequence represents faults which are genetically related to the formation of the caldera in the central Bonanza area, and which may be very significant with regard to the mineralization at the Klondike mine.

Although there are some distinct contrasts between several of the Tertiary volcanic lithologies in subarea 2, it was impossible to identify the various lithologies with any degree of certainty. Thus, most of the possible lithologic contacts that were seen in the photointerpretation were simply traced and marked as a dotted line on the interpretation. The identification of these contacts and the decisions as to which ones were boundaries between mappable units was left to the field investigation.

It is interesting to note that the small outcrop of Precambrian quartz monzonite in the northeastern corner of Section 30, T 45 N, R 7 E was located in the photointerpretation and noted as an anomalous area, but it could not be identified by photointerpretation. It was very encouraging to find that there was a visible contrast between the Precambrian quartz monzonite and the overlying andesites of the Rawley Formation, especially after the effort to distinguish between Precambrian quartz monzonite and andesitic breccias of the Rawley Formation in the Ute Pass and Findley Gulch areas had failed (p. 151).

The only units in the area that could be identified with confidence were the Quaternary units. The Quaternary units in subarea 2 include alluvium, alluvial fans, stream terraces, valley-fill deposits, and landslides. Most of these units could be accurately identified by their characteristic morphology. Also, the boundaries of the various Quaternary features could be traced more easily and more accurately on the photography than in the field.

The mapping of subarea 3 was used as a test of the maximum utility of the Mission 105 color photography. The photointerpretation for the entire area was completed before any field work was done in the area. In this test I had the advantage of being familiar with many of the geologic units that were present in the area because I had worked with most of these same units in subareas 1 and 2. In making the photointerpretation for area 3, I forced myself to identify each feature on the photointerpretation and to identify every area according to its lithology and local geologic name. In short, I constructed a complete geologic map on the basis of the photointerpretation (plate 2, in pocket). The entire area was then field checked in detail, and the necessary additions and corrections were made in order to produce a complete and accurate geologic map. As the area was checked, a record was kept of the number of features and

areas that were 1) correctly identified, 2) incorrectly identified, 3) overlooked, and 4) not verifiable from field relations. Using these data, percentages were computed to give a rough measure of the accuracy of the photogeologic interpretation. The geologic units in subarea 3 fall into two catagories; unconsolidated Quaternary deposits and Tertiary volcanic rocks. The apparent accuracy of identification of units within the two catagories differs markedly, so the two were treated separately in the percentage analysis. The accuracy of identification of structural features does not appear to be influenced by any special factors, so all the structures were analyzed as a single group. Table 1 lists the percentages computed for the groups.

Table 1. Accuracy of photointerpretation of structures and lithologies in the southwestern Bonanza region (subarea 3).

	STRUCTURES (faults)		LITHOLOGIES			
			Quaternary		Tertiary	
	No.	%	No.	%	No.	%
Correctly Identified	44	57.1	14	92.9	78	61.9
Incorrectly Identified	14	18.3	1	7.1	48	38.1
Not Identified (overlooked)	15	19.4	0	0.0	0	0.0
Not Verifiable	4	5.2	0	0.0	0	0.0
Totals	77	100.0	15	100.0	126	100.0

The significance of the data presented in table 1 is rather difficult to determine, but, with the proper considerations, these data provide a rough measure of the usefulness of the photography. Among the factors that must be considered in evaluating the data are: 1) only one class of structures is present in the mapped area--faults; 2) the area contains five Quaternary units and four Tertiary units, none of which are entirely unique in composition; 3) faults and lithologies vary considerably in size and extent, the smaller faults and smaller areas are more difficult to detect and identify; 4) the interpretation and field check were performed by a single individual, therefore, the determinations are not completely objective; and 5) the determinations were made in a limited area under a unique set of physical conditions and can not be directly translated to any other area or set of conditions.

From these few considerations it becomes obvious that the results of this test have significance only in a qualitative sense, and that many such sets of data are required if quantitatively meaningful and widely applicable results are to be obtained. Nevertheless, this type of data and analysis are necessary in order to gain a quantitative measure of the utility of remote-sensing data.

Comparison of the effectiveness of the Mission 105 photography as it was used in three different roles brings me to the rather simple and subjective conclusion that the

utilization of the large-scale photography in the first application (subarea 1) was relatively inefficient. The use of the photography for mapping in subareas 2 and 3 represents a much more efficient use of the photography, with its use in subarea 2 being very nearly optimum on a "total time spent" basis. The actual rate of mapping in subarea 2 was more than twice that in subarea 1 (1.1 sq mi/day vs 0.5 sq mi/day), but a good deal of extra time was spent in getting familiar with the various lithologic units during the mapping of subarea 1. Still less time was spent in the field mapping in subarea 3 (1.3 sq mi/day) even though subarea 3 is more rugged and a greater portion is heavily forested. Thus, on the basis of "time spent in the field", the technique used in subarea 3 was most efficient. However, if one considers the time spent in the laboratory prior to going to the field (i.e. on the basis of "total time spent"), the technique used in subarea 2 is most efficient.

Multiband Photography

Multiband photography provides a means of separating the reflectance information normally recorded on a photograph into several wavelength-limited components. This separation allows the interpreter the advantage of comparing objects not only with regard to their total

reflectance, but also, with regard to the relative contributions of components that constitute that total reflectance.

There are two approaches to the use of multiband photography. The scene can be recorded in a standard array of band-limited photographs (usually blue, green, red, and infrared bands) and then recombined in various proportions and combinations to yield an enhanced image. The composite image may be in black and white or false-color, depending on the technique used in the reconstruction. This technique offers little advantage over color or color infrared photography which records each of these same bands in a separate emulsion and displays each as a separate color. The only real advantage of standard multiband photography over color photography is the flexibility it offers in forming combinations. One, two, three, or four bands can be used in various combinations and, with a color-additive viewer, these can be composited in various colors and with different intensities.

A second multiband technique involves preliminary field and/or laboratory work in which the spectral reflectance curves are measured for samples of materials to be discriminated. These curves are compared to determine where, within the photographic range, the spectral reflectance values differ most. Special film/filter combinations

can then be selected to produce images showing maximum contrast between the objects being distinguished. This technique offers the same flexibility in presentation as the standard-band technique, but provides the additional advantage of maximization of the significant contrasts.

Multiband photography in the Bonanza area was obtained on Mission 101 (August, 1969), Mission 105 (October, 1969), and Mission 153 (October, 1970). The three standard bands of Mission 101 multiband photography were taken with Hasselblad EL 500 cameras (70-mm focal length) from an altitude of 60,000 ft amsl (50,000 ft amt). The scale of the photography is approximately 1:200,000. The coverage is complete but non-stereoscopic (10%-20% end-lap). Mission 101 was flown before any field spectral measurements were made, so a standard film/filter configuration was employed. Table 2 lists the film/filter combinations and spectral bands for the Mission 101 multiband photography.

Table 2. Mission 101 film/filter combinations.

Band	Film	Filter	Spectral Band*
A	2402 (black & white)	W57	480-590 nm (green)
B	2402 (black & white)	W25A	590-700 nm (red)
C	SO246 (black & white IR)	W89B	700-900 nm (infrared)

*Note: Band limits denote the spectral region of >10% transmission of the limiting filter.

The major problem with the Mission 101 multiband photography is the small scale. Secondarily, much of the area is obscured by clouds (fig. 51). The purpose of the multiband photography was to discriminate lithologies on the basis of enhanced tonal contrasts. Most outcrop patterns in the Bonanza area are intricate and they are seldom continuous for distances of more than one mile. Such patterns are represented on the Mission 101 multiband photography as features no more than 0.25 in. long and the contrasts are generally subtle so that the patterns can not be detected on the photography.

Additional problems with the Mission 101 multiband photography were the overexposure of the green band (480-590 nm) and static discharge marks on the infrared band (700-900 nm). The infrared band was further degraded by light and dark streaks across the film strip produced in the processing of the film. The various problems with the Mission 101 multiband photography not only rendered it useless for evaluating the multiband photography as a tool, but also spoiled the comparison of the bands so that their relative value could not be determined. Several of the regional topographic features which were evident on the Mission 101 multiband photography represent faults, but no geologically significant features were located on the multiband photography that were not more apparent on the Mission 101 color and/or color infrared photography.

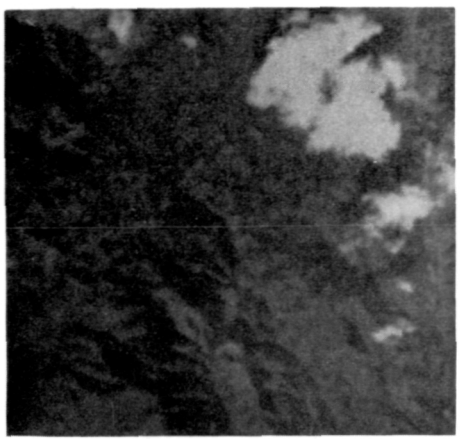

Green (480-590 nm)

Red (590-700 nm)

Infrared (700-900 nm)

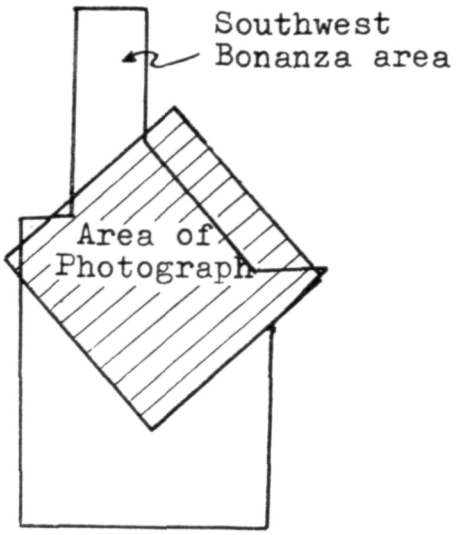

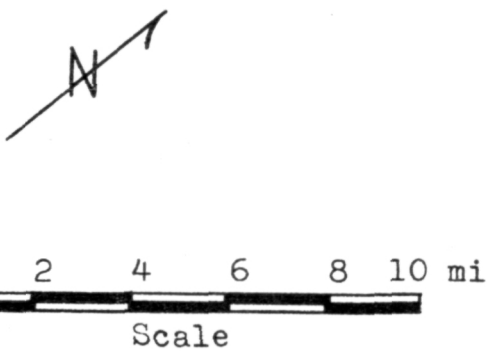

Figure 51. Comparison of three bands of Mission 101 high-altitude photography. Note overexposure of the green band, static discharge marks, and light and dark streaks across the infrared photograph, all defects in the original photography.

NASA Mission 105 obtained complete, non-stereoscopic, multiband coverage of the southwest Bonanza area in four bands. This multiband photography was obtained with a suite of four Chicago Aerial KA-62 cameras on the same flight that obtained large-scale color and color infrared photography of the Bonanza area. The KA-62 cameras, equipped with 3-in. focal length lenses, produced 1:30,000-scale photography with a 4½- by 4½-in. format. Enlarged prints (2X) were then made to facilitate interpretation of the multiband data and to allow a better comparison of the multiband photography with the color and color infrared photography. The film/filter combinations of the Mission 105 multiband photography are listed in table 3.

Table 3. Mission 105 multiband film/filter combinations.

Band	Film	Filter	Spectral Band
A	2402 (B & W panchromatic)	W25A	590-700 nm (red)
B	2402 (B & W panchromatic)	W47	350-515 nm (blue)
C	2402 (B & W panchromatic)	W58	465-610 nm (green)
D	SO246 (B & W infrared)	W89B	700-900 nm (infrared)

Mission 105 was flown before specific objectives had been defined and before spectral field data could be compiled. Consequently, no special requirements were outlined and no special film/filter combinations were specified. With no background data, this standard configuration seemed as likely to produce results as any other.

The work of L. C. Rowan (1972) with standard multiband remote sensing suggests that lithologies may be distinguishable by their iron oxide content using a comparison of the red and infrared bands. Significant differences in iron content were anticipated for the rocks of the Bonanza area and I hoped that these differences could be detected with the standard multiband photography, but comparison of the red and infrared bands of the Mission 105 photography revealed no contrasts that could be related to iron oxide content.

Bands A (red) and C (green) of the Mission 105 multiband photography provide the best resolution and contrast in most areas (fig. 52). It appears that rock outcrops and vegetation can best be distinguished in these bands. Band D (infrared) is underexposed and lacks the necessary quality for meaningful comparison. However, stream channels, soil moisture, and some vegetation are best delineated on band D due to the low reflectance of water and the high reflectance of vigorous vegetation in the

Band	Spectral Region	
A	Red	580-700 nm
B	Blue	350-515 nm
C	Green	470-615 nm
D	Infrared	700-900 nm

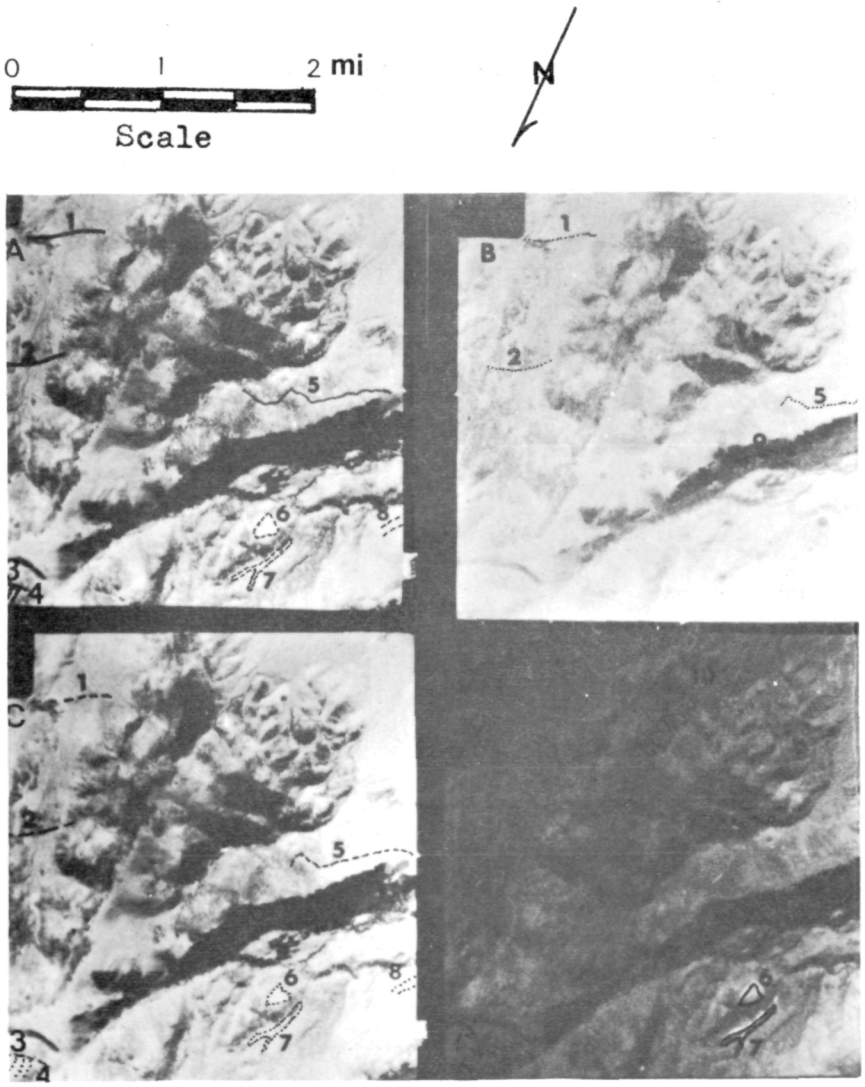

Figure 52. Comparison of four bands of Mission 105 multiband photography. Band B (blue) is slightly overexposed and hazy, and band D (infrared) is slightly underexposed. (Explanation of annotations, p. 169)

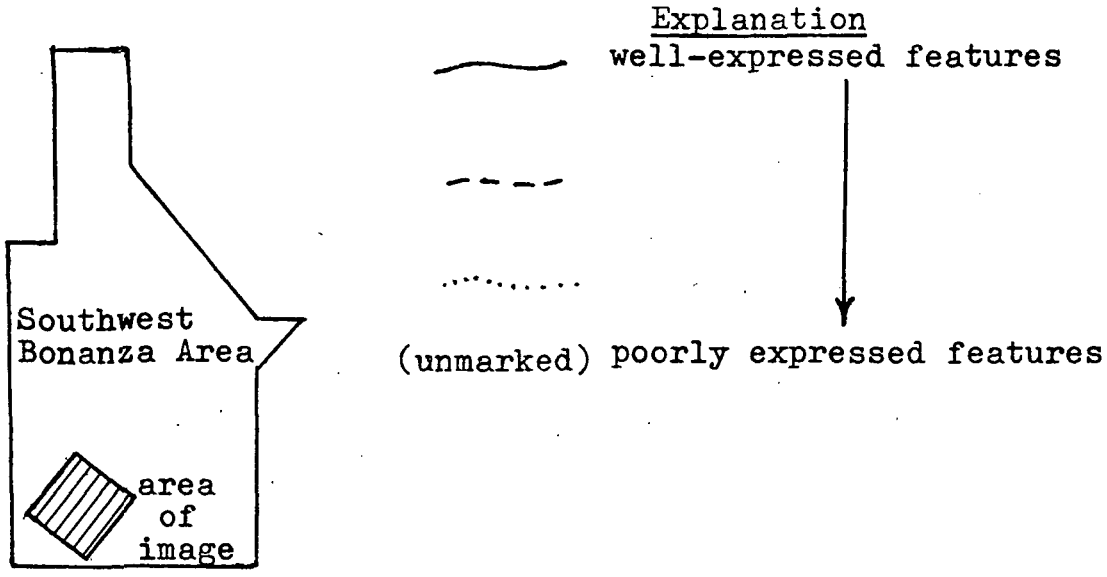

Number	Represented Feature
1	Fault: shown by vegetation
2	Fault: shown by vegetation
3	Lithologic contact (covered)
4	Subtle topography: may reflect buried structure
5	Lithologic contact (exposed in outcrop)
6	Alteration zone
7	Alteration zone (exposed in gulley)
8	Lithologic contact (exposed in outcrop)
9	Lithologic contact in deep shadow

Table 4. Index map and explanation of annotations for figure 52.

near infrared portion of the spectrum. Band B appears to have low resolution (fuzzy), probably due to scattering of the blue light by the atmosphere.

Photogeologic interpretation of the Mission 105 multiband photography was hampered by the lack of stereo coverage, but a comparative evaluation of several of the bands of photography was made. In general, the comparison of interpretations of the Mission 105 multiband photography with interpretations of the color and color infrared photography indicates that there is very little information on the multiband photography not available from the color and/or color infrared photography. Features which may be more apparent on the multiband photography include 1) features which lie in deep shadows and which can best be seen in the band B (blue) photography because they are illuminated by scattered light, 2) variations in the appearance of some conifers which may be distinguishable in the blue-green spectral range. No geologically significant information was extracted from the Mission 105 multiband data due to either of these observations, but they may be important considerations in other applications of multiband photography.

Color-additive viewing and video-image processing were used in an attempt to differentiate low outcrops of Precambrian quartz monzonite and gneiss from Quaternary

alluvial gravels in the Findley Gulch area. This work was performed by Martin Marietta Corporation personnel using a Clark multispectral projection system (model 5005) for color-additive viewing, and a video-image processing system. The color-additive viewing tests, as reported by Gliozzi and others (1971, p. 2·45 and 2·47), produced no definite distinction between the Precambrian crystalline rocks and the Quaternary gravel deposits, but some indication of improved contrast was observed with the band and filter combinations listed in table 5.

Table 5. Multiband photography and filter combinations yielding some contrast improvement between Precambrian crystalline rocks and alluvial gravels in the Findley Gulch area.

Combination	Band			
	A	B	C	D
1	No filter	Blue	-----	---
2	No filter	Red	-----	---
3	---------	Green	Blue	---
4	Red	Green	-----	---
5	Red	-----	Blue	---
6	Red	-----	Green	---
7	---------	-----	Green	Red

Not all possible combinations of photography bands and filters were tried, but the combinations that were tried suggest that the information necessary to make definite distinctions between the test lithologies is not present in the photography of Mission 105. Tests with the video-image processor using individual bands and combinations of bands of the Mission 105 photography tend to confirm this conclusion. There appears to be no correlation between the mapped geologic contacts and the patterns which appear on the processed images (fig. 53).

These negative results and similarly discouraging results for other tests in the Bonanza test site (Muhm, Lee, Raines and others, 1970, personal communications), show that the "standard band" approach to the use of multiband photography is not effective in the Bonanza test site. The multiband film/filter combinations must be specifically designed for each job if they are to produce the desired distinction between the various lithologic units.

In order to design the proper film/filter combinations for a task, it is necessary to measure the spectral reflectances of the various lithologies to be discriminated. Hornblende andesites of the Rawley Formation and the biotite latite ash-flow tuff of the Bonanza Formation were selected as two units to be distinguished in the southwest Bonanza area. The spectral reflectance curves for these

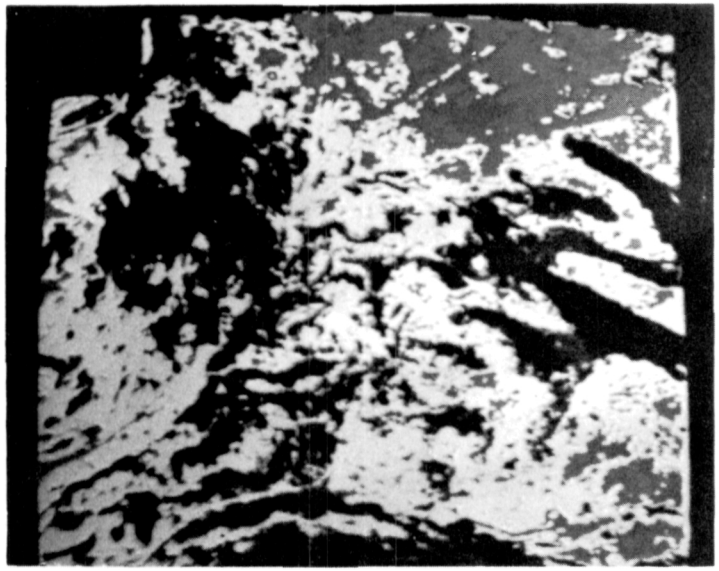

Density segregated video image displayed on color picture tube in contrasting colors.

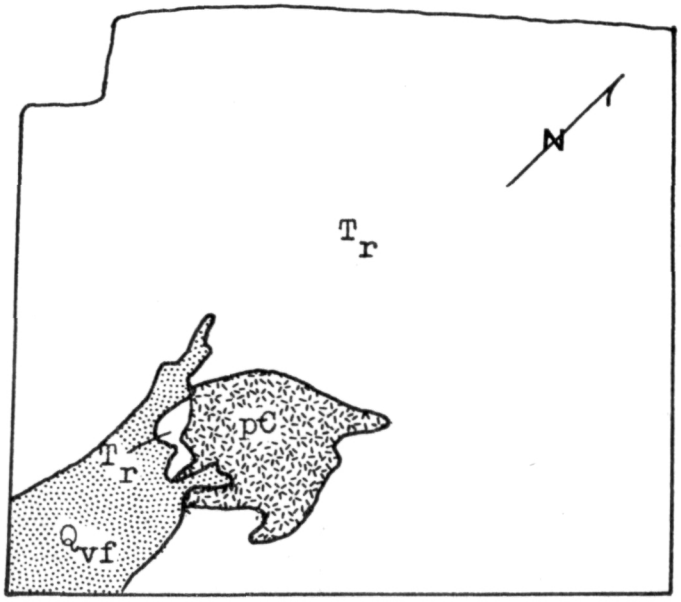

Generalized outcrop map.

0 1 2 mi

Scale

Q_{vf} Quaternary valley fill

T_r Tertiary Rawley Formation

pC Precambrian crystalline rocks

Figure 53. Video-image processed photography and outcrop map of the Findley Gulch area (after Martin Marietta Corporation Annual Report 2, p. 2·49). Note the complete lack of correlation between the video image (which enhances density contrasts) and the outcrop pattern.

and other units were determined using an ISCO spectro-radiometer. Spectral reflectance curves for the Rawley hornblende andesite and the Bonanza ash-flow tuff are given in figures 42 and 43 (p. 135-136). Comparison of the spectral curves indicates that there may be no band in the visible spectrum which offers sufficiently different reflectance values for discrimination of the Rawley and Bonanza formations. The variations between spectra for the same unit are as large as those between spectra of the Rawley and Bonanza lithologies. The spectra for the Rawley Formation (fig. 42) do exhibit a slight reflectance high in the 1,000- to 1,100-nm range (infrared) and a low in the 600- to 700-nm range (red). The infrared film is not sensitive beyond 1,000 nm. Thus, the reflectivity peak in that range does not provide opportunity for discrimination of the Rawley and Bonanza formations with multiband photography.

The reflectance low in the 600- to 700-nm range of the Rawley spectra is only slightly stronger than a similar low in spectra for the Bonanza tuff, but there is some possibility for discrimination. Discrimination between the Rawley and Bonanza formations on the basis of this slight spectral difference would certainly require optimum exposure and carefully controlled processing of the film, but the band-limited multiband photography

should provide more contrast between the units than standard photography.

Both Mission 101 and Mission 105 included multiband photography in the red band. On neither mission, however, was the photography optimum, and no marked distinction can be seen between Rawley and Bonanza formations. This lack of distinction was probably due, in part, to soil and vegetation cover which obscured the lithologic contacts.

Mission 153 multiband photography was flown in October, 1970. Five Hasselblad EL 500 cameras with 3-in. focal length lenses were used with film/filter combinations designed specifically for a test conducted in the Canon City area. Although the film/filter combinations were not designed for the Bonanza area, several lines were requested in order to obtain better photography for some of the bands which had been flown before but had not turned out well. The coverage was obtained along with the Mission 153 color and color infrared photography in the area between Hayden Peak and Saguache. The snow-cover, clouds, and cloud-shadows (p. 148) effectively spoiled the multiband photography and no comparison could be made between it and the multiband photography that was flown on Missions 101 and 105.

Low Sun-Angle Photography

One line of low sun-angle photography (LSAP) was flown in the Bonanza area to determine whether or not the low sun-angle photography would enhance topographic and geomorphic features that might be geologically significant. This line, which trends north-northwest across the Bonanza area along Kerber Creek, was obtained by NASA's NC130B aircraft flying 18,000 ft above mean terrain (amt). The LSAP was taken with a Wild-Heerbrugg RC-8 camera with a 6-in.-focal-length lens and using black and white infrared film (2424) with a Wratten 25 filter, so that shadows would appear very dark. The LSAP was flown between 7:13 and 7:19 AM MDT on June 15, 1971. At that time the sun was approximately 19 degrees above the horizon.

The quality of the Mission 168 LSAP is excellent. The sun-angle was low enough to give the appropriate shadowing to topographic features; the shadows are black; the resolution is excellent; and the contrast is good.

Attempts to delineate major structural features from this low sun-angle photography have, in general, been rather disappointing. Failure of the low sun-angle photography to delineate structure is mostly due to the large scale of the LSAP. The photography provides too much detail and lacks the regional scope necessary for tracing large topographic alignments.

The large-scale (1:36,000) Mission 168 LSAP accentuates small structures that are topographically expressed. However, in the Bonanza area, very few of the small structures have an appreciable topographic expression. The topography is dominated by ridges and drainages that reflect the major structural trends, but the original topographic expressions of most smaller structures has been removed by erosion.

Attempts to detect and identify characteristic geomorphic patterns were somewhat more encouraging. Quaternary features generally can be identified and/or distinguished from other units by their geomorphic expressions which are enhanced on the LSAP. The LSAP is also capable of enhancing subtle drainage features in areas of low relief. Perhaps the most encouraging aspect of the LSAP investigation is the enhancement of areas of sedimentary outcrop near Kerber and Little Kerber creeks (fig. 54). The upturned sedimentary strata in that area commonly develop minor relief which compliments the bedding. The alternating shadowed and lighted bands resulting from the low-angle illumination causes them to stand out strongly on the LSAP.

These observations show that LSAP is capable of providing marked enhancement of subtle topographic features. Also, it has the additional advantage of better resolution than side-looking radar, which also enhances topographic

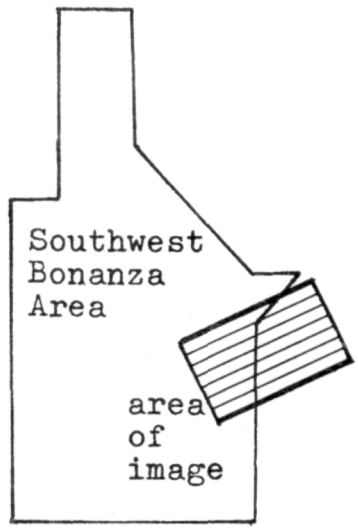

Boundary of sedimentary rock outcrops

Lineations (topographic linears parallel to bedding)

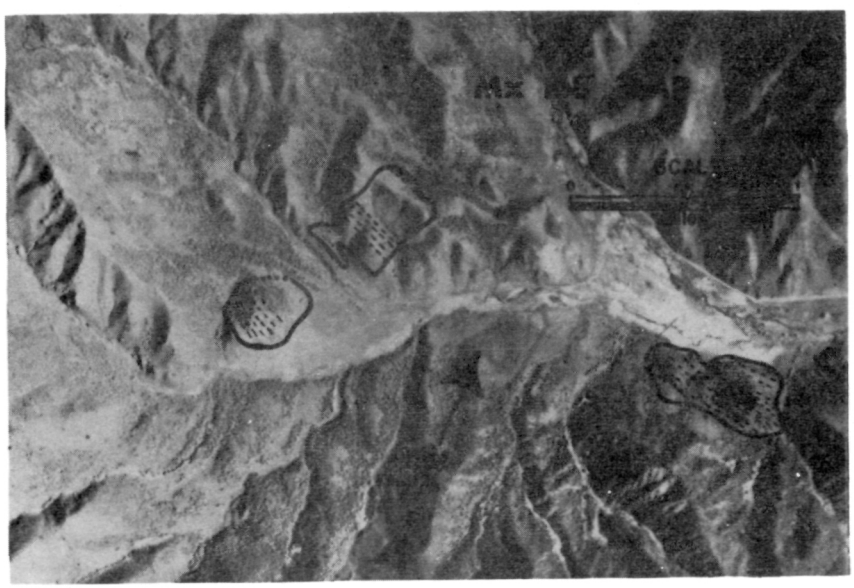

Figure 54. Mission 168 low sun-angle photography at the junction of Kerber and Little Kerber creeks. The distinctive light and dark pattern in areas of sedimentary outcrop reflect small-scale topographic lineaments resulting from differential weathering of different beds in the sedimentary sequence.

features. The experience with Bonanza LSAP emphasizes the importance of choosing the proper scale of photography for a given application. Enhancement of regional topographic features requires very small-scale photography. Considering both the Mission 101 high-altitude photography and the Mission 168 LSAP, with scales of 1:100,000 and 1:36,000 respectively, it appears that a scale smaller than 1:100,000 is desirable for locating regional structural trends with LSAP. For enhancement of local or low-relief features such as microdrainage patterns or weathering anomalies, larger-scale photography is necessary. Scales in the range of 1:20,000 or 1:30,000 might be optimum for such applications if high-resolution photography can be obtained. Stereoscopic coverage is highly desirable so that apparent topographic features can be positively identified. LSAP with a very low angle of illumination best enhances low-relief structures.

In addition to its intended uses, the Mission 168 LSAP provided an opportunity for comparison of the Mission 105 color and color infrared photography with black and white infrared photography of comparable resolution. The Mission 168 photography was enlarged so that the scales were comparable, and the three types of photography were compared. An effort was made to restrict all comparisons to areas that were well illuminated on all photography. These comparisons led to the

following conclusions regarding the relative utility of the different types of photography.

1. The low sun-angle photography is definitely superior to both the color and color infrared photography for mapping areas characterized by small-scale topographic features. Small ridges, microdrainages and areas of coarse texture are most easily seen on the LSAP. Vegetative patterns can also be enhanced where the individual plants or plant groups are large enough to cast a shadow.

2. The infrared photography (both color and black and white) display vegetative contrasts better than the color photography. One striking example is seen in the Quaternary pediments of the southwest Bonanza area. The pediments are characterized by low, circular mounds 3-6 in. high, 4-10 ft in diam) that appear as randomly spaced dots on an aerial photograph. These mounds are difficult to see on the color photography, but they stand out very well on the infrared photography. The mounds have sufficient relief to cause a moisture differential that affects the distribution of vegetation. As a result, the mounds are reflected as spots on the infrared photography which is extremely sensitive to vegetation contrasts.

3. Alteration is most apparent on the color and color infrared photography. Zones of argillic alteration show the strongest contrast with the surroundings on the color

infrared photography but are easily mapped on the color photography also.

4. Most contrasts related to lithologic changes (both normal and fault contacts) are best expressed on the color photography. Some contacts show contrasting tones and can be detected on any properly exposed photograph, others are largely marked by changes in hue. These changes in hue seem most apparent on the color photography except where vegetation contrasts are important.

Thermal Infrared Imagery

Both mid-day and pre-dawn thermal infrared flights were scheduled as part of Mission 105, flown by NASA's P3A aircraft equipped with a RS-14 thermal scanner*. The requested mid-day thermal imagery was obtained but the pre-dawn thermal infrared flight had to be cancelled because of bad weather. The imagery is high quality and it appears that both the 3- to 5- and 8- to 14-μm bands of the RS-14 scanner were working well.

The first attempt to evaluate the daytime thermal imagery in the Bonanza area was an experiment designed to determine the maximum utility of the infrared imagery for

*The thermal data from the RS-14 are recorded on film and magnetic tape, both of which were furnished by NASA. But, programs were not available to process or reduce the tape data so only the film-recorded thermal data were analyzed.

geologic mapping. The thermal imagery covering the geologically complex area of the central Bonanza mining district (near Elkhorn Gulch) was chosen for this test because that area offers a variety of geologic features and had been mapped in detail. The central Bonanza area is highly fractured and mineralized and is a region of high topographic relief with 70-80 per cent forest cover. Some of the major faults are reflected in the topography and some of the lithologic contacts are expressed by changes in vegetation. The major volcanic lithologies that are exposed in the test area are in both normal- and fault-contact with one another.

The test area was mapped by Burbank (1932) in the early 1930's, at a time of much mining activity; consequently, Burbank had access to shafts and adits from which he was able to gain underground geologic information. By combining surface and subsurface data, he was able to produce a detailed (1:12,000) map of the area. Burbank (1932, plate 1) mapped more than 200 faults in the test area; many of which are less than 500 ft long and of undetermined displacement.

Both the 3- to 5- and the 8- to 14-μm infrared imagery from Mission 105 were interpreted. Features noted on the interpretation were mostly linear anomalies, most of which represent faults (fig. 55). The surface expressions of the features include topographic alignments or

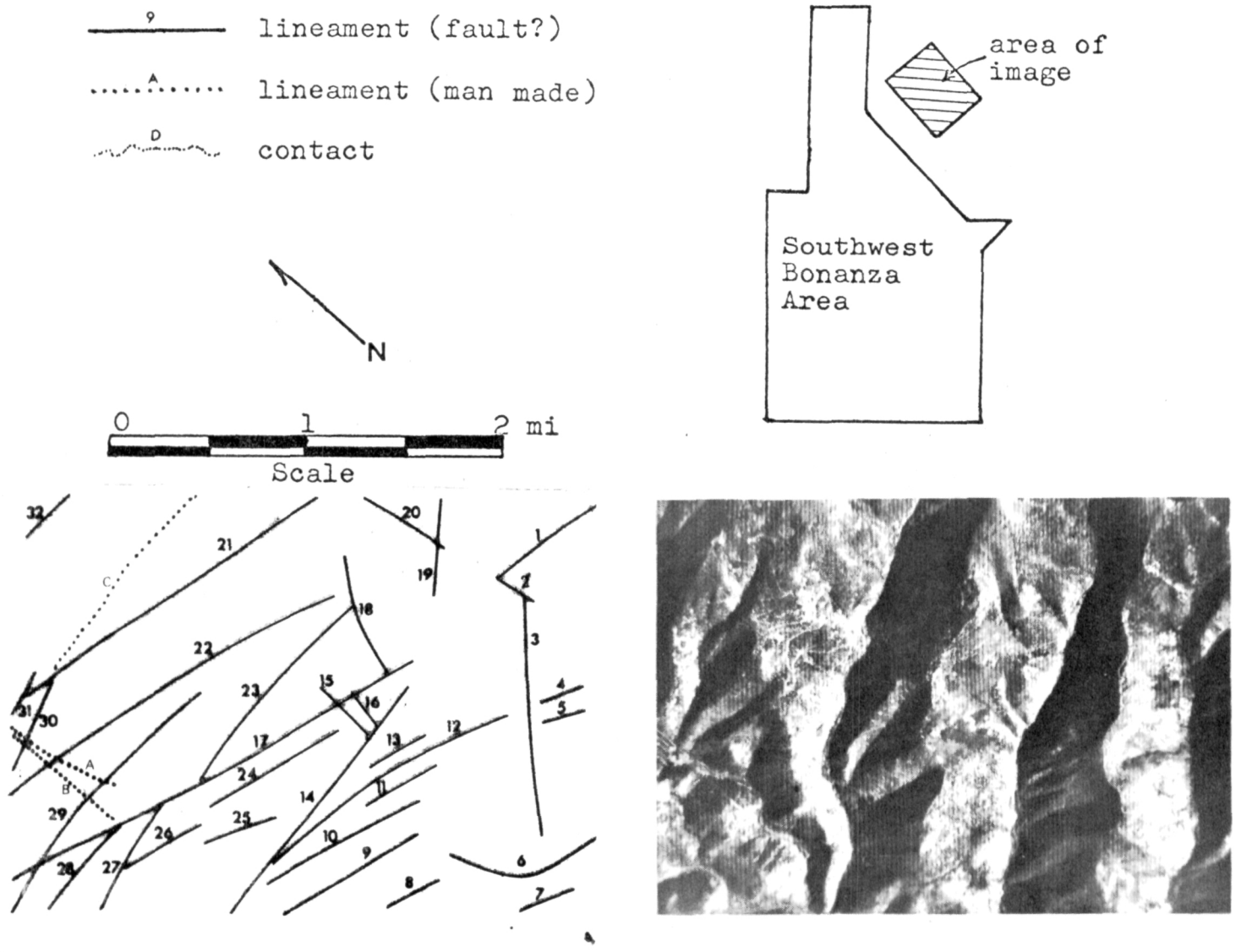

Figure 55. Interpretation of 8- to 14-um daytime thermal infrared imagery of the central Bonanza mining district.

breaks; changes in condition, type, and/or density of vegetation; some changes in soil or outcrop; and combinations of these variations.

After the imagery had been interpreted, the anomalies were graded according to their relative degree of apparentness. The interpretation was then compared to Burbank's geologic map. Of the 200 faults mapped by Burbank, 25 had been located and identified as faults on the infrared imagery. All of the faults of major proportions (and which are not masked by a stronger feature such as a stream valley) were found in the interpretation. Faults that were not identified were those lying in areas of very heavy forest cover or having a surface outcrop less than 500 ft long (less than 0.12 in. on the 1:42,000-scale imagery). The infrared imagery indicates continuity of some faults that were not mapped continuously. Only seven lineaments were located on the infrared imagery that were not mapped by Burbank (features 1, 2, 15, 16, 18, 19, and 31). No geologic significance could be established for these lineaments.

Lithologic contacts generally could not be located and identified from visual interpretation of the infrared imagery. The only exception was a contact between Rawley andesite and Bonanza latite ash-flow tuff, which coincides

roughly with the edge of a grove of aspen trees (feature D, fig. 55). The trees probably produce the observed contrast, but their distribution may be controlled by the lithologies.

Martin Marietta Corporation personnel interpreted the Mission 105 multiband photography in the Elkhorn Gulch area by visual, color-additive, and video-image-processing techniques. This work also brought out the correspondence between the contact and the aspen trees, but the multiband data also failed to provide any definite distinction between the Rawley andesite and Bonanza latite independent of the concentration of aspen trees (Gliozzi and others, 1971, p. 2·54 through 2·59). Interpretations of photography and infrared imagery in other parts of the Bonanza area demonstrate that aspen trees, in themselves, are not good indicators of Bonanza Formation outcrop.

Several man-made features were identified on the infrared imagery of the Elkhorn Gulch area. These included roads, a power line (feature C, fig. 55), old aerial tramlines (features A and B, fig. 55), mine dumps, and prospect pits. These were identified as cultural features from their appearance on the imagery.

All anomalies seen on the 3- to 5-μm infrared imagery were also found on the 8- to 14-μm imagery. Comparison of the quality of the two bands of imagery by addition of

"apparentness grades"* assigned to the various anomalies indicates that the anomalies are about 12% more apparent on the 3- to 5-μm imagery (table 6). This may be influenced by the somewhat higher contrast of the 3- to 5-μm imagery.

The Elkhorn Gulch thermal infrared imagery and its interpretation were compared to the Mission 105 color photography. All but four of the features seen on the infrared imagery could also be seen on the color photography (features 14, 26, 29, and 32). Most of the anomalies which appear both on the photography and on the infrared imagery are more apparent on the infrared imagery, but many features are visible on the photography which can not be seen on the infrared imagery. An accurate appraisal of the relative utility of infrared imagery as compared to color photography was impossible because of the difference in scale between the photography and the infrared imagery (1:12,000 vs 1:42,000), and because it was difficult to compare the continuity of features which encountered frame edges on the photography but not on the imagery.

Study of the thermal infrared imagery in the central Bonanza area demonstrates that the daytime thermal imagery is dominated by thermal contrasts related to topography.

*Numbers from 1 to 10 were assigned to each feature on each image according to its relative apparentness with 10 representing a very obvious feature and 1 representing a subtly expressed feature.

Table 6. Comparison of 3- to 5-μm, 8- to 14-μm infrared imagery and color photography by apparentness grades (refer to fig. 55 to see numbered anomalies).

Features	Apparentness Grades (1=poor 10=excellent) 8- to 14-μm thermal IR	3- to 5-μm thermal IR	Color photography	Slope	Interpretation of feature	Map Representation
1	3	2	2	West wooded	Fault	None
2	10	10	10	South - top	Ridge peak or dike	None
3	5	6	3	South	Fault	Fault
4	1	2	7	North wooded	Fault	Fault
5	2	3	8	North wooded	Fault	Fault
6	8	7	4	South - bottom	Fault	Fault
7	3	3½	5	North wooded	Fault	Fault
8	3	3	1	North wooded	Fault	Fault
9	4	4	3	North and South	Fault	Fault
10	4	4	5	North and South	Fault	Fault
11	3	3	5	North wooded	Fault	Fault
12	5	4	5	North and South	Fault	Fault
13	3	3	5	North wooded	Fault	Fault
14	3	5	0	South	Fault	Fault
15	7	8	6	South	Fault and gulley	None
16	7	8	6	South	Fault and gulley	None

Continued

Table 6. (continued)

Features	Apparentness Grades (1=poor 10=excellent) 8- to 14-μm thermal IR	3- to 5-μm thermal IR	Color photography	Slope	Interpretation of feature	Map Representation
17	5	5	3	South and North	Fault	Fault
18	5	5	3	Bottom	Fault	None
19	3	2	2	South - bottom	Fault	None
20	1	3	2	South	Fault	Fault
21	5	5	1	North and South	Fault	Fault
22	2	3	1	North and South	Fault	Fault
23	3	4	4	Bottom	Fault	Fault
24	5	6	7	North and South	Fault	Fault
25	1	2	1	North	Fault	Fault
26	1	2	0	North and South	Fault	Fault
27	4	4	4	North and South	Fault	Fault
28	2	3	4	North and South	Fault	Fault
29	3	5	0	North and South	Fault	Fault
30	6	7	5	North and South	Fault	Fault
31	1	2	7	North wooded	Fault	Fault
32	3	3	0	North wooded	Fault	Fault

In an attempt to evaluate the thermal imagery in an area where topographic effects are not as strong, portions of lines 18 and 20 in the lower Findley Gulch region were interpreted.

Interpretation of the line 18 imagery for the vicinity of Findley Ridge (Sec 23, T 45 N, R 7 E) reveals lineaments that extend from the steep topography of the ridge out across the gravel and alluvial deposits of the Findley Gulch valley (fig. 56, A, B, and C). These lineaments are traceable in the valley because of moisture patterns. Some of the more obvious moisture patterns have been marked with a stippled pattern on the interpretation. Comparison of the annotated infrared imagery with mapped features (plate 1) shows that most of the lineaments seen on the infrared imagery correspond to mapped faults. Lineaments that do not represent mapped faults may correspond to faults that were not detected in the field.

Other features that are apparent on the daytime thermal imagery are the prominent outcrops of the Bonanza Formation which are exposed continuously along the slopes of Findley Ridge. These bands of outcrop image cool on the daytime thermal imagery.

Figure 57 shows an interpretation of a portion of line 20 of the Mission 105 mid-day thermal imagery. Lineaments can be seen transecting the area where Precambrian quartz

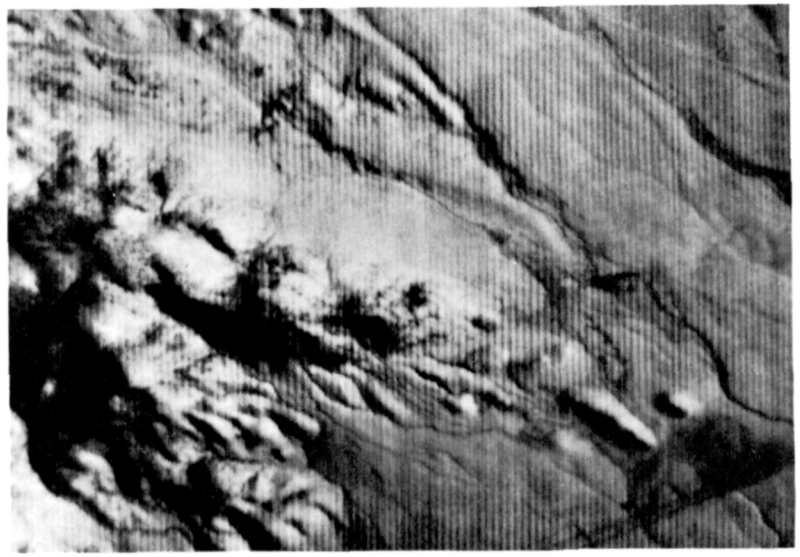

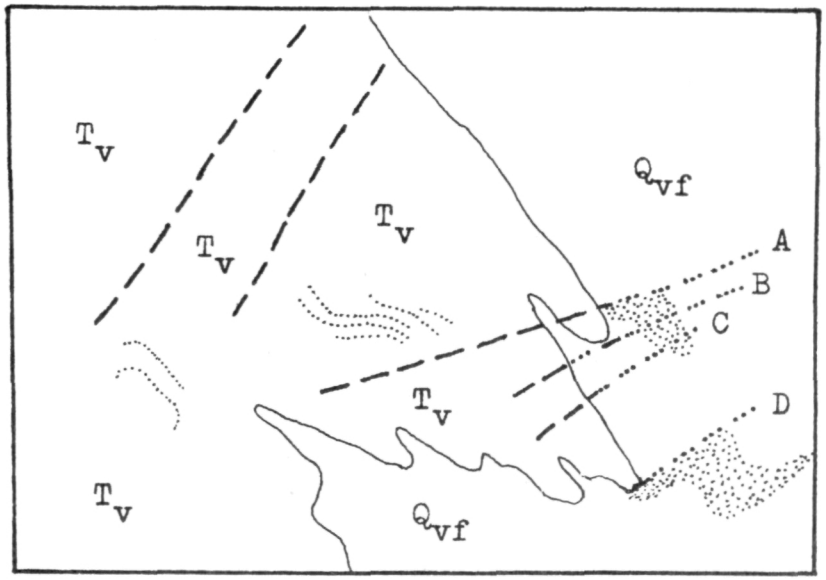

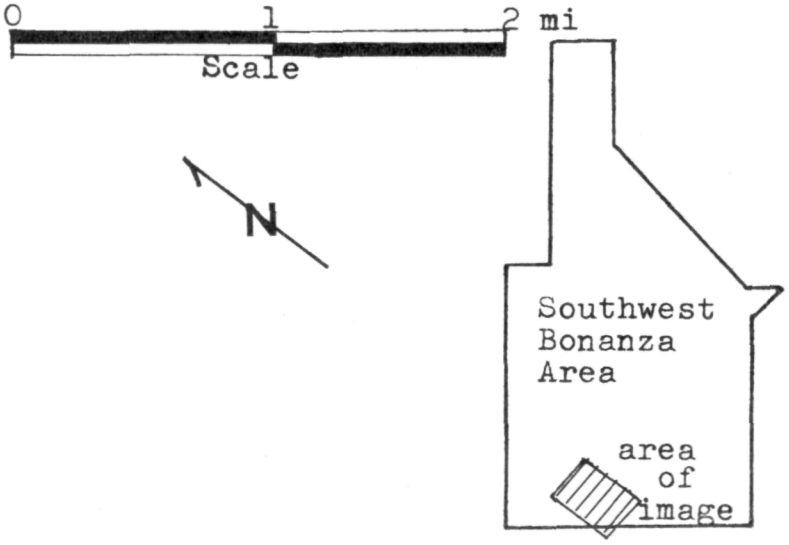

Q_{vf} Quaternary valley fill (gravels)

T_v Tertiary volcanic rocks

Areas of anomalous moisture

Lithologic contact

Lineament (possible contact)

Fault

Covered fault

Figure 56. Interpretation of Mission 105, 8- to 14-μm, daytime thermal imagery in the Findley Gulch area (line 18). Note faults A, B, C, and D which extent into area of valley fill. Areas of anomalous moisture appear to be controlled by these faults.

monzonite and gneiss crop out. These lineaments may represent major foliation within the Precambrian rocks. However, similar lineaments corresponding to minor drainage channels occur in areas of volcanic rock outcrop. Consequently, the northwest-trending lineaments are not unique to the Precambrian terrane and the precise boundaries of the Precambrian outcrop can not be traced on the thermal imagery.

In summary, the interpretation of the daytime thermal imagery shows that the thermal infrared scanner is capable of producing imagery that contains considerable detail, but much of the geologically meaningful information is submersed in the stronger contrasts produced by non-geologic phenomena. The daytime infrared imagery does not appear to be as useful for geologic mapping as the color photography, but some features are easier to see on the thermal imagery. There is very little intrinsic difference between the 3- to 5-μm and the 8- to 14-μm daytime imagery.

Pre-dawn thermal imagery in the southern Bonanza area (1:17,000) was obtained on Mission 168. Again, the thermal data were provided by the RS-14 thermal scanner aboard NASA's NP3A aircraft. The quality of the imagery is good but only the 8- to 14-μm channel of the RS-14 was operative. Since previous daytime imagery had been flown in the area on Mission 105, identical daytime coverage had to be omitted from Mission 168 in order to cut down the total length of the mission. Therefore, the daytime and

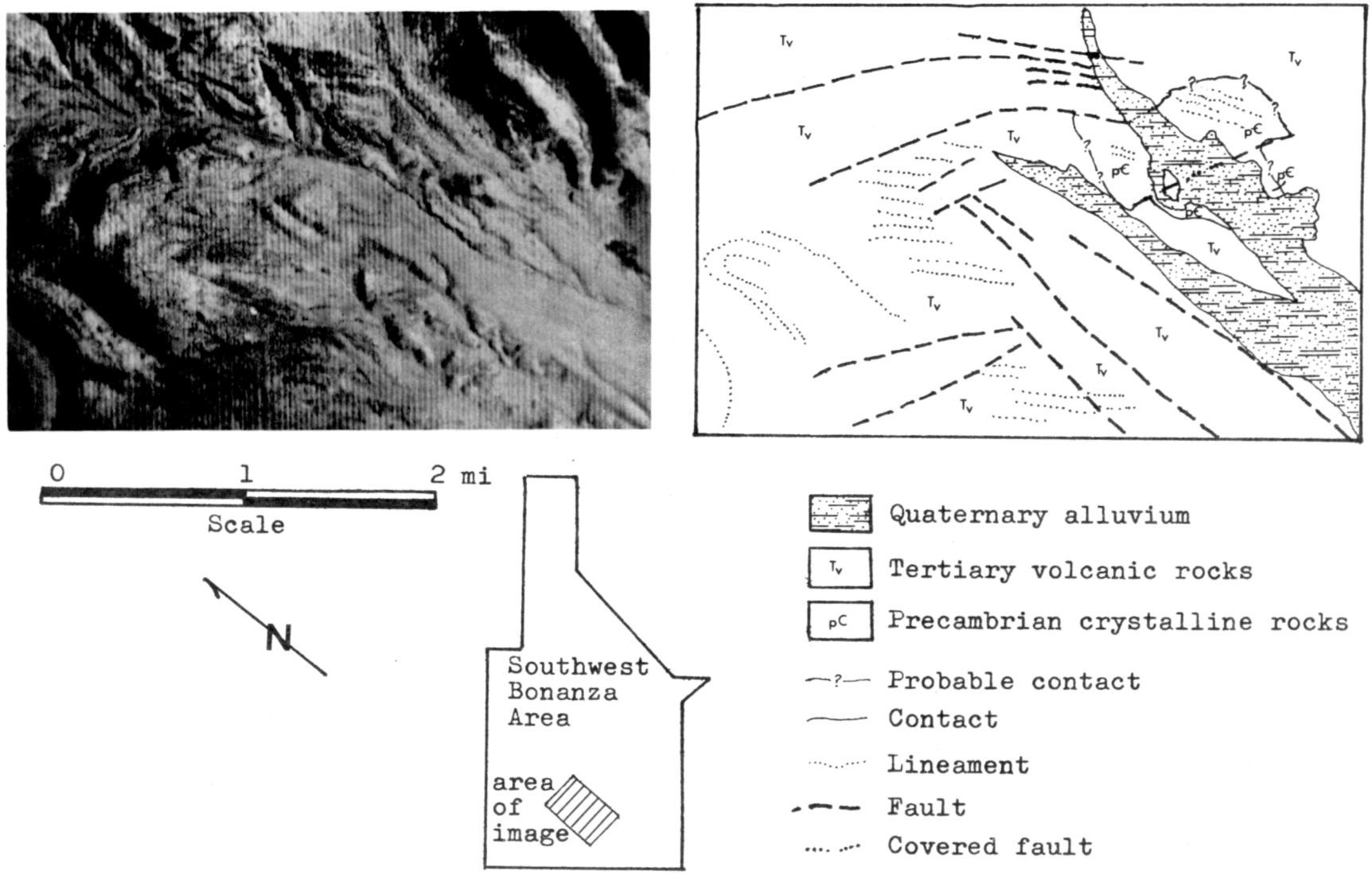

Figure 57. Interpretation of Mission 105, 8- to 14-μm, daytime thermal infrared imagery in the Findley Gulch area (line 20), showing lineaments in areas of outcrop of Precambrian crystalline rocks. Note that the lineaments in the volcanic terrain differ slightly from those cutting across the Precambrian outcrop.

pre-dawn infrared imagery in the Bonanza area are not directly comparable, not only because the scale of the imagery obtained on the two missions was different, but because weather, soil moisture, and vegetation conditions were not identical for the two missions. In order to avoid misleading conclusions regarding the relative utility of the mid-day and pre-dawn thermal imagery, no direct comparisons were made.

Interpretation and evaluation of Mission 168 pre-dawn thermal imagery reveals that it, like the daytime thermal imagery, presents many strong thermal contrasts that reflect topography. Among the parameters that are related to topography and affect the thermal values are slope-angle and direction (relative to the sun's illumination angle), and near-surface microclimate.

The pre-dawn thermal contrasts are generally low, and the gain of the RS-14 scanner must be increased to compensate for the low level of the thermal energy received. As a result, scan lines appear on the imagery. When a greater amount of thermal energy is being received, as in the daytime imagery, the gain can be turned down and the scan lines are no longer apparent on the imagery. In spite of the degradation of the imagery by the scan lines, the increased gain of the thermal scanner increases the instrument's capability to record the relatively low-level thermal energy emitted during the pre-dawn hours and allows a useable image to be produced.

Pre-dawn thermal imagery is often considered superior to daytime thermal imagery for geologic applications because thermal contrasts related to topographic effects may be subdued relative to thermal contrasts reflecting differences in the soils and rocks. After sunset, thermal contrasts produced by differential heating of slopes during the daylight hours begin to diminish along with all other thermal contrasts. But the rate of cooling of all areas is controlled by the thermal diffusivity of the exposed materials. As the total heat budget is depleted, thermal differences that reflect the contrasting diffusivities of various soils and lithologies may be maintained longer than those related solely to differential heating of slopes. As a result, these geologically significant contrasts may be most apparent on the pre-dawn thermal imagery.

Figures 58 and 59 are examples of the Mission 168 pre-dawn thermal imagery in areas of moderately high relief (600 ft). Figure 58 is the area surrounding Studhorse Meadow along the eastern edge of the southwest Bonanza area. Both features A and B are stream valleys. In area B, a spring produces a zone of very high moisture along the major drainage. The high-moisture area is evident as a cold (dark) area superimposed on the cool (grey) background of alluvium which is surrounded by the warm (light) areas of shallow soil and rock. The parallel, curvilinear features in the upper right of figure 58 (near C) coincide

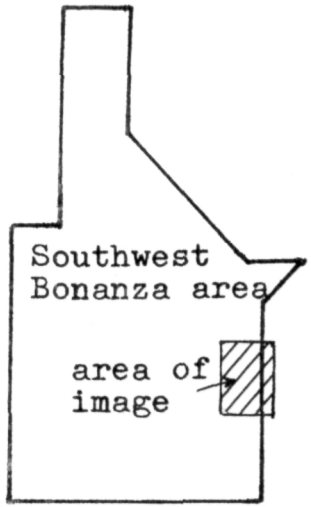

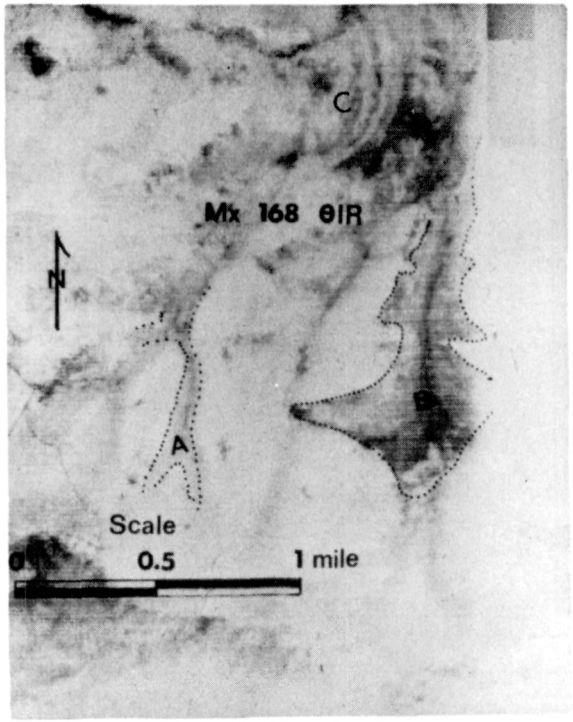

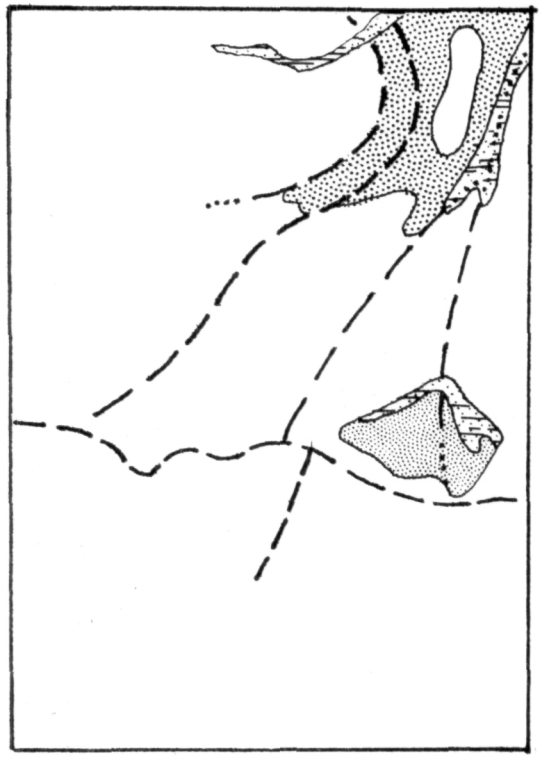

Quaternary alluvium

Quaternary alluvial fan

Quaternary gravel

Tertiary Rawley Formation

Fault

Lithologic contact

Figure 58. Comparison of Mission 168 pre-dawn, 8- to 14-μm thermal infrared imagery of the Studhorse Meadow area and geologic map of the same area.

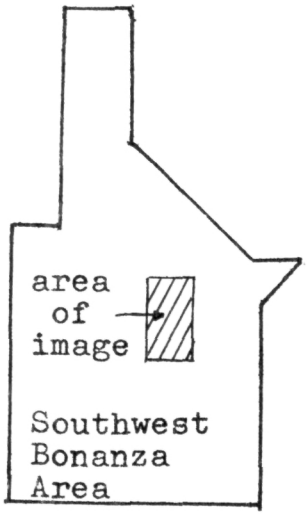

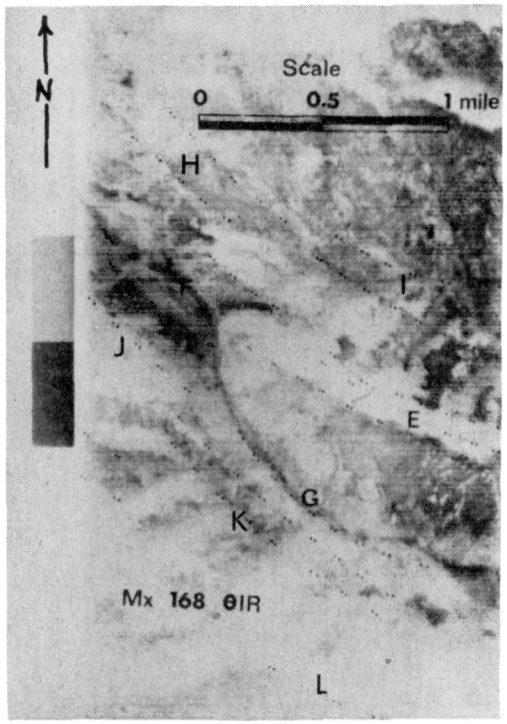

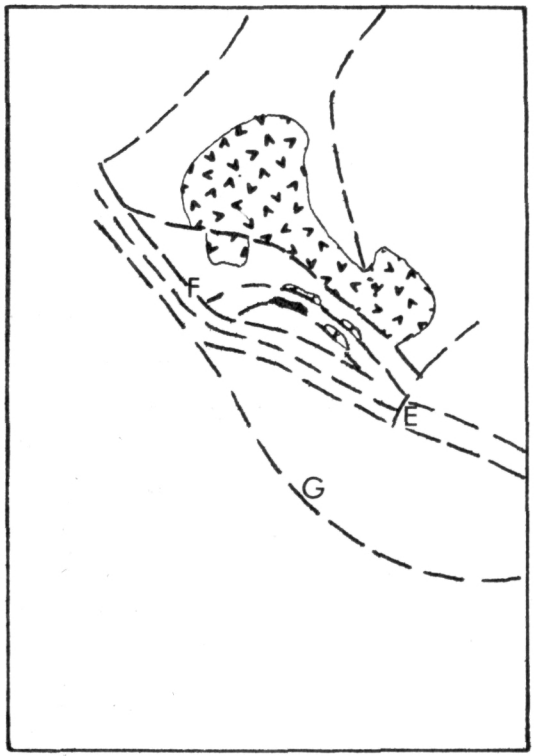

Tertiary Rawley Formation

Tertiary Bonanza Formation

Precambrian quartz monzonite

Fault

Contact

Figure 59. Comparison of Mission 168 pre-dawn, 8- to 14-μm thermal infrared imagery to the generalized geologic map for the Little Kerber Creek area. Lineaments noted on the imagery are marked by double rows of dots.

with the major elements of a large fault zone. At this point, the fault zone is topographically expressed as a series of curved drainage channels.

Figure 59 is the thermal imagery in the area of Little Kerber Creek along the west edge of T 46 N, R 8 E. The lineaments near E, F, and G correspond to elements of a major fault zone along the southwest side of the Bonanza caldera (plate 1). These same lineaments can be traced on the Mission 105 photography. However, the parallel and sub-parallel lineaments seen to the northeast (near H and I) and southwest (near J, K, and L) were not mapped in the field nor found on the photography. Their similarity to lineaments representing mapped faults suggest that they are a part of the same fault system. The fact that these features were not detected in the field may only mean that they are covered or have very minor displacements. Their expression on the thermal imagery would certainly lead one to suspect corresponding faults even though there is no visible evidence of them in the field.

Three lithologies crop out in the area of figure 59 but no difference can be detected in the infrared emittances of the units as seen on the pre-dawn imagery. The three lithologies present in this particular area are

Precambrian quartz monzonite, Rawley andesite, and Bonanza latite ash-flow tuff. Laboratory tests to determine the 8- to 14-μm thermal infrared reflectances of twenty samples representing these and other units within the Bonanza area were conducted by personnel of Martin Marietta Corporation. The spectral emissivity curves computed from these reflectance measurements (Gliozzi and others, 1970; this report, p. 127-128) give little insight into the behavior of total emittance values as measured by the thermal imaging system of the aircraft. However, the emissivity curves do suggest that differences in emittance (a function of the total area under the emissivity curve) may be small for the sampled lithologies and that weathering and viewing angle can have considerable influence on the emittance values. Other factors that undoubtedly influence the emittance values recorded by the thermal scanner are surface roughness and interference from other material on (or near) the surface or in the atmosphere.

Whether from lack of contrast or as a result of complicating factors, the lithologies in the Bonanza area could not be identified or even differentiated on the basis of their infrared emittances as recorded by the thermal scanner.

Infrared Spectrometry

Infrared spectrometric data in the Bonanza area were obtained on line 27 of Mission 105 and line 65 of Mission 184. In both cases, photography and thermal scanner imagery were also flown at the same time. Boresight photography and 8- to 14-μm radiometric data were obtained for location and calibration of the spectrometer data. In addition, calibration lines were flown over Russell Lakes.

The Airborne Rapid-Scan Spectrometer (ARSS) aboard NASA's NP3A aircraft records 6.7- to 13.2-μm infrared radiation emitted from the earth's surface and is capable of producing measurements with an accuracy equivalent to 0.2° C. The ARSS scans its spectral range 6.5 times per second, and records a complete 6.7- to 13.2-μm spectrum every 27 ft when flown at 300 mph.

The ARSS was operating properly on Mission 105 and the data appeared to be useable. It was hoped that infrared spectrometric curves obtained could be correlated with the various lithologies that had been mapped on the ground and tested in the laboratory. The identified curves, in turn, could be correlated with one another in order to see if there was any uniqueness upon which to base lithologic identifications.

A computer technique for comparing the spectrometric curves was developed by Martin Marietta Corporation investigators (Gliozzi and others, 1971a). Preliminary tests in areas of broad homogeneous outcrop indicated that some rock types, particularly the carbonates, might be distinguishable. Unfortunately, an accurate appraisal of the data and the interpretation system could not be made because the spectrometer boresight camera was badly misaligned. As a result, the spectrometer data could not be precisely correlated with the respective ground points.

Line 65 of Mission 184 spectrometry, flown in September, 1971, covers almost the same area as line 27 of Mission 105. The spectrometric tapes for line 65 have not yet been received, so they have not been evaluated. However, the hard copy plots have been received and indicate that good spectrometric data were recorded on Mission 184. If the boresight camera functioned properly, an evaluation of the Mission 184 spectrometer data should soon be possible.

Side-Looking Airborne Radar (SLAR)

Mission 105, 168, and 184 provided side-looking airborne radar imagery of the Bonanza area. All of the SLAR lines were flown approximately 25,000 ft amsl with the Philco-Ford DPD-2 (16.5 GHz) radar system. The scale on all the Bonanza area SLAR is approximately 1:160,000. Imagery at this scale provides no detailed information. It is best used for regional structural interpretations based on textural patterns and lineaments that reflect topography. In an area as geologically complex as the Bonanza area and where lithologies show relatively little physical contrast, there is little chance that the SLAR data can provide lithologic discrimination.

The Mission 105 SLAR looks westward across the Bonanza volcanic center. The Bonanza area and some of its major topographic features, such as Studhorse and Kerber drainages, can be recognized on the radar imagery. However, the SLAR equipment was not functioning at its best and the imagery quality is poor. All of the near range information was lost, and there is a great deal of signal break-up and noise across the entire line. Consequently the Mission 105 SLAR data were judged inadequate for proper evaluation of the imagery for geologic studies.

The DPD-2 radar set flown on Mission 168 has been modified by NASA so that it operates simultaneously as a brute-force and synthetic-aperture system. Because the

system transmits both the vertically and horizontally polarized portions of the returning energy, it can simultaneously produce four varieties of radar images. Furthermore, the radar operator has the option of recording either the vertically polarized or horizontally polarized mode for the returning signal. Thus, two passes of the aircraft can produce eight different radar images.

A first step in the evaluation of the radar was to determine which, of all the radar modes, produces the best radar imagery for geologic applications. In this determination, "best" is taken to mean "that which produces the greatest amount of useful information". To determine this, a few radar lines were flown twice so that all eight varieties of radar imagery could be obtained. The radar images were then compared. Figure 60 compares the various radar modes and configurations on line 61 of Mission 168, which looks east across the northern San Luis Valley toward the Sangre de Cristo range. Comparison of each of the polarization combinations in brute-force and synthetic-aperture modes shows that the horizontally received brute-force image is definitely better than the horizontally received synthetic aperture return regardless of the polarization of the transmitted energy. A similar comparison shows that the synthetic aperture system yields the best image when recording vertically received returns, although the difference is not as

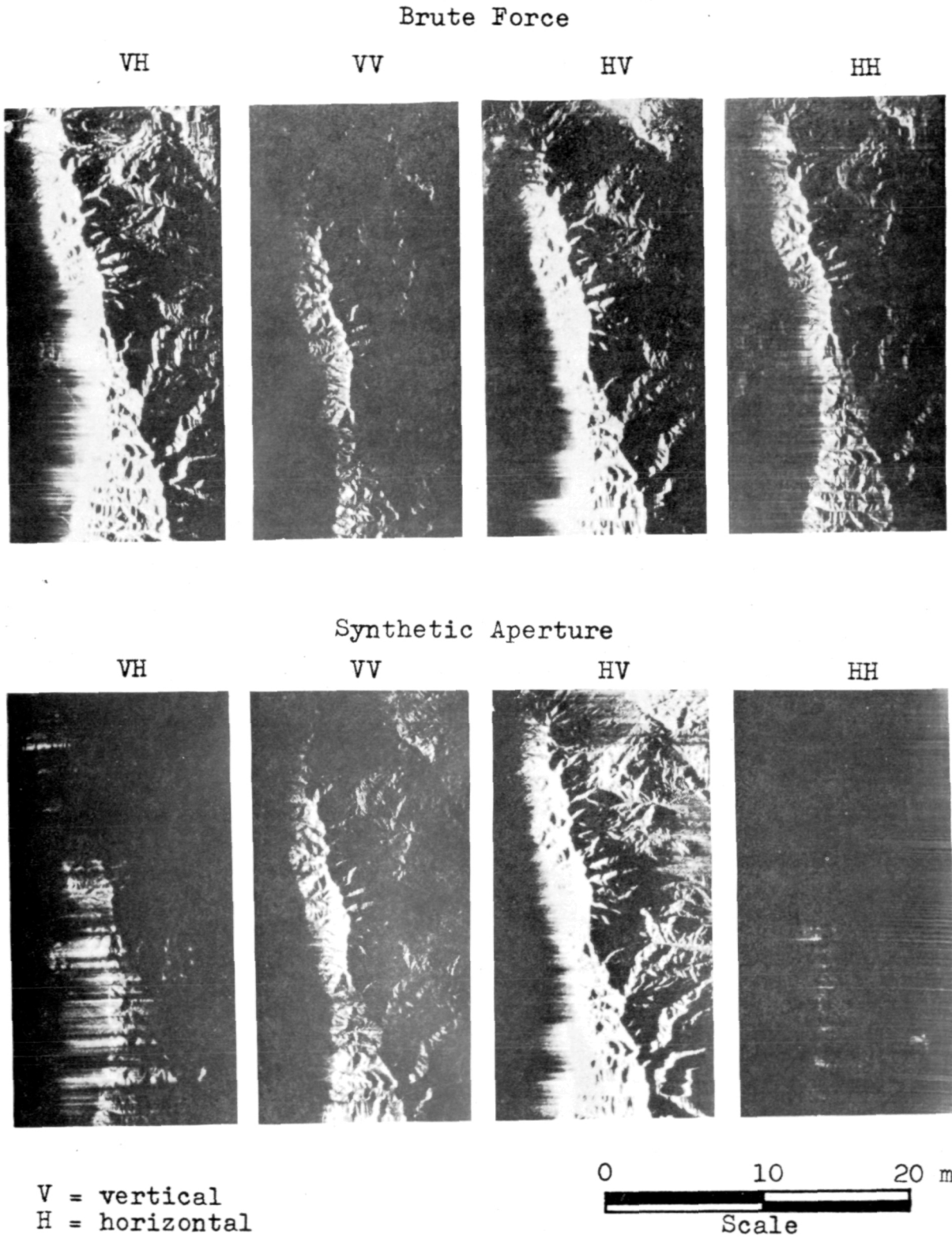

V = vertical
H = horizontal

Figure 60. Comparisons of various polarization modes and imaging configurations for Philco-Ford DPD-2 radar system. Mission 168 SLAR, line 61, covering the northern Sangre de Cristo range. VH indicates vertically polarized energy transmitted and horizontally polarized energy recorded, etc.

striking. Further comparison of the brute-force and synthetic-aperture data indicates that the synthetic aperture might be more susceptible to signal loss and excessive noise (note the dark bands where all image detail is lost). The texture of the brute-force radar is smoother, giving it a better appearance, and, possibly, somewhat better resolution than the synthetic-aperture data.

Assuming that the photographic processing was the same for each of the various radar polarization modes, comparison shows that brighter images are produced by oppositely-polarized transmit-return modes (VH and HV). The HV data is definitely the brightest of the synthetic-aperture imagery, but the VV mode produces only slightly less useful information. Similarly, the VH brute-force imagery is brightest, but each of the other brute-force images yields nearly the same amount of useful data. The dominant slope-direction (with respect to the look-angle) is clearly an important consideration. The like-polarized radar modes yield the greatest amount of information on the near slope of the mountain range, while the cross-polarized images reveal the greatest detail on the far slope.

Table 7 summarizes the different systems and polarizations of the Mission 168 SLAR and gives a rating for each type on a 1-5 basis. This rating yields a relative measure of the quality of the Bonanza area imagery.

Table 7. Results of quality comparison on various radar modes based on Mission 168 radar data.
(Rating system: 1=poorest 5=best)

System	Transmit Polarization	Receive Polarization	Rating
Brute Force	Vertical	Horizontal	4
Brute Force	Horizontal	Horizontal	5
Brute Force	Vertical	Vertical	3
Brute Force	Horizontal	Vertical	4
Synthetic Aperture	Vertical	Vertical	4
Synthetic Aperture	Horizontal	Vertical	5
Synthetic Aperture	Vertical	Horizontal	2
Synthetic Aperture	Horizontal	Horizontal	1

The Bonanza area was imaged on four lines of the Mission 168 SLAR. Each of the four lines has a different "look" direction across the Bonanza caldera. Interpretation and comparison of the images from the different lines gives an indication of the effect of viewing direction on the SLAR data and some idea of the importance of having SLAR with the best look-direction in any given area.

The Bonanza area is particularly amenable to an investigation into the effects of look-direction because the dominant radial and concentric structural and topographic pattern includes structural features at different angles to the radar beam regardless of look-direction. At the

same time, the topographic relief is high and provides various slope-angle situations, yet there is no strongly dominant slope direction persisting throughout the area.

Initial interpretation of all four lines of SLAR imagery in their area of common coverage revealed 16 features that correspond to structures mapped in the field. The features seen on the SLAR imagery are the major features among more than 100 faults mapped in this area. Twelve of the 16 features (75%) were located on the radar image with a southeast look-direction. On the other extreme, only 8 of 16 features (50%) were apparent on the southwest-looking image. Combinations of two look-directions yield results varying from 69% to 94% of the information available from all four images, with the best combination of two images being with look-directions differing by 90 degrees. The Mission 168 SLAR interpretations suggest that a look-direction perpendicular, or nearly perpendicular, to a given structure provides the best topographic enhancement of that structure. Therefore, in areas of strongly oriented structure, SLAR flight lines should be flown parallel to the structure. Also, better enhancement of topographically expressed structure is achieved by SLAR which looks "down-slope"; that is, radar that is flown with the aircraft nearest to the higher elevations and covering the lower-elevation terrain in the far range of the radar imagery. This holds true

except when the slope-angle is so steep that the down-slope is shadowed (fig. 61). These observations are in keeping with the geometry of radar return (Rydstrom, 1966) which is largely dependent on dihedral and trihedral specular reflections of the radar energy (figs. 62a and 62b). With this geometry, a lower illumination angle favors high contrast between topographic anomalies and the dominant slope.

The overall contribution of the four lines of Mission 168 SLAR to the geological data in the south and west Bonanza area consists of 32 linear features (only 16 of which lie in the area of common coverage). Twenty-six of the 33 linears correspond to mapped faults (fig. 63). The remaining 7 features (nos. 4, 12, 14, 20, 23, 26, and 27) represent strong topographic alignments which, according to field evidence, do not represent structural features.

SLAR coverage of the central Bonanza district and the Bonanza volcanic field was obtained on two Mission 184 lines. These two opposite-looking lines were very precisely spaced and flown so that their coverage is very nearly identical. HH and VH polarized data were recorded on both the brute-force and synthetic-aperture channels for both lines. The brute-force imagery on both lines is sharper and contains more useful data than does the synthetic-aperture imagery. Also, the cross-polarized (VH) imagery

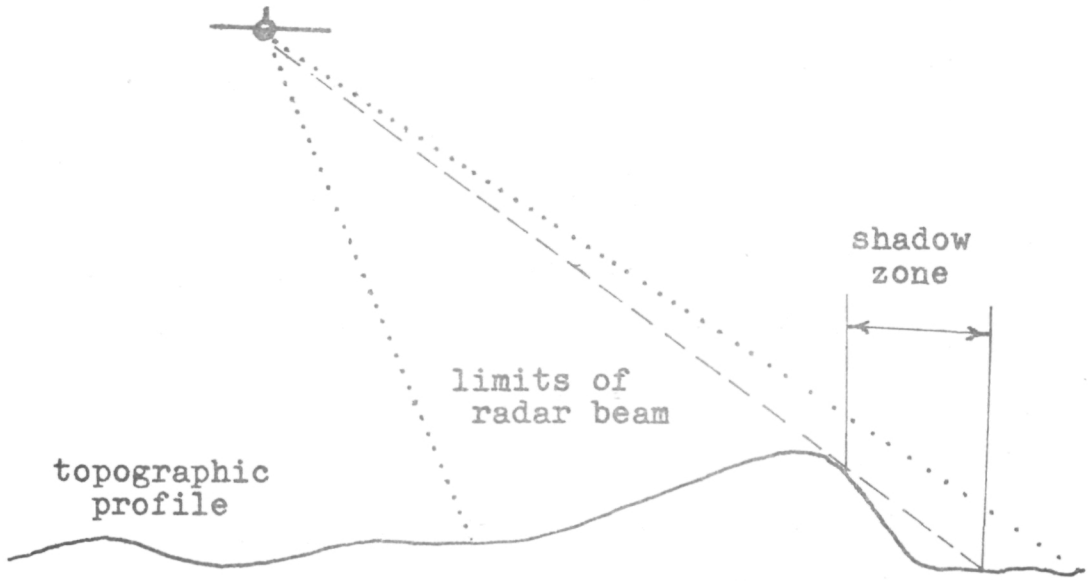

Figure 61. Diagram showing conditions under which a portion of the far slope of topographic high lies within a shadow zone and is not imaged.

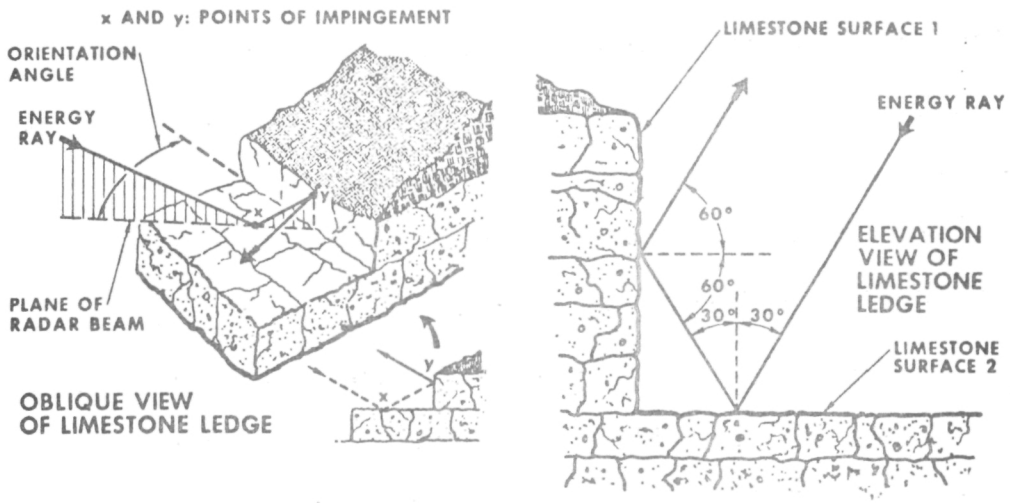

Figure 62. Diagrams depicting important modes of radar reflection (after Rydstrom, 1966, p. 196).

FIGURE 63

SOUTHWEST BONANZA AREA

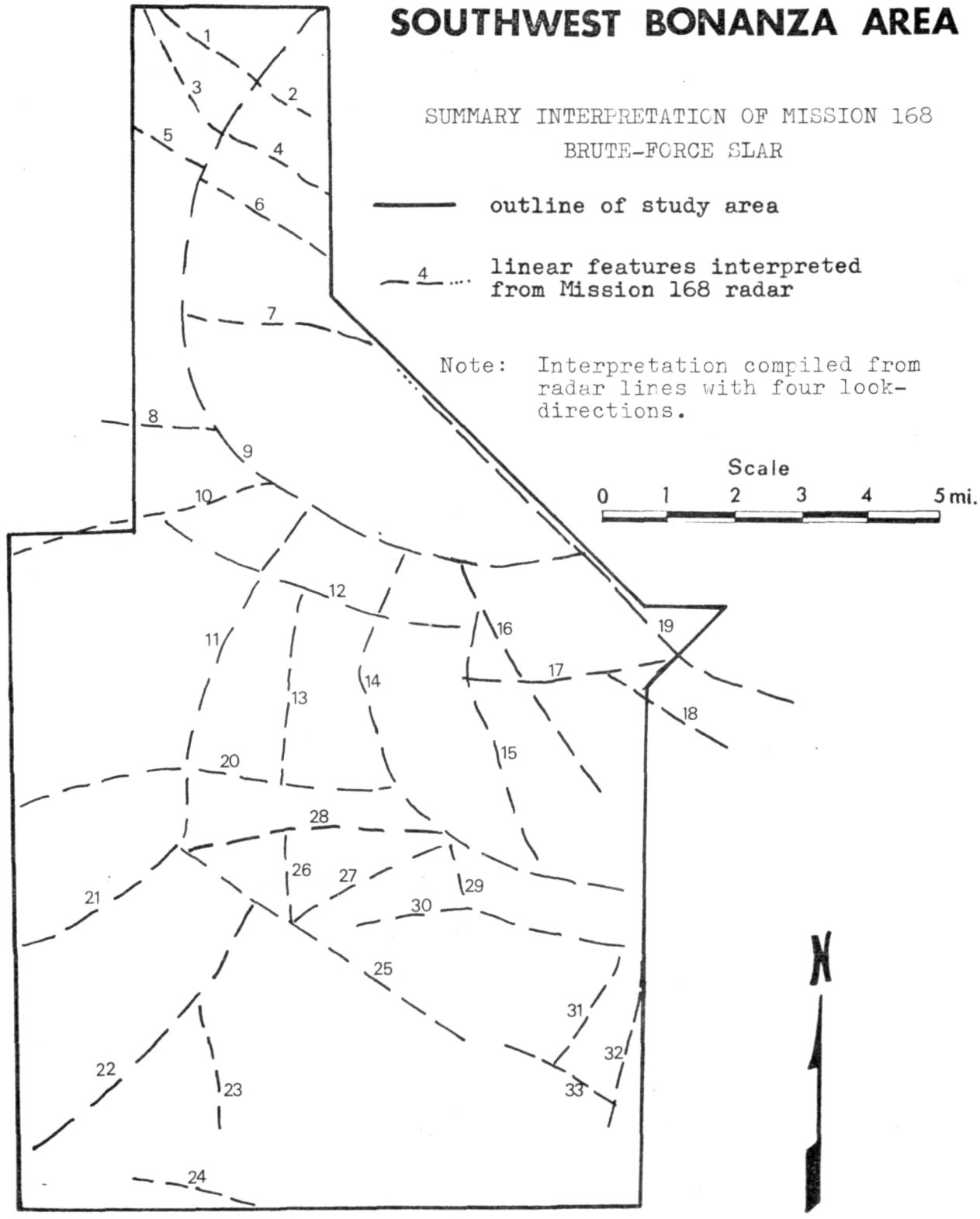

from both channels shows greater contrast than the like-polarized (HH).

The Mission 184 radar imagery displays the Bonanza caldera very well and many of the concentric and radial faults related to the caldera are also accentuated on the SLAR imagery. In the southwest Bonanza area, 32 lineaments were found on the Mission 184 SLAR which correspond to mapped faults (fig. 64 and plate 1). Twenty-three other lineaments were found on the SLAR imagery which do not correspond to faults or could not be verified from the field relations. Thirty-two additional lineaments lying outside the southwest Bonanza area were also noted, but no attempt was made to establish their significance.

Interpretation of Mission 184 SLAR imagery in the southern part of the Bonanza district reveals that most of the same features seen on the east-looking imagery are also well expressed on the west-looking imagery. One notable exception to this is the region of high relief around the caldera itself, where structures of the steeply westward-sloping terrain are best revealed on the west-looking imagery while those on the steeply eastward-sloping terrain are best expressed on the east-looking imagery. These observations confirm the conclusion derived from the Mission 168 SLAR interpretation; topographically-expressed structures are best enhanced by radar that looks down the slope of the terrain.

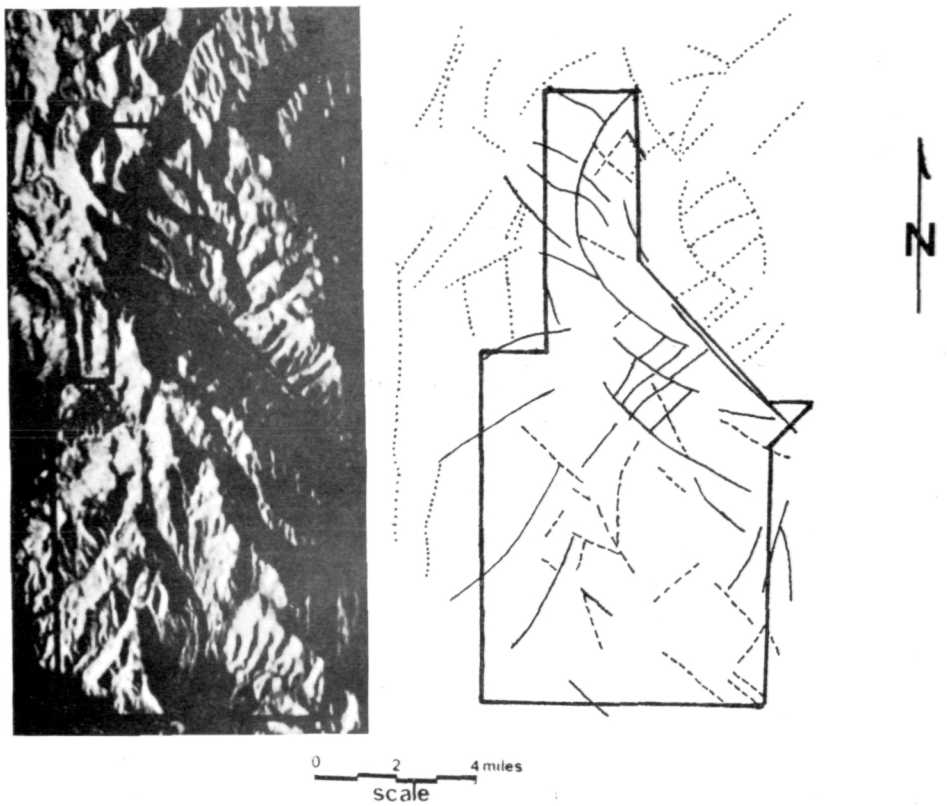

Outline of southwest Bonanza area

Radar linears in the southwest Bonanza area corresponding to mapped faults

Radar linears of the southwest Bonanza area that do not correspond to mapped faults

Unconfirmed radar linears outside the southwest Bonanza area

Figure 64. Interpretation of Mission 184 SLAR of the southwest Bonanza area (line 80, brute-force, VH polarization).

In evaluating the observations drawn from interpretation and comparison of the Mission 168 and Mission 184 SLAR imagery of the southwest Bonanza area, one must keep in mind that all the images were produced by the NASA DPD-2 SLAR system. The SLAR images used in this evaluation were not of the highest quality and most of the evaluations are severely limited by this lack of quality. Other critical factors in these evaluations are the assumptions that the photographic processing was the same for each image and that the initial exposure and film selection was optimum. The general appearance of the imagery suggests that a better combination of film type, exposure, and processing might have been chosen and, certainly, this could influence the quality of the various images considerably. Nevertheless, some of the conclusions derived from the various comparisons and interpretations may serve as a qualitative guide in selecting polarization modes, flight line directions, and look directions for SLAR imaging.

Radar Scatterometry

Five lines of 13.3 GHz scatterometry were flown on Mission 153. Three of these lines are in the southwest Bonanza area between Hayden Peak and Saguache. Preliminary evaluation of the "time history" curves from the scatterometer revealed problems with noise and difficulties in relating the data and reference signals. In subsequent discussion with NASA personnel, it was learned that the scatterometer had not been working properly for some time. Inspection of the quadrature channel readouts from the Mission 153 scatterometer data tapes showed differences of such magnitude that no quantitative information and, probably no reliable qualitative information would be retrievable. As a result, the Mission 153 scatterometer data were not suitable for making any sort of sensor evaluation. Therefore, it was decided, upon recommendation from NASA, to make no attempt to evaluate the Mission 153 scatterometry.

SUMMARY AND CONCLUSIONS

The work described in this report demonstrates that remote-sensing techniques can provide extremely valuable information for geologic mapping in either a partially known or unknown area. The information provided by some sensors increases the data base and the efficiency of the mapping program enough that the geologist should no longer be limited to using standard black-and-white photography as his only aid in mapping. However, color and/or color infrared photography are the only remote-sensing tools which warrant routine use. Other techniques are, as yet, capable of producing optimum results only when their use is carefully controlled and aimed at a particular application. The proper use of these sensors and the interpretation of the data require additional training on the part of the geoscientist. He must be able to select the proper sensor for the problem he wishes to solve, specify the manner in which data are to be gathered, and interpret the data.

The geologic data accumulated in this study, coupled with information from previous studies in adjacent areas, have made possible a much more complete assessment of the geology of the Bonanza center and its relation to the regional tectonics. The post-Paleozoic geologic history of the area, as reconstructed from these data, can be summarized in seven steps.

1. Precambrian crystalline rocks and Paleozoic sedimentary rocks were folded and faulted into a series of northwest-trending anticlines and synclines with complimentary high-angle reverse faults on their flanks. These are thought to have formed as an early stage of Laramide deformation in response to northeast-southwest compressive stresses associated with the uplift of the Sawatch arch.

2. Late Laramide uplift of a basement block (the Sierra Blanca Massif) to the south may have produced the northward-directed stresses which resulted in low-angle thrusting in the Kerber area.

3. Intermediate to silicic volcanism in early and middle Oligocene time was accompanied by local doming in the area of Bonanza. A concentric and radial fault pattern developed on the domed area in response to the upward- and outward-directed forces exerted by a subsurface magma. The radial faults served as planes of minor structural adjustment between the concentric faults which served as planes of primary stress-release.

4. Eruption continued as the magma evolved from andesite to latite. The major portion of volcanism was culminated with the explosive eruption of a thick sequence of latite ash-flow tuffs.

5. Sufficient material (≈25 cu mi) was removed from the magma chamber during eruption of the ash-flow sequence that the pressures were relieved and the central portion of the domed area began to subside within the concentric fractures. Small intrusive and extrusive bodies forced their way up along major fractures as the central area sank deeper into the magma chamber.

6. Hydrothermal fluids which formed as a dying phase of the volcanic activity followed the radial fault pattern outward from the central area and produced zones of alteration and mineralization wherever the fractured volcanic rocks provided adequate channels and a favorable temperature-pressure environment.

7. Regional east-west taphrogenic forces began to affect the area in Miocene time, and the northern Rio Grande rift began to develop. The complexly faulted caldera area provided a zone of weakness to accommodate the down-to-the-east movement of the northern San Luis Valley and to serve as an area of transition between the graben structure of the northern San Luis-Arkansas Valley area and the broad, hinge structure of the main San Luis Valley. Consequently, movements complimentary to the presently active Rio Grande rift system have affected the overall structural picture in the Bonanza area.

The development of the Bonanza mining district has long been hampered by an inadequate knowledge of the geology of the surrounding area. Recognition of the structural pattern and knowledge of post-volcanic adjustment is a very important part of the geologic picture. Insight gained in this study into these geologic aspects may serve as the basis for an effective minerals exploration program in the Bonanza area.

APPENDIX A

Petrographic Descriptions of Rock Samples from the Southwest Bonanza Area

Thin section analysis were made of forty-nine rock samples from the Bonanza area. Most of these analysis were made to obtain a better understanding of the character of the rocks for purposes of correlation and description. However, some of the samples were subjected to spectral reflectance measurements, and the petrographic studies were necessary in order to better interpret the test results.

Ten of the samples (PRC-1 thru 10) were collected specifically for infrared spectral reflectance studies and, although they are from the Bonanza district, they are not from the southwest Bonanza area, which is the subject of this report. The thin section analysis and spectral emittance measurements from these samples are included in this report because the samples are representative of rock types seen in the southwest Bonanza area and the spectral measurements were made in connection with the southwest Bonanza area remote-sensing evaluations.

Ten other samples (PRC-11 thru 20) were collected in the southwest Bonanza area as geologically representative samples to be studied for description and correlation purposes, and were later selected for spectral

measurements. The remaining 28 samples were selected and studied strictly for correlation and interpretation. No spectral measurements were made on them.

Compositions of samples from locations 1 thru 10 were determined by modal analysis (1,500 points counted). Other compositions are estimated. Compositions of plagioclase feldspars were determined using the Michel-Levy statistical method (Heinrich, 1965, p. 360). Selective staining of feldspars was used as an aid in determining relative abundances of feldspars in some samples.

PRC No.	Page	Field Number	Map Unit	Petrographic Designation	Location Section	Township	Range
1	A-52	6-4-69-1B		Vein Material	24	47N	7E
2	A-39	6-4-69-2B	T_{uv}	Biotite Hornblende Andesite	14	47N	7E
3	A-18	6-4-69-3B	T_b	Biotite Latite Ash-Flow Tuff	14	47N	7E
4	A-19	6-4-69-4B	T_b	Biotite Latite Ash-Flow Tuff	23	47N	7E
5	A-20	6-4-69-5B	T_b	Biotite Latite Ash-Flow Tuff	24	47N	7E
6	A-49	6-4-69-6B	T_i	Latite	1	46N	7E
7	A-8	6-4-69-7B	P_l	Dolomite and Chert	26	46N	8E
8	A-5	6-4-69-8B	pC	Quartz Monzonite	23	46N	8E
9	A-6	6-4-69-8D	pC	Hornblende Gneiss	23	46N	8E
10	A-7	6-4-69-8F	pC	Migmatite	23	46N	8E
11	A-9	J-1A	T_r	Hornblende Basalt	29	46N	8E
12	A-10	J-2C	T_r	Altered Hornblende Augite Basalt	29	46N	8E
13	A-40	J-5C	T_{uv}	Latite Ash-Flow Tuff	11	46N	8E
14	A-41	A-17A	T_{uv}	Hornblende Augite Biotite Andesite	1	46N	7E
15	A-21	A-12A	T_b	Biotite Latite Ash-Flow Tuff	35	48N	8E
16	A-11	A-11?	T_r	Biotite Hornblende Andesite	4	45N	8E
17	A-42	A-17B	T_{uv}	Hornblende Biotite Andesite	1	46N	7E
18	A-12	S-157	T_r	Augite Basalt	12	45N	7E
19	A-13	S-201	T_r	Biotite Augite Basalt	26	46N	7E
20	A-14	S-178	T_r	Augite Biotite Basalt	12	45N	7E
21	A-22	M-4	T_b	Biotite Latite Ash-Flow Tuff	28	45N	7E
22	A-23	M-5	T_b	Biotite Latite Ash-Flow Tuff	28	45N	7E
23	A-24	M-6	T_b	Biotite Latite Ash-Flow Tuff	28	45N	7E
24	A-25	M-7	T_b	Biotite Latite Ash-Flow Tuff	28	45N	7E

PRC No.	Page	Field Number	Map Unit	Petrographic Designation	Location Section	Township	Range
25	A-26	M-8	T_b	Biotite Latite Ash-Flow Tuff	28	45N	7E
26	A-27	M-9	T_b	Biotite Latite Ash-Flow Tuff	28	45N	7E
27	A-28	M-10	T_b	Biotite Latite Ash-Flow Tuff	28	45N	7E
28	A-29	M-11	T_b	Biotite Latite Ash-Flow Tuff	28	45N	7E
29	A-30	M-12	T_b	Biotite Latite Ash-Flow Tuff	28	45N	7E
30	A-31	M-13	T_b	Biotite Latite Ash-Flow Tuff	28	45N	7E
31	A-32	M-14	T_b	Biotite Latite Ash-Flow Tuff	28	45N	7E
32	A-33	M-15	T_b	Biotite Latite Ash-Flow Tuff	28	45N	7E
33	A-34	M-16	T_b	Biotite Latite Ash-Flow Tuff	28	45N	7E
35	A-35	M-18B	T_b	Biotite Latite Ash-Flow Tuff	28	45N	7E
36	A-36	M-19	T_b	Biotite Latite Ash-Flow Tuff	28	45N	7E
37	A-43	M-21	T_{uv}	Hornblende Biotite Andesite	28	45N	7E
38	A-44	M-22	T_{uv}	Hornblende Biotite Andesite	28	45N	7E
39	A-37	845-70	T_b	Biotite Latite Ash-Flow Tuff	31	46N	7E
40	A-48	805	T_{pp}	Biotite Rhyolite	11	47N	7E
41	A-45	1150	T_{uv}	Biotite Andesite	16	46N	7E
42	A-46	1163	T_{uv}	Lithic Ash-Flow Tuff	17-18	46N	7E
43	A-17	319	T_r	Augite Andesite	28	45N	7E
44	A-15	203	T_r	Silicified Biotite Latite	3	45N	7E
45	A-16	103	T_r	Augite **Andesite**	5	45N	8E
46	A-47	1300	T_{uv}	Hornblende Biotite Andesite	26	47N	7E
47	A-50	1196A	T_i	Leucocratic Biotite Aphanite	13	46N	7E
48	A-51	1196B	T_r	Hornblende Biotite Andesite	13	46N	7E
49	A-38	484	T_b	Biotite Latite Ash-Flow Tuff	28	46N	8E

Quartz Monzonite (pЄ)

PRC-8

Field Number: 6-4-69-8B (8B-f)

Texture and Fabric: Holocrystalline granular with coarse subhedral and anhedral crystals. Feldspars are subhedral and quartz crystals are anhedral.

Composition: (by modal analysis)

Plagioclase: 40.8% (Oligoclase-An_{10-15})

Microcline: 35.2% (two varieties)

Quartz: 22.0%

Biotite and Muscovite: 1.5%

Accessories: 0.5%

Alteration: Perthitic microcline and plagioclase are slightly sericitized.

Remarks: Plagioclase has tiny quartz inclusions which are aligned parallel to cleavage. Two types of microcline are present: slightly sericitized perthitic microcline and a later variety with well-developed quadrille twinning.

Petrographic Designation: Quartz Monzonite

Hornblende Gneiss (pC)

PRC-9

Field Number: 6-4-69-8D (8D-f)

Texture and Fabric: Holocrystalline with fine grained, prismatic, amphibole crystals strongly aligned and concentrated in zones, imparting a nematoblastic texture and gneissose structure to the rock. Crystals are mostly subhedral and both hornblende and plagioclase are commonly **poikiloblastic.**

Composition: (by modal analysis)

Hornblende: 69.8% (blue-green, highly pleochroic)

Plagioclase: 29.4% (Andesine, An_{20-25})

Accessories: 0.8%

Alteration: Relatively minor, some alteration of hornblende to biotite and magnetite.

Remarks: Alternating lenses of high hornblende concentration and zones high in plagioclase give gneissose structure. Lenses of hornblende are arcuate and discontinuous.

Petrographic Designation: Hornblende Gneiss **or Gneissic Amphibolite**

Migmatite (pC)

PRC-10

Field Number: 6-4-69-8-F (8F-f)

Texture and Fabric: Hornblende gneiss as described in sample 8D-f (p. A-6) intruded by veins of medium-grained, hypidiomorphic-granular, quartz diorite. The quartz diorite veinlet is about 1 cm wide paralleling the gneissose structure.

Composition: (by modal analysis)

Gneiss: 65%

Hornblende: 47.2%

Plagioclase: 50.1%

Biotite and Quartz: 2.7%

Quartz Diorite: 35%

Quartz: 53.2%

Plagioclase: 43.7% (Oligoclase)

Chlorite, microcline, and clinozoisite: 3.1%

Alteration: Slight sericitization of plagioclase; **some alteration of hornblende to biotite and magnetite.**

Remarks: Microcline appears to be a late stage replacement product in the quartz diorite.

Petrographic Designation: **Gneissic Hornblende Quartz Diorite Migmatite**

Manitou Dolomite (P_1)

PRC-7

Field Number: 6-4-69-7-C (7C-f)

Texture and Fabric: Dolomite occurs as fine-grained, homogeneous, subhedral crystals which appear tan or brown and contain small patches of carbonatious material. Chert is grey, cryptocrystalline quartz with tiny voids and veinlets filled with crystalline quartz.

Composition: (by modal analysis)

Chert: 51.4%

Dolomite: 42.8%

Crystalline Quartz: 4.0%

Carbonaceous material: 1.8%

Remarks: Fine veinlets of dolomite penetrate the chert.

Petrographic Designation: Dolomite and Chert

Rawley Hornblende Basalt (T_r)

PRC-11

Field Number: J-1A-B (1A-f)

Texture and Fabric: Porphyritic-aphanitic with fine to medium euhedral and subhedral phenocrysts randomly oriented in a cryptocrystalline, grey groundmass.

Composition: (estimated)

Phenocrysts: 40%

Plagioclase: 16% (Labradorite An_{55})

Hornblende: 12%

Magnetite: 5% (replacing hornblende)

Augite: 4%

Quartz: 3% (secondary

Groundmass: 60% (mostly plagioclase microlites)

Alteration: Groundmass shows some sericitization. Hornblende and augite altering to magnetite.

Remarks: Most plagioclase phenocrysts are strongly zoned (more calcic toward the center). Unzoned crystals tend to be more nearly euhedral. Hornblende is also weakly zoned.

Petrographic Designation: Hornblende Basalt

Altered Rawley Andesite (T_r)

PRC-12

Field Number: J-2C-B (2C-f)

Texture and Fabric: Porphyritic-aphanitic with abundant, fine to medium, euhedral and subhedral phenocrysts randomly oriented in a cryptocrystalline groundmass.

Composition: (estimated)

Phenocrysts: 58%

Plagioclase: 35% (Labradorite ?)

Magnetite: 9% (alteration product)

Orthoclase: 4% (badly altered)

Augite & Hornblende: 9% (completely altered)

Quartz: 1% (secondary)

Groundmass: 42% - mostly made up of highly-altered feldspar microlites.

Alteration: Extreme sericitization; mafics completely altered to sericite, chlorite, and magnetite. Some characteristic textures of hornblende and augite are still recognizable. Alteration appears partly hydrothermal with veinlets and voids filled with crystalline quartz and some replacement of crystals by silica.

Remarks: Plagioclase shows oscillitory zoning. Many crystals appear broken.

Petrographic Designation: Highly Altered Hornblende Augite **Basalt**

Rawley Hornblende Biotite Andesite (T_r)

PRC-16

Field Number: A-117A-B (117A-f)

Texture and Fabric: Porphyritic-aphanitic with fine and medium phenocrysts in a dark-grey groundmass. Prismatic phenocrysts are aligned, but groundmass microlites are randomly oriented. Crystals are euhedral and subhedral.

Composition: (estimated)

Phenocrysts: 41%

Plagioclase: 26% (Andesine-An_{44})

Hornblende: 6% (badly altered)

Biotite: 4% (often bent)

Orthoclase: 3%

Magnetite: 2%

Voids: 2%

Groundmass: 57% (mostly altered plagioclase microlites)

Alteration: Some crystals and the groundmass are strongly altered. Other crystals are relatively fresh.

Remarks: Plagioclase is strongly zoned. Altered phenocrysts and relatively fresh ones indicate two generations of phenocrysts, the earlier one being magmatically altered.

Petrographic Designation: **Biotite Hornblende Andesite**

Rawley Augite Andesite (T_r)

PRC-18

Field Number: S-157-B (S-157)

Texture and Fabric: Porphyritic-aphanitic with fine to medium, euhedral and anhedral phenocrysts randomly oriented in a groundmass of subparallel microlites.

Composition: (estimated)

Phenocrysts: 35%

Plagioclase: 22% (Labradorite An_{51})

Augite: 9%

Orthoclase: 3%

Magnetite: 1%

Groundmass: 65% (mostly plagioclase microlites)

Alteration: Some sericitization of feldspars; some augite altering to magnetite.

Remarks: Very little zoning of plagioclase; augite crystals often aggregated; groundmass microlites aligned parallel to phenocryst boundaries. A few ghosts of andesitic lithic fragments remain. The mineralogy is relatively simple.

Petrographic Designation: Augite **Basalt**

Rawley Biotite Augite Andesite (T_r)

PRC-19

Field Number: S-201-B (S-201)

Texture and Fabric: Porphyritic-aphanitic with fine to coarse phenocrysts set in dark-grey, microcrystalline groundmass. Euhedral and subhedral, prismatic phenocrysts and microlites are aligned to give a pilotaxitic structure.

Composition: (estimated)

Phenocrysts: 41%

Plagioclase: 25% (Labradorite An_{58})

Orthoclase: 4%

Augite: 6%

Biotite: 4%

Magnetite: 2% (replacing biotite and augite)

Groundmass: 59% (mostly aligned plagioclase microlites)

Alteration: Very slight; some sericitization of feldspars; magnetite replacing biotite and augite.

Remarks: The mineralogy is fairly simple but smaller feldspar phenocrysts are zoned (more calcic at center), and larger feldspars are not. Pyroxene appears simple.

Petrographic Designation: Biotite Augite **Basalt**

Rawley Augite Biotite Basalt (T_r)

PRC-20

Field Number: S-178-B

Texture and Fabric: Porphyritic-aphanitic with fine phenocrysts in a dark-grey, randomly oriented groundmass. Crystals are euhedral and subhedral.

Composition: (estimated)

Phenocrysts: 43%

Plagioclase: 26% (Labradorite An_{53})

Biotite: 7%

Augite: 5%

Magnetite: 2%

Hornblende: 3%

Groundmass: 57% (large percentage of plagioclase microlites showing slight pilotaxitic texture)

Alteration: Considerable sericitization; hornblende and biotite are mostly altered to magnetite.

Remarks: All plagioclase crystals are rather strongly zoned. Augite crystals are small. Hornblende crystals and biotite flakes are large and show considerable alteration.

Petrographic Designation: Augite Biotite Basalt

Rawley Banded Biotite Latite (T_r)

PRC-44

Field Number: S-203

Texture and Fabric: Porphyritic-vitric with fine and medium phenocrysts oriented subparallel to strong flow structure in the partially devitrified groundmass. Flow structure is emphasized by alteration and silicification. Hand specimen shows distinct banding.

Composition: (estimated)

Phenocrysts: 22%

Plagioclase: 10% (Andesine An_{33})

Biotite: 5%

Orthoclase: 5%

Magnetite: 2%

Crystalline Quartz: 8% (in veinlets and voids)

Groundmass: 70% (glass and iron oxides)

Alteration: Some devitrification of groundmass. Mafics other than biotite and magnetite completely altered. A few recognizable pseudomorphs of hornblende are present. Secondary silicification in veins parallels flow structure.

Remarks: Appears much like an ash-flow tuff, but lacks pyroclastic fragments.

Petrographic Designation: Silicified Biotite Latite

Rawley Augite Basalt (T_r)

PRC-45

Field Number: A-103

Texture and Fabric: Porphyritic-aphanitic with fine to medium phenocrysts in a groundmass of fine crystals; slightly pilotaxitic with euhedral and subhedral crystals.

Composition: (estimated)

Phenocrysts: 40%

Plagioclase: 28% (Andesine An_{47})

Augite: 10%

Magnetite: 2%

Groundmass: 60%

Plagioclase: 45% (Andesine An_{38})

Augite: 12%

Magnetite: 3%

Alteration: Augite altering to magnetite

Remarks: This rock looks much like an intrusive with its fine grained groundmass. Its mineralogy is very simple. Most plagioclase crystals are weakly zoned.

Petrographic Designation: Augite **Andesite**

Rawley Augite Andesite (T_r)

PRC-43

Field Number: 319

Texture and Fabric: Porphyritic-aphanitic with fine phenocrysts subparallelly aligned in a somewhat pilotaxitic groundmass of microlites. Crystals are euhedral and subhedral.

Composition: (estimated)

Phenocrysts: 38% (Andesine to Labradorite An_{40-55})

Plagioclase: 21%

Orthoclase: 4%

Augite: 11%

Magnetite: 2%

Hornblende: <1%

Groundmass: 62% (mostly plagioclase microlites)

Alteration: Hornblende is almost completely altered to magnetite. Considerable sericitization of feldspars.

Remarks: Altered hornblende and strongly zoned plagioclase crystals indicate some complexity, but the mineralogy is relatively simple.

Petrographic Designation: Augite Andesite

Bonanza Tuff (T_b)

PRC-3

Field Number: 6-4-69-3-B (3-f)

Texture and Fabric: Pyroclastic with definite compaction layering; contains abundant, angular, lithic fragments and phenocrysts in a glassy groundmass. Phenocrysts are fine to medium. Contains numerous, tiny, quartz veinlets. Small particles of uncrystallized glass are poikilitically enclosed in feldspar crystals.

Composition: (by modal analysis)

Phenocrysts: 34.6%

Plagioclase: 11.2% (Andesine ?)

Orthoclase and Sanidine: 12.4%

Biotite: 5.2%

Magnetite: 1.8%

Glass Shards: } 4.0%
Quartz: }

Groundmass: 43.8% (mostly devitrified glass)

Lithic Fragments: 21.6% (finely crystalline grey biotite andesite or basalt)

Alteration: Shows marked alteration which includes devitrification of groundmass, extreme sericitization, and biotite altering to magnetite and chlorite.

Remarks: The most notable things about this sample are the extreme alteration, and the remarkable compaction layering which distinguishes it as an ash-flow tuff. Lithics are relatively abundant.

Petrographic Designation: Biotite Latite Ash-Flow Tuff

Bonanza Tuff (T_b)

PRC-4

Field Number: 6-4-69-4-B (4-f)

Texture and Fabric: Pyroclastic with compaction layering emphasized in flattened pumice fragments; rather crystal-rich and contains many grey, angular, lithic fragments (finely crystalline biotite andesite). Groundmass is red-brown devitrified glass. Phenocrysts are fine to medium and lithics are medium- to coarse-grained. Small glass blebs are poikilitically enclosed in feldspar crystals.

Composition: (by modal analysis)

Phenocrysts: 32.2%

Plagioclase: 15.8%

Orthoclase and Sanidine: 13.6%

Biotite: 2.0%

Magnetite: 0.8%

Glass Shards: and Quartz: } 5.2%

Groundmass: 56.2% (mostly devitrified glass)

Lithic Fragments: 6.4%

Alteration: Groundmass is badly devitrified. Phenocrysts are highly sericitized and chloritized.

Remarks: Fewer lithics indicate that this sample may have come from higher in the section than sample 3-f. Many phenocrysts are broken or bent.

Petrographic Designation: Biotite Latite Ash-Flow Tuff

Bonanza Tuff (T_b)
(Highly Altered)

PRC-5

Field Number: 6-4-69-5-B (5-f)

Texture and Fabric: Pyroclastic with obvious compaction layering evident in flattened pumice lapilli; crystals also bent, broken, and aligned subparallel to compaction structures; contains a few fine to coarse andesitic, lithic fragments. Crystals, lithics and pumice are set in a matrix of altered and devitrified glass.

Composition: (by modal analysis)

Phenocrysts: 49.8%

Plagioclase: 3.8%

Orthoclase and Sanidine: 16.6%

Micas (Biotite, Chlorite, Muscovite): 3.2%

Magnetite and Pyrite: 2.0%

Quartz and Glass Shards: 24.2%

Groundmass: 46.2% (mostly devitrified glass)

Lithic Fragments: 4.0% (andesite)

Alteration: Shows extreme alteration, probably hydrothermal; feldspars highly sericitized. Biotite is replaced by chlorite and muscovite. Some magnetite is replaced by pyrite. Veinlets and vesicules are quartz-filled. The groundmass is largely devitrified.

Remarks: Relative scarcity of lithic fragments indicates that sample is high in the sequence. Hydrothermal alteration may indicate proximity to a fault or fissure.

Petrographic Designation: Altered Biotite Latite Ash-Flow Tuff

Bonanza Tuff (T_b)

PRC-not on map, along Alder Creek

Field Number: A-12A-B (12-f)

Texture and Fabric: Pyroclastic with extremely well-developed compaction layering; large, flattened, pumice fragments* up to 1 in. long. Fine to medium crystals are set in a slightly devitrified, brown, glassy matrix. Angular, grey lithics (fine to coarse) are altered, hornblende andesite. Crystals of the ash-flow are euhedral to subhedral; often broken.

Composition: (estimated)

Phenocrysts: 40%

Plagioclase: 9% (Andesine An_{48})

Sanidine: 15%

Biotite: 9% (highly altered)

Magnetite: 4% (alteration product)

Quartz and Glass Shards: 3%

Groundmass: 24% (red-brown, vitric, slightly devitrified)

Lithic Fragments: 36% (hornblende andesite and biotite latite ash-flow)

Alteration: Feldspars are somewhat sericitized; biotite is altered to chlorite and magnetite. Groundmass is partially devitrified.

Remarks: The presence of large lithics of latite ash flow and sparsity of andesite lithics indicates that this sample is from high in the ash-flow sequence. The sample is from a highly welded portion of the flow.

Petrographic Designation: Biotite Latite Ash-Flow Tuff

*The large pumice fragments are ash-flow lapilli which are somewhat less indurated than the surrounding flow material.

Bonanza Tuff (T_b)
(Lower Flow 1-A: Findley Ridge section)

PRC-21

Field Number: M-4

Texture and Fabric: Pyroclastic with subhedral crystals in a matrix of glass and pumice. Compaction layering is present, but not extremely obvious. Abundant grey lithics seen in hand specimen are not abundant in this thin section.

Composition: (estimated)

Crystals: 29%

Plagioclase: 17% (Andesine An_{32-50})

Sanidine: 7%

Biotite: 4%

Magnetite: 1%

Matrix: 57% (glass and pumice fragments)

Lithic Fragments: 4% (andesitic)

Voids: 10%

Alteration: Crystals relatively fresh, glass is partly devitrified. Spheroidal recrystallization is apparent in both the glass and the pumice.

Remarks: Feldspars are difficult to distinguish in thin section. Feldspar staining of thin-section slab reveals much of the K-feldspar is concentrated in the matrix. Sanidine is commonly found in crystal aggregates with plagioclase.

Petrographic Designation: Biotite Latite Ash-Flow Tuff

Bonanza Tuff (T_b)

(Lower Welded Flow 1-A: Findley Ridge Section)

PRC-22

Field Number: M-5

Texture and Fabric: Pyroclastic with fine- to medium-grained crystals and lithic fragments in a matrix of strongly layered glass and pumice. The very abundant crystals are subhedral and aligned parallel to flow structures.

Composition: (by modal analysis)

- Crystals: 41.5%
  - Plagioclase: 30.3% (Andesine An_{32-51})
  - Sanidine: 6.1% (most has been removed by weathering)
  - Biotite: 2.7%
  - Magnetite: 1.4%
  - Augite: 1.0%
- Matrix: 46.0%
  - Pumice: 25.0%
  - Glass: 21.0%
- Lithic Fragments: 3.6% (andesite)
- Voids: 8.9%

Alteration: Very minor; some devitrification of groundmass.

Remarks: Excellent compaction layering may reflect good to moderate welding. Stained slab shows most of the sanidine crystals have been weathered out and the bulk of the K-feldspar is concentrated in the matrix.

Petrographic Designation: Biotite Latite Ash-Flow Tuff

Bonanza Tuff (T_b)

(Middle Welded Flow 1-A: Findley Ridge Section)

PRC-23

Field Number: M-6

Texture and Fabric: Pyroclastic with fine to medium, subhedral phenocrysts in a groundmass of pumice and glass. Compaction layering is apparent in the flattened pumice fragments and glass shards. Blebs of crystalline quartz are dispersed throughout the pumice fragments.

Composition: (estimated)

- Crystals: 35%
  - Plagioclase: 24% (Andesine An_{32-52})
  - Sanidine: 6%
  - Biotite: 4%
  - Magnetite: 1%
  - Augite: < 1%
- Matrix: 56% (Glass and Pumice)
- Lithic Fragments: 2%
- Voids: 7%

Alteration: Vitric matrix is partially devitrified. Secondary quartz is concentrated in pumice as crystal blebs.

Remarks: Fewer lithics suggest that the lithic fragments are concentrated near the base of the flow. Crystal proportions and compositions are evidence that this sample is part of ash-flow #1. Augite may be accidental. Again, the stained slab indicates most sanidine is weathered out. This might account for many of the voids in the thin section.

Petrographic Designation: Biotite Latite Ash-Flow Tuff

Bonanza Tuff (T_b)

(Upper Welded Flow 1-A: Findley Ridge Section)

PRC-24

Field Number: M-7

Texture and Fabric: Pyroclastic with fine and medium subhedral crystals subparallelly aligned in a matrix of pumice and glass.

Composition: (by modal analysis)

Crystals: 38%

Plagioclase: 23.2% (Andesine An_{30-46})

Sanidine: 7.2%

Biotite: 3.3%

Augite: 2.3%

Magnetite: 2.0%

Matrix: 55.5% (glass and pumice)

Lithic Fragments: 3.0%

Voids: 3.5% (some partially filled with crystalline quartz)

Alteration: Matrix is partially devitrified. Mafics are partially altered to magnetite.

Remarks: Augite is particularly abundant in this sample. The augite crystals are anhedral but don't show reaction rims. They appear to be primary minerals. Some sanidine has been weathered out but a greater proportion remains.

Petrographic Designation: Biotite Latite Ash-Flow Tuff

Bonanza Tuff (T_b)

(Upper Moderately Welded Flow 1-A: Findley Gulch Section)

PRC-25

Field Number: M-8

Texture and Fabric: Pyroclastic with subhedral phenocrysts in a matrix of compacted pumice and glass.

Composition: (estimated)

Crystals: 25%

Plagioclase: 16% (Andesine An_{30-50})

Sanidine: 5% (many other crystals weathered out)

Biotite: 3%

Magnetite: ≃1%

Matrix: 33%

Voids: 40% (thin section cut too thin)

Lithic Fragments: 2% (fine-grained andesite)

Alteration: Glass in matrix is somewhat devitrified. A few small blebs of quartz are present in the matrix. Biotite is partly altered to chlorite.

Remarks: The estimate of composition may be in error because only a few of the voids in the thin section were originally present due to weathering. Most of the voids were produced when material was torn out while cutting the thin section. No augite was found.

Petrographic Designation: Biotite Latite Ash-Flow Tuff

Bonanza Tuff (T_b)
(Lower Flow 1-B: Findley Ridge Section)

PRC-26

Field Number: M-9

Texture and Fabric: Pyroclastic with subhedral crystals in a pumiceous matrix. Numerous tiny quartz-lined vesicles are present in the matrix. Compaction is evident in the flattened glass shards.

Composition: (by modal analysis)

Crystals: 32.7%

Plagioclase: 20.7% (Oligoclase An_{26} - Andesine An_{45})

Sanidine: 6.9%

Biotite: 2.1%

Augite: 2.0% — (Some with centers of ???, some poikilitically enclosed in plagioclase, another pyroxene crystal in a pumice fragment.)

Magnetite: 1.0%

Matrix: 61.7%

Pumice: 57.2%

Glass: 4.5%

Lithic Fragments: 4.9% (andesite and ash-flow tuff)

Voids: 0.7%

Alteration: Most of the glass in the matrix is not devitrified. There are thousands of tiny, quartz-lined vesicles in the pumice-rich matrix. Most phenocrysts are fairly fresh. Pyroxene is altering to magnetite.

Remarks: The relative abundance of lithics indicates this sample is from the lower part of a flow. Some of the lithic fragments are ash-flow tuff indicating previous eruptions of ash flow. Crystal abundance suggest the sample is part of ash flow #1 of the Bonanza Tuff.

Petrographic Designation: Biotite Latite Ash-Flow Tuff

Bonanza Tuff (T_b)

(Poorly Welded Middle Flow 2: Findley Ridge Section)

PRC-27

Field Number: M-10

Texture and Fabric: Pyroclastic with euhedral and subhedral crystals (often broken) in a matrix of pumice. Compaction structures are present, but not obvious.

Composition: (estimated)

- Crystals: 32%
  - Plagioclase: 14% (Oligoclase An_{27} - Andesine An_{48})
  - Sanidine: 12%
  - Biotite: 4%
  - Magnetite: 2%
- Matrix: 61% (mostly pumice)
- Lithics: 3% (andesite and ash-flow tuff)
- Voids: 4%

Alteration: Considerable sericitization on the edges of some crystals and in places in the matrix. Fan-shaped growths of crystalline quartz occur in the groundmass. Highly altered places in matrix may have been pyroxene or amphibole crystals.

Remarks: No pyroxene in this thin section. Condition of stained slab prevents accurate estimate, but the **sanidine/plagioclase** ratio is noticeably higher. These observations are evidence that this represents a different flow.

Petrographic Designation: Biotite Latite Ash-Flow Tuff

Bonanza Tuff (T_b)

(Moderately Welded Flow 3: Findley Ridge Section)

PRC-28

Field Number: M-11

Texture and Fabric: Pyroclastic with extremely good compaction layering. Fine to medium subhedral phenocrysts are strongly aligned in a matrix of pumice and glass.

Composition: (by modal analysis)

Crystals: 29.4%

Plagioclase: 19.5% (Andesine An_{29-47})

Sanidine: 6.7%

Biotite: 2.8%

Magnetite: 0.4%

Matrix: 61% (mostly pumice and pumice fragments)

Lithic Fragments: 0.7%

Voids: 8.8%

Alteration: A few crystals (probably mafics) have been completely replaced by sericite, muscovite, magnetite, and calcite. Some biotite altering to magnetite.

Remarks: Except for the absence of augite, the composition of this sample is very much like the upper part of flow 1. The sanidine/plagioclase ratio suggests that it is a different flow than sample M-10.

Petrographic Designation: Biotite Latite Ash-Flow Tuff

Bonanza Tuff (T_b)

(Moderately Welded Middle Flow 4: Findley Ridge Section)

PRC-29

Field Number: M-12

Texture and Fabric: Pyroclastic with rather sparse, fine and medium crystals in a matrix of pumice showing a very subtle compaction layering.

Composition: (estimated)

Crystals: 22%

Plagioclase: 11% (Andesine An_{30-48})

Sanidine: 8%

Biotite: 2%

Magnetite: 1%

Matrix: 71% (mostly pumice)

Voids: 7%

No Lithic Fragments

Alteration: Biotite is heavily altered to magnetite. Some chloritization around edges of magnetite and biotite.

Remarks: Relatively high sanidine/plagioclase ratio is apparent in stained slab. This thin section contains no lithic fragments and no augite. It differs from sample M-11 in that it has more sanidine.

Petrographic Designation: Biotite Latite Ash-Flow Tuff

Bonanza Tuff (T_b)

(Highly Welded Middle Flow 5: Findley Gulch Section)

PRC-30

Field Number: M-13

Texture and Fabric: Pyroclastic with euhedral and subhedral, fine- to medium-grained crystals in a matrix of brown glass and pumice. Compacted pumice fragments and matrix lineaments strikingly reflect compaction layering.

Composition: (estimated)

Crystals: 38%

Plagioclase: 20% (Oligoclase and Andesine An_{26-50})

Sanidine: 11% (some removed by weathering)

Biotite: 4%

Augite: 2%

Magnetite: 1%

Hornblende: Tr

Matrix: 53% (mostly brown glass)

Lithic Fragments: 3%

Voids: 6%

Alteration: Very minor, some alteration of mafics. Matrix is slightly devitrified.

Remarks: The composition of this flow is still different from all others. Augite is present with considerable sanidine. Plagioclase is slightly less calcic. Lithics are very sparse.

Petrographic Designation: Biotite Latite Ash-Flow Tuff

Bonanza Tuff (T_b)

(Highly Welded Upper Flow 5: Findley Gulch Section)

PRC-31

Field Number: M-14

Texture and Fabric: Pyroclastic with euhedral and subhedral crystals in a matrix of glass and pumice which shows strong compaction layering. Crystals are fine- to medium grained.

Composition: (estimated)

Crystals: 47%

Plagioclase: 20% (Andesine An_{30-47})

Sanidine: 19%

Biotite: 5%

Augite: 2%

Magnetite: <1%

Hornblende: <1%

Matrix: 51% (mostly glass)

Lithic Fragments: 2% (crystal-rich andesite)

Alteration: Minor; some devitrification of groundmass; mafics slightly altered.

Remarks: There are a few flattened vesicles or veinlets filled with secondary quartz. Mafics and calcic plagioclase is concentrated in pumice and lithic fragments. Stained slab shows sanidine/plagioclase abundances very well. Composition is very similar to that of M-13 if missing K-feldspar of M-13 is taken into account.

Petrographic Designation: Biotite Latite Ash-Flow Tuff

Bonanza Tuff (T_b)
(Lower Middle Flow 6: Findley Gulch Section)

PRC-32

Field Number: M-15 (marked 18-A)

Texture and Fabric: Pyroclastic with fine to medium subhedral crystals in a pumiceous matrix.

Composition: (estimated)

- Crystals: 34%
  - Sanidine: 16%
  - Plagioclase: 13% (Oligoclase-Andesine An_{23-44})
  - Biotite: 4%
  - Magnetite: 1%
- Matrix: 58% (mostly pumice)
- Lithic Fragments: 5% (some vitric, others andesitic)
- Voids: 3%

Alteration: Some devitrification; some preferential sericitization, particularly within lithic fragments.

Remarks: Secondary quartz (chalcedony) filling some elongate vesicles. Abundance of lithics is typical of the basal portion of a flow. Sanidine/plagioclase ratio is high while augite and hornblende are absent. This indicates a different flow than for sample M-14.

Petrographic Designation: Biotite Latite Ash-Flow Tuff

Bonanza Tuff (T_b)
(Lower Flow 7: Findley Gulch Section)

PRC-33

Field Number: M-16

Texture and Fabric: Pyroclastic with very little compaction or flow structure. Fine to medium crystals set in a matrix largely composed of microcrystalline quartz and feldspar. Crystals are subhedral to anhedral and embayed at edges.

Composition: (estimated)

Crystals: 16%

Sanidine: 10%

Plagioclase: 5% (Oligoclase An_{23})

Hornblende: < 1%

Biotite: < 1%

Magnetite: < 1%

Other: < 1%

Matrix: 76%

Lithic Fragments: 2% (ash-flow tuff and latite)

Voids: 6%

Alteration: Biotite and other mafics altering to magnetite. Quartz in groundmass may be recrystallized.

Remarks: Fluted edges of large crystals indicate recrystallization. Outlines of elongate vesicles (or replaced pumice) filled with tridymite are visible. Quartz must be secondary or recrystallized. Lack of mafics and unique mineralogy set this sample apart. It must be a different flow and probably from a different source.

Petrographic Designation: Rhyolite Ash-Flow Tuff

Bonanza Tuff (T_b)
(Upper Flow 7: Findley Gulch Section)

PRC-35

Field Number: 18-B

Texture and Fabric: Pyroclastic with fine and medium subhedral crystals in a matrix of microcrystalline quartz and glass which shows subtle compaction layering.

Composition: (estimated)

Crystals: 33%

Sanidine: 24%

Plagioclase: 7% (Andesine An_{40})

Biotite: 1%

Magnetite: 1%

Matrix: 63% (glass and microcrystalline quartz)

Lithics: 1% (fine crystalline andesite)

Voids: 3%

Alteration: Biotite altering to magnetite, fluted edges on feldspars indicate partial resorption. Considerable recrystallization of matrix quartz is evident.

Remarks: This is a very distinct ash flow. Abundance of matrix quartz would certainly push its chemical composition to a rhyolite. It is very poor in mafics. Vesicles are lined with tiny quartz crystals. This is like M-16 but not so highly silicified.

Petrographic Designation: Rhyolite Ash-Flow Tuff

Bonanza Tuff (T_b)
(Lower Flow 8: Findley Gulch Section)

PRC-36

Field Number: M-19

Texture and Fabric: Pyroclastic with fine and medium subhedral and euhedral crystals subparallelly aligned in a matrix of glass and pumice. Compaction layering is well developed.

Composition: (estimated)

Crystals: 44%

Plagioclase: 26% (Andesine)

Sanidine: 11%

Biotite: 5%

Augite: 2%

Magnetite: 1%

Matrix: 46% (pumice and glass)

Lithic Fragments: 4% (andesitic)

Voids: 6%

Alteration: Matrix somewhat devitrified; mafics partly altered to magnetite.

Remarks: This looks like a sample from flow #1. This flow is certainly distinct from M-16 and M-18. Mafics are relatively abundant and the texture is similar to ash-flow lower in the sequence.

Petrographic Designation: Biotite Latite Ash-Flow Tuff

Bonanza Tuff (T_b)

PRC-39

Field Number: 845-70

Texture and Fabric: Pyroclastic with obvious compaction layering. Fine and medium, subhedral crystals are set in a matrix of glass and pumice. Elongate crystals parallel the compaction layering.

Composition: (estimated)

Crystals: 44%

Plagioclase: 21% (Andesine An_{36-45})

Sanidine: 13%

Biotite: 7%

Quartz: 2%

Magnetite: 1%

Matrix: 64% (pumice and glass)

Lithic Fragments: 2% (highly altered)

Alteration: Slight sericitization; glass partially devitrified; biotite altering to magnetite.

Remarks: Lack of lithics in this sample indicate that it represents a unit well above the base of the Bonanza ash-flow sequence.

Petrographic Designation: Biotite Latite Ash-Flow Tuff

Bonanza Tuff (T_b)

PRC-49

Field Number: 484

Texture and Fabric: Pyroclastic with distinct compaction layering and abundant crystals, many of which are bent or broken. Secondary crystalline quartz is concentrated in pods and lenses parallel to compaction foliation. Elongate crystals are subparallelly aligned.

Composition: (estimated)

Crystals: 48%

Plagioclase: 15% (Andesine An_{35-45})

Sanidine: 11%

Biotite: 11%

Quartz: 9%

Magnetite: 2% (secondary)

Matrix: 47% (devitrified glass and altered pumice)

Lithics: 5% (highly altered)

Alteration: Some sericitization; considerable hematitic alteration and silicification; biotite altering to magnetite.

Remarks: Silicic alteration has preferentially invaded some of the larger feldspar crystals and replaced some mafics. It has also preferentially concentrated in pumice zones of the matrix.

Petrographic Designation: Silicified Biotite Latite Ash-Flow Tuff

Andesite of the Upper Volcanic Sequence (T_{uv})
(Squirrel Gulch)

PRC-2

Field Number: 6-4-69-2-B (2-f)

Texture and Fabric: Porphyritic-aphanitic with euhedral and subhedral phenocrysts varying from very fine to medium. Microlites in the groundmass and phenocrysts are randomly oriented.

Composition: (by modal analysis)

Phenocrysts: 31.2%

- Plagioclase: 19.2% (An_{30} to An_{50})
- K-Feldspar: 2.4%
- Hornblende: 3.8%
- Biotite: 2.4%
- Augite: 1.4%
- Magnetite: 1.0%
- Sphene: 1.0%

Groundmass: 68.8% (mostly plagioclase microlites)

Alteration: Fairly fresh, but with some sericitization. Some mafics are partially altered to magnetite.

Remarks: Larger plagioclase phenocrysts are more calcic than smaller phenocrysts. The cores of some of these may even be labradorite. Amphiboles are of two types, the larger phenocrysts often show reaction rims of magnetite. Some of the smaller hornblende crystals have augite cores. This complex mineralogy indicates fluctuation of the environment of the parent melt. Possibly, continued evolution of the magma after pressure release by eruption or migration.

Petrographic Designation: Biotite Hornblende Andesite*

***This unit has previously been called a latite, but the modal analysis indicates that it is, petrographically, an andesite. Chemically, the rock may be a latite if there is an abundance of K-feldspar in the groundmass.**

Younger Latite Ash-Flow Tuff (T_{uv})

PRC-13

Field Number: J-5C-B (5C-f)

Texture and Fabric: Pyroclastic with fine to medium crystals, quartz-lined **vesicles, and groundmass microlites aligned** parallel to compaction layering.

Composition: (estimated)

Crystals: 27%

Plagioclase: 10% (Andesine An_{46})

Biotite: 11%

Sanidine: 4%

Magnetite: 2% (replacing biotite)

Lithics and Accidentals: 2%

Groundmass: 46% (mostly ash)

Quartz lined **Vesicles: 27%**

Alteration: Slight sericitization; biotite altering to magnetite. Quartz was introduced as secondary mineral after removal of pumice fragments. The degree of feldspar alteration varies from crystal to crystal.

Remarks: Biotite crystals are often bent or broken. Silica may have been introduced hydrothermally. Groundmass is largely devitrified. This ash-flow tuff differs from Bonanza ash-flow tuff mostly because it lacks the andesitic lithic fragments and contains fewer crystals.

Petrographic Designation: Biotite Latite Ash-Flow Tuff

Andesite of the Upper Volcanic Sequence (T_{uv})
(Squirrel Gulch)

PRC-14

Field Number: A-17A-B (17A-f)

Texture and Fabric: Porphyritic-aphanitic with mostly fine, euhedral and subhedral phenocrysts randomly oriented in a grey groundmass of microlites.

Composition: (estimated)

Phenocrysts: 38%

- Plagioclase: 21%
- Orthoclase: 4%
- Augite: 4%
- Biotite: 4%
- Hornblende: 3%
- Magnetite: 2%
- Sphene: >1%

Groundmass: 62% (mostly plagioclase microlites)

Alteration: Relatively fresh; some alteration of mafics to magnetite; some sericitization of feldspars.

Remarks: Zoned plagioclase crystals are more calcic toward the center. Several aggregates of small crystals occur. Most mafics show magnetite reaction rims.

Petrographic Designation: Hornblende Augite Biotite Andesite*

*This unit has previously been called a latite. Chemically, it may be a latite; but, petrographically, it is an andesite.

Andesite of the Upper Volcanic Sequence (T_{uv}) (Brewer Creek)

PRC-17

Field Number: A-17B-B (17B-f)

Texture and Fabric: Porphyritic-aphanitic with fine to medium phenocrysts in a groundmass of randomly oriented microlites. Phenocrysts are euhedral and subhedral.

Composition: (estimated)

Phenocrysts: 28%

Plagioclase: 12% (Andesine An_{47})

Orthoclase: 4%

Biotite: 5%

Hornblende: 4%

Magnetite: 2%

Quartz: 1%

Groundmass: 72% (mostly feldspar microlites)

Alteration: Some sericitization; magnetite replacing feldspars and mafics.

Remarks: Some feldspars show oscillatory zoning.

Petrographic Designation: Hornblende Biotite Andesite*

*Previously mapped as a latite.

Andesite of the Upper Volcanic Sequence (T_{uv})
(Dry Gulch)

PRC-37

Field Number: M-21

Texture and Fabric: Porphyritic-aphanitic with fine and medium phenocrysts subparallelly aligned in a strongly pilotaxitic groundmass of microlites.

Composition: (estimated)

Phenocrysts: 37%

Plagioclase: 22% (Andesine An_{45})

Orthoclase: 4%

Biotite: 4%

Hornblende: 3%

Augite: 2%

Magnetite: 2%

Groundmass: 63% (mostly plagioclase-microlites)

Alteration: Minor alteration; magnetite replacing mafics, especially hornblende; some hematitic alteration.

Remarks: This unit is, compositionally, very similar to the Squirrel Gulch andesite (samples 2-f and 17A-f). However, the texture is considerably different. The **crystallites** of the groundmass are larger and show definite pilotaxitic structure. The phenocrysts are more nearly euhedral. They are separate units.

Petrographic Designation: Hornblende Biotite Andesite

Andesite of the Upper Volcanic Sequence (T_{uv}) (Dry Gulch)

PRC-38

Field Number: M-22

Texture and Fabric: Porphyritic-aphanitic with fine to medium phenocrysts and groundmass microlites exhibiting a strong pilotaxitic texture. Most crystals are euhedral, some are subhedral.

Composition: (estimated)

Phenocrysts: 35%

Plagioclase: 21% (Andesine An_{42})

Orthoclase: 4%

Biotite: 4%

Hornblende: 3%

Augite: 2%

Magnetite: ≈1%

Groundmass: 65% (fine crystals and microlites)

Alteration: Mafics are partly altered to magnetite.

Remarks: Practically identical to sample M-21, but has slightly less alteration (no hematitic alteration) and the plagioclase may be slightly more sodic.

Petrographic Designation: Hornblende Biotite Andesite

Andesite of the Upper Volcanic Sequence (T_{uv}) (Dry Gulch)

PRC-41

Field Number: 1150

Texture and Fabric: Porphyritic-aphanitic with fine to medium phenocrysts in a slightly pilotaxitic groundmass. Crystals are euhedral and subhedral.

Composition: (estimated)

Phenocrysts: 38%

Plagioclase: 21% (Andesine An_{46})

Orthoclase: 4%

Biotite: 6%

Hornblende: 3%

Augite: 3%

Magnetite: 1%

Groundmass: 62% (fine crystals and microlites)

Alteration: Minor; mafics are altering to magnetite.

Remarks: This sample is petrographically similar to M-21 and M-22. The groundmass is not so strongly oriented. Alteration in some feldspars yields sieve structure. Mineralogy of mafics is simple, but feldspars are zoned.

Petrographic Designation: Biotite Andesite

Lithic-Rich Ash-Flow Tuff of the Upper Volcanic Sequence (T_{uv})

PRC-42

Field Number: 1163

Texture and Fabric: Pyroclastic with extremely abundant lithics in a meager matrix of glass and crystals. Compaction layering is present, but obscure. Crystals are mostly subhedral and anhedral.

Composition: (estimated)

Crystals: None recognized as essential minerals

Matrix: 15% (probably latite, but crystals belonging to matrix and accidentals are indistinguishable)

Lithics: 85% (Porphyritic-aphanitic hornblende biotite latite)

Alteration: Feldspars are highly sericitized. Mafics are altered almost beyond recognition. They are replaced by magnetite chlorite and sericite. Secondary silica is present as crystal blebs and veinlets.

Remarks: There is some doubt as to the pyroclastic origin of this rock. It could be a finely brecciated hornblende andesite that was partially remobilized, relithified, and altered by hot, silica-rich fluids. If it were an ash flow, it carried an extreme abundance of andesitic lithics.

Petrographic Designation: Highly Altered, Lithic-Rich, Ash-Flow Tuff

Andesite of the Upper Volcanic Sequence
(Brewer Creek)

PRC-46

Field Number: 1300

Texture and Fabric: Porphyritic-aphanitic, fine to medium phenocrystalline, with subhedral and anhedral phenocrysts in a grey groundmass of subparallelly oriented microlites.

Composition: (estimated)

Phenocrysts: 42%

Plagioclase: 23% (Andesine An_{38})

Orthoclase: 8%

Biotite: 6% - } altering to magnetite

Hornblende: 3% - }

Magnetite: 2%

Groundmass: 58% (mostly microlites of feldspars)

Alteration: Leucocratic minerals are fairly fresh, but mafics are badly altered.

Remarks: Plagioclase crystals are strongly zoned. Most phenocrysts are broken and somewhat rounded. Hornblende appears to have been partially replaced by biotite, and then magnetite.

Petrographic Designation: Hornblende Biotite Andesite

Porphyry Peak Rhyolite (T_{pp})

PRC-40

Field Number: 805

Texture and Fabric: Porphyritic-aphanitic with fine to medium phenocrysts in an aphanitic groundmass. Groundmass microlites are slightly pilotaxitic and phenocrysts are weakly aligned. In hand specimen, banding is apparent.

Composition: (estimated)

Phenocrysts: 23%

Plagioclase: 5% (Oligoclase An_{27})

Sanidine: 14%

Biotite: 3%

Magnetite: 1%

Groundmass: 69% (microlites of feldspar and crystalline quartz)

Voids: 8%

Alteration: Very little; some sericitization; biotite being replaced by magnetite.

Remarks: No phenocrysts of quartz are present in this sample, so it might be classed as a trachyte; but sufficient quartz is present in the groundmass to confirm that it is a rhyolite. Most of the quartz in the groundmass is in veins parallel to banding.

Petrographic Designation: Biotite Rhyolite

Tertiary Intrusive (T_i)
(Eagle Gulch Latite)

PRC-6

Field Number: 6-4-69-6-B (6-f)

Texture and Fabric: Porphyritic-holocrystalline; fine to coarse subhedral phenocrysts in a very fine crystalline groundmass. Groundmass appears randomly oriented and rather granular.

Composition: (estimated)

Phenocrysts: 25%

The only recognizable phenocrysts are plagioclase and potassium feldspar in nearly equal amounts.

Groundmass: 75%

Mostly feldspar; some quartz and magnetite.

Alteration: Extreme alteration consisting of sericitization and argillization. Mafics, if present, are no longer recognizable. Concentrations of magnetite and other alteration products **(chlorite and epidote) may indicate former locations of mafic phenocrysts.**

Remarks: Alteration appears to have affected phenocrysts and groundmass equally.

Petrographic Designation: **Porphyritic Quartz Monzonite**

Tertiary Intrusive (T_i)

PRC-47

Field Number: 1196-A

Texture and Fabric: Very fine grained leucocratic aphanite. Zones of extremely fine-grained material alternate with zones of very fine material to yield banding parallel to the slightly pilotaxitic alignments of microlites.

Composition: (estimated)

Feldspar Microlites: 60%

Biotite Microlites: 7%

Magnetite: 11%

Other??: 22%

Alteration: Sericitization is the only recognizable alteration.

Remarks: Extremely fine grain-size of the sample may have been caused by very rapid cooling or pressure release from an entirely molten magma.

Petrographic Designation: Leucocratic Biotite Aphanite

Altered Rawley Andesite (T_r)
(Adjacent to intrusive-1196A)

PRC-48

Field Number: 1196-B

Texture and Fabric: Porphyritic-aphanitic with fine and medium, subhedral phenocrysts in an aphanitic groundmass. Elongate phenocrysts are subparallelly aligned, but groundmass microlites are randomly oriented. Anhedral grains of quartz are dispersed throughout.

Composition: (estimated)

Phenocrysts: 45%

- Plagioclase: 22% (Andesine An_{38}) — Badly altered
- Orthoclase: 6% — Badly altered
- Mafics (Biotite and Hornblende): 9% — Badly altered
- Magnetite: 2%
- Quartz (late): 6%

Groundmass: 55% (microlites of feldspars and mafics)

Alteration: All minerals except quartz are badly altered. Mafics are altered to magnetite, chlorite, and hematitic minerals. Feldspars are highly sericitized.

Remarks: The condition of the primary rock minerals indicates severe alteration (probably hydrothermal) prior to, or contemporaneous with the introduction of silica which crystallized to form anhedral quartz grains.

Petrographic Designation: Altered and Silicified Hornblende Biotite Andesite

Vein Material - Cocomongo Mine

PRC-1

Field Number: 6-4-69-1-B (1-f)

Texture and Fabric: Fine- and medium-grained allotriomorphic granular. **Fine crystals occur in veinlets within the** coarser material. One large (1 cm) subhedral quartz crystal appears as an island within one of the veinlets.

Composition: (by modal analysis)

Quartz: 88.2%

Rhodochrosite: 8.6%

Opaques: 3.2% (pyrite and galena)

Remarks: Rhodochrosite and opaques also occur as veinlets associated with the fine-grained quartz. The rock is generally quite fresh. The coarse-grained quartz was introduced into the vein early, and later invaded by siliceous material that filled veinlets with fine-grained quartz, rhodochrosite, and sulfides. The large quartz crystal must have cooled in place from the same late material.

Petrographic Designation: Rhodochrosite Quartz **Pyrite Galena Vein Material**

BIBLIOGRAPHY

Anderson, E. M., 1936, The dynamics of the formation of cone-sheets, ring-dykes, and caldron subsidences: Proc. Royal Soc., Edinburgh, v. 56, p. 128-157.

Beloussov, V. V., 1969, Continental rifts, in Hart, P. J. (editor), The Earth's crust and upper mantle: Am. Geophys. Union Mon. 13, p. 539-543.

Bridwell, R. J., 1968, Geology of the Kerber Creek area, Saguache County, Colorado: Colo. School of Mines thesis 1177, 104 p.

Bruns, D. L., 1971, Geology of the Lake Mountain NE quadrangle, Saguache County, Colorado: Colo. School of Mines thesis 1367, 79 p.

Bruns, D. L., Epis, R. C., Weimer, R. J., and Steven, T. A., 1971, Stratigraphic relations between Bonanza center and adjacent parts of the San Juan volcanic field, south-central Colorado, in James, H. L. (editor), Guidebook of the San Luis Basin, Colorado: New Mexico Geol. Soc., p. 183-190.

Burbank, W. S., 1932, Geology and ore deposits of the Bonanza mining district, Colorado: U. S. Geol. Survey Prof. Paper 169, 166 p., map.

_____ 1947, The Bonanza (Kerber Creek) mining district, Saguache County, in Vanderwilt, J. W., Mineral resources of Colorado: Colo. Mineral Resources Board, p. 443-446.

Chapin, C. E., 1971, The Rio Grande rift, part I: Modifications and additions, in James, H. L. (editor), Guidebook of the San Luis Basin: p. 191-202.

Chapin, C. E., and Epis, R. C., 1964, Some stratigraphic and structural features of the Thirtynine Mile volcanic field, central Colorado: Mountain Geologist, v. 1, no. 3, p. 145-160.

Cook, D. R., 1960, Bonanza project, Bear Creek Mining Co.: Am. Inst. Mining, Metall., and Petroleum Engineers Trans., v. 217, p. 285-295.

Del Rio, S. M., 1960, Mineral resources of Colorado-first sequel: Colo. Mineral Resources Board, p. 266-271 and p. 364.

De Voto, R. H., Peel, F. A., and Pierce, W. H., 1971, Pennsylvanian and Permian stratigraphy, tectonism and history, northern Sangre de Cristo range, Colorado, in James, H. L. (editor), Guidebook of the San Luis Basin, Colorado: New Mexico Geol. Soc., p. 141-165.

Endlich, F. M., 1874a, Report on mining districts of Colorado and geology of the San Luis district: U. S. Geol. Survey, Territorial Survey (Hayden), 7th annual rept., p. 343-351.

_____ 1874b, Report on the erupted rocks of Colorado: U. S. Geol. Survey, Territorial Survey, 10th annual rept.

Epis, R. C., and Chapin, C. E., 1968, Geologic history of the Thirtynine Mile volcanic field, central Colorado, in Cenozoic volcanism in the southern Rocky Mountains: Colo. School of Mines Quart., v. 63, no. 3, p. 51-85.

Faul, Henry, 1966, Ages of rocks, planets, and stars: McGraw Hill Book Co., New York, 109 p.

Fisher, R. V., 1960, Criteria for recognition of laharic breccias, southern Cascade Mountains, Washington: Geol. Soc. America Bull., V. 71, p. 127-132.

_____ 1960, Classification of volcanic breccias: Geol. Soc. America Bull., v. 71, p. 973-982.

_____ 1961, Proposed classification of volcaniclastic sediments and rocks: Geol. Soc. America Bull., v. 72, p. 1409-1414.

_____ 1963, Classification of volcanic breccias: a reply: Geol. Soc. America Bull., v. 74, p. 87.

_____ 1966, Rocks composed of volcanic fragments and their classification: Earth Sci. Rev., v. 1, no. 4, p. 287-298.

Gableman, J. W., 1952, Structure and origin of northern Sangre de Cristo range, Colorado: Am. Assoc. Petroleum Geologists Bull., v. 36, no. 8, p. 1574-1612.

Gaca, J. R., 1965, Gravity studies in the San Luis Valley area, Colorado: Colo. School of Mines thesis 1021, 73 p.

Gliozzi, J., and others, 1970, Application of remote sensor data to geologic and economic analysis of the Bonanza test site, Colorado: Martin Marietta Corp. First Year Summary Rept., prepared under Colo. School of Mines Contract 9-W-06040, 200 p.

_____ 1971a, Application of remote sensor data to geologic and economic analysis of the Bonanza test site, Colorado: Martin Marietta Corp. Second Year Summary Rept., prepared under Colo. School of Mines Contrast 9-W-06040, 110 p.

_____ 1971b, Ground instruments applicable to remote sensing: Martin Marietta Corp. Rept. R-71-48680-005, prepared under Colo. School of Mines Contract 9-W-06040, 30 p.

Green, D. H., and Ringwood, A. E., 1969, The origin of basalt magmas, in Hart, P. J. (editor), The Earth's crust and upper mantle: Am. Geophys. Union Mon. 13, p. 489-495.

Haun, J. D., and Kent, H. C., 1965, Geologic history of Rocky Mountain region: Am. Assoc. Petroleum Geol. Bull., v. 49, no. 11, p. 1781-1800.

Hayden, F. V., 1869, Preliminary field report, (third) Annual report on the U. S. Geological and Geographical Survey of the territories, Colorado and New Mexico: Washington, U. S. Govt. Print. Off., 155 p.

Healy, J. H., and Warren, D. H., 1969, Explosion seismic studies in North America, in Hart, P. J. (editor), The Earth's crust and upper mantle: Am. Geophys. Union Mon. 13, p. 208-219.

Heinrich, E. Wm., 1965, Microscopic identification of minerals: McGraw Hill Book Co., New York, 414 p.

Henderson, C. W., 1926, Mining in Colorado: U. S. Geol. Survey Prof. Paper 138, p. 26, 55, 208, 209.

Ho, Chieh, and Wang, S. Y., 1913, Geology of the Rawley Mine and its vicinity, Saguache County, Colorado: Colo. School of Mines thesis 374, 34 p.

Hudson, W. C., and Bigley, A. C., 1913, A topographical and geological survey of a portion of the Kerber Creek District, Saguache County, Colorado: Colo. School of Mines thesis 354, 52 p.

Jackson, W. H., and Pakiser, L. C., 1965, Seismic study of crustal structure in the southern Rocky Mountains: U. S. Geol. Survey Prof. Paper 525-D, p. D85-D92.

Johnson, R. B., 1968, Volcanic terrains adjoining the central Sangre de Cristo mountains of Colorado and New Mexico (abs): in Cenozoic volcanism in the southern Rocky Mountains, Colo. School of Mines Quart., v. 63, no. 3, p. 239-240.

Karig, D. E., 1965, Geophysical evidence of a caldera at Bonanza, Colorado: U. S. Geol. Survey Prof. Paper 525-B, p. B9-B12.

Kempner, Helen A., 1971, Bonanza and the Kerber Creek district: The San Luis Valley historian, v. 3, no. 2, 46 p.

Knepper, D. H., Jr., 1970, Structural framework of the Rio Grande rift zone; Mineral Hot Springs to Poncha Springs, Colorado (abs): paper given before New Mexico Geol. Soc.

_____ 1972, NASA Mission 184 ninety-day report: Bonanza Remote Sensing Project, Colo. School of Mines, prepared under NASA grant NGL 06-001-015, 29 p.

Knepper, D. H., Jr., and Marrs, R. W., 1971, Geological development of the Bonanza-San Luis Valley-Sangre de Cristo Range area, south-central Colorado, in James, H. L. (editor), Guidebook of the San Luis Basin, Colorado: p. 249-264.

_____ 1972, Remote sensing aids geologic mapping: Eighth Internat. Symp. on Remote Sensing of Environment, University of Mich. (in press).

Kuno, H., 1953, Formation of calderas and magmatic evolution: Am. Geog. Union Trans., v. 34, p. 267-280.

Kushiro, I., and Kuno, H., 1963, Origin of primary basalt magmas and classification of basaltic rocks: Jour. Petrology, v. 4, p. 75-89.

Lachenbuch, A. H., 1957, Three-dimensional heat conduction in permafrost beneath heated buildings: U. S. Geol. Survey Bull. 1052-B, p. 51-69.

Larsen, E. S., Jr., and Cross, W., 1956, Geology and petrology of the San Juan region, southwestern Colorado: U. S. Geol. Survey Prof. Paper 285, 303 p.

Lee, Keenan, and others, 1970, Application of remote-sensor data to geologic and economic analyses of the Bonanza test site, Colorado: Bonanza Remote Sensing Project, Colo. School of Mines, prepared under NASA grant NGL 06-001-015, 34 p.

_____ 1971, NASA Mission 105, flight 5, summary report: Bonanza Remote Sensing Project, Colo. School of Mines, prepared under NASA grant NGL 06-001-015, 53 p.

Lipman, P. W., and others, 1966, A compositionally zoned ash-flow sheet in southern Nevada: U. S. Geol. Survey Prof. Paper 524-F, 47 p.

Lipman, P. W., and Steven, T. A., 1971, Reconnaissance geology and economic significance of the Platoro caldera, southeastern San Juan mountains, Colorado, in James, H. L. (editor), Guidebook of the San Luis Basin, Colorado: p. 221-230.

Lipman, P. W., Steven, T. A., and Mehnert, H. H., 1970, Volcanic history of the San Juan Mountains, Colorado, as indicated by potassium-argon dating: Geol. Soc. America Bull., v. 81, p. 2329-2352.

Litsey, L. R., 1958, Stratigraphy and structure of the northern Sangre de Cristo mountains: Geol. Soc. America Bull., v. 69, no. 9, p. 1143-1178.

Luedke, R. G., and Burbank, W. S., 1968, Volcanism and cauldron development in the western San Juan mountains, Colorado, in Cenozoic volcanism in the southern Rocky Mountains: Colo. School of Mines Quart., v. 63, no. 3, p. 175-208.

Lyon, R. J. P., and Burns, E. A., 1963, Analysis of rocks and minerals by reflected infrared radiation: Econ. Geology, v. 58, no. 2, p. 274-285.

Lyon, R. J. P., and Patterson, J. W., 1966, Infrared spectral signatures--a field geological tool: Fourth Internatl. Symp. on Remote Sensing of Environment, University of Mich.

McBirney, A. R., 1969, Andesitic and rhyolitic volcanism of orogenic belts, in Hart, P. J. (editor), The Earth's crust and upper mantle: Am. Geophys. Union Mon. 13, p. 501-507.

McTaggart, K. C., 1960, The mobility of nuees ardentes: Am. Jour. Sci., v. 258, p. 369-382.

Malahoff, Alexander, 1969, Gravity anomalies over volcanic regions; in Hart, P. J. (editor), The Earth's crust and upper mantle: Am. Geophys. Union Mon. 13, p. 364-378.

Marrs, R. W., 1972a, Geology of the Bonanza caldera, Saguache County, Colorado (abs.): Geol. Soc. America, Abstracts with Programs, v. 4, no. 6, p. 391.

_____ 1972b, Application of remote sensing techniques to geologic mapping in the Bonanza volcanic center, Saguache County, Colorado (abs.): Geol. Soc. America, Abstracts with Programs, v. 4, no. 6, p. 390.

Mayhew, J. D., 1969, Geology of the eastern part of the Bonanza volcanic field, Saguache County, Colorado: Colo. School of Mines thesis 1226, 94 p.

Mertzman, S. A., 1971, The Summer Coon volcano, eastern San Juan mountains, Colorado, in James, H. L. (editor), Guidebook of the San Luis Basin, Colorado: p. 265-272.

Moore, J. G., 1967, Base surge in recent volcanic eruptions: Bull. Vulcanologique, v. 30, p. 337-363.

Nelson, R. A., 1969, Handbook of Rocky Mountain plants: Dale Stuart King, Tucson, Arizona, 331 p.

Nolting, R. M., III, 1970, Pennsylvanian-Permian stratigraphy and structural geology of the Orient-Cotton Creek area, Sangre de Cristo mountains, Colorado: Colo. School of Mines thesis 1311, 102 p.

Patton, H. B., 1915, Geology and ore deposits of the Bonanza district, Saguache County, Colorado: Colo. Geol. Survey Bull. 9, 136 p.

Perry, H. A., 1971, Geology of the northern part of the Bonanza volcanic field, Saguache County, Colorado: Colo. School of Mines thesis 1362, 72 p.

Peterson, D. W., 1970, Ash-flow deposits--their character, origin, and significance: Jour. Geology, v. 18, no. 2, p. 66-76.

Powell, W. J., 1958, Ground water resources of the San Luis Valley, Colorado: U. S. Geol. Survey Water Supply Paper 1379, 284 p.

Preston, R. J., Jr., 1968, Rocky Mountain trees: Dover Pubs., New York, 285 p.

Prucha, and others, 1965, Basement controlled deformation in the Rocky Mountains: Am. Assoc. Petroleum Geol. Bull., v. 40, p. 966-992.

Ransom, Rastus W., and Daman, J., 1913, Topographical and geological survey around Bonanza, Saguache County, Colorado: Colo. School of Mines thesis 341, 44 p.

Ratte, J. C., 1968, Identification of ash-flow boundaries within densely welded tuff, Creede Area, Colorado (abs.), in Cenozoic volcanism in the southern Rocky Mountains: Colo. School of Mines Quart., v. 63, no. 3, p. 237.

Ratte, J. C., and Steven, T. A., 1964, Magmatic differentiation in a volcanic sequence related to the Creede caldera, Colorado: U. S. Geol. Survey Prof. Paper 475-D, p. D49-D53.

Ray, L. L., 1940, Glacial chronology of the Southern Rocky mountains: Geol. Soc. America Bull., v. 51, p. 1851-1918.

Reeves, R. G., and others, 1971, Application of remote-sensor data to geologic analysis of the Bonanza test site, Colorado: Bonanza Remote Sensing Project, Colo. School of Mines, prepared under NASA grant NGL 06-001-015, 19 p.

Richmond, G. M., 1965, Glaciation of the Rocky Mountains, in Wright, H. E., Jr., and Frey, D. E. (editors), The Quaternary of the United States: Princeton Univ. Press, Princeton, N. J., p. 217-230.

Ross, C. S., and Smith, R. L., 1961, Ash-flow tuffs; their origin, geologic relations, and identification: U. S. Geol. Survey Prof. Paper 366, 81 p.

Rowan, L. C., 1972, Near infrared iron absorption bands: Application to geologic mapping and mineral exploration: Fourth Annual Earth Resources Program Review, Natl. Aeronautics and Space Administration-MSC, v. III, p. 60-1 thru 60-18.

Rydstrom, H. O., 1966, Interpreting local geology from radar imagery: Fourth Internatl. Symp. on Remote Sensing of Environment, University of Mich., p. 193-201.

Scott, G. R., 1970, Quaternary faulting and potential earthquakes in east-central Colorado: U. S. Geol. Survey Prof. Paper 700-C, p. C11-C18.

Seibenthal, C. E., 1910, Geology and water resources of the San Luis Valley, Colorado: U. S. Geol. Survey Water Supply Paper 240.

Simon, Ruth B., 1968, Earthquake interpretations: Colo. School of Mines Research Foundation Unpublished Rept., 88 p.

_____ 1969, Seismicity of Colorado: Consistency of recent earthquakes with those of historical record: Science, v. 165, p. 897-899.

Simonds, F. M., and Burns, E. Z., 1913, A problem of mining together with some data of tunnel driving: Am. Inst. Mining Engineers Bull. 75, p. 37.

Smith, R. L., 1960a, Ash flows: Geol. Soc. America Bull., v. 71, no. 6, 47 p.

_____ 1960b, Zones and zonal variations in welded ash flows: U. S. Geol. Survey Prof. Paper 354-F, p. 149-159.

Smith, R. L., and Bailey, R. A., 1966, The Bandelier Tuff: a study of ash-flow eruption cycles from zoned magma chambers: Bull. Vulcanologique, v. 29, p. 83-104.

Stephens, F. M., and Gregg, D. B., 1913, The Geology of the Kerber Creek mining district, Saguache County, Colorado: Colo. School of Mines thesis 380, 37 p.

Steven, T. A., and Epis, R. C., 1968, Oligocene volcanism in south central Colorado, in Cenozoic volcanism in the southern Rocky Mountains: Colo. School of Mines Quart., v. 63, no. 3, p. 241-258.

Steven, T. A., Mehnert, H. H., and Obradovich, J. D., 1967, Age of volcanic activity in the San Juan mountains, Colorado: in Geol. Survey research 1967, U. S. Geol. Survey Prof. Paper 575-D, p. D47-D55.

Steven, T. A., and Ratte, J. C., 1964, Revised Tertiary volcanic sequence in the central San Juan mountains, Colorado: U. S. Geol. Survey Prof. Paper 475-D, p. D54-D63.

Turner, F. J., and Verhoogen, John, 1960, Igneous and metamorphic petrology: McGraw Hill Book Co., New York, 694 p.

U. S. Air Force Aeronautical Chart and Information Center, 1968, Transcontinental geophysical survey (35°-39°N), Bouguer gravity map from 100° to 112° W longitude: U. S. Geol. Survey Misc. Geol. Inv. Map I-533-B.

U. S. Geological Survey, 1958, Suggestions to authors of the reports of the U. S. Geological Survey (5th edition): U. S. Geol. Survey, 255 p.

Van Alstine, R. E., 1968, Tertiary trough between the Arkansas and San Luis Valleys, Colorado: U. S. Geol. Survey Prof. Paper 600-C, p. C158-C160.

_____ 1969, Geology and mineral deposits of the Poncha Springs NE quadrangle, Chaffee County, Colorado: U. S. Geol. Survey Prof. Paper 626, 52 p.

_____ 1970, Allochthonous Paleozoic blocks in the Tertiary San Luis-upper Arkansas graben, Colorado: U. S. Geol. Survey Prof. Paper 700-B, p. B43-B51.

Van Alstine, R. E. and Lewis, G. E., 1960, Pliocene sediments near Salida, Chaffee County, Colorado: U. S. Geol. Survey Prof. Paper 400B, p. B-245.

Verhoogen, J., 1951, Mechanics of ash formation: Am. Jour. Sci., v. 249, p. 729-739.

Wentworth, C. K., and Williams, H., 1932, The classification and terminology of pyroclastic rocks: Natl. Research Council Repts., Bull. 89, p. 19-53.

Wilcox, R. E., 1965, Volcanic-ash chronology, in Wright, H. E., Jr., and Frey, D. G. (editors), The Quaternary of the United States: Princeton Univ. Press, Princeton, N. J., p. 807-816.

Williams, H., 1932, History and character of volcanic domes: University Calif. Pubs., Dept. Geol. Sci., v. 21, no. 5, p. 51-149.

_____ 1941, Calderas and their origins: University Calif. Pubs., Bull of Dept. Geol. Sci., v. 25, p. 239-346.

Williams, H., and McBirney, A., 1968, Geologic and geophysical features of calderas: Natl. Aeronautics and Space Administration-MSC Rept., Houston, Texas, 87 p.

Williams, H., Turner, F. J., and Gilbert, C. M., 1954, Petrography--an introduction to the study of rocks in thin section: Freeman and Co., San Francisco, 406 p.

Woollard, G. P., 1969, Tectonic activity in North America as indicated by earthquakes, in Hart, P. J. (editor), The Earth's crust and upper mantle: Am. Geophys. Union Mon. 13, p. 125-133.

Wychgram, D. C., 1972, Geology of the Hayden Pass-Orient Mine area, northern Sangre de Cristo mountains, Colorado: a geologic remote-sensing evaluation: Colo. School of Mines thesis

Wright, A. E., and Bowes, D. R., 1963, Classification of volcanic breccia: a discussion: Geol. Soc. America Bull., v. 74, p. 79-86.

Wuench, C. E., 1923, Secondary enrichment at the Eagle mine, Bonanza, Colorado: Am. Inst. Mining Engineers Trans., v. 69, p. 96-109.

Yoder, H. S., Jr., and Tilley, C. E., 1962, Origin of basalt magmas; an experimental study of natural and synthetic rock systems: Jour. Petrology, v. 3, p. 342-352.

Zietz, Isidore, and Kirby, J. R., Jr., 1968, Transcontinental geophysical survey (35°-39°N), magnetic map from 100° to 112° W longitude: U. S. Geol. Survey, Misc. Geol. Inv. Map I-533-A.

_____ 1972, Aeromagnetic map of Colorado: U. S. Geol. Survey, Geophys. Inv. Map GP-880.

DATA REFERENCES

The following is a listing of the remote-sensor data used in the study of the southwest Bonanza area. All of these data can be purchased in print and/or transparency form from:

U. S. Geological Survey
EROS Data Center
Sioux Falls, South Dakota

The data used in this report are also on file at the Colorado School of Mines, Remote Sensing Laboratory, and may be cursorily examined at that laboratory by appointment.

Figure	Scale	Original Data Description	NASA Mission	Date	Film Roll	Lines or Frames
45	1:100,000	color infrared photo	101	8/11/69	1	5057
46	1:100,000	color photo	101	8/11/69	2	4720-4723
	1:50,000	color photo	101	8/11/69	3	163-164
	1:100,000	color infrared photo	101	8/11/69	1	5056-5059
49	1:15,000	color photo	105	10/2/69	4	5856
50	1:15,000	color photo	105	10/2/69	3	5703
51	1:250,000	multiband photo (green)	101	8/11/69	6	64389
	1:250,000	multiband photo (red)	101	8/11/69	5	64474
	1:250,000	multiband photo (IR)	101	8/11/69	8	66103
52	1:30,000	multiband photo (red)	105	10/2/69	1A/1	412
	1:30,000	multiband photo (blue)	105	10/2/60	1B/1	unreadable

continued

Figure	Scale	Original Data Description	NASA Mission	Date	Film Roll	Lines or Frame
52	1:30,000	multiband photo (green)	105	10/2/69	1C/1	356
	1:30,000	multiband photo (IR)	105	10/2/69	1D/1	787
54	1:32,000	b&w low sun-angle photo	168	6/15/71		7759
55	1:42,000	thermal infrared imagery	105	10/2/59	1	L-27
56	1:42,000	thermal infrared imagery	105	10/2/59	1	L-18
57	1:42,000	thermal infrared imagery	105	10/2/69	1	L-20
58	1:28,000	thermal infrared imagery	168	6/17/69	13	L-40
59	1:28,000	thermal infrared imagery	168	6/17/69	13	L-39
60	1:160,000	side-looking radar	168	6/16/69	8	L-61
63	1:160,000	side-looking radar	168	6/16/69	8	L-60
	1:160,000	side-looking radar	168	6/16/69	8	L-62
	1:160,000	side-looking radar	168	6/16/69	8	L-63
	1:160,000	side-looking radar	168	6/16/69	8	L-64
64	1:160,000	side-looking radar	184	10/14/71	32	L-80

Plate 2 was compiled from interpretations of many stereo photo pairs. These include both color and color infrared photographs from rolls 3, 4, and 5 of the NASA Mission 105 photography.

Plate 1

GEOLOGIC MAP OF THE SOUTHWEST BONANZA AREA

Saguache County, Colorado

R. W. Marrs Thesis no. 1531 March, 1973

TOPOGRAPHIC BASE COMPILED FROM USGS KLONDIKE MINE AND GRAVEYARD GULCH 7½′ QUADRANGLES AND BONANZA 15′ QUADRANGLE

R 7 E | R 8 E

T 47 N / T 46 N

T 46 N / T 45 N

38°15′

1 ½ 0 1 mile

Scale

N MN 14½°

Explanation

- Zone of alteration
- Lithologic contact
- Probable contact
- Covered contact
- Fault
- Probable fault
- Covered fault
- 25 Foliation dip and strike in igneous, metamorphic and volcanic rocks
- 34 Bedding dip and strike
- 74 Dip and strike of joints
- Joint with 90° dip
- 21 Plunge and strike of lineation
- OVERTHRUST PLATE Thrust fault
- ●2 Location of drill hole (Cook, 1960)
- ⑫ Sample location (corresponds to PRC number)

Cenozoic — Quaternary
- Qal Alluvium
- Ql Landslide
- Qaf Alluvial fan
- Qvf Valley fill
- Qgt Gravel terrace

Cenozoic — Tertiary
- Tuv Upper intermediate volcanic sequence
- Ti Silicic flows and intrusives (includes Porphry Peak Rhyolite)
- Tb Bonanza Formation
- Tr Rawley Formation

Mesozoic
- Mtb Tectonic breccia

Precambrian — Paleozoic
- Pu Upper sedimentary sequence
- Pl Lower sedimentary sequence

Precambrian
- pЄ Gneiss, schist and quartz monzonite

Plate 2

GEOLOGIC INTERPRETATION OF COLOR AND COLOR INFRARED PHOTOGRAPHY

Saguache County, Colorado

R.W. Marrs Thesis no. 1531 March, 1973

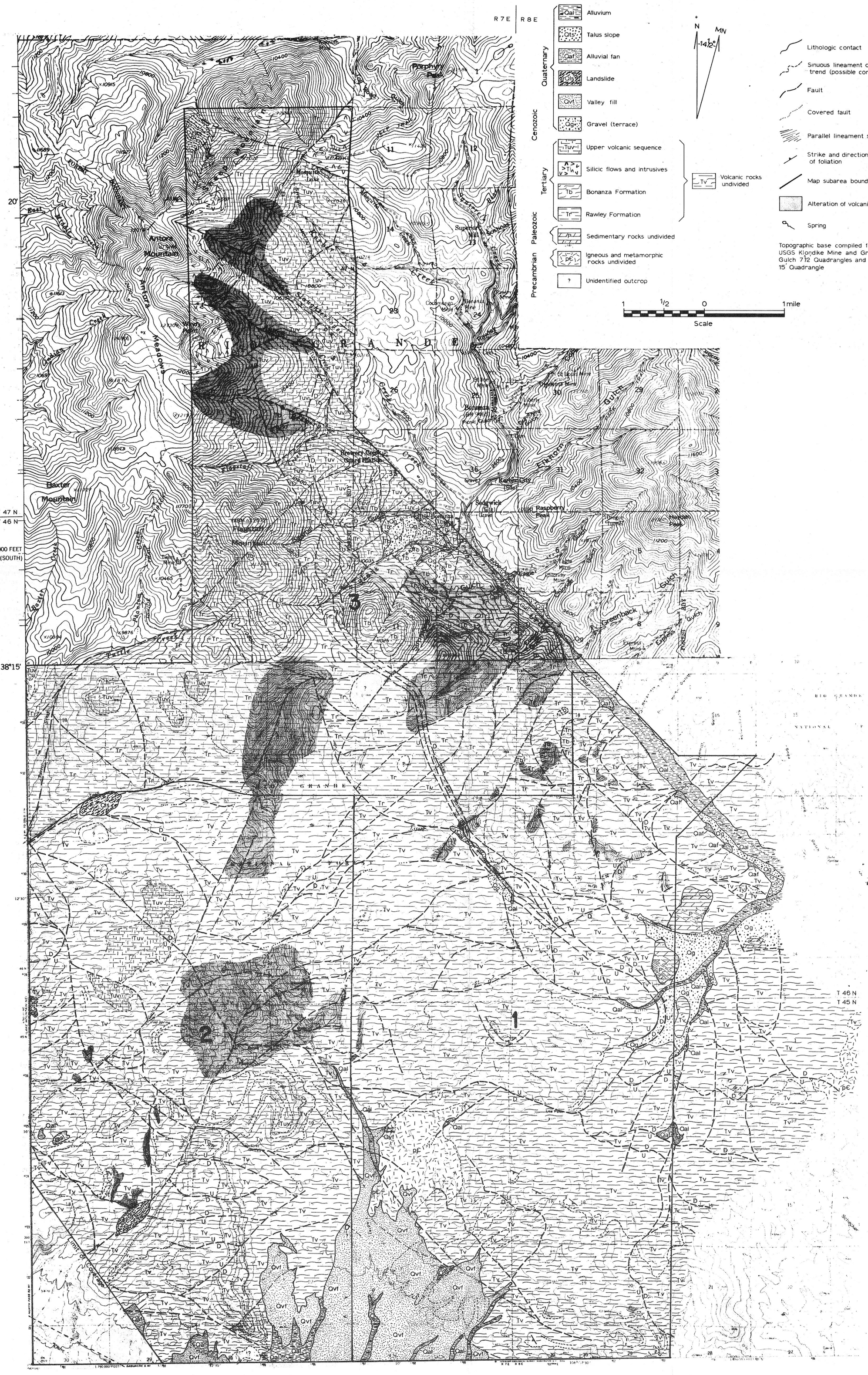

Plate 3

CROSS SECTIONS

R. W. Marrs Thesis no. 1531 March, 1973

Explanation

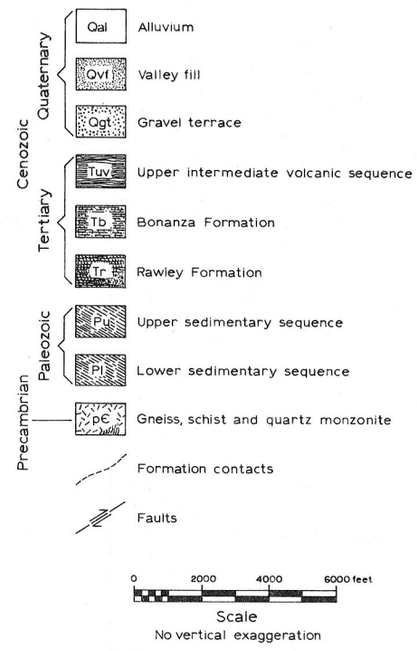

Cross Section A-A'

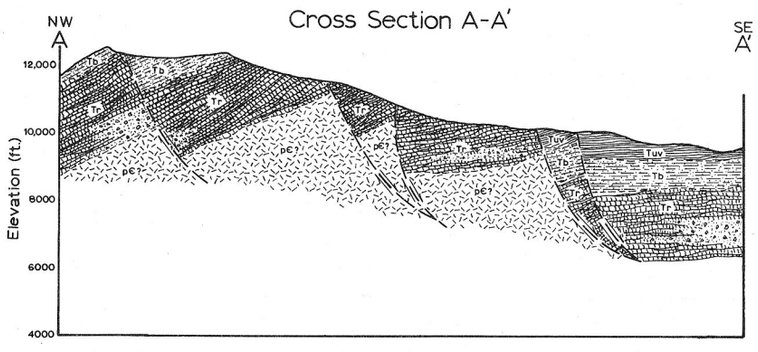

Cross Section B-B'

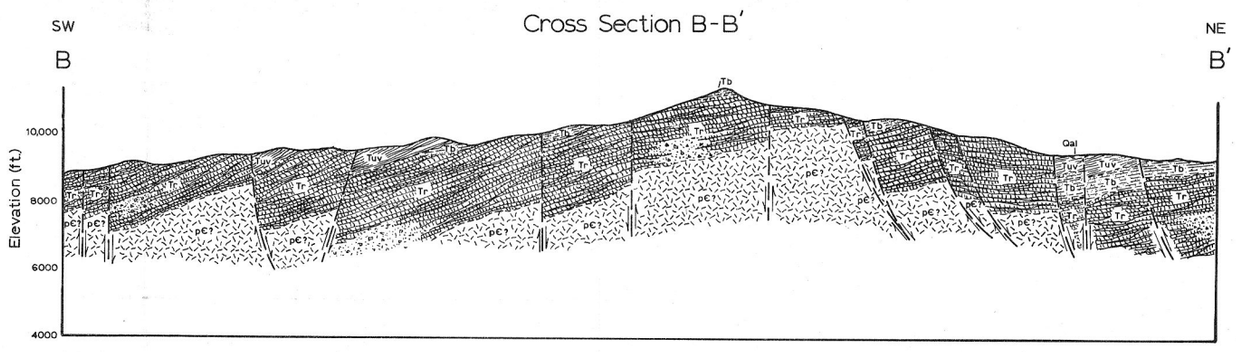

Cross Section C-C'

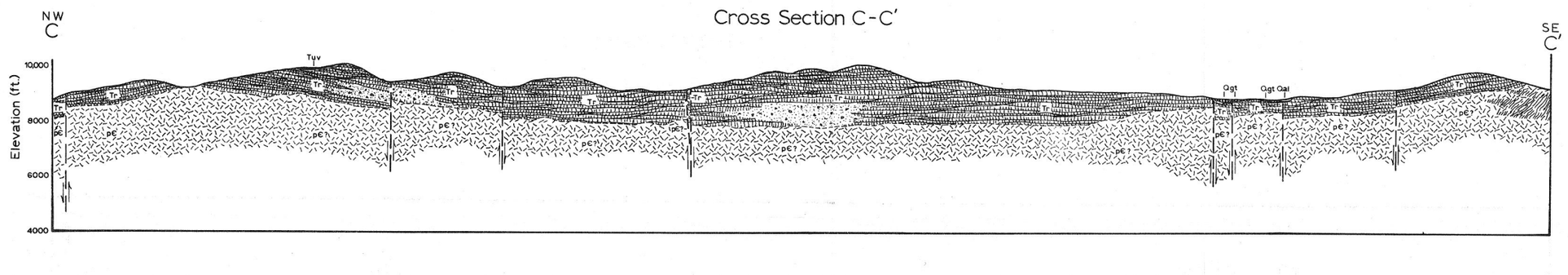

Cross Section D-D'

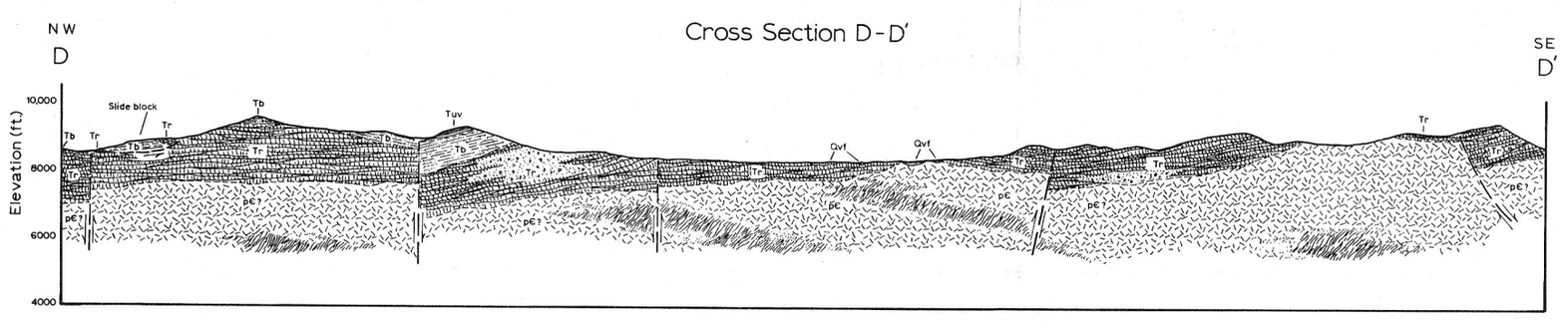

Cross Section E-E'

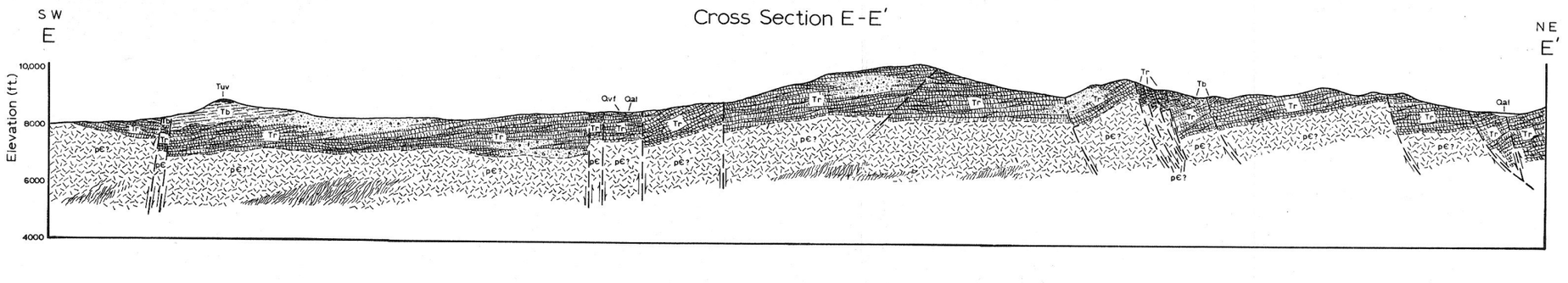

Cross Section F-F'